NASA CONTRACTOR REPORT

DEGRADATION OF MULTIPLIER PHOTOTUBES EXPOSED TO SPATIAL RADIATIONS

by M. John Brown, M. S. Bae, and S. Park

Prepared by
EMR-AEROSPACE SCIENCES
WESTON INSTRUMENTS, INC.
College Park, Md.
for Langley Research Center

NATIONAL AERONAUTICS AND SPACE ADMINISTRATION • WASHINGTON, D. C. • MARCH 1969

NASA CR-1304

DEGRADATION OF MULTIPLIER PHOTOTUBES EXPOSED TO SPATIAL RADIATIONS

By M. John Brown, M. S. Bae, and S. Park

Prepared under Contract No. NAS 1-7648 by

EMR-AEROSPACE SCIENCES
WESTON INSTRUMENTS, INC.
College Park, Md.

for Langley Research Center

NATIONAL AERONAUTICS AND SPACE ADMINISTRATION

For sale by the Clearinghouse for Federal Scientific and Technical Information
Springfield, Virginia 22151 – CFSTI price $3.00

FOREWORD

Multiplier phototubes, used in scientific spacecraft for detector applications, are designed to be extremely rugged and stable in the spatial environment of vacuum, temperature, and radiations from solar, planet and charged particles. But, like many electronic devices, the operating characteristics of multiplier phototubes are dependent upon exposure to their indigenous environments. The experimental program and analysis of test measurements were used to evaluate the stability and reliability of the anticipated end usage of multiplier phototubes. This task was conducted under the Technical Monitoring of Mr. J. A. Holland, Langley Research Center, Hampton, Virginia.

ACKNOWLEDGEMENT

The authors wish to express their gratitude to others on the technical staff of Langley Research Center who contributed to the overall success of the program by their recommendations and technical discussions. In particular, appreciation is expressed to Messrs. W. Dixon and T. M. Walsh.

Thanks are also due to the laboratory personnel who participated in setting up and conducting the experimental program.

TABLE OF CONTENTS

LIST OF ILLUSTRATIONS

LIST OF SYMBOLS

S	Stray sunlight	watts/cm^2
E_s	Earth Albedo of the sun	watts/cm^2
M	Moon Albedo of the sun (moonlight)	watts/cm^2
M_a	Moon Albedo attenuated by sunshield	watts/cm^2
E_m	Earth Albedo of the moon	watts/cm^2
H^+	Proton flux	P/cm^2/day
e	Electron flux	e/cm^2/day
I_a	Anode current	Amperes
I_k	Cathode current	Amperes
I_{13}	Dynode current (subscript denotes stage)	Amperes
σ_a	Anode radiant sensitivity	Amperes/watt
σ_k	Cathode radiant sensitivity	Amperes/watt
G	Gain	
Q.E.	Quantum efficiency	percent
λ	Wavelength	A^o or n.m.
p	Incident power at the phototube cathode	watts/cm^2/second
A	Current unit	Amperes
μA	Current unit	Microamperes
$H(\lambda)$	Solar Irradiance	watts/cm^2/nanometer
θ	Angle of incident illumination	degrees

h	Altitude above surface of earth	kilometers
Å	Wavelength unit	Angstrom (10^{-10}m)
nm	Wavelength unit	Nanometers
t	Time	
T	Temperature	
τ	Transmission	percent
KM	Distance	kilometers
Torr.	Pressure	mm Hg.
cm	Length	centimeters
M	Direct moonlight	watts/cm^2
rpm	Rotation	revolutions per minute
R	Radius of earth	6370 kilometers
W	Electrical energy	watts
m	Visual magnitude of space body	
A.U.	Astronomical Unit	1 A.U. = 1.49 x 10^8KM
P(λ)	Normalized Quantum Efficiency of Phototube	
V(λ)	Normalized human eye response	

DEGRADATION OF MULTIPLIER PHOTOTUBES EXPOSED TO SPATIAL RADIATIONS

By M. John Brown, M. S. Bae, S. Park
EMR-Aerospace Sciences
College Park, Maryland 20740

SUMMARY

The degradation of multiplier phototubes was determined from properties measured in situ during exposure to simulated spatial radiations. A complete analysis of the orbital environments for a specific spacecraft was accomplished to determine operational parameters of a phototube detector. The experimental apparatus was then arranged to provide the spatial environments at real time conditions. Exposure of four identical phototubes was conducted to evaluate the synergistic effect of combined radiations including solar, lunar, and earth irradiances and electron-proton accelerated particle radiations over a seven month period.

The phototubes were fabricated for high stability using beryllium copper dynodes in each of fourteen stages and their spectral sensitivity was from 250 to 700 nanometers. Selection of the phototube was based on detector requirements in starmapping from an orbiting spacecraft.

Laboratory test results indicate that the phototube is relatively stable when exposed to single radiation sources of solar and charged particles, but degrades when exposed to combined radiations, especially when the irradiation profile included lunar viewing. Degradation in properties was enhanced greatly for the phototube exposed to lunar radiations. Therefore, in the design of detector systems for space exploration, consideration must be given to protect the phototube sensing element from excess irradiation fluxes which eminate from specific sources.

SECTION 1.0
INTRODUCTION

The stability of spacecraft detectors becomes more critical as we increase our knowledge of the universe and consequently demand more resolution from the on-board instrumentation. The inadequacy

of applying previous flight experience to future spacecraft missions compels the scientist to seek his answers in the laboratory. With a laboratory program the scientists and engineers can establish a level of confidence in the ability of data acquisition systems to obtain specific measurements. During a typical spacecraft mission on-board detectors are exposed to a variety of environments and radiating sources which consist mainly of: a) low pressure vacuum, b) solar illumination, c) earth, moon, and planet albedo illumination, d) electron and proton charged particles, and e) temperature. Therefore, an adequate test program to evaluate detector stability is one that simulates each of the irradiating fluxes in their proper sequence, at appropriate levels, and for specific orbit conditions. The purpose of the present investigation was to measure the degradation of a multiplier phototube detector in simulated radiation environments for a spacecraft orbiting the earth at an altitude of 500 KM.

The approach taken in this program is to simulate, at real time conditions, the environs of space and impose those conditions on a group of four phototubes. Irradiation of the phototubes is programmed to determine the degree of interaction which exists to enhance or decrease the amount of degradation when the radiations are additive. The experimental apparatus and sequence of irradiations are established in accordance with the results of detailed analyses conducted for a specific spacecraft polar orbit, inclined at 95°. During exposure and with the phototubes remaining in the vacuum enclosure, measurements of electrical and optical properties of the phototubes are made in situ periodically throughout their lifetime.

SECTION 2.0

ORBITAL ANALYSIS

The experimental program was conducted in a simulated space environment which the spacecraft and enclosed multiplier phototube encounters during its orbiting lifetime. The specific conditions selected for this study corresponded to a spacecraft in an earth orbit at an altitude of 500 KM, polar orientation in the three o'clock position, and for a period of 90 minutes. The spacecraft is a "rolling wheel" spinning at the rate of three rpm with its spin axis tangential to the Earth's curvature, illustrated in Figure 2.0-1. This orbiting condition results in the spacecraft being illuminated by the sun for 60 percent of the period (54 minutes) and shadowed by the earth for the remaining 40 percent of the period (36 minutes).

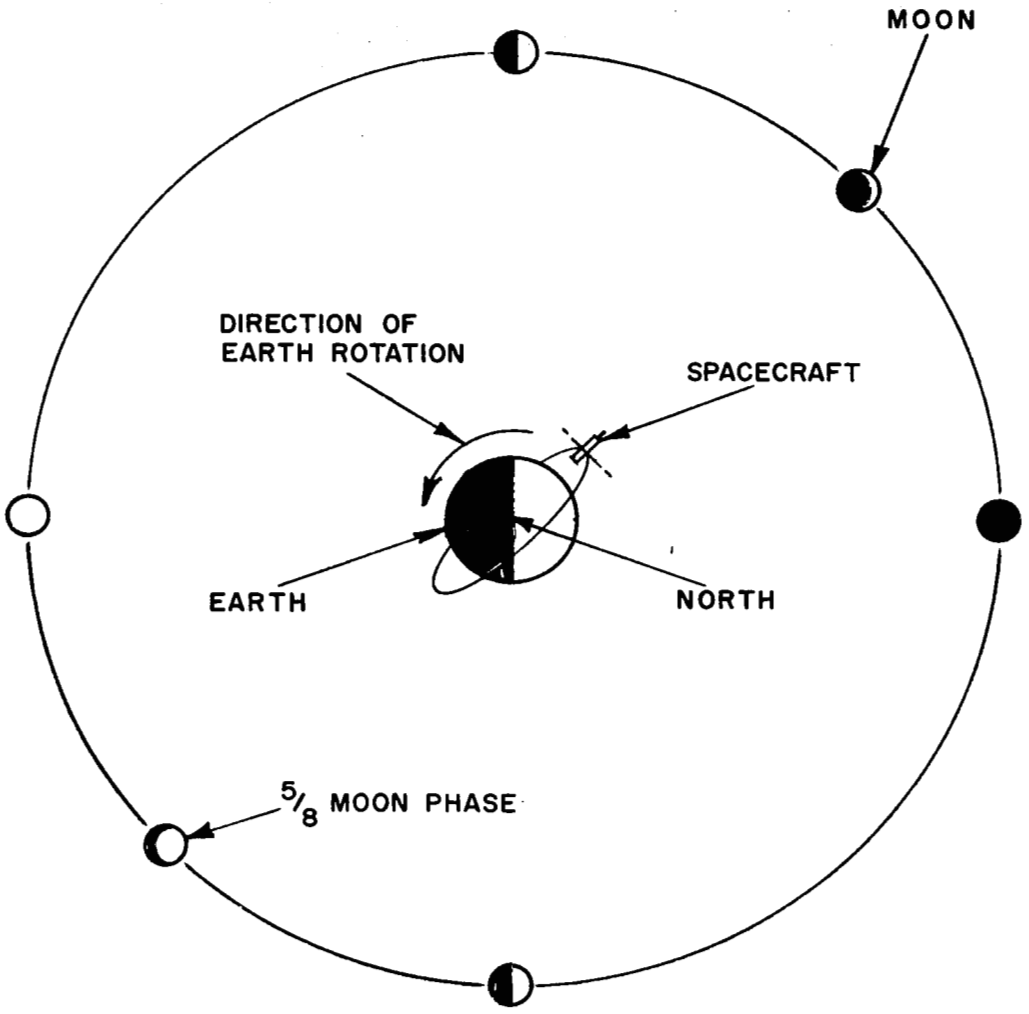

FIGURE 2.0-1 SPACECRAFT ORBITAL CONDITION

2.1 SPACE ENVIRONMENT

Spacecraft which are placed into orbit around the Earth for scientific exploration, encounter large doses of charged particles and electromagnetic radiations are of special concern to the design of data collecting devices. Specifically, exposure to electrons and ultraviolet radiations can cause changes in optical and thermal properties of surface materials and can result in detector outputs beyond comprehension and analysis.

2.1.1 Natural Space Environments

2.1.1.1 Pressure

A reasonable estimate of the pressure in space is one particle per cubic centimeter for interstellar regions and is equal to approximately 10^{-16}torr. In describing the near Earth atmosphere, concentrations of approximately 10^{9} particles/cm^{3} exist at an altitude of 200 miles above the earth. This corresponds to the pressure of approximately 10^{-7}torr.

2.1.1.2 Electromagnetic Radiation

Approximately 98 percent of the solar energy lies between the wavelengths of 0.3 and 4.0 microns and is contained in a beam collimated to 32 minutes of an arc. The total radiant flux, at a distance of 1 A.U. from the sun, (outside the Earth's atmosphere) is the "solar constant" with a value which has been established at 0.14 watts/cm^{2}. Figure 2.1.1.2-1 shows spectral energy curves related to the sun.

2.1.1.3 Charged Particles

The charged particle environment of space, close to the Earth, is due primarily to the geomagnetically trapped radiation belts, shown in Figure 2.1.1.3-1. Approximately 99 percent of the trapped radiation consists of protons and electrons. These regions of trapped particles are commonly known as the Van Allen radiation belts and can be roughly attributed to two overlapping regions or belts. The inner region is composed of high energy protons and low to moderate electrons and reaches its maximum intensity at approximately 1.5 earth radii. The outer belt reaches its maximum intensity at approximately 4 earth radii and is composed of electrons and low energy protons.

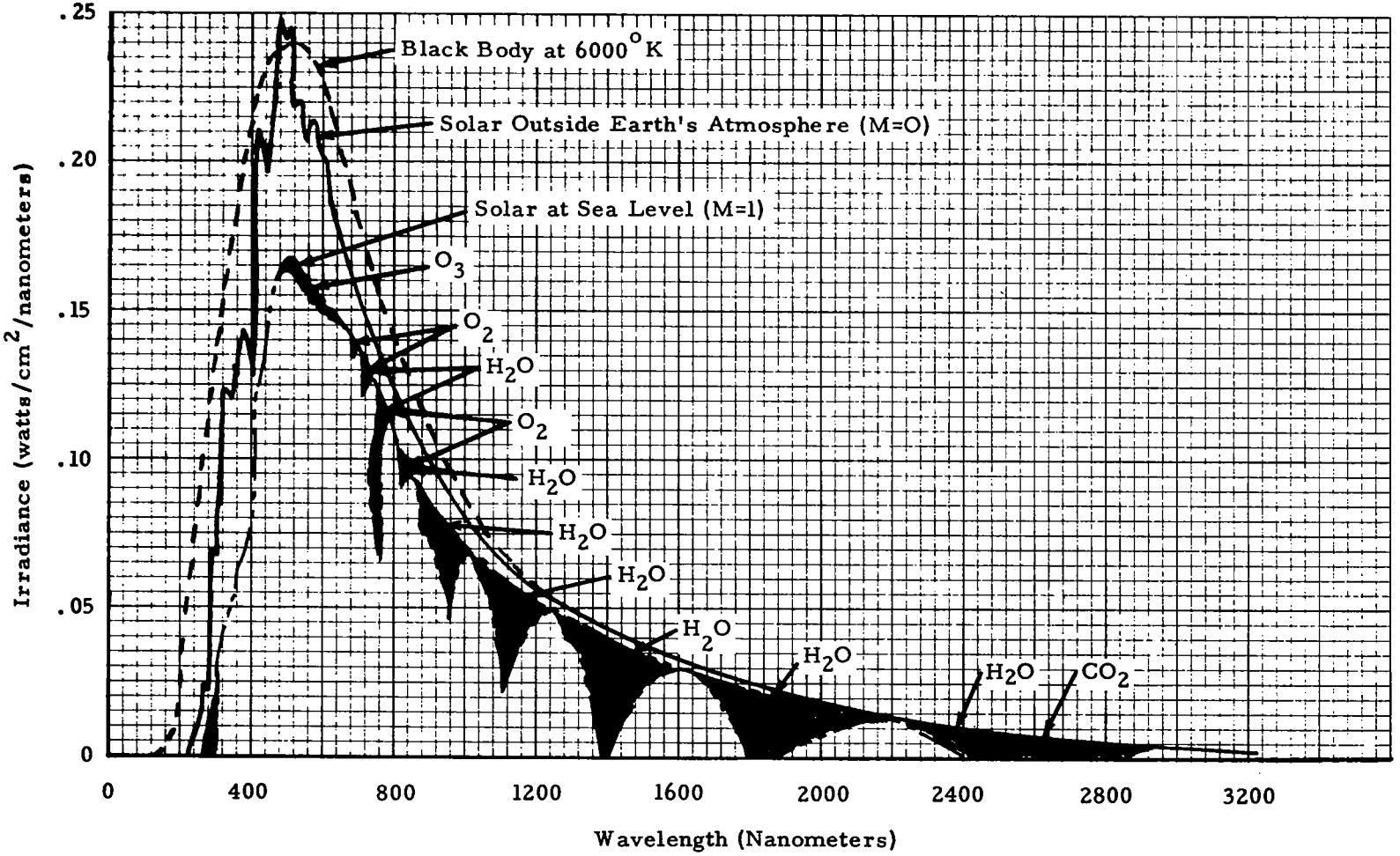

FIGURE 2.1.1.2-1 SPECTRAL ENERGY CURVES RELATED TO THE SUN

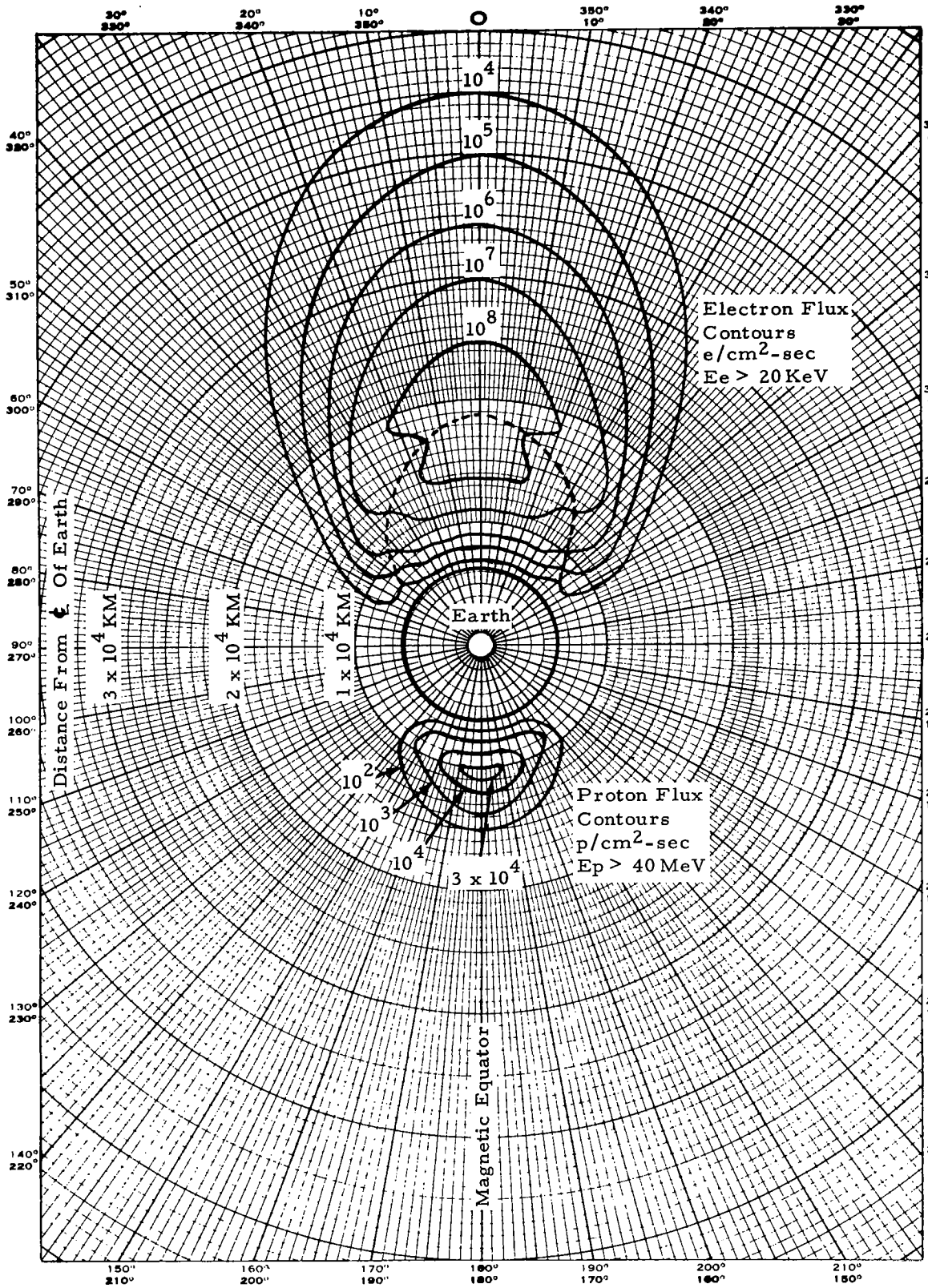

FIGURE 2.1.1.3-1 TRAPPED RADIATION ABOUT THE GEOMAGNETIC EQUATOR

2.1.1.4 Planet Radiation and Albedo

Radiation from the surface of a planet stems from two sources. The first source is thermal radiation of the planet itself and is a direct function of the surface temperature of the planet and its atmosphere. The second source is referred to as the planet's albedo and is reflected solar radiation from the planet and its atmosphere. Both of these radiations are thermal and vary continuously with the position of the sun and the climatic and atmospheric conditions of the surface of the planet.

The radiation spectrum of a planet will have a Plankian energy distribution dictated by the surface temperature of the planet and modified by the emissivity characteristics of the surface and atmosphere. The spectrum may vary from point to point with changes in surface and atmospheric composition, i.e., barren land, verdant land, water, ice, cloud cover, etc. Figure 2.1.1.4-1 shows intensity distributions of direct and earth reflected sunlight.

2.1.1.5 Miscellaneous

Additional parameters of the natural space environment which are important to spacecraft performance, but not included in this study, include the following:

a.) Space heat sink
b.) Meteoric impact
c.) Cosmic Radiation
d.) Gamma and X radiations
e.) Low and non-gravitational fields
f.) Magnetic fields

2.1.2 Artificial Space Environment

2.1.2.1 Electron Belt

A significant number of artificial radiation belts have been made by high altitude explosions of nuclear bombs since 1958 and 1962 which result in trapped energetic charged particles mostly electrons. Above 1.7 earth radii the artificial belts have experienced unusually rapid decay although there are still significant numbers of electrons trapped in the central part of the belts.

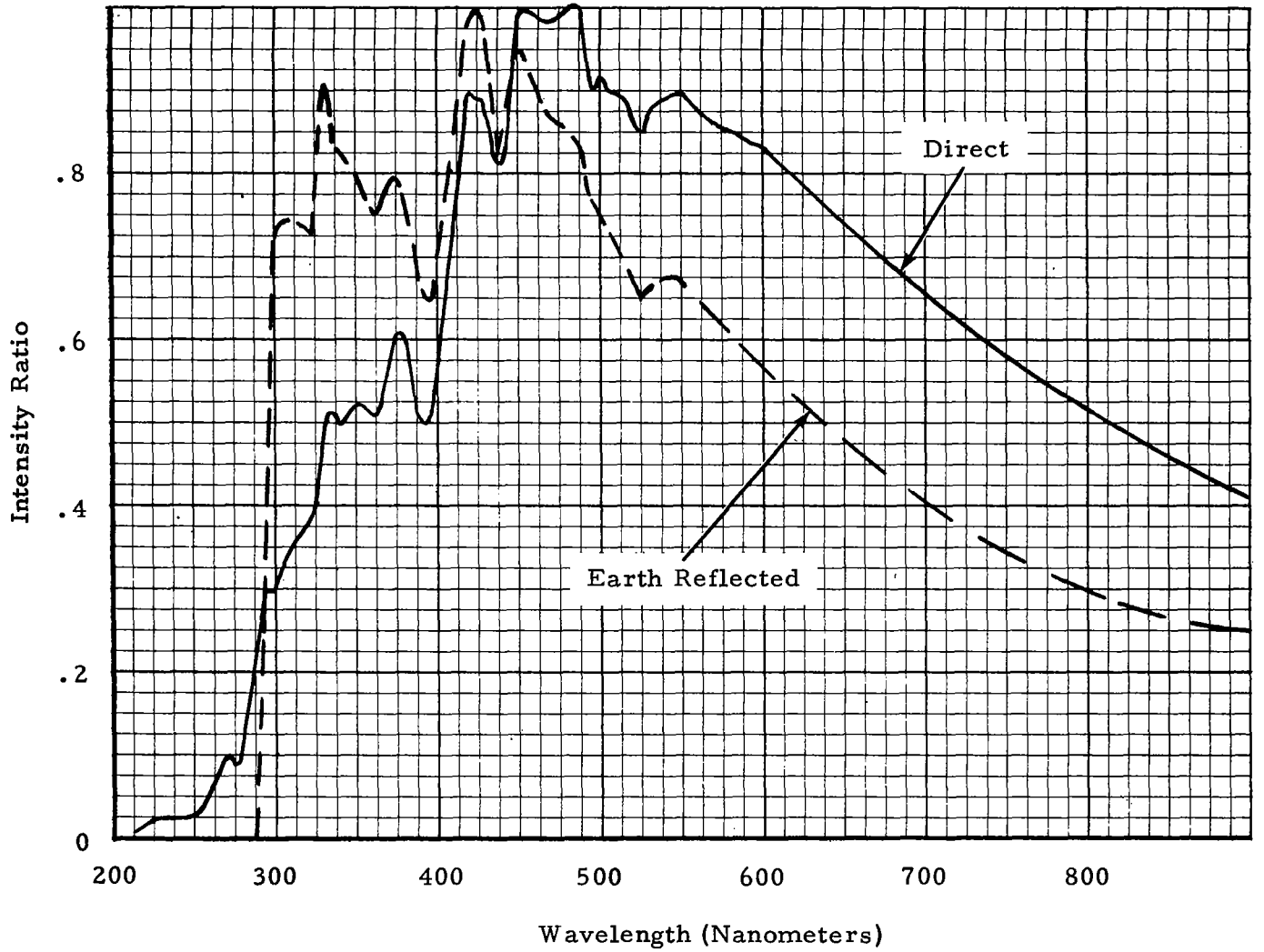

FIGURE 2.1.1.4-1 INTENSITY DISTRIBUTION OF DIRECT AND EARTH REFLECTED SUNLIGHT

2.1.2.2 Nuclear Power Sources

The use of nuclear power sources in orbiting spacecraft introduces an artificial radiation environment due to leakage and inadequate shield design. Damage to spacecraft is related to specific applications.

2.1.2.3 Rocket Plumes

The products of exhausts from solid and liquid fueled rockets are highly detrimental to many spacecraft elements, such as, thermal control coatings, solar cells, and optical experiments. Contamination by rocket plumes and subsequent effect of the space radiation environment on the contaminant films requires further definition.

2.2 SPACECRAFT AND ITS ORBIT

Figure 2.2-1 shows the spacecraft and its components. The spacecraft is at an altitude of 500 KM for a 90 minute period in a polar orbit and in the three o'clock direction. The spacecraft is a "rolling wheel", spinning at a rate of three rpm with the spin axis tangential to the Earth's curvature, as illustrated in Figures 2.2-2 and 2.2-3. A study of the spacecraft orbit revealed that it will be in the daylight portion of the Earth for 60 percent of the period (about 54 minutes) and in the dark portion for 40 percent (about 36 minutes) as shown in Figure 2.2-4.

2.3 MULTIPLIER PHOTOTUBE AND ITS OPTICAL SYSTEM

2.3.1 Multiplier phototubes

The phototubes were the model 541, type N, manufactured by EMR Photoelectric, EMR Division of Weston Instruments, Inc., Princeton, New Jersey.

2.3.2 The conceptual schematic and tentative design of the starmapper which uses the subject phototube is shown in Figures 2.3.2-1 and 2.3.2-2. The starmapper consists of a sun and earth light shield, objective and condensing lens system with reticle slits, and the phototube detector.

Figure 2.3.2-3 shows the geometry of the reticle slits. The lens system has a three inch aperture and an optical efficiency without the reticle slits of about 70 percent. The reticle slits further attenuate the light with an attenuation factor that is different for each angle of illumination. The total attenuation factor due to the lens system and reticle slits for different angles of off optical axis were calculated. In each case the

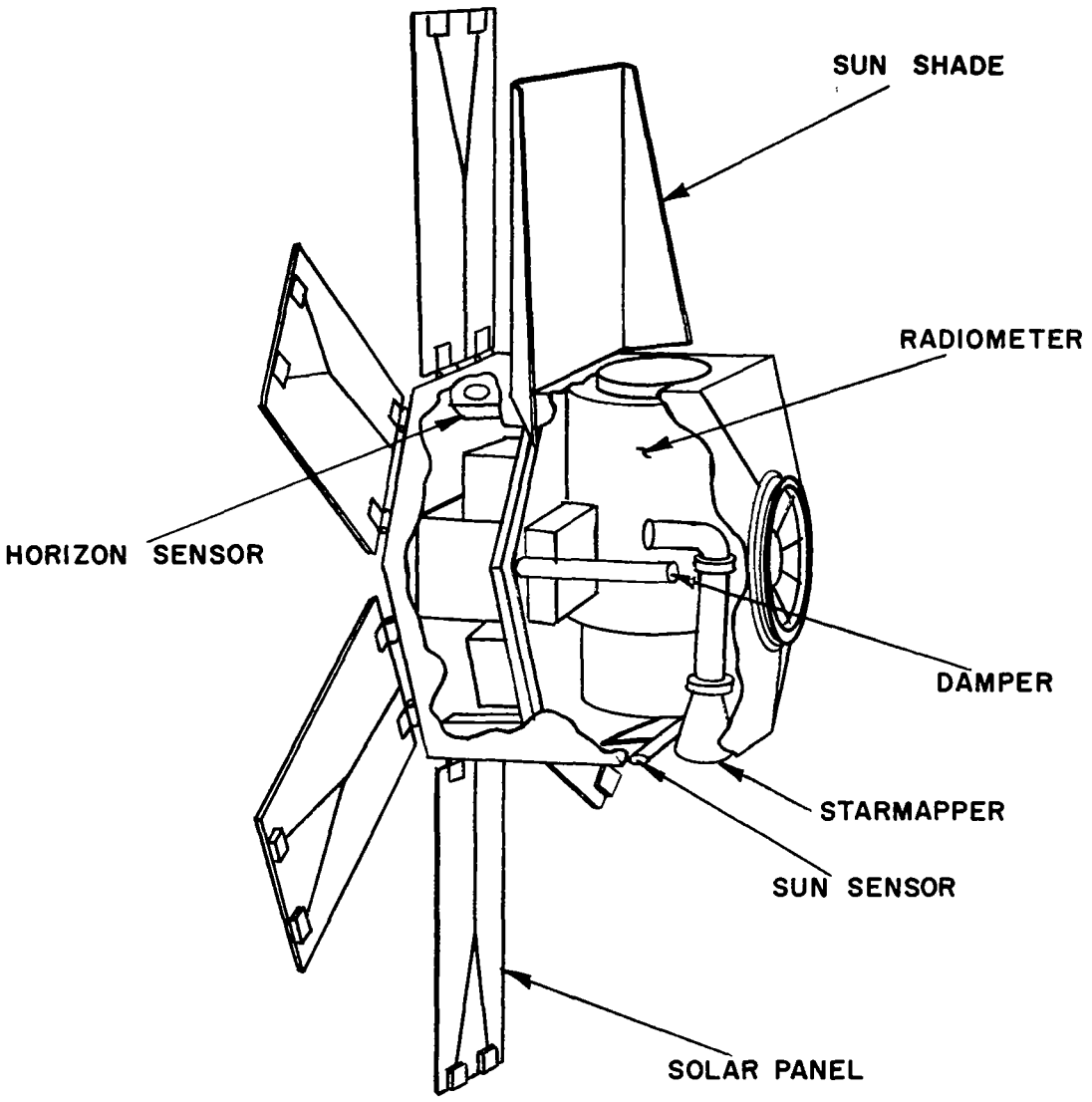

FIGURE 2.2-1 CONFIGURATION OF SPACECRAFT AND DETECTORS

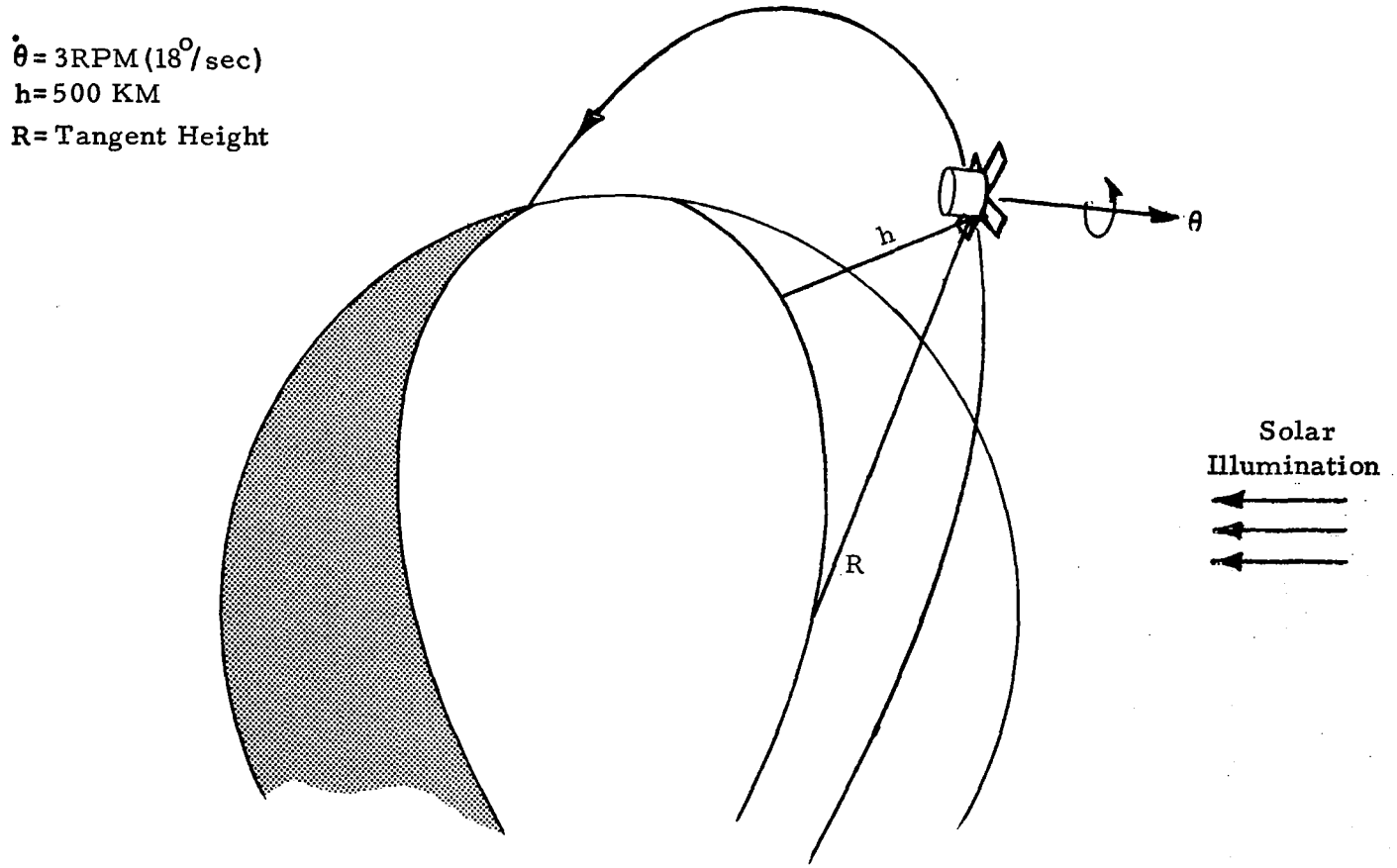

FIGURE 2.2-2 CONSTRAINTS OF THE SPACECRAFT SYSTEM

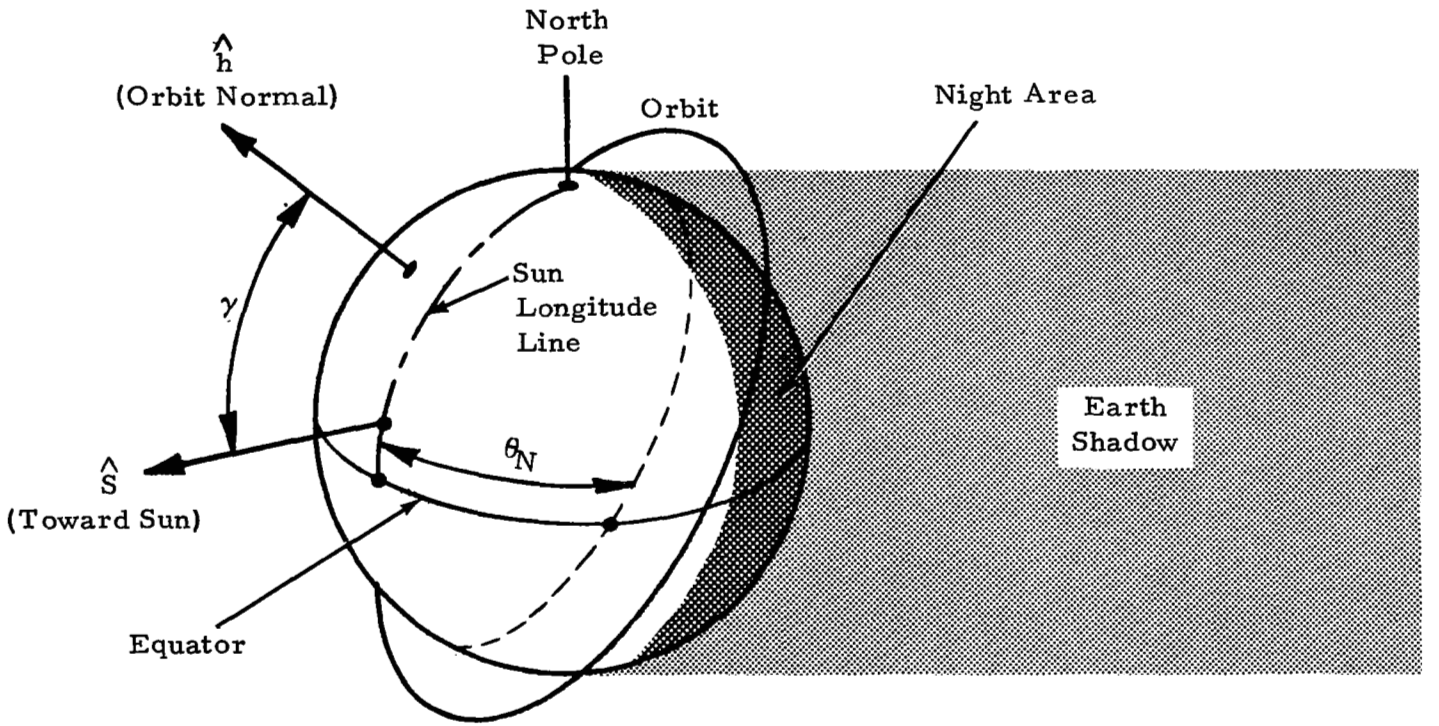

Orbit-Normal/Sun-Line Angle = γ
Shadow Fraction = Percentage of Total Orbit in Earth Shadow
Ascending Node = θ_N

FIGURE 2.2-3 SPACECRAFT ORBIT GEOMETRY

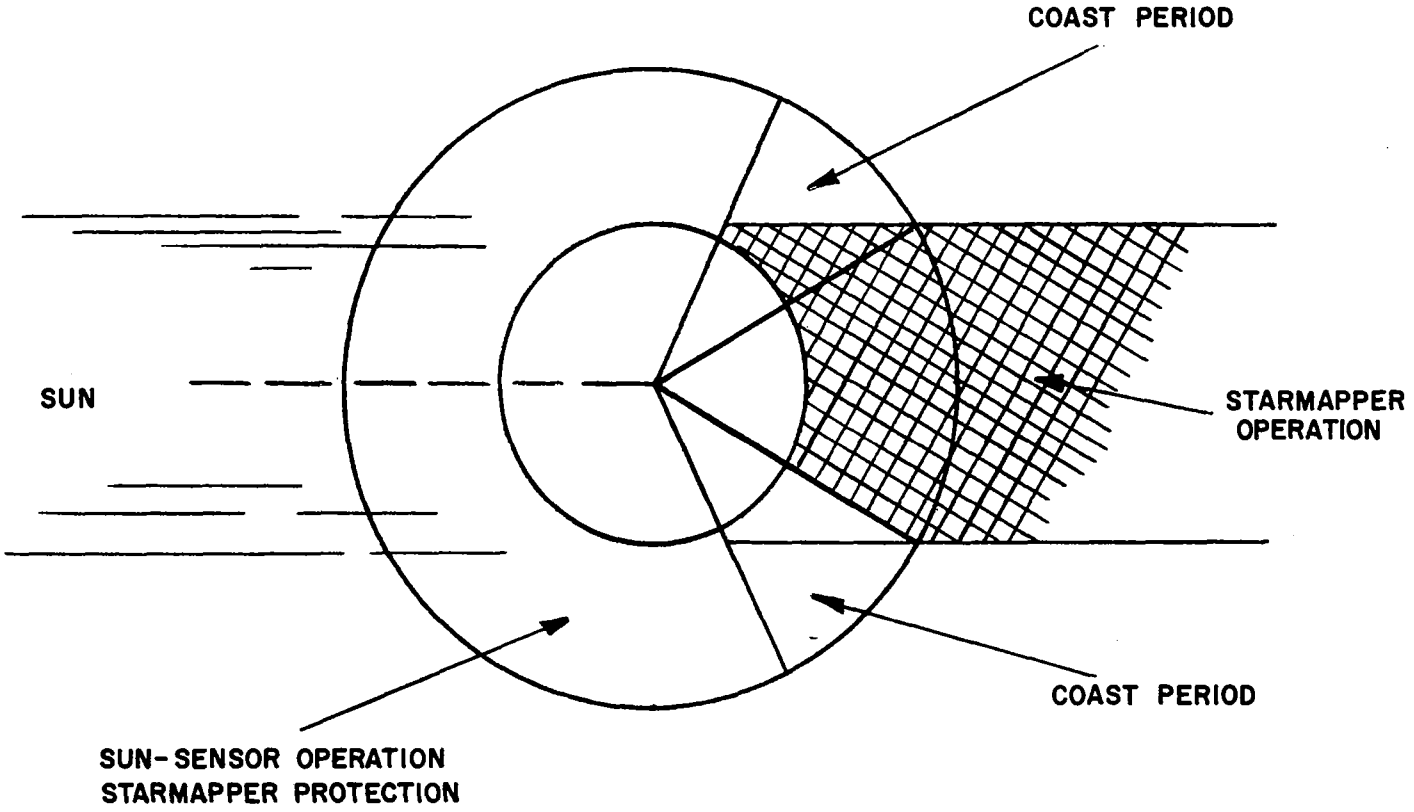

FIGURE 2.2-4 SPACECRAFT OPERATIONAL REGIMES

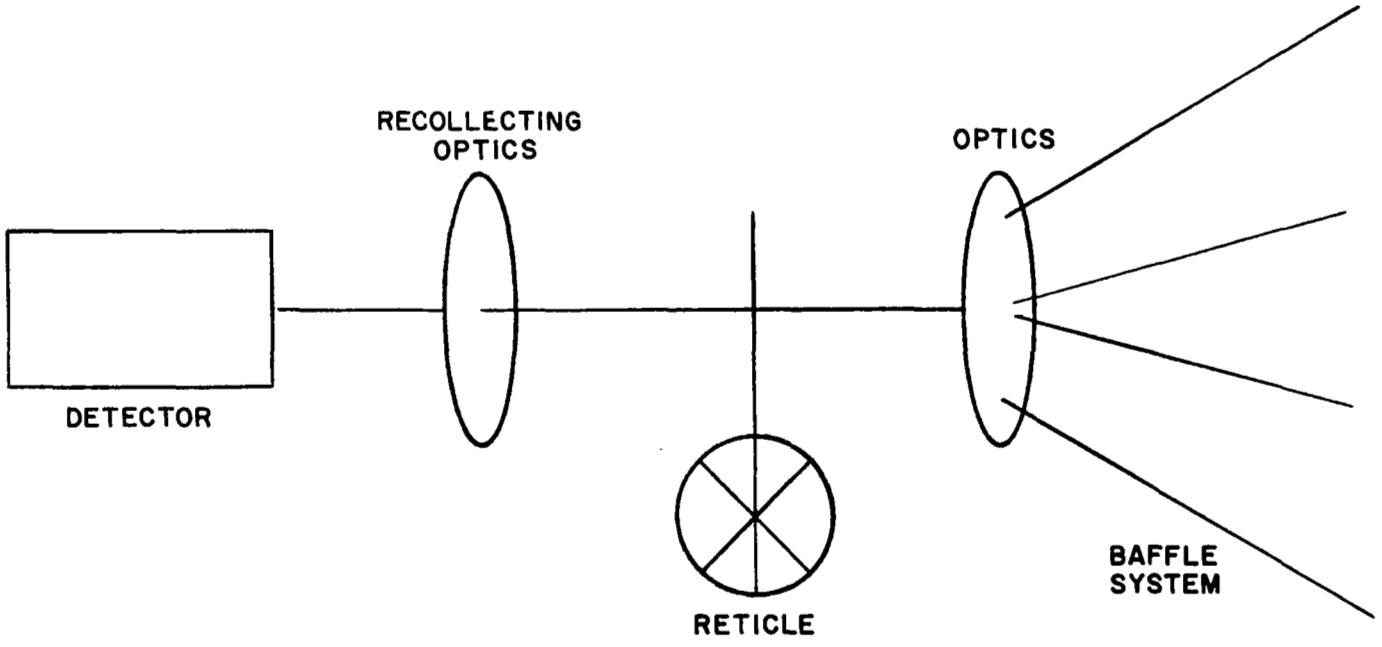

FIGURE 2.3.2-1 CONCEPTUAL SCHEMATIC OF STARMAPPER

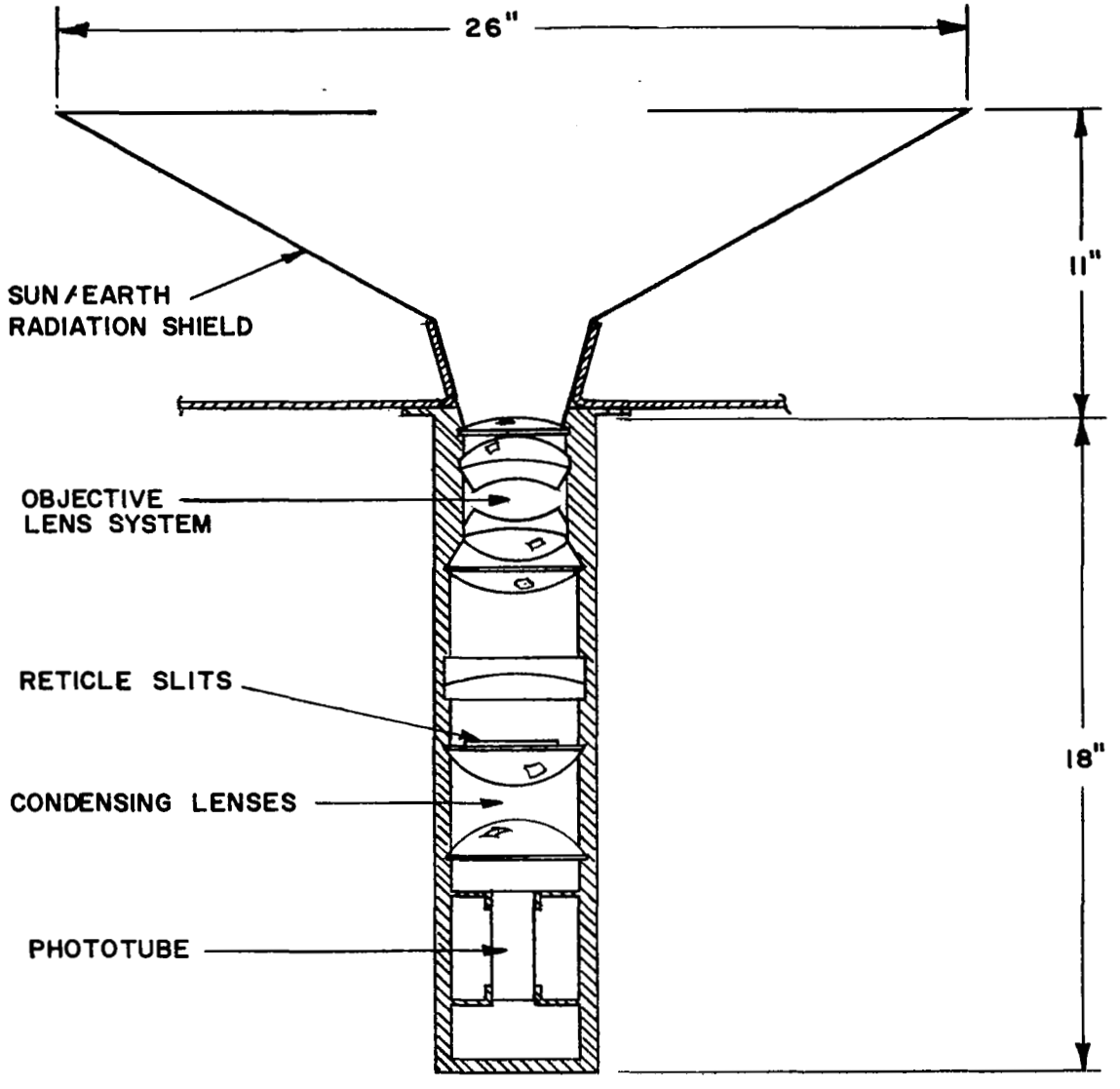

FIGURE 2.3.2-2 TENTATIVE DESIGN OF STARMAPPER

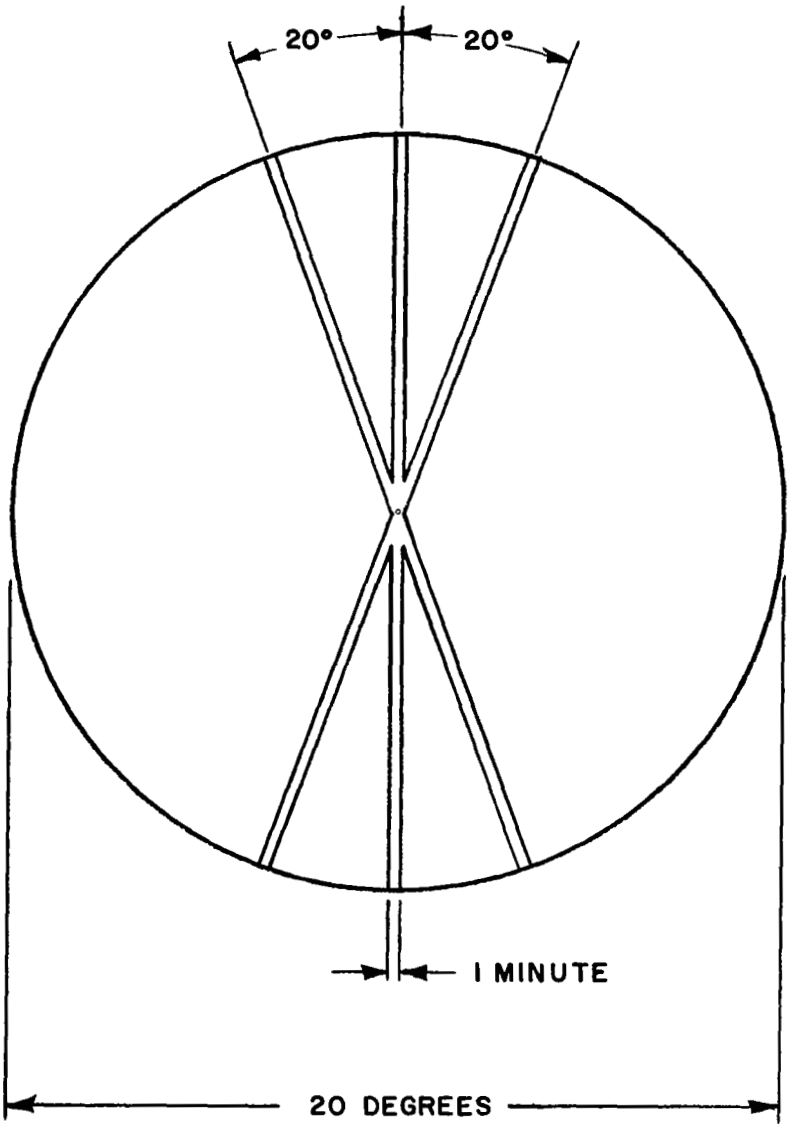

FIGURE 2.3.2-3 RETICLE GEOMETRY

optical efficiency is 0.7 and a factor of optical ratios is 9 as follows:

The light through a three inch aperture lens system is collected by a one inch diameter photocathode of the phototube in accordance with the relationship where:

$$\frac{\text{Aperture area}}{\text{Photocathode area}} = \frac{\pi \left(\frac{3''}{2}\right)^2}{\pi \left(\frac{1''}{2}\right)^2} = 9$$

2.3.2.1 Attenuation of moonlight (M) within the total field of view (10° off optical axis).

The moon is focused on the reticle and the image of the moon on the reticle has a size equal to 33' of an arc:

$$\frac{3 \times 1' \times 33'}{\pi \left(\frac{33'}{2}\right)^2} = 0.116$$

where: 1' = the width of the reticle slits and
3 = the number of slits.

Therefore, the apparent total attenuation factor becomes:

$$0.116 \times 0.7 \times 9 = 0.7308$$

2.3.2.2 Attenuation within the sunshield (between 10° and 25° off optical axis).

Although the moon is no longer focused on the reticle, perfect diffused light will continue to be collected through the three inch aperture with the following reticle attenuation factor:

$$\frac{\text{Clear field of view}}{\text{Total field of view}} = \frac{(1 \text{ deg})^2}{\pi (10 \text{ deg})} 2 = \frac{1}{\pi} \times 10^{-2}$$

$$= 3.18 \times 10^{-3}$$

Therefore, the total attenuation factor becomes:

$$3.18 \times 10^{-3} \times 0.7 \times 9 = 2.0 \times 10^{-2}$$

2.3.2.3 Beyond 25° off the optical axis, the attenuation decreases logarithmically.

At 45° off the optical axis the attenuation is approximately 10^{-5} and at 90°, approximately 10^{-11}. Figure 2.3.2.3-1 shows the overall attenuation curve for the starmapper detector system.

2.3.2.4 Attenuation of earth reflected moonlight (E_m)

Since all the light is collected by the starmapper through a three inch aperture, the resulting attenuation is:

2×10^{-2} (See Section 2.3.2.2)

However, the attenuation factor has to be modified by the effective area of the earth as viewed by the phototube.

The field of view of the earth at an altitude of 500 KM is approximately 136°, (see Section 2.4.1); but since the phototube has only a 20° field of view, attenuation becomes:

$$\frac{\pi (10^{\circ})^2}{\pi (\frac{136^{\circ}}{2})^2} = \frac{100}{(68)^2} = \frac{1}{46.2} = 2.2 \times 10^{-2}$$

2.4 SPACECRAFT ROTATION

As the satellite spins at a rate of three rpm, the phototube will see the earth and moon for different time periods. Calculations of the chopper duty cycles to simulate these conditions are as follows:

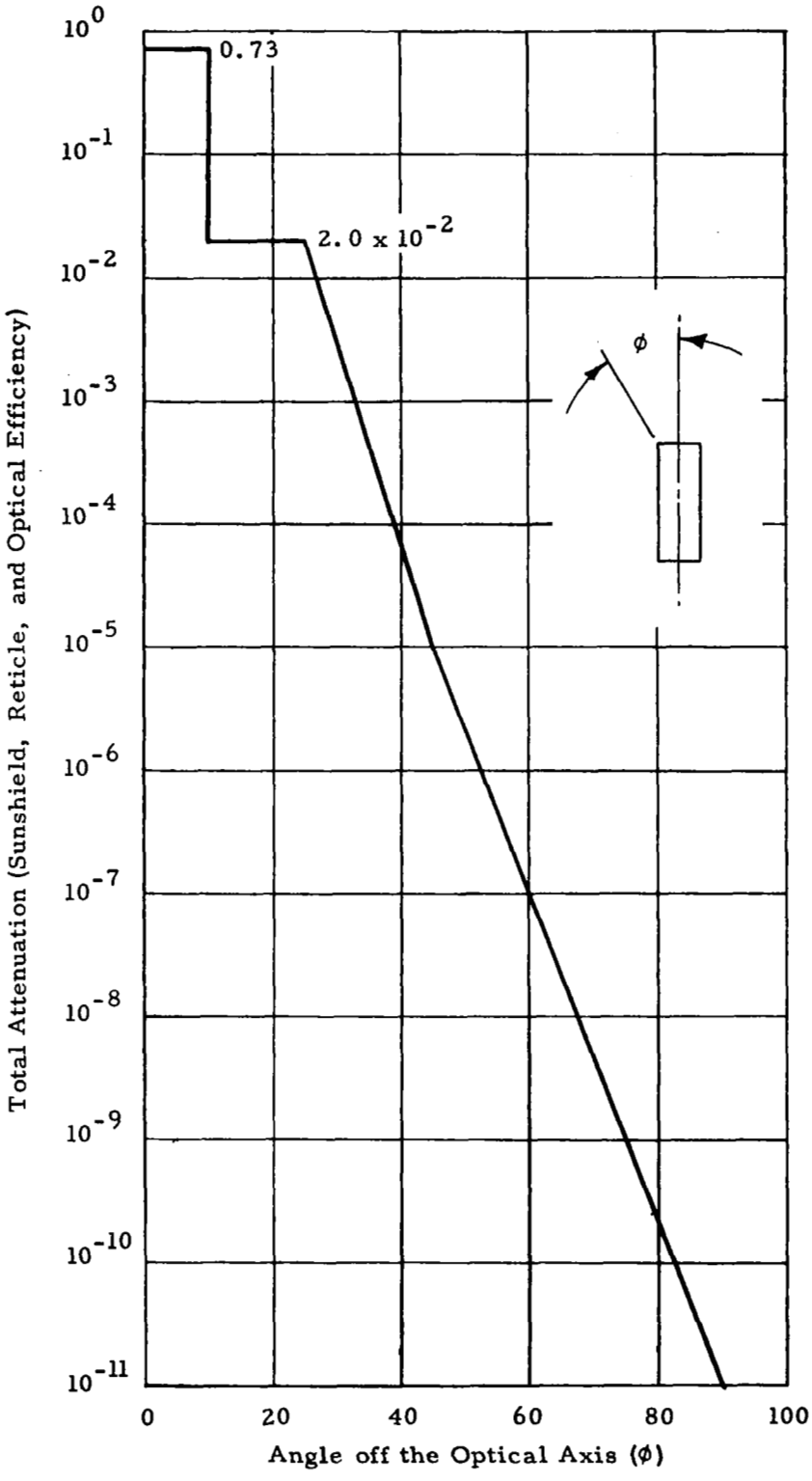

FIGURE 2.3.2.3-1 OVERALL ATTENUATION

2.4.1 Field of View of the Satellite at an Altitude of 500 KM:

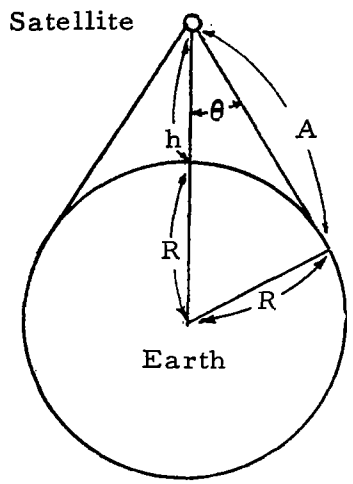

h = 500 KM

R = 6370 KM

2θ = Field of View

A = Tangent Height

θ is given by the equation:

$$\theta = \tan^{-1} \frac{R}{A}$$

where:

$$A = \sqrt{(R + h)^2 - R^2}$$

$$= \sqrt{2\,Rh + h^2}$$

$$= \sqrt{2 \times 6370 \times 500 + 250000}$$

$$= 2575 \text{ KM}$$

therefore:

$$\theta = \tan^{-1} \frac{6370}{2575} = \tan^{-1} 2.474$$

$$= 67^{\circ}\ 59.5'$$

$$\approx 68^{\circ}$$

field of view of the satellite is:

$$2\theta = 136^{\circ}$$

2.4.2 Duty Cycles of the Chopper

2.4.2.1 Earth Albedo (E_s or E_m)

The spacecraft and its phototube detector with a 20^o field of view is shown below:

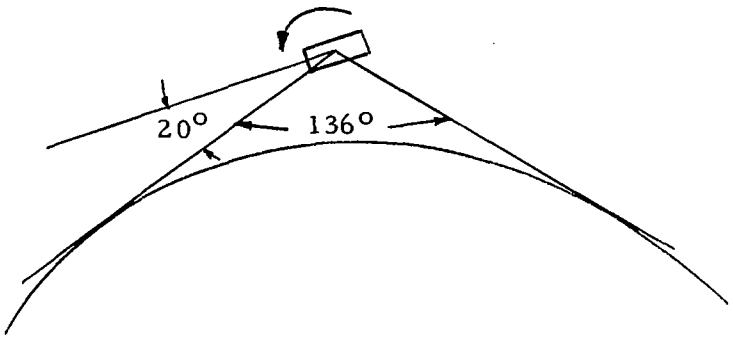

Therefore, the total apparent field of view of the phototube viewing the earth is:

$$136^o + 20^o = 156^o$$

and a duty cycle of the chopper for earth albedo would be:

$$20 \text{ sec.} \times \frac{156^o}{360^o} = 8.66$$

$$\approx 8.7 \text{ sec.}$$

or: 8.7 sec. out of every 20 sec.

2.4.2.2 Moon Radiance (M)

Since the size of the moon is approximately 33' and the phototube has a 20^o field of view, the period of direct moon viewing becomes:

$$20 \text{ sec.} \times \frac{20^o}{360^o} = 1.1 \text{ sec.}$$

or: 1.1 sec. out of every 20 sec.

2.4.2.3 Sunshield Attenuated Moon Radiance (M_a)

The sunshield has a 50^o field of view and its duty cycle becomes:

$$20 \text{ sec.} \times \frac{50^o}{360^o} = 2.8 \text{ sec.}$$

or 2.8 sec. out of every 20 sec.

2.5 ILLUMINATION ANALYSIS

In order to completely understand the magnitude of each irradiation source and their relationship to the phototube capability, an analysis was conducted. Since illuminating intensities during daylight portions of the spacecraft orbit were beyond the phototube capacity, it was decided that the phototube would be turned on only during the dark portion of the orbit. The remaining sources, which illuminated the phototube during the time that power was supplied, were the moon and the earth albedo of the moon. The following analysis was conducted for each irradiation source.

2.5.1 Stray Sunlight (S)

The total irradiance of the sun in the range of a type 541N phototube is given by:

$$\int_0^\infty H(\lambda)\ P(\lambda) = 31.2 \text{ mw/cm}^2$$

where: $H(\lambda)$ = the solar irradiance curve (Fig. 2.5.1-1)

$P(\lambda)$ = the normalized Q.E. curve of the phototube (Figure 2.5.1-2).

$H(\lambda)\ P(\lambda)$ curve is as shown in Figure 2.5.1-3. Spacecraft is in three o'clock orbit. Stray sunlight will be 45^o off the optical axis.

The attenuation factor is 10^{-5}.

Therefore, the apparent irradiance of stray sunlight at the photocathode is:

$$p(S) = 0.0312 \text{ W/cm}^2 \times 10^{-5} = 3.12 \times 10^{-7} \text{ W/cm}^2$$

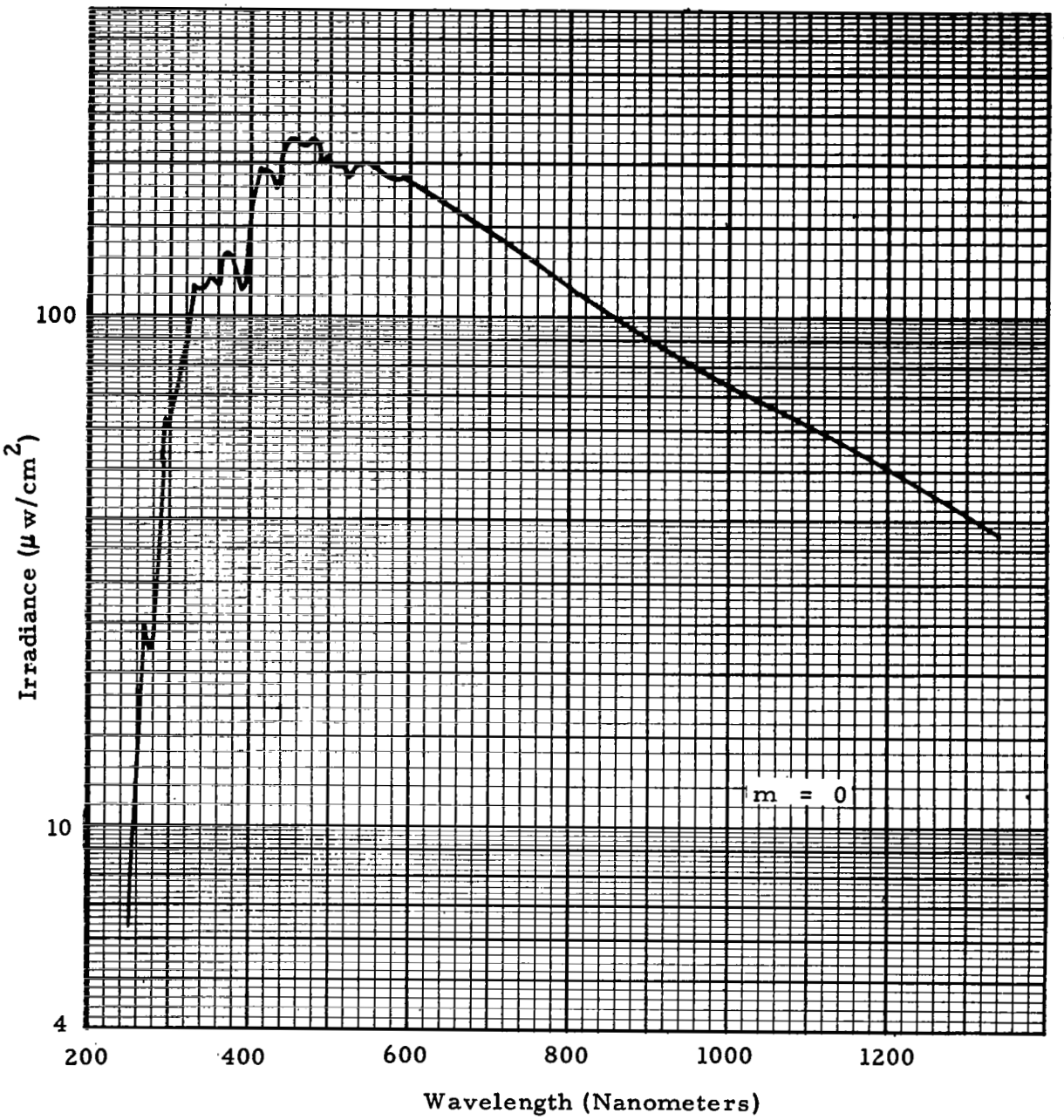

FIGURE 2.5.1-1 SOLAR SPECTRAL IRRADIANCE

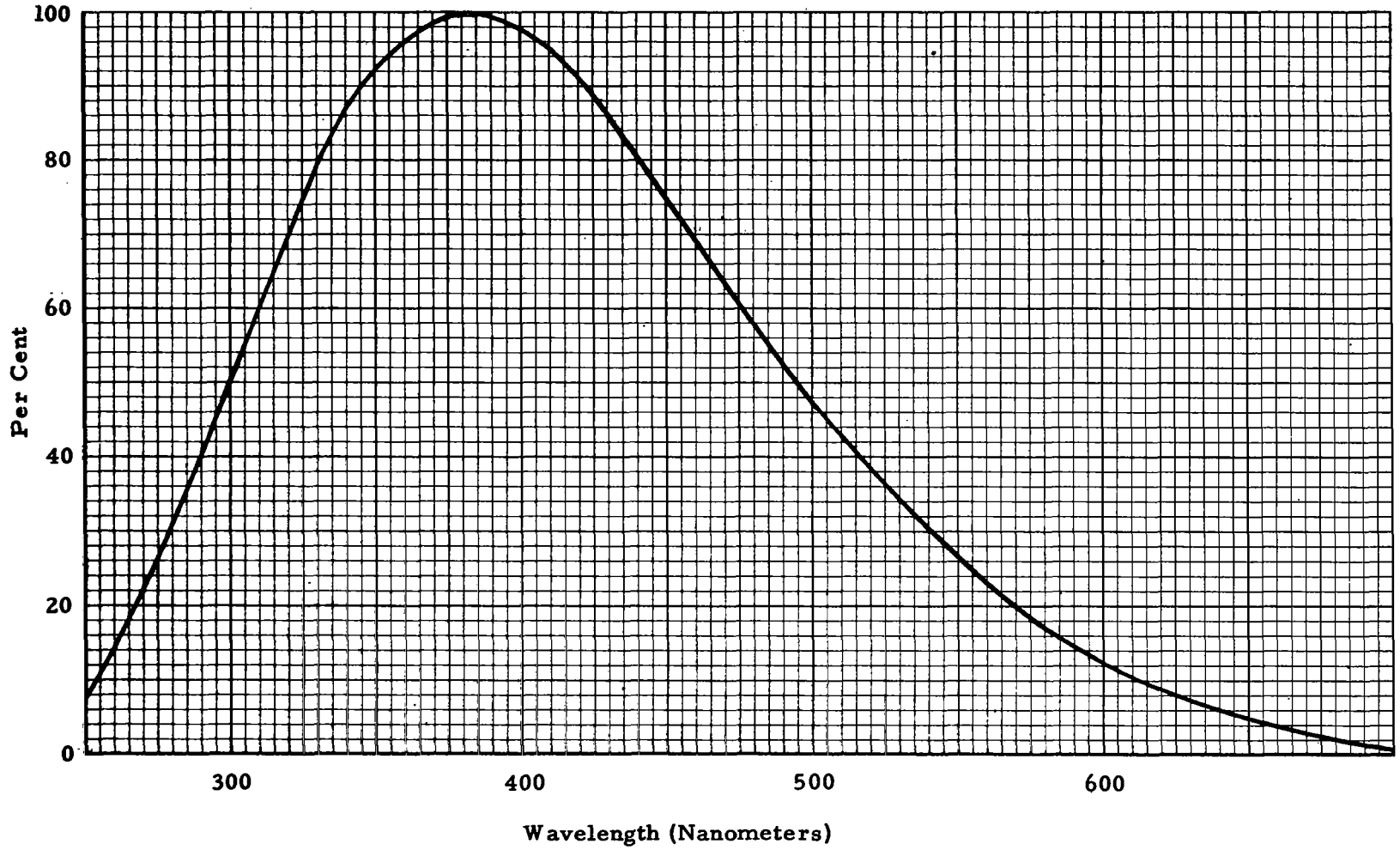

FIGURE 2.5.1-2 LUMINOUS EFFICIENCY [P (λ)] OF 541N PHOTOTUBE

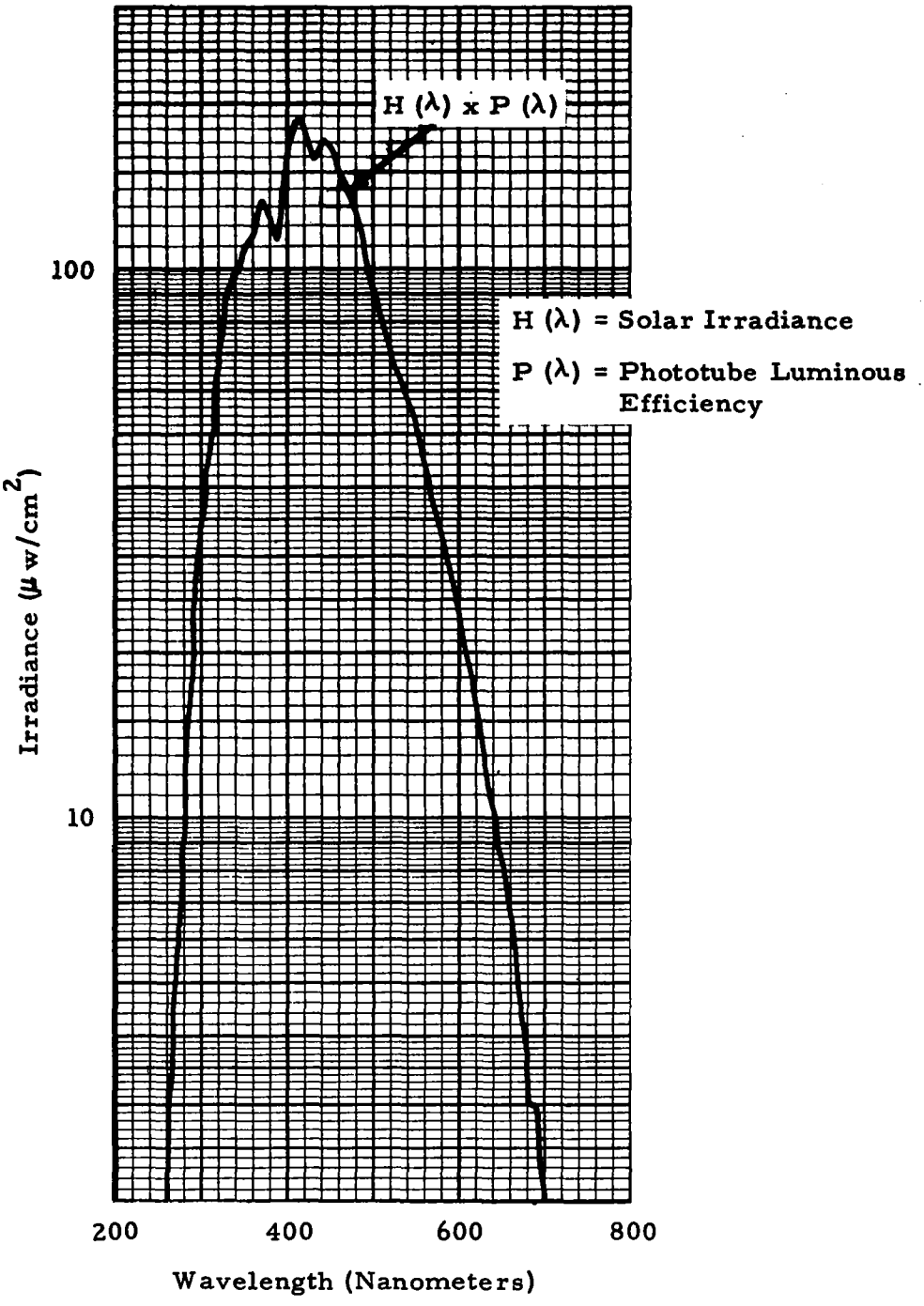

FIGURE 2.5.1-3 SPECTRAL RESPONSE OF PHOTOTUBE RELATIVE TO SOLAR IRRADIANCE

2.5.2 Earth Albedo of the Sun (E_s)

Solar radiation reflected from the Earth is variable and depends also on surface conditions of the Earth. The albedo which is a spectral image of the sun modified by reflectance characteristics of surface elements of the Earth is also a function of the angle of the sun relative to that portion of the surface under consideration. In Figure 2.5.2-1 an earth albedo at 45° off the sun line (three o'clock orbit) is approximately 0.25 (assuming 500 KM altitude) and the attenuation factor for E_s is 2.0×10^{-2} (see Section 2.3.2.2). Therefore, apparent irradiance at the photocathode due to E_s is:

$$p(E_s) = 0.0312\ W/cm^2 \times 0.25 \times 2.0 \times 10^{-2} = 1.56 \times 10^{-4}\ W/cm^2$$

2.5.3 The Moon (M)

2.5.3.1 Four different brightness calculations were derived and each was within the same order of magnitude.

2.5.3.1.1 Meisenholter made a theoretical model calculation in his report "Planet Illumination", (Ref. 1) for all the planets and moon of the solar system. According to his tabulated data, the illuminance of the full moon at the distance of the Earth was given as:

$1.6 \times 10^{-8}\ W/cm^2$

2.5.3.1.2 The visual brightness values of the moon as measured on earth are 0.02 to 0.03 lumens/ft.^{2} (Ref. 2, 3). These values are after the atmospheric attenuation; therefore, a correction is required. Assuming that the spectral distribution of moon light is the same as the sun's (see discussion below) a correction factor between air mass 0 and air mass 1 of the solar spectrum needs to be applied to the case of the moon. In the visible region of the spectrum, approximately 20 percent of the air mass zero spectrum is attenuated on Earth (air mass one).

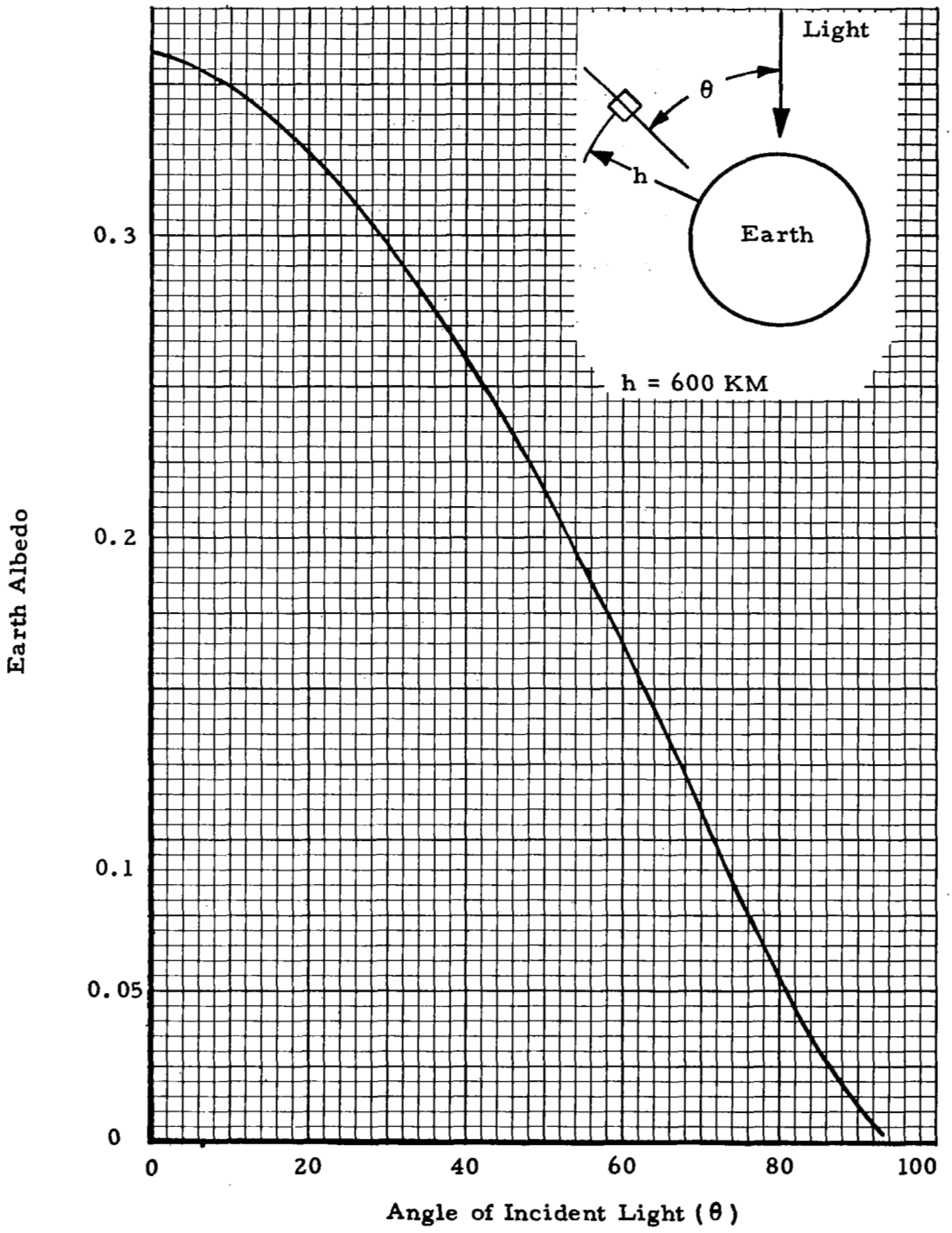

GURE 2.5.2-1 EARTH ALBEDO VERSUS ANGLE OF INCIDENT LIGHT

Using 0.025 lumens/ft.^{2} as the illuminance of a full moon on Earth and outside the Earth's atmosphere one obtains:

$$0.025 \times 5/4 = 0.0313 \text{ lumens/ft.}^2$$

The conversion factor of lumens to watts is 685 lumens per watt for the visible range of the spectrum (1 ft.^{2} = 930 cm^2) therefore:

$$0.0313 \text{ lumens/ft.}^2 = 0.0313 \times 1/685 \times 1/930$$
$$= 4.93 \times 10^{-8} \text{ W/cm}^2$$

2.5.3.1.3. Fessenkov (Ref. 4) states that the color of the moon does not differ greatly from that of the sun. Measurements with different filters show that the difference in color indices is 0.13 to 0.33. The color indices selected are 0.8 for the sun and 1.1 for the moon. Therefore, it will be within the limit of error range for the calculations if the shape of irradiance spectrum of the moon in the visible range is similar to that of the sun. Knowing the difference in the visual magnitude, one computes the brightness of the moon as follows:

Visual Magnitude (m) of the sun = 26.7
Visual Magnitude (m) of the moon = 12.7
$\Delta m = 14 = 5 + 5 + 4$
Brightness factor = (100) x (100) x (40)
$= 4 \times 10^5$

Therefore, in the visible range, the sun is about 4×10^5 times brighter than the full moon.

The total irradiance of the sun in the visible range is given by the integral:

$$\int_0^\infty H(\lambda)\, V(\lambda)\, d(\lambda) = 19.2m \text{ W/cm}^2$$

where:

$H(\lambda)$ = the solar irradiance curve, (Figure 2.5.1-1), and

$V(\lambda)$ = the normalized human eye response.

Therefore, brightness of a full moon is:

$$\frac{19.2\text{m W/cm}^2}{4 \times 10^5} = 4.8 \times 10^{-5} \text{ mW/cm}^2$$

or: $= 4.8 \times 10^{-8}$ W/cm^2

2.5.3.1.4. Since the human eye response is not the same as a photoelectric device, the following calculations are based on photoelectric measurements.

Photoelectric Magnitude (m) of the sun = 26.16 (Ref. 5)

Photoelectric Magnitude (m) of the moon = 11.74 (Ref. 4)

$\Delta m = 14.42 \approx 14.5 = 5 + 5 + 4 + 0.5$

Brightness factor $= 100 \times 100 \times 40 \times 1.585$

$= 6.34 \times 10^5$

The total radiance of the sun in the range of a type 541N phototube is given by:

$$H(\lambda)\, P(\lambda)\, d(\lambda) = 31.2\text{mW/cm}^2$$

Therefore, an apparent brightness of the full moon as seen by the phototube is:

$$\frac{31.2\text{mW/cm}^2}{6.34 \times 10^5} = 4.92 \times 10^{-5} \text{ mW/cm}^2$$

or: $= 4.92 \times 10^{-8}$ W/cm^2

The above calculations show very close agreement with the theoretically calculated values which are of the same order of magnitude.

Therefore, the value used for brightness of

the full moon was:

5×10^{-8} W/cm^2

As shown in Figure 2.5.3.1.4-1.

2.5.3.2 As the moon travels from full moon position (0° phase moon) to the 5/8 moon position (-45° phase moon) the phototube will see the moon light starting at the -20° phase which also corresponds to an angle of 25° off the optical axis of the phototube and is the angle of the sun light shield (see Figures 2.5.3.1.4-1 and 2.5.3.2-1). Calculations of the apparent moon irradiance (M) at different moon phases on the photocathode are as follows:

2.5.3.2.1 When the moon is 45° off the optical axis of the phototube and is at full moon position (0° phase):

$M = 5 \times 10^{-8}$ W/cm^2 (see Fig. 2.5.3.1.4-1)

Attenuation = 10^{-5}

$p(M) = 5 \times 10^{-13}$ W/cm^2

2.5.3.2.2 When the moon is 25° off the optical axis (within sunshield) and the moon is at a -20° phase:

$M = 3.36 \times 10^{-8}$ W/cm^2

Attenuation = 2.0×10^{-2}

$p(M) = 6.72 \times 10^{-10}$ W/cm^2

2.5.3.2.3 When the moon is 10° off the optical axis (within the field of view of the phototube) and at a -35° phase:

$M = 2.45 \times 10^{-8}$ W/cm^2

Attenuation just before 10° = 2.0×10^{-2}

$p(M) = 2.45 \times 10^{-8} \times 2.0 \times 10^{-2}$

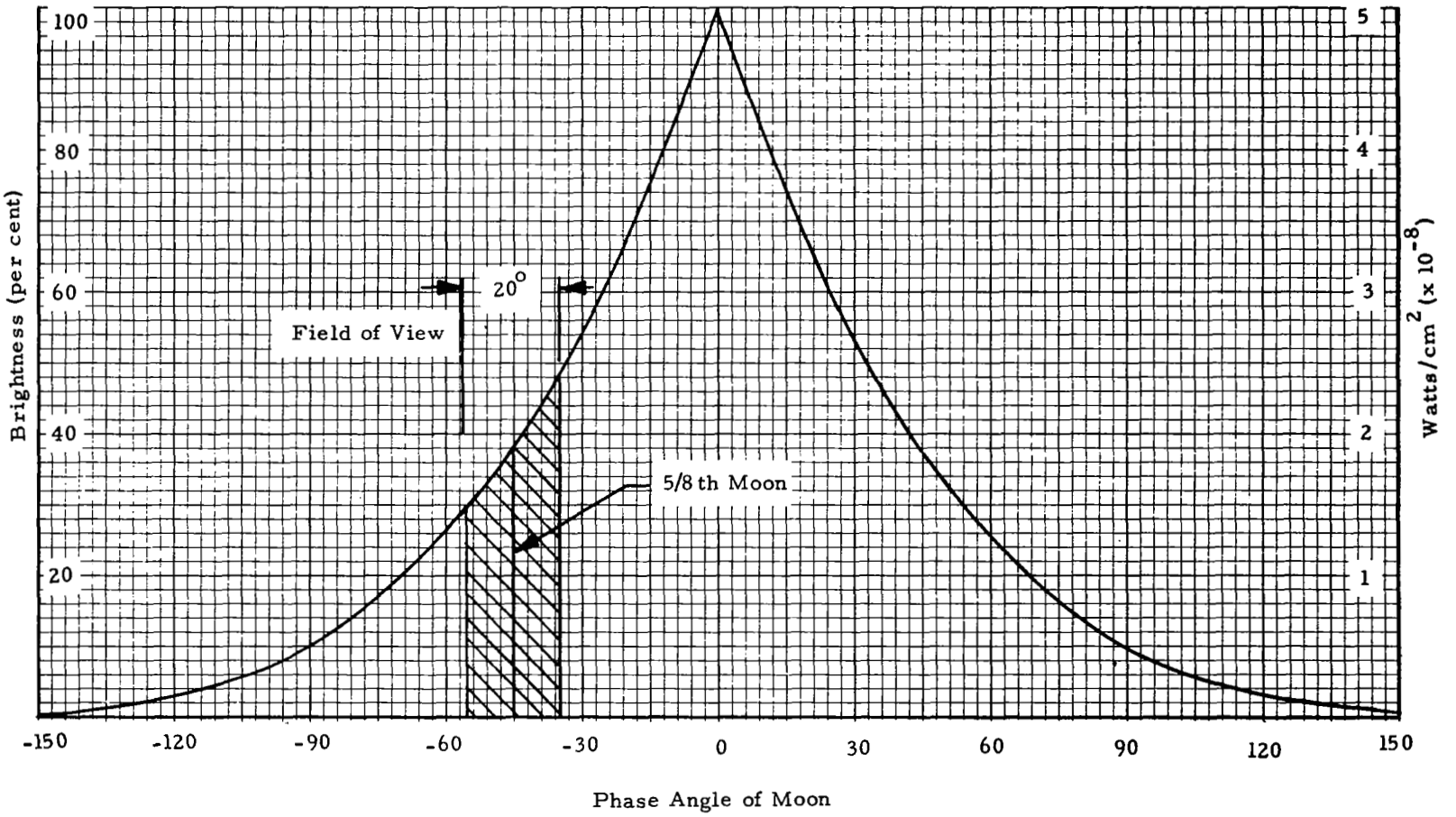

FIGURE 2.5.3.1.4-1 VARIATION OF THE NORMALIZED AND ABSOLUTE BRIGHTNESS OF THE MOON

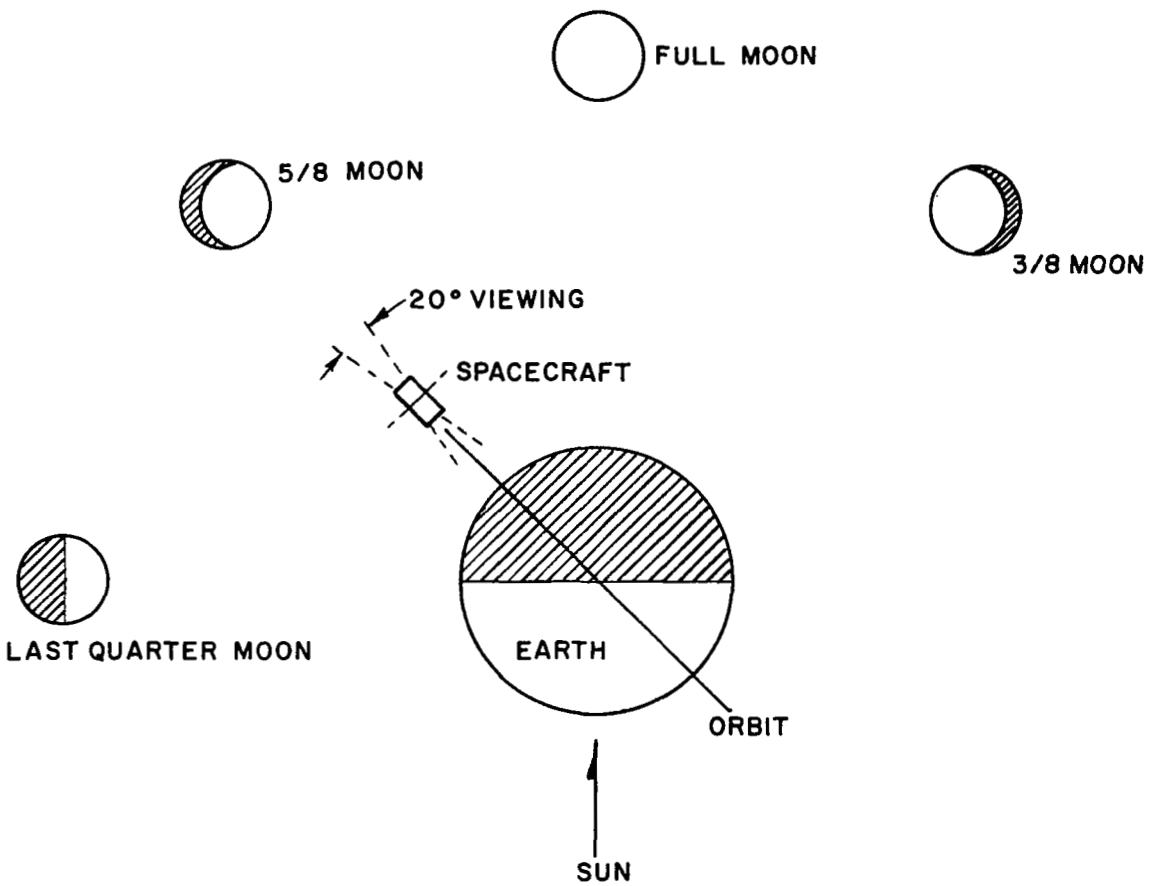

FIGURE 2.5.3.2-1 SPACECRAFT - EARTH - MOON - SUN RELATIONSHIP

$= 4.9 \times 10^{-10} W/cm^2$

Attenuation just after $10^\circ = 0.73$

$p(M) = 2.45 \times 10^{-8} \times 0.73$

$= 1.79 \times 10^{-8} W/cm^2$

2.5.3.2.4 When the moon is 10° off the optical axis and is at a -55° phase:

$M = 1.45 \times 10^{-8} W/cm^2$

Attenuation just before $10^\circ = 0.73$

$p(M) = 1.45 \times 10^{-8} \times 0.73$

$= 1.06 \times 10^{-8} W/cm^2$

Attenuation just after $10^\circ = 2.0 \times 10^{-2}$

$p(M) = 1.45 \times 10^{-8} \times 2.0 \times 10^{-2}$

$= 2.9 \times 10^{-10} W/cm^2$

2.5.3.2.5 When the moon is 25° off the optical axis and is at a -70° phase:

$M = 0.93 \times 10^{-8} W/cm^2$

Attenuation $= 2.0 \times 10^{-2}$

$p(M) = 1.86 \times 10^{-10} W/cm^2$

2.5.3.2.6 When the moon is 45° off the optical axis and is at a -90° phase (last quarter moon):

$M = 0.45 \times 10^{-8} W/cm^2$

Attenuation $= 10^{-5}$

$p(M) = 4.5 \times 10^{-14} W/cm^2$

Figure 2.5.3.2.6-1 shows apparent moon irradiance at the photocathode for different phases as calculated above.

2.5.4 Moon Light Reflected by the Earth

Meisenholter (Ref. 1) made theoretical calculations of various planet illuminations for different angles of incident light relative to detector position and altitude. Figure 2.5.2-1 was derived from the above reference and shows albedo values of the Earth at an altitude of 600 KM for different angles of incident light. Since the projected spacecraft is in a three o'clock orbit and the phase of the moon changes as shown in Figure 2.5.3.2-1, a combination of curves in Figures 2.5.3.2.6-1 and 2.5.3.2-1 produces the earth reflected moon light for different phases of the moon as shown in figure 2.5.4-1.

Calculations of irradiance at the photocathode due to E_m when the moon is in the 0^o phase (full moon):

$$E_m = 1.19 \times 10^{-8} W/cm^2$$

$$\text{Attenuation} = 4.4 \times 10^{-4}$$

$$p(E_m) = 1.19 \times 10^{-8} \times 4.4 \times 10^{-4}$$

$$= 5.24 \times 10^{-12} W/cm^2$$

Figure 2.5.4-2 shows the irradiance curve at the photocathode due to E_m for different phases of the moon.

2.6 CALCULATIONS OF ANODE CURRENT

2.6.1 Anode Current Calculation

In Section 2.5, all possible irradiances due to various light sources were derived. It is necessary also to calculate the expected anode current (Ia) due to these light sources and to determine when the phototube should be on or off to prevent failure of the phototube. The basic equation to calculate

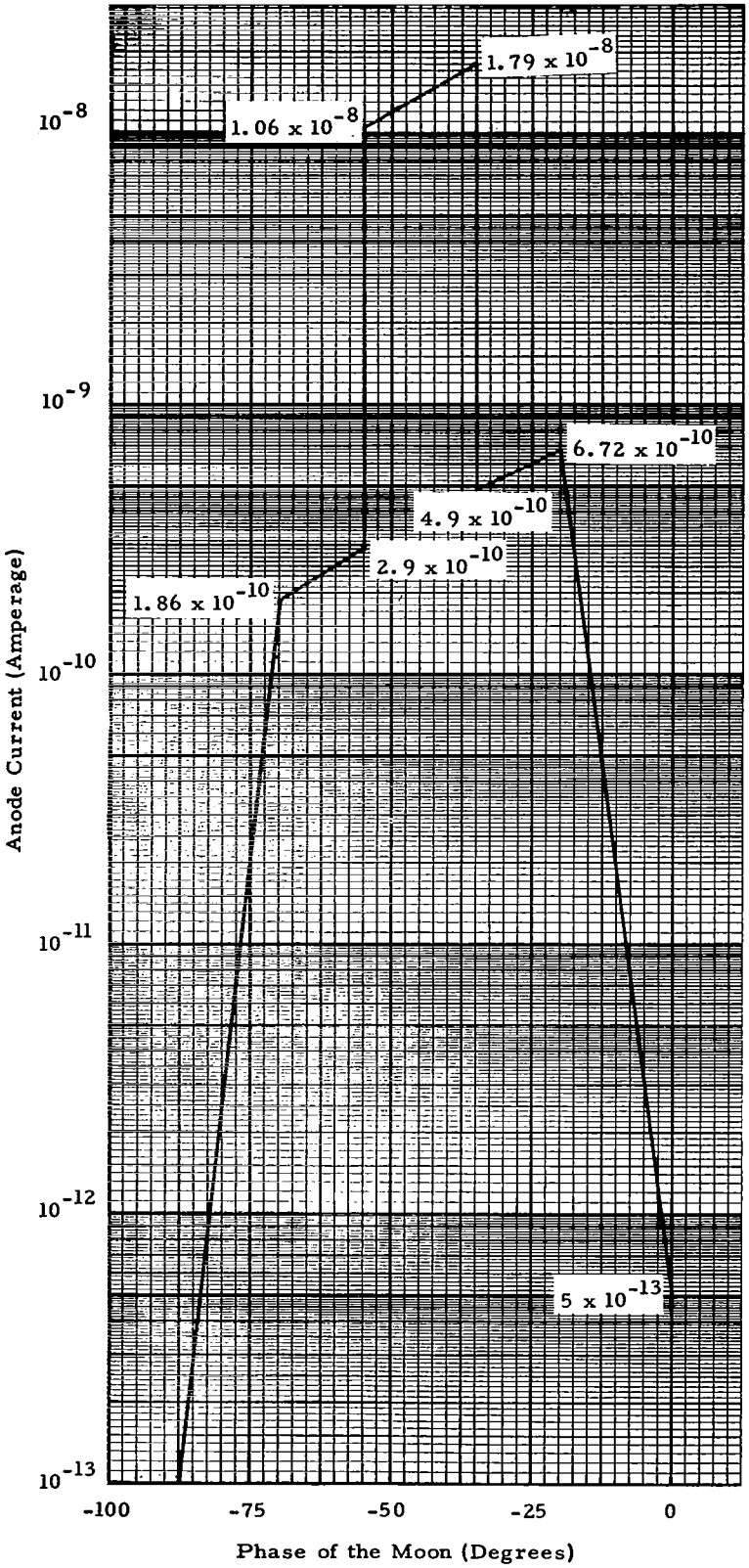

FIGURE 2.5.3.2.6-1 MOON IRRADIANCE AT THE PHOTOCATHODE

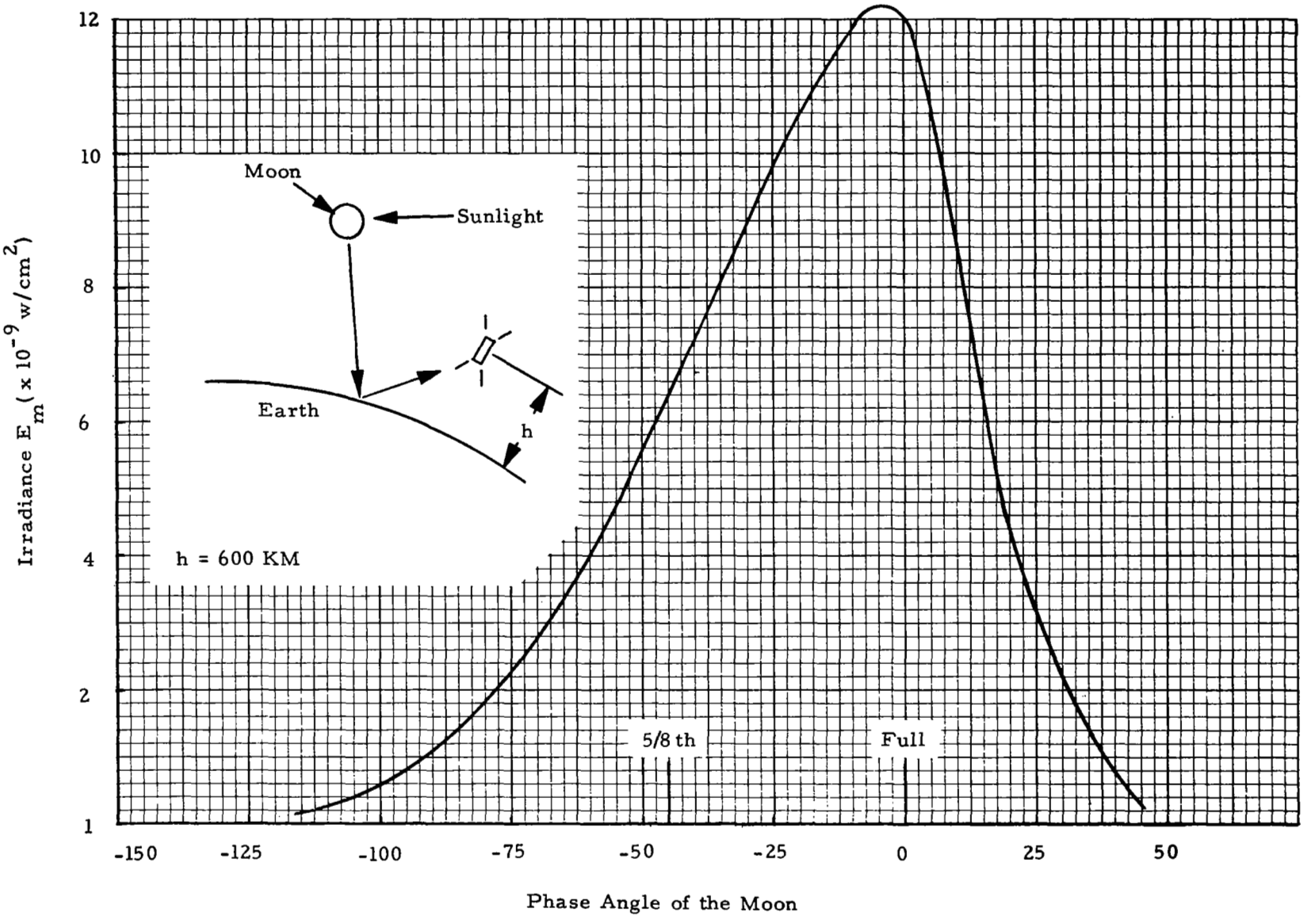

FIGURE 2.5.4-1 EARTH REFLECTED MOON LIGHT AT THE SPACECRAFT POSITION

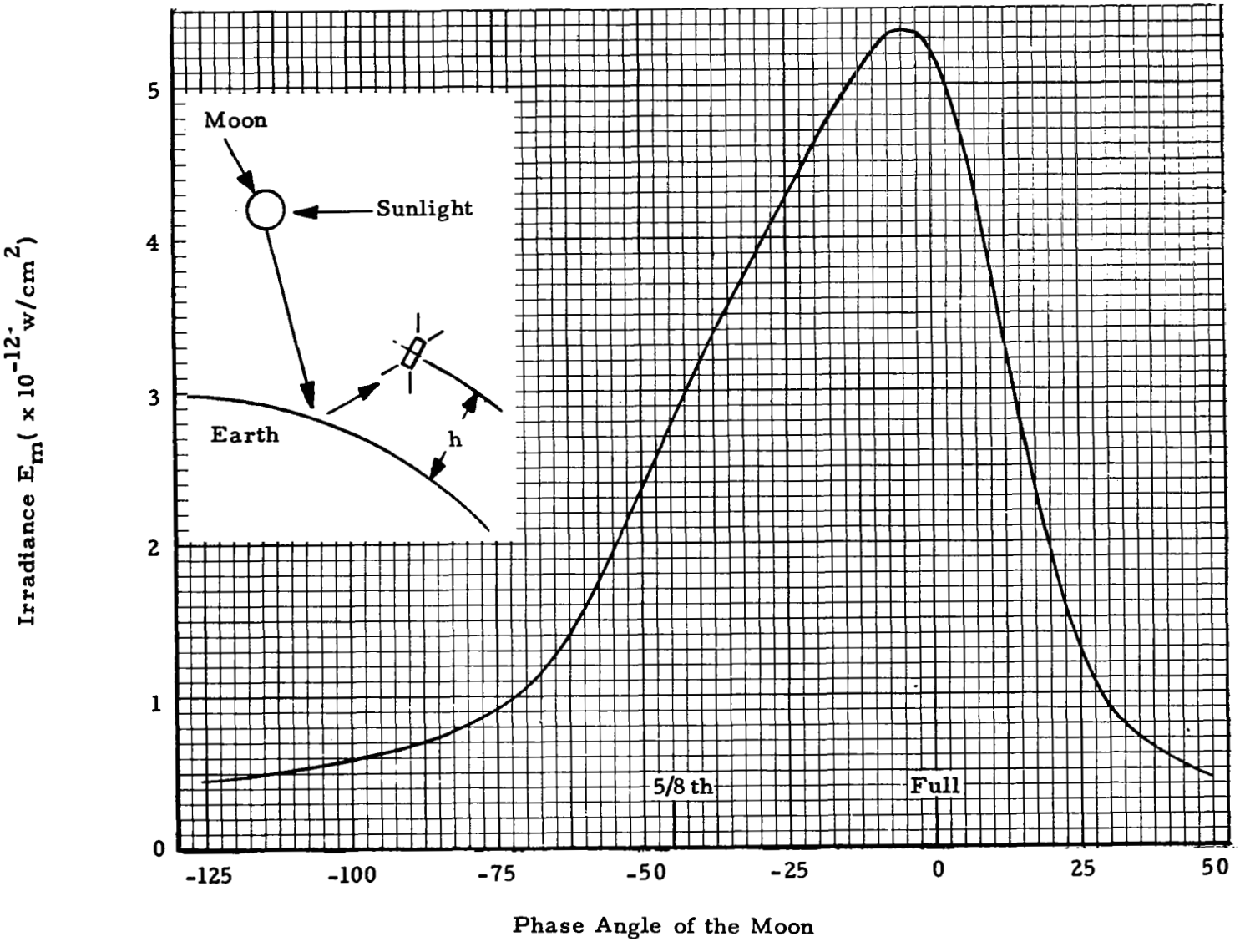

FIGURE 2.5.4-2 EARTH REFLECTED MOON IRRADIANCE AT THE PHOTOCATHODE

anode current is given by:

$$Ia = p \times \sigma_k \times G \times A$$

$$= p\ (W/cm^2) \times 1.6 \times 10^5 \text{ amperes}$$

as derived in Appendix 9.2.

2.6.1.1 Anode current due to stray sunlight (S)

$$p\ (S) = 3.12 \times 10^{-7}\ W/cm^2$$

$$Ia\ (S) = 3.12 \times 10^{-7} \times 1.6 \times 10^5 \text{ amperes}$$

$$= 5 \times 10^{-2} \text{ amperes} = 50 \text{ mA.}$$

2.6.1.2 Anode current due to E_s

$$p\ (E_s) = 1.56 \times 10^{-4}$$

$$Ia\ (E_s) = 1156 \times 10^{-4} \times 1.6 \times 10^5 = 25 \text{ amperes!!!}$$

The two calculations above indicate that power to the phototube should definitely be off during daylight portions of the spacecraft orbit.

2.6.1.3 Anode current due to M

The p(M) curve for different moon phases shown in Figure 2.5.3.2.6-1 and the constant multiplication factor of 1.6×10^5 gives the desired anode current curve as shown in the upper curve of Figure 2.6.1.3-1,

In Figure 2.6.1.3-1, $I_a(M)$ shows a rapid increase in anode current at the -10° phase of the moon and a further increase into the mA current range for the 5/8th period. During the 5/8th period the moon is directly above the phototube, but then goes out of view rapidly at the -75° phase. Since the burn-in current of the phototube is 5 μ A, the phototube power should be off between moon phases of 5° to 75°.

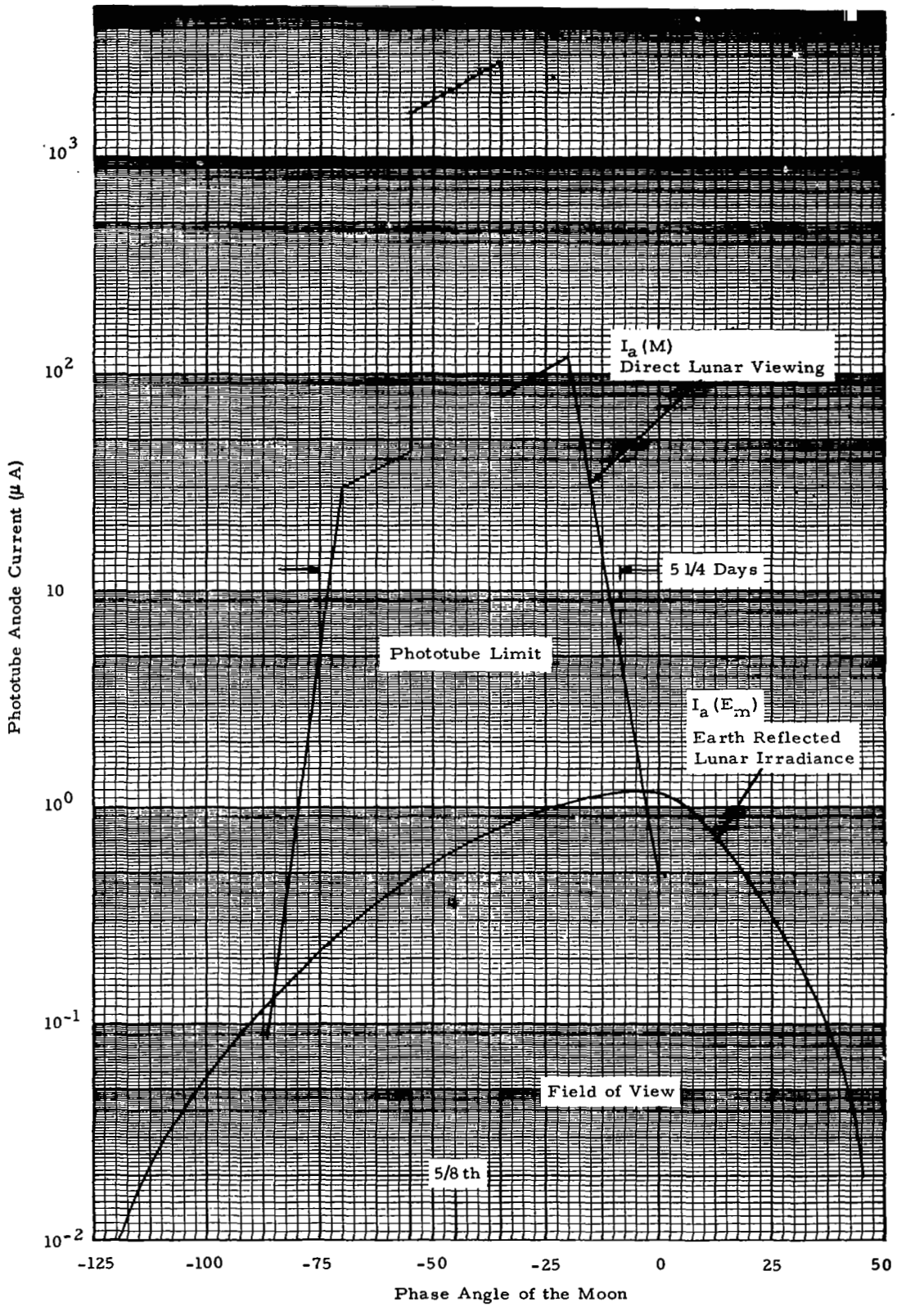

FIGURE 2.6.1.3-1 PHOTOTUBE ANODE CURRENT DUE TO LUNAR ILLUMINATION

2.6.1.4 Anode Current due to Em

Figure 2.5.3.2.6-1 shows the values for p(Em). A constant multiplication factor of 1.6×10^5 results in the Ia(Em) curve as shown in the lower curve of Figure 2.6.1.3-1. Between -10° to -75° phases of the moon period Ia(Em) is almost negligible as compared to the Ia(M).

2.7 SIMULATED LEVELS OF ILLUMINATION

2.7.1. Stray Sunlight (S) and Earth Reflected Sunlight (Es)

Calculations in Sections 2.5.1 and 2.5.2 show that the stray sunlight is negligible as compared to the earth reflected sunlight. Therefore, the irradiance of:

$$S = 3.12 \times 10^{-7} \text{ W/cm}^2$$

and

$$E_s = 1.56 \times 10^{-4} \text{ W/cm}^2$$

was simulated with a single tungsten lamp. The lamp was arranged with a water filter to cut off the IR spectrum, and a neutral density screen filter to reduce the intensity so that the total irradiance at the phototube was 1.57×10^{-4} W/cm^2 The lamp was turned on for 54 minutes and off for 36 minutes to simulate orbit conditions, and three rpm mechanical chopping was used to simulate rotation of the spacecraft.

2.7.2 Moonlight (M) and Earth Reflected Moonlight (E_m)

The irradiances of combined moon and earth reflected illumination at the photocathode are shown in Figure 2.7.2-1. One tungsten lamp was used with different sets of neutral density screen filters to obtain the desired flux levels. The lamp was turned off for 54 minutes and on for 36 minutes, and three rpm mechanical chopping was used to simulate spacecraft rotation. The following simulated flux levels were used:

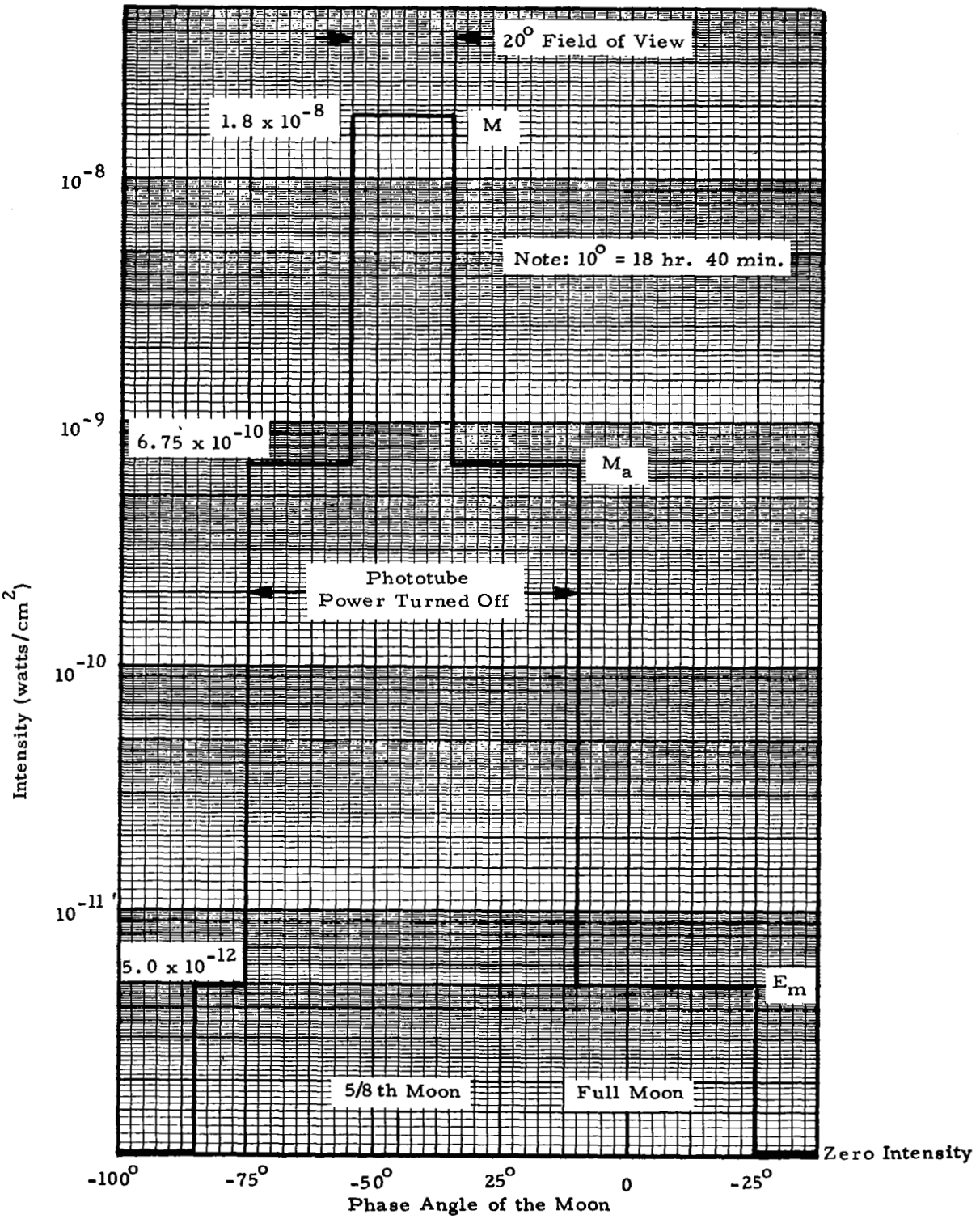

FIGURE 2.7.2-1 SIMULATED FLUX LEVELS FOR MOON AND EARTH REFLECTED MOON IRRADIANCE

$$E_m = 5.0 \times 10^{-12} \text{ W/cm}^2$$

$$M_a = 6.75 \times 10^{-10} \text{ W/cm}^2$$

$$M = 1.8 \times 10^{-8} \text{ W/cm}^2$$

2.8 SIMULATED FLUX LEVELS FOR CHARGED PARTICLES

Irradiation of the phototubes with protons and electrons was accomplished with a low energy Van de Graaff accelerator. The program of exposure was arranged so that the phototubes were irradiated with protons (H^+) for a one week period and then with electrons (e^-) for a one week period. During the first two weeks of exposure, the proton and electron particles were accelerated at an energy level of 20 KeV. During the remainder of the test program, an energy level of 35 KeV was utilized.

The rate of irradiating fluxes and total flux levels were measured with a Faraday cup located within the test chamber and in the plane of the phototubes. Measurements of irradiating fluxes were made at least daily. The flux levels were:

Protons: 4×10^7 particles/cm^2 - day

Electrons: 10^{10} particles/cm^2 - day

The flux levels and rates for high energy irradiation were selected from data derived at NASA/GSFC on March, 1967. The data were obtained from spacecraft flights at 400 KM altitude and a 90^o polar orbit. In summary, the following data were derived:

Electrons		Protons	
Flux	Energy (MeV)	Flux	Energy (MeV)
3.35×10^9 e/cm^2- day	> 0	$\approx 10^7$ p/cm^2- day	> 0
5.19×10^8	> .5	6.43×10^6	> 3
1.77×10^8	> 1	4.82×10^6	> 5
3.11×10^7	> 2	1.04×10^6	> 15
7.36×10^6	> 3	8.88×10^5	> 30
2.11×10^6	> 4	7.29×10^5	> 50
6.66×10^5	> 5	3.47×10^5	> 100
2.18×10^5	> 6		
7.43×10^4	> 7		

Since the desired orbit conditions for the subject study are established at 500 KM and 95^o polar orbit, an increase of 10-20 percent in the values above are reasonable. Therefore, integrated fluxes at rates of 10^{10} electrons/cm^2-day and 4×10^7 protons/cm^2-day are selected for use in testing the phototube.

SECTION 3.0

EXPERIMENTAL APPARATUS

Exposure of the multiplier phototubes to spatial environments combining solar, planet, and charged particle radiations was conducted in a vacuum enclosure arranged as illustrated in Figure 3.0-1. Four identical phototubes were arranged so that the following schedule of exposure was accomplished:

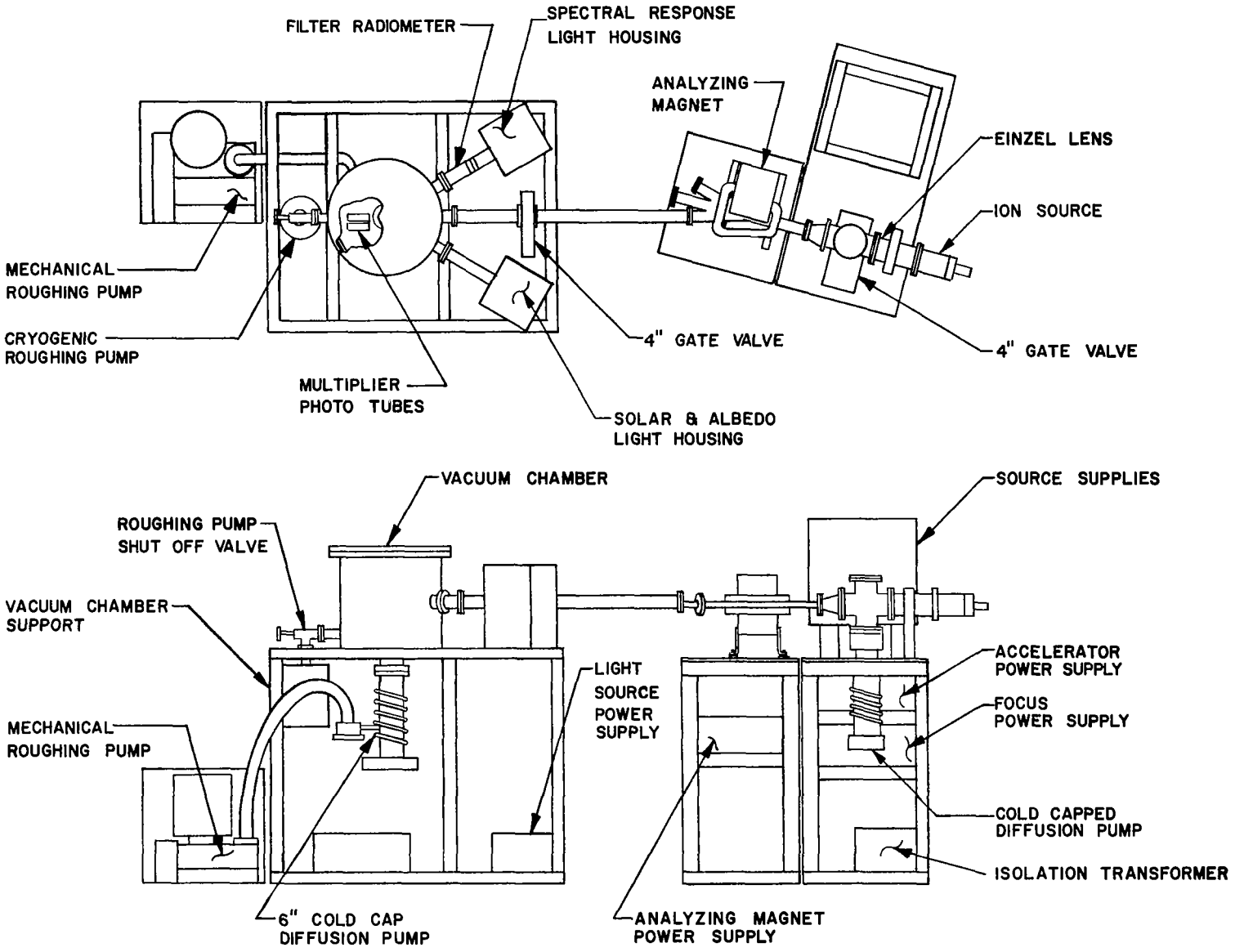

FIGURE 3.0-1 GENERAL ARRANGEMENT OF THE EXPERIMENTAL APPARATUS

Phototube 11644: electron and proton irradiation

Phototube 11762: electron, proton, and earth albedo irradiation

Phototube 11647: electron, proton, earth albedo, and lunar illumination irradiation

Phototube 11664: earth albedo irradiation

The entire testing facility was arranged to facilitate the experimental program and provide for in situ measurements of optical and electrical properties on each phototube. A program of irradiation and measurement was conducted for seven months (total exposure time) without disturbing the enclosure environment. A detail description of each major component of the experimental apparatus is presented below and illustrated on the block diagram, Figure 3.0-2.

3.1 VACUUM ENCLOSURE

A stainless steel bell jar eighteen inches high by eighteen inches in diameter was modified (Figure 3.1-1) to provide a vacuum enclosure for the phototubes. The bell jar flange was grooved to accommodate a single viton o-ring for sealing the top closure plate. A number of openings were cut and flanges welded in place to provide optical and vacuum parts. Two optical parts were required to illuminate the phototubes during simulated earth and lunar irradiation and during measurements of spectral response. Each of these optical parts had a quartz window sealed to the port by a viton o-ring. The additional ports which were cut into the bell jar enclosure were arranged with flanges to accommodate the accelerator flight tube and two vacuum pumps. The top closure plate had provisions for mounting the phototube assembly and corresponding electrical feed-throughs required for power and measurements. Additional feed-throughs were provided in the top plate for thermocouples, Faraday cup, and phototube positioner. The top closure plate (Figure 3.1-2) was fabricated from 304 stainless steel plate, one-half inch thick and bolted in place on the bell jar o-ring flange.

All interior surfaces of the vacuum enclosure were covered with 3-M black velvet paint to reduce internal reflections of illumination. This surface treatment was apparently successful because

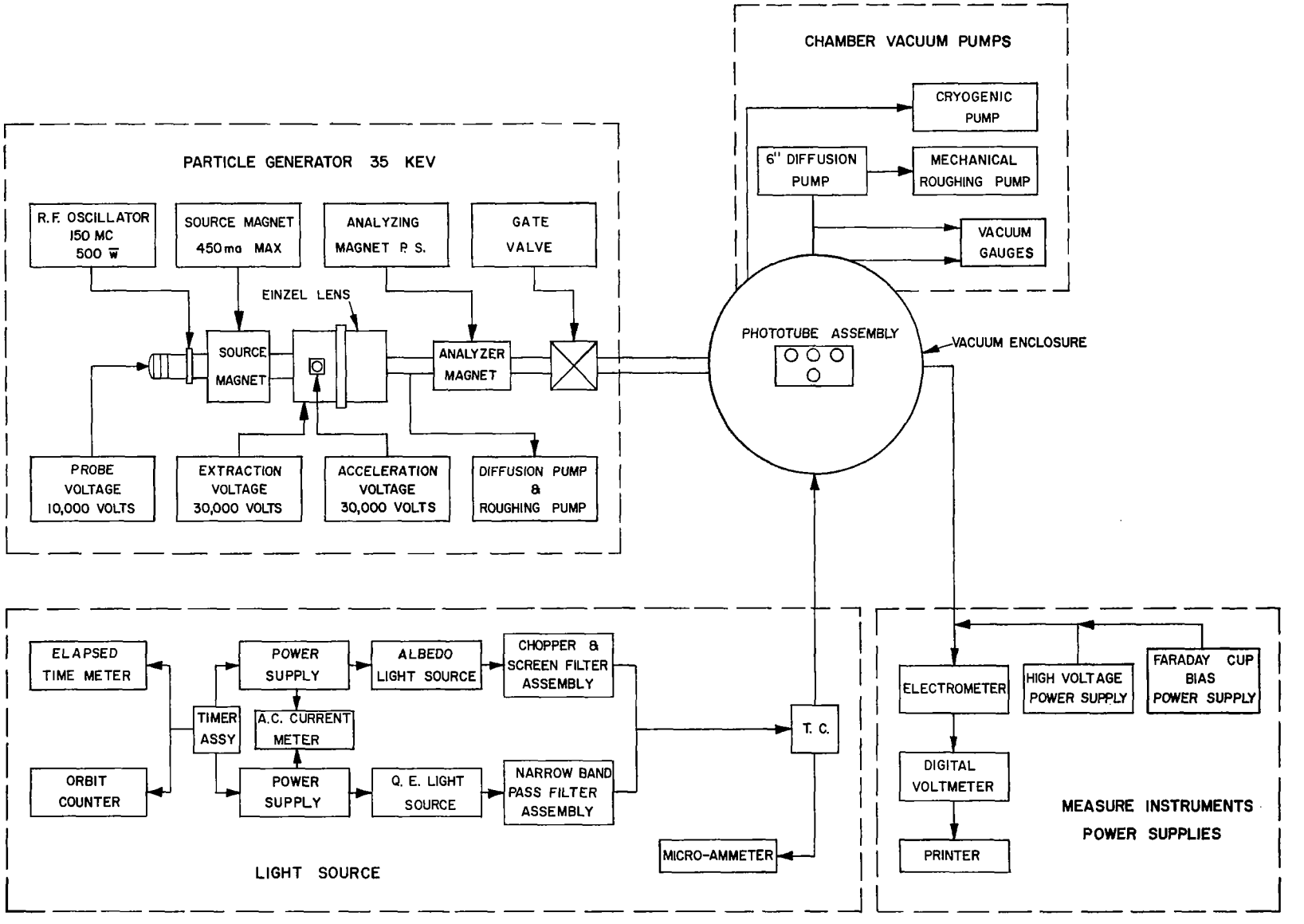

FIGURE 3.0-2 BLOCK DIAGRAM OF EXPERIMENTAL APPARATUS

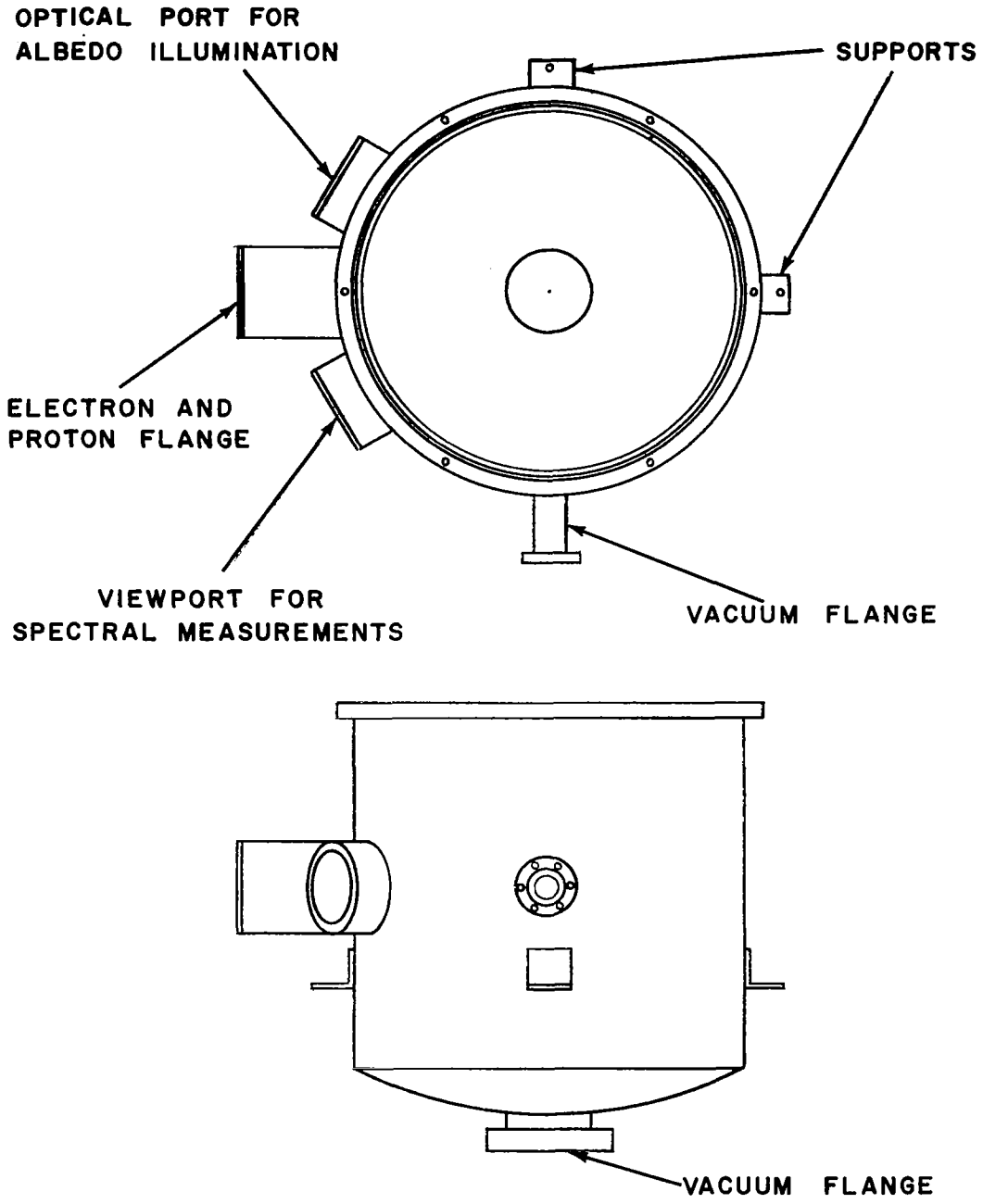

FIGURE 3.1-1 BELL JAR MODIFICATION FOR VACUUM ENCLOSURE

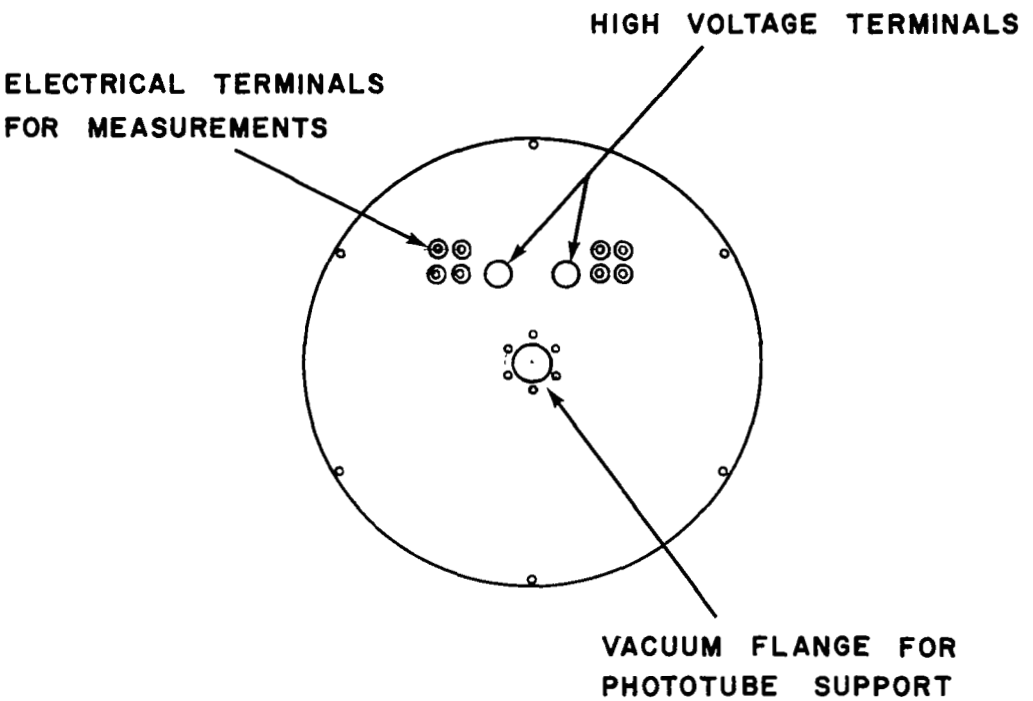

FIGURE 3.1-2 TOP CLOSURE PLATE ASSEMBLY

we could not measure any change in response of one dark phototube when the remaining three were illuminated. In addition to the internal black coating, a baffle type configuration was designed to hold the phototubes and eliminate unwanted radiations and secondary reflections on specific phototubes. The baffle configuration (Figure 3.1-3) was painted black also and was supported on a vacuum feed-through to permit rotary and linear motion of the entire assembly. In addition to the phototubes, the holder assembly supported a Faraday cup to measure electron and proton flux levels. The faces of all four phototubes and the Faraday cup were on the same measuring - irradiating plane.

3.2 VACUUM PUMPS

Vacuum pumps were provided in the experimental apparatus to maintain an operating pressure below 10^{-6} torr in the test enclosure. A Vac-ion pump which was initially designed for use in the facility had to be replaced with an oil diffusion pump when it was discovered that an electrical field effect from the ion pump magnet was strong enough to deflect the stream of electrons from the accelerator. The same difficulty was also encountered when an attempt was made to use a cold cathode vacuum gage which incorporated a ring magnet. Therefore, vacuum pumping and measurement was accomplished void of any magnetic fields. In addition to a six inch diffusion pump used on the test chamber enclosure, a four inch diffusion pump was incorporated into the accelerator module. The total capacity of these two pump systems was more than adequate to achieve high evacuation rates and to maintain desired pressure levels. Each diffusion pump was arranged with a water cooled cold cap to prevent backstreaming of oil into the system. Rough pumping was achieved with mechanical pumps connected to each diffusion pump. Initial evacuation of the test enclosure was achieved with a liquid nitrogen cryopump. Measurements of pressure were made periodically using hot filament ionization gauges located on the accelerator and on the test enclosure. The pressure was consistently below 10^{-6} torr. and at no time during the test program did it rise above 10^{-6} torr.

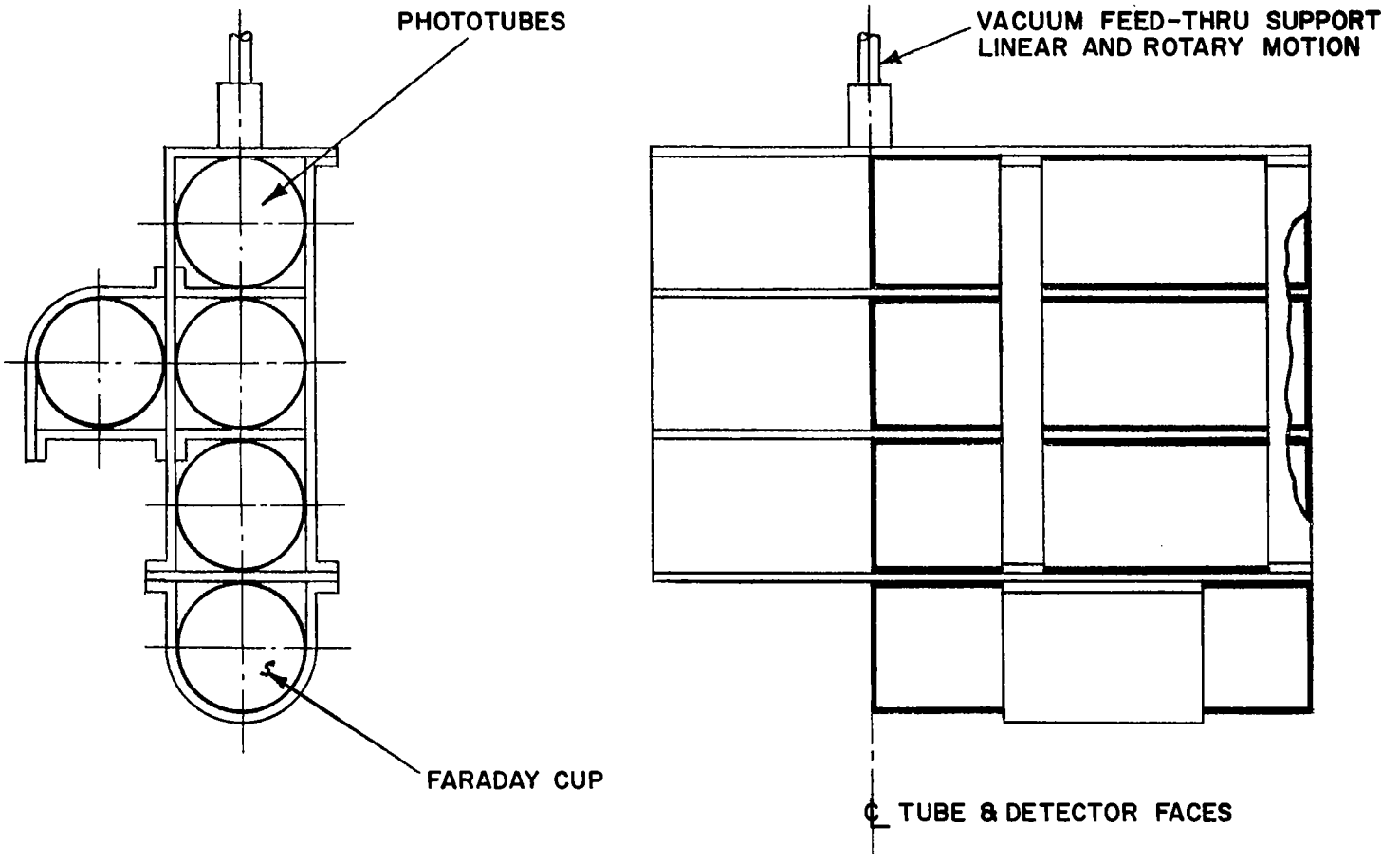

FIGURE 3.1-3 SUPPORT OF PHOTOTUBES WITHIN THE VACUUM ENCLOSURE

3.3 ELECTRON-PROTON ACCELERATOR

Irradiation of the phototubes with electrons and protons up to an energy level of 35 KeV was accomplished with a model SO-173K Ion accelerator manufactured by High Voltage Engineering. The accelerator was used at an energy level of 35 KeV and fluxes of 4×10^{7} protons/cm^2/day and 10^{-10} electrons/cm^2/day for all but the first two weeks of exposure. During the first two weeks the phototubes were irradiated at an energy level of 20 KeV and flux levels noted above. The accelerator has a maximum beam current capability of approximately 1.5×10^{-3} amperes. An Einzel lens was used for beam focusing and an analyzing magnet was utilized to extract protons or electrons from the beam. Hydrogen gas used in the accelerator was passed through a palladium leak and ionized to form a confined plasma. The plasma, which was excited by RF capacitive coupling, was confined and positioned with an axial magnetic field. The accelerator output was optimized by control of gas pressure, magnetic field, oscillator loading, and acceleration voltages. A Faraday cup located in the test chamber was used to measure and monitor the level of exposure to charged particles. The drift tube and all connections were fabricated from non-magnetic materials and covered with mu metal to eliminate stray magnetic fields. The distribution of particle flux was determined by translating the Faraday cup vertically in the face plane of the phototubes. Data of electron and proton distribution illustrated in Figure 3.3-1 indicate that a maximum deviation of 25 percent from minimum to maximum values could be expected during irradiation. This magnitude of difference in exposure values is well within the capability of experimental technology.

3.4 FARADAY CUP

Measurements of charged particle irradiation were conducted with a Faraday cup (Figure 3.4-1) located in the test chamber. Since the Faraday cup was located on the phototube holder and directly below the phototubes it was convenient to check the level of irradiating flux periodically throughout the test program.

3.5 TEST MEASUREMENTS

Measurements of phototube properties and characteristics were obtained periodically throughout the period of irradiation.

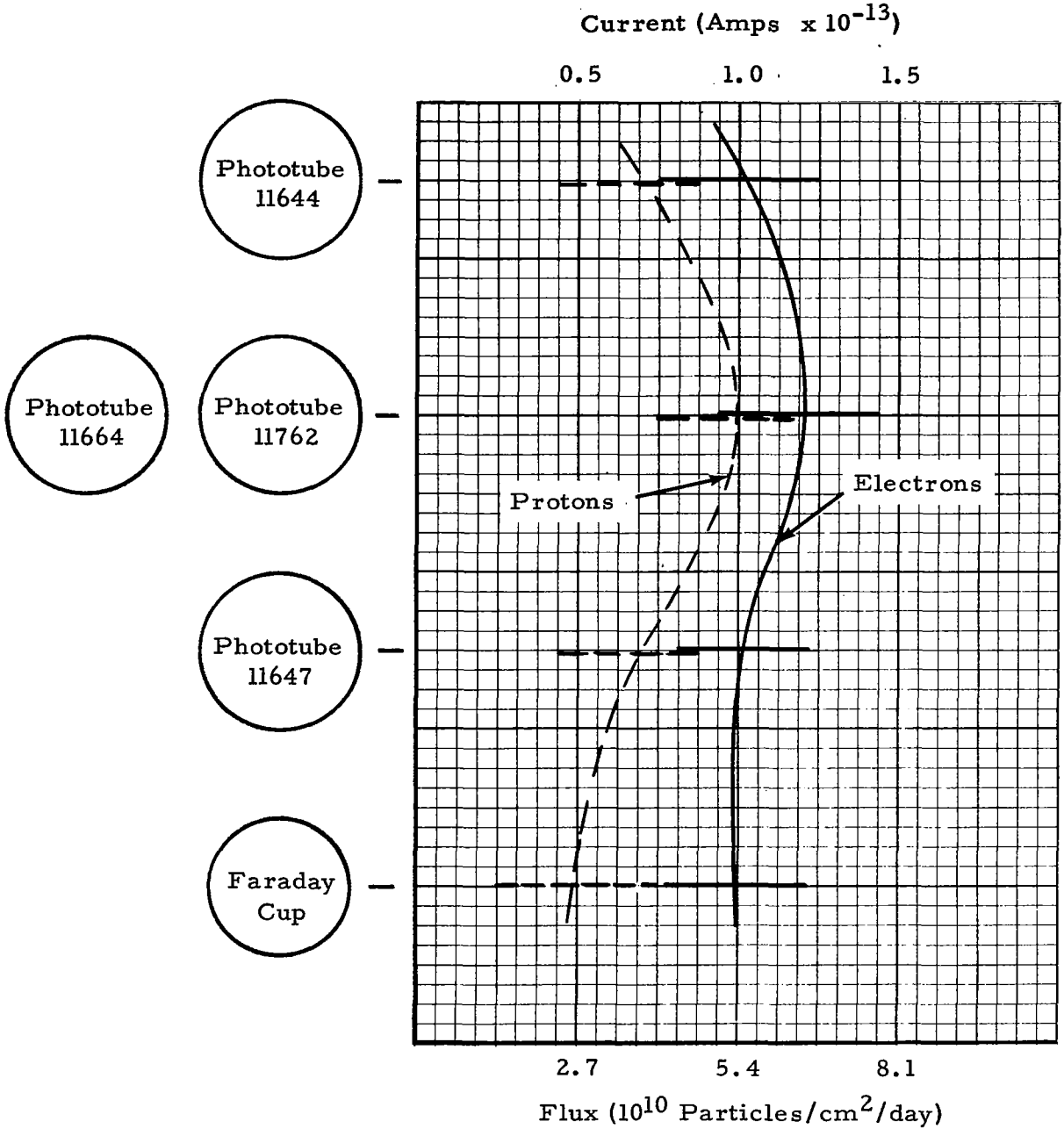

FIGURE 3.3-1 DISTRIBUTION OF ELECTRONS AND PROTONS

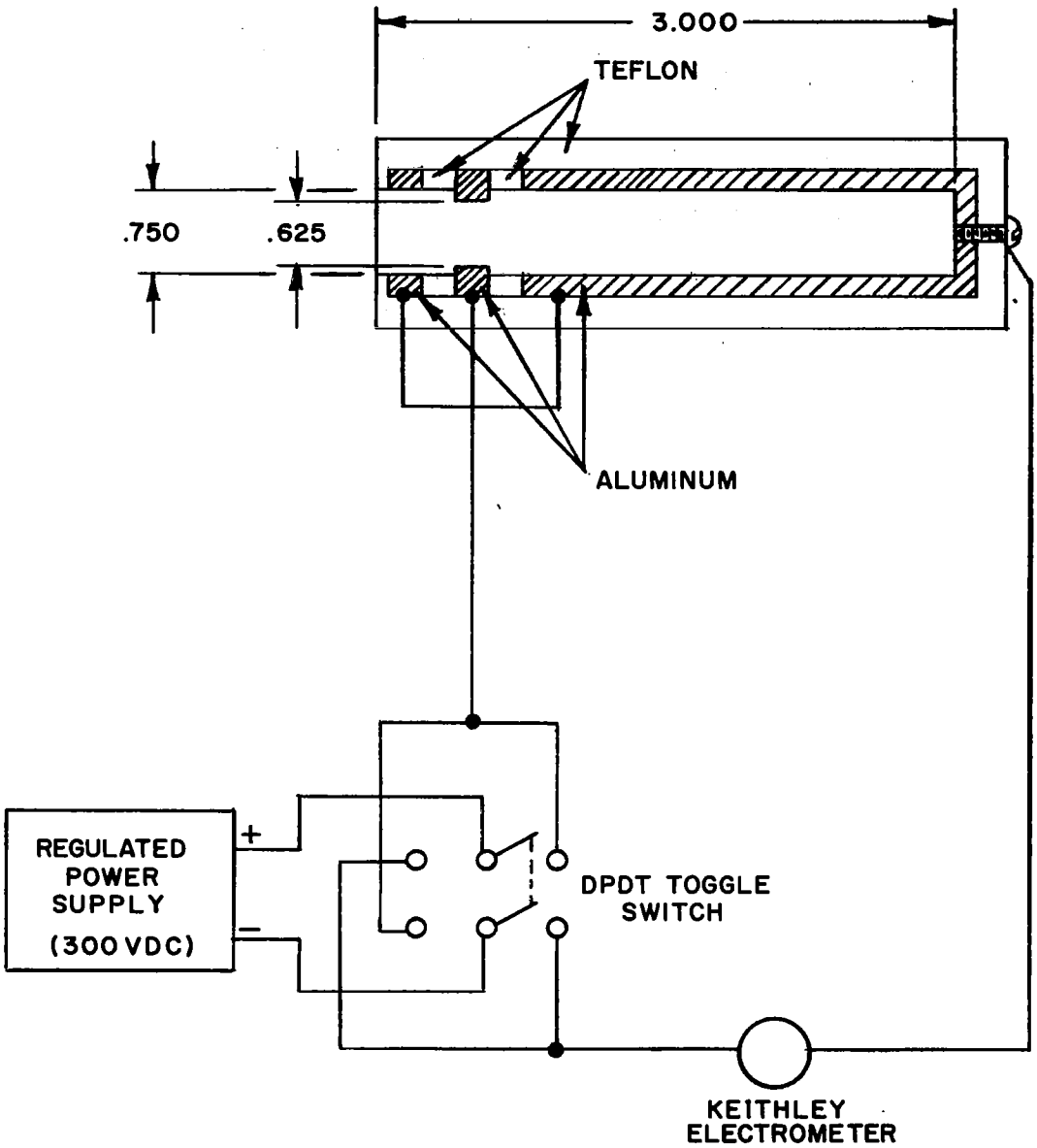

FIGURE 3.4-1 FARADAY CUP ARRANGEMENT

These data were obtained with the phototubes in situ and consisted of the following items:

Spectral response (Quantum Efficiency)
Current-Voltage gain characteristics
Dark current

In addition to phototube properties, measurements were made also on the test system parameters and consisted of temperature, vacuum, orbit number, and total elapse time.

3.5.1 Spectral Response (Quantum Efficiency)

Characteristics of spectral response of the phototubes is a measure of cathode radiant sensitivity in amperes per watt as a function of spectral wavelength. Mathematically, the quantum efficiency is expressed as a function of the anode current where:

$$I_a = p \times G \times \lambda \times Q.E. \times 8.0658 \times 10^{-7} \text{ Amps/cm}^2$$

and:

p = incident power (W/cm^2)

G = Gain (10^6)

λ = wavelength ($\mathring{A}$)

Q.E. = Quantum Efficiency (%)

Therefore, by measuring I_a and p experimentally at a given λ and for a gain of 10^6 the calculation for quantum efficiency becomes:

$$Q.E. = I_a / p \times \lambda \times 8.0658 \times 10^{-1}$$

During measurement of spectral response, incident power (p) was recorded with a calibrated thermopile detector and monochromatic light (λ) was obtained with a set of narrow bandpass filters. During these measurements, the phototubes were connected as a diode (Figure 3.5.1-1) with a forward bias of 150 volts DC. The voltage level of 150 was sufficient to saturate the phototube and establish a stable electrical condition for measurement. The spectral

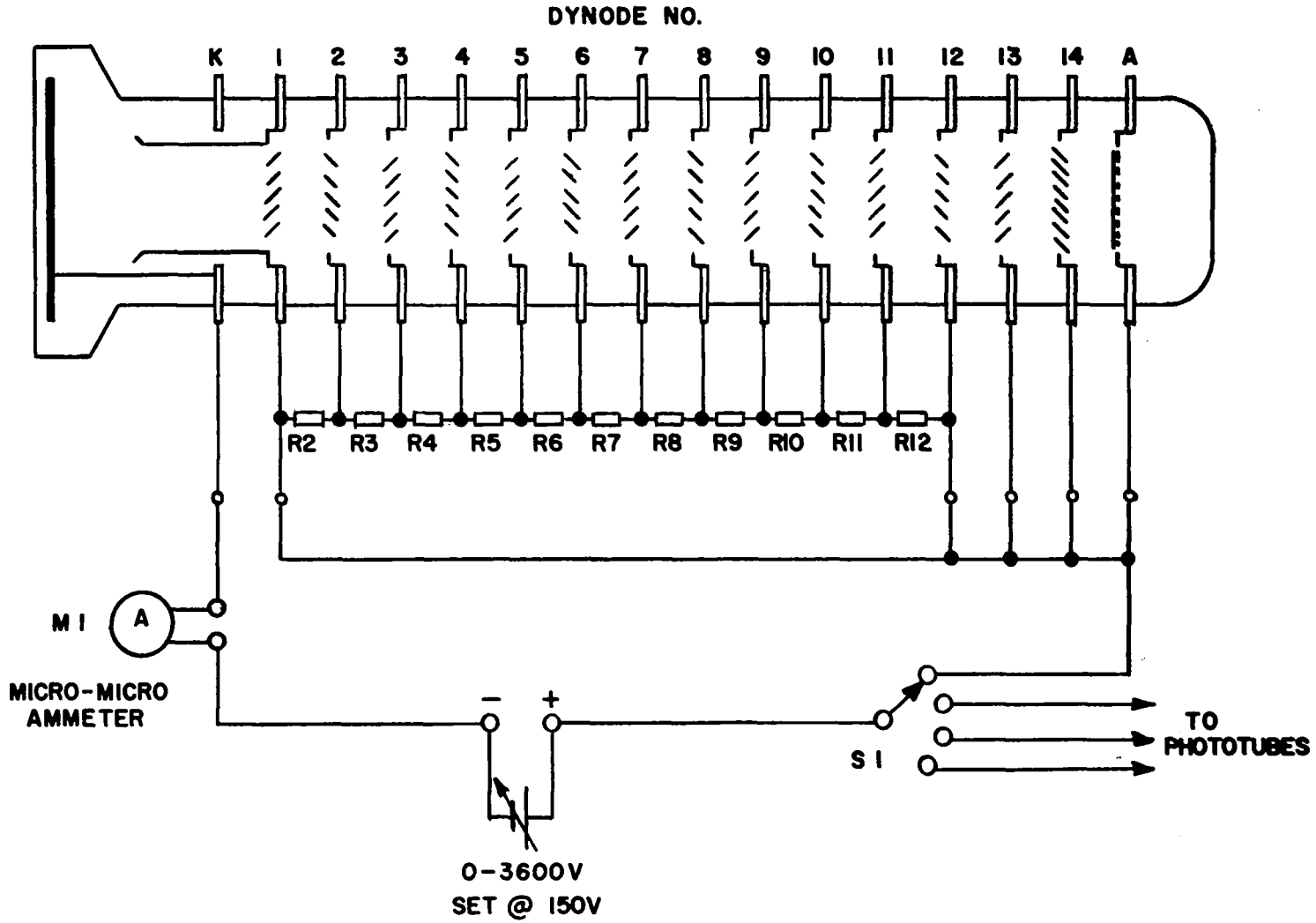

FIGURE 3.5.1-1 PHOTOTUBE ARRANGED FOR MEASUREMENT OF CATHODE CURRENT

response property is then a function of the total cathode current output divided by the total incident monochromatic energy on the cathode.

The optical system for spectral response measurements was arranged as a filter radiometer (Figure 3.5.1.-2). Each narrow bandpass filter (Figure 3.5.1-3) permitted approximately 30 percent transmission at the principle wavelength and 5 to 10 percent at the second order in the infrared region. This excess energy in the infrared spectrum was eliminated by a second order cutoff filter. The thermopile detector was used to set equal monochromatic energy through each filter and was then removed from the beam path during illumination of the phototube. Figure 3.5.1-4 shows the linear response and sensitivity of the thermopile used for equal energy measurements.

During initial check-out measurements of spectral response with the filter radiometer, an error in use of the filters caused some erratic results. Although the filters were purchased and measured to have very narrow wavelength transmission properties, the presence of small second order bandpasses were responsible for overall errors in spectral response properties. When a filter was endowed with the capability to transmit more than one bandpass order, the reference thermopile detected an overall increase in radiant energy. This increased energy level was then adjusted to a constant energy level. As a result of sequential events, the phototube output became lower as the second order transmissions increased. An evaluation of all filters was made over the wavelength range of 0.25 to 15 microns and spectral cut-off filters were introduced to block out the unwanted second orders. The resulting data with cut-off filters were in complete agreement with published curves for the phototubes, Figure 3.5.1.-5.

3.5.2 Current-Voltage Gain

Electrical gain factors for the last two dynode stages and anode of each phototube for various voltages on the cathode were obtained with the phototube arranged electrically as

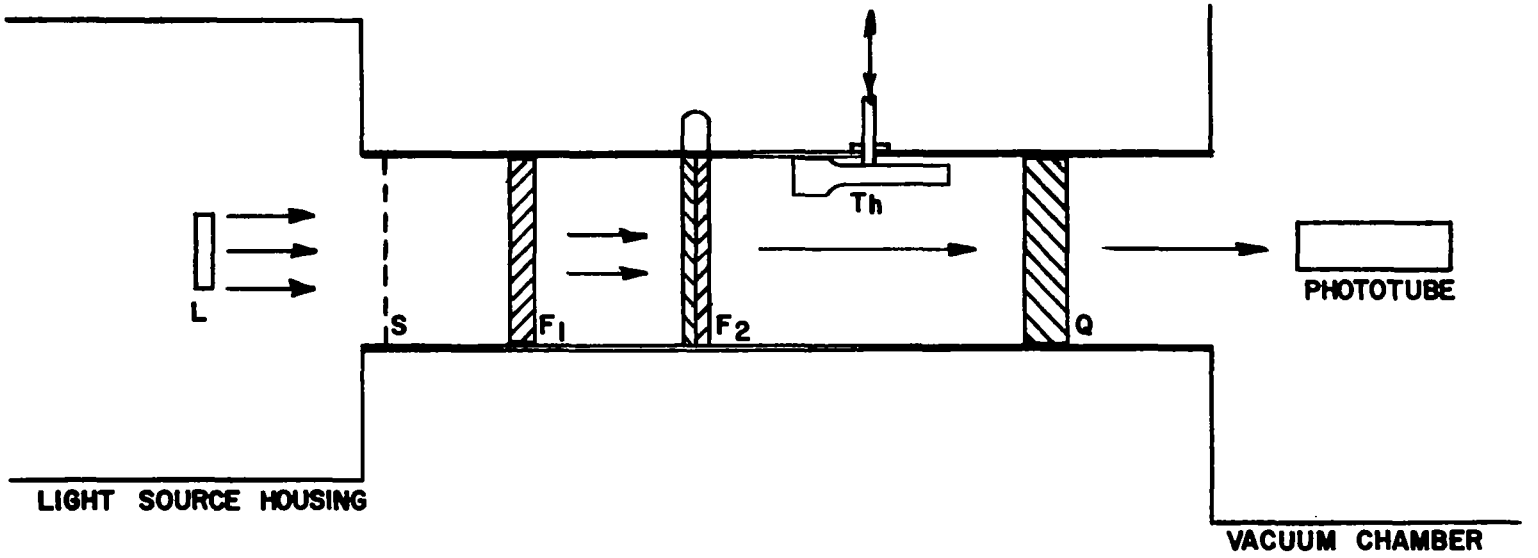

L — LIGHT SOURCE

S — SCREEN FILTER

F_1 — SECOND ORDER CUT OFF FILTER

F_2 — NARROW BANDPASS FILTER; INTERCHANGEABLE FROM .31 MICRONS TO .7 MICRONS

Q — QUARTZ WINDOW

Th — THERMOPILE DETECTOR

FIGURE 3.5.1-2 FILTER RADIOMETER ARRANGEMENT FOR SPECTRAL RESPONSE MEASUREMENTS

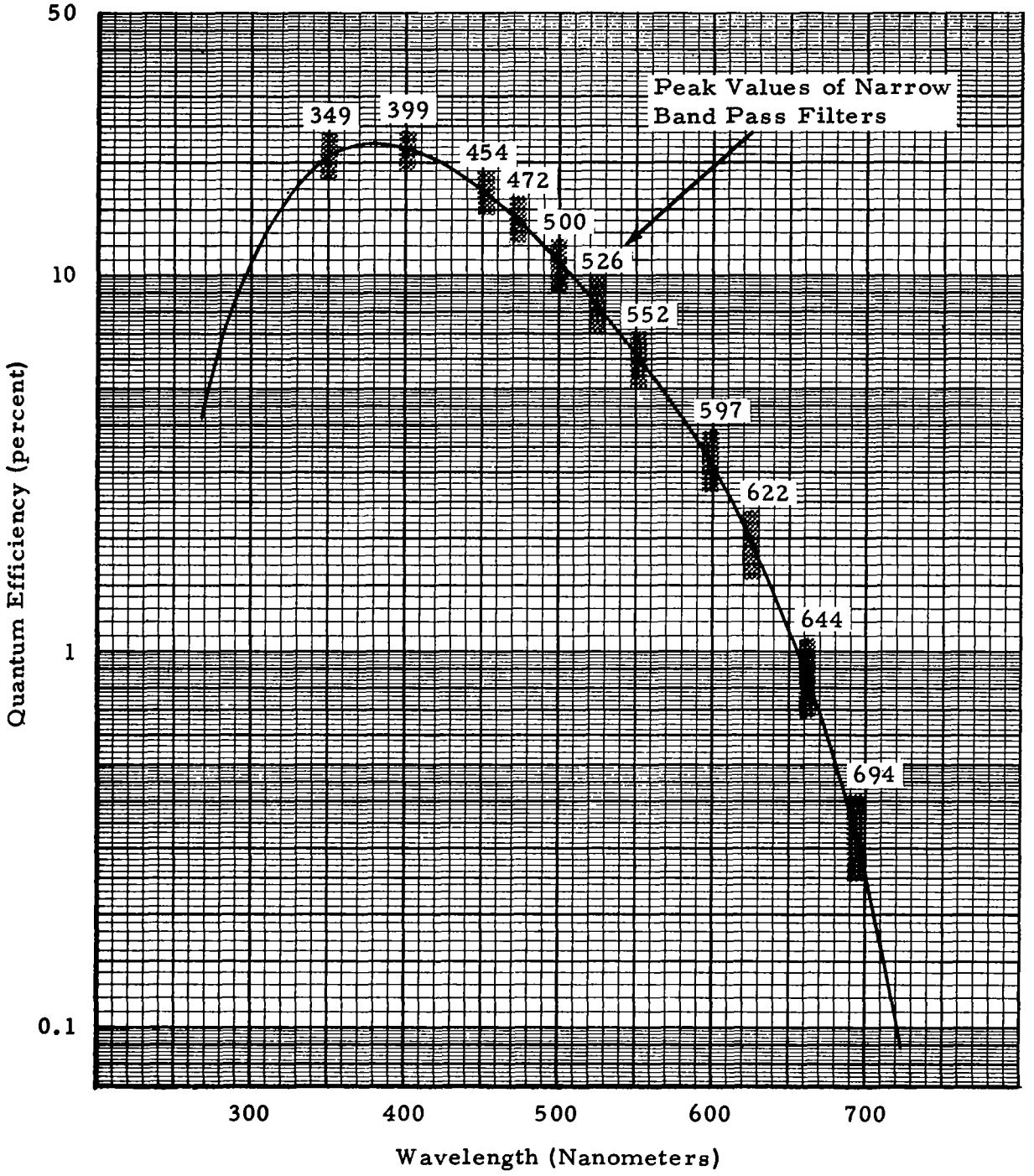

FIGURE 3.5.1-3 LOCATIONS OF MONOCHROMATIC FILTERS FOR SPECTRAL RESPONSE MEASUREMENTS

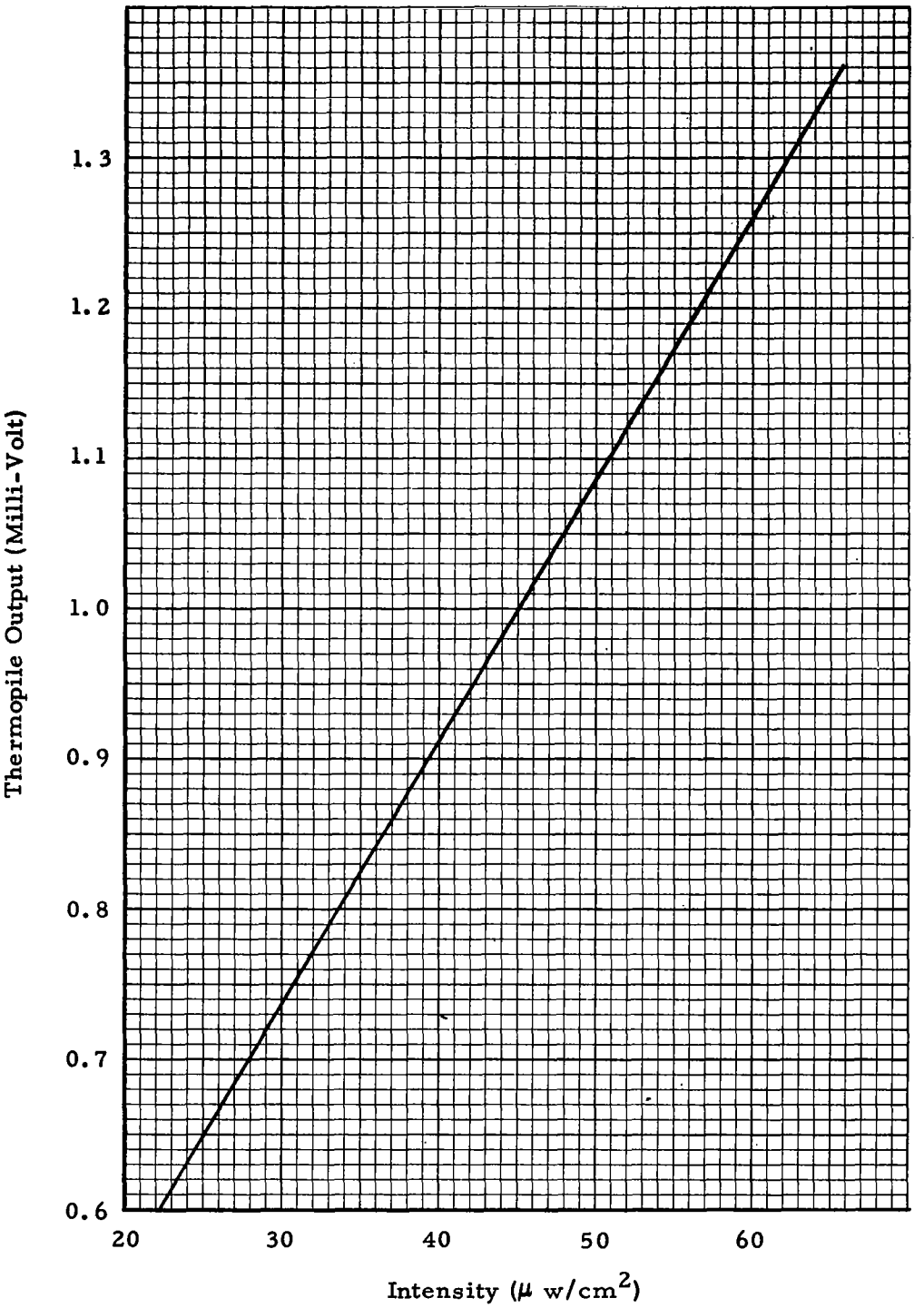

FIGURE 3.5.1-4 SENSITIVITY OF REFERENCE THERMOPILE

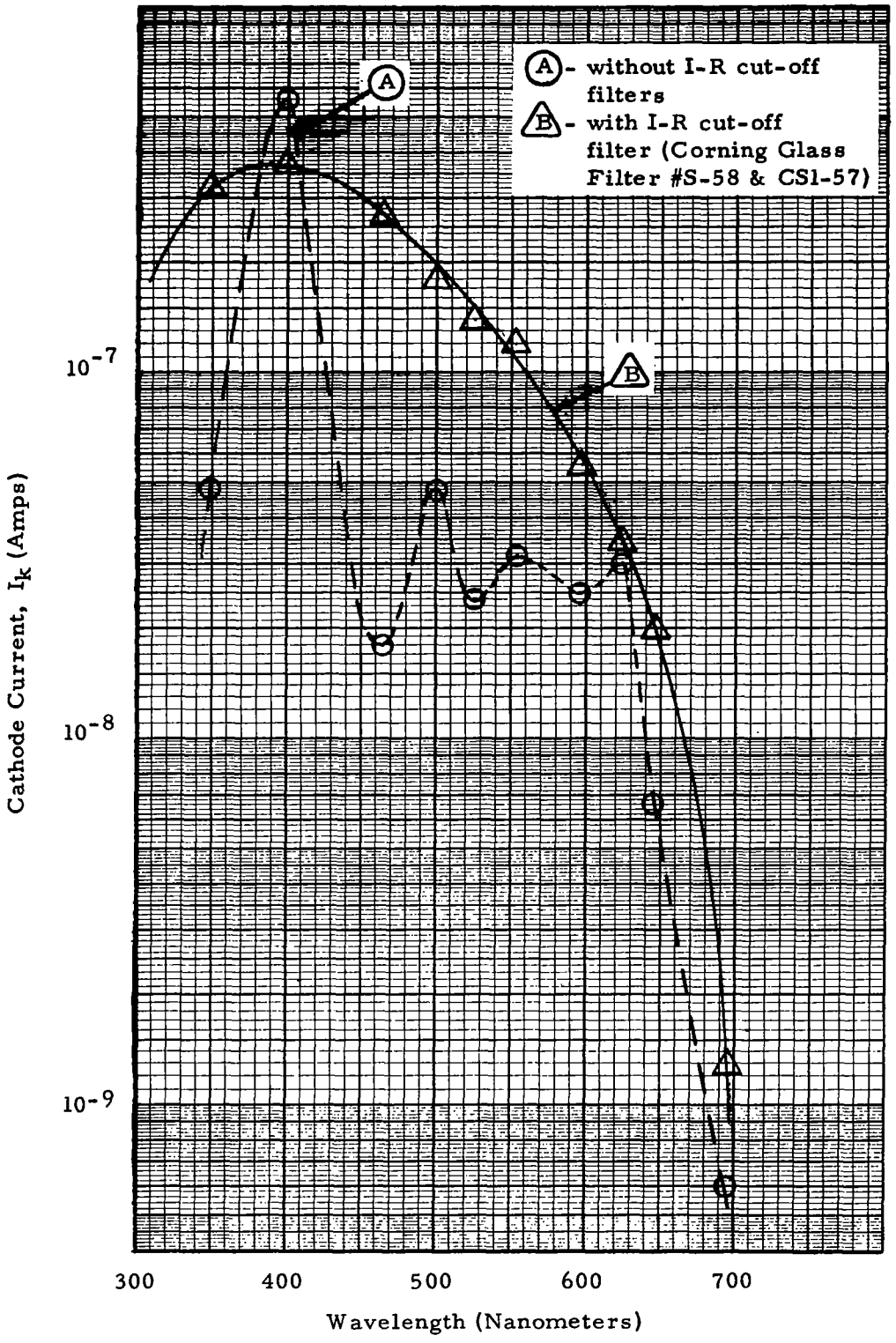

FIGURE 3.5.1-5 SPECTRAL RESPONSE MEASUREMENTS OF A PHOTOTUBE WITH BANDPASS FILTERS

shown in Figure 3.5.2-1. During measurements of current-voltage gain the phototube was illuminated at a constant level throughout the range of testing. The light level was selected to produce a cathode current (I_k) of 2×10^{-12} amperes and to maintain the anode current (I_a) well below the phototube burn-in current of 5×10^{-6} amperes. The precise measurements of very low cathode currents were made with a dc powered Keithley Electrometer and illumination was provided by a tungsten lamp.

3.5.2.1 The following procedure was used:

Once the light level of illumination was established to obtain an I_k of 2×10^{-12} amperes, voltage on the phototube was increased until an I_a of 2×10^{-8} amperes was obtained. This voltage corresponded to a gain in the phototube of 10^4. Similarly, the phototube voltages were established for an I_a of 2×10^{-7} amperes which was proportional to a gain of 10^5 and an I_a of 2×10^{-6} amperes which was proportional to a gain of 10^6. During each period of measurement the current values for the last two dynode stages I_{13} and I_{14} were obtained also.

3.5.2.2 Measurements of gain previous to Orbit No. 400 were accomplished in accordance with the vendor's recommended procedure and was as follows:

The light level was set so that the cathode current (I_K) indicated 10^{-10} amperes with the phototube arranged electrically as a diode. The phototube was then arranged electrically as a multiplier and the anode voltage (V_A) was adjusted so that the anode current (I_A) indicated a level of 10^{-6} amperes which, therefore, resulted in a gain of 10^4. Holding the voltage constant, the light level was reduced so that I_A decreased to 10^{-7} amperes. Holding this new light level constant, the anode voltage (V_A) was then increased to obtain a value of 10^{-6} amperes

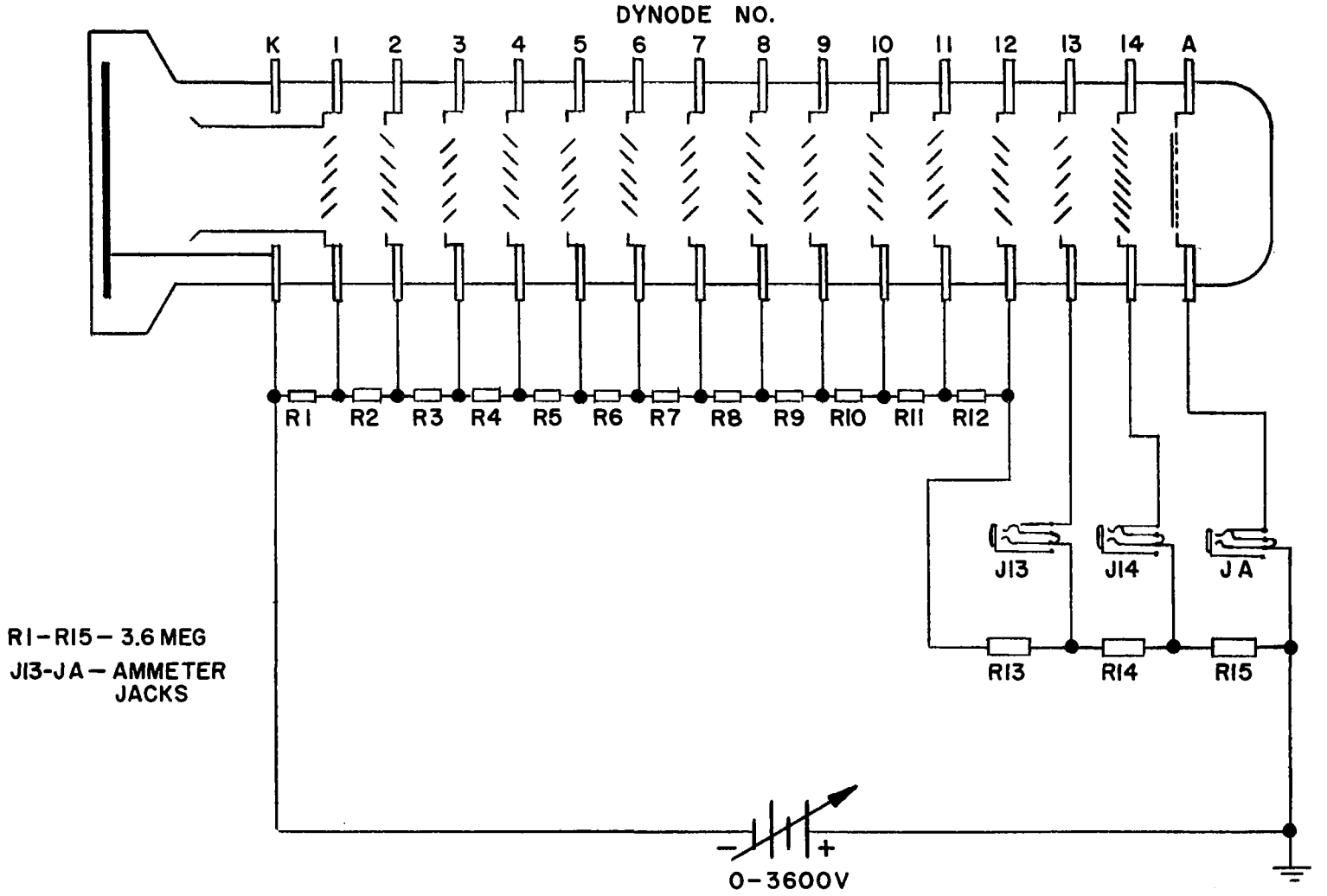

FIGURE 3.5.2-1 PHOTOTUBE ARRANGED FOR MEASUREMENT OF CURRENT VOLTAGE GAIN

for the anode current (I_A) which resulted in a gain of 10^5. This process was then repeated again for the voltage required to obtain a gain of 10^6.

The procedure outlined above which gave satisfactory results was not desirable because it required a couple of hours for the cathode current to settle down after each measurement of gain. In addition, there was constant apprehension and rechecking to be sure that the light levels were set properly. Therefore, the measurements of Orbit 400 and thereafter were obtained as described in Section 3.5.2.1.

3.5.3. Dark Current

The phototubes were darkened (no illumination on the phototubes) for a minimum period of four hours prior to recording dark current data. Typical periods of time for each phototube to recover their initial condition after being illuminated are shown in Figure 3.5.3-1. The dark current was measured at the anode with an applied voltage on the phototube equal approximately to that required for a gain of 10^6. The voltages used were those determined previously during current voltage gain measurements.

3.6 ALBEDO ILLUMINATION

To obtain the correct level of illumination to simulated S, E_s, M, M_a, and E_m during irradiation of the phototubes, a combination of slit aperatures and neutral density filters was utilized. The geometry for illumination was arranged as shown in Figure 3.6-1 and the levels of irradiances on the phototubes were measured for each condition of simulation.

The source of illumination consisted of two tungsten filament quartz envelope lamps operating at their rated power of 1000 watts; and to obtain maximum energy in the ultraviolet spectrum, lamps with 3200°K filaments (Figure 3.6-2) were used. The total energy of illumination viewed by the phototubes was attenuated to simulated levels by placing the following items in the beam path: a) Water filter. A one-half inch thick water filter was constructed of a quartz plate

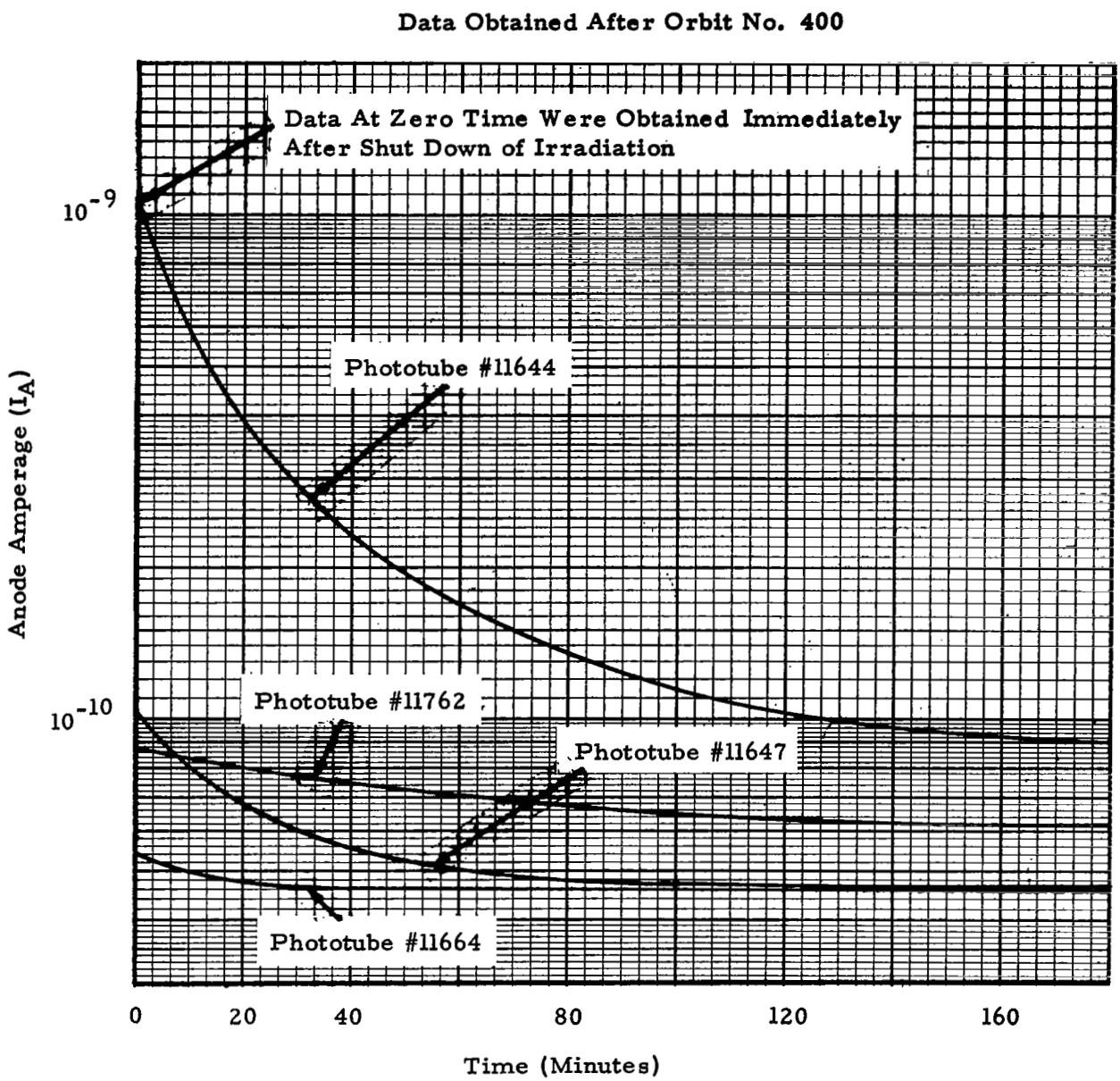

FIGURE 3.5.3-1 RECOVERY OF DARK CURRENT

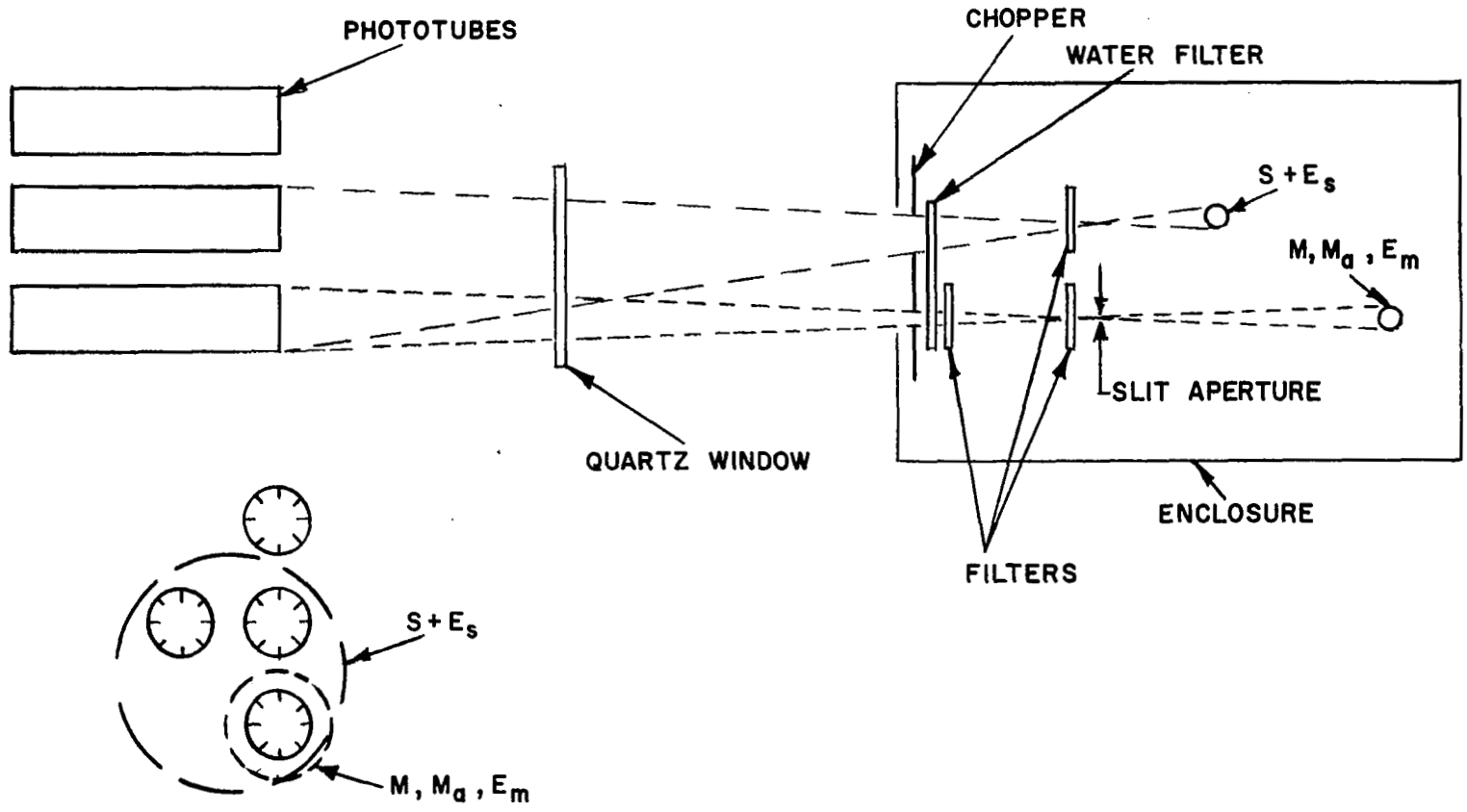

FIGURE 3.6-1 OPTICAL SCHEMATIC OF IRRADIATION BY SIMULATED ILLUMINATING SOURCES

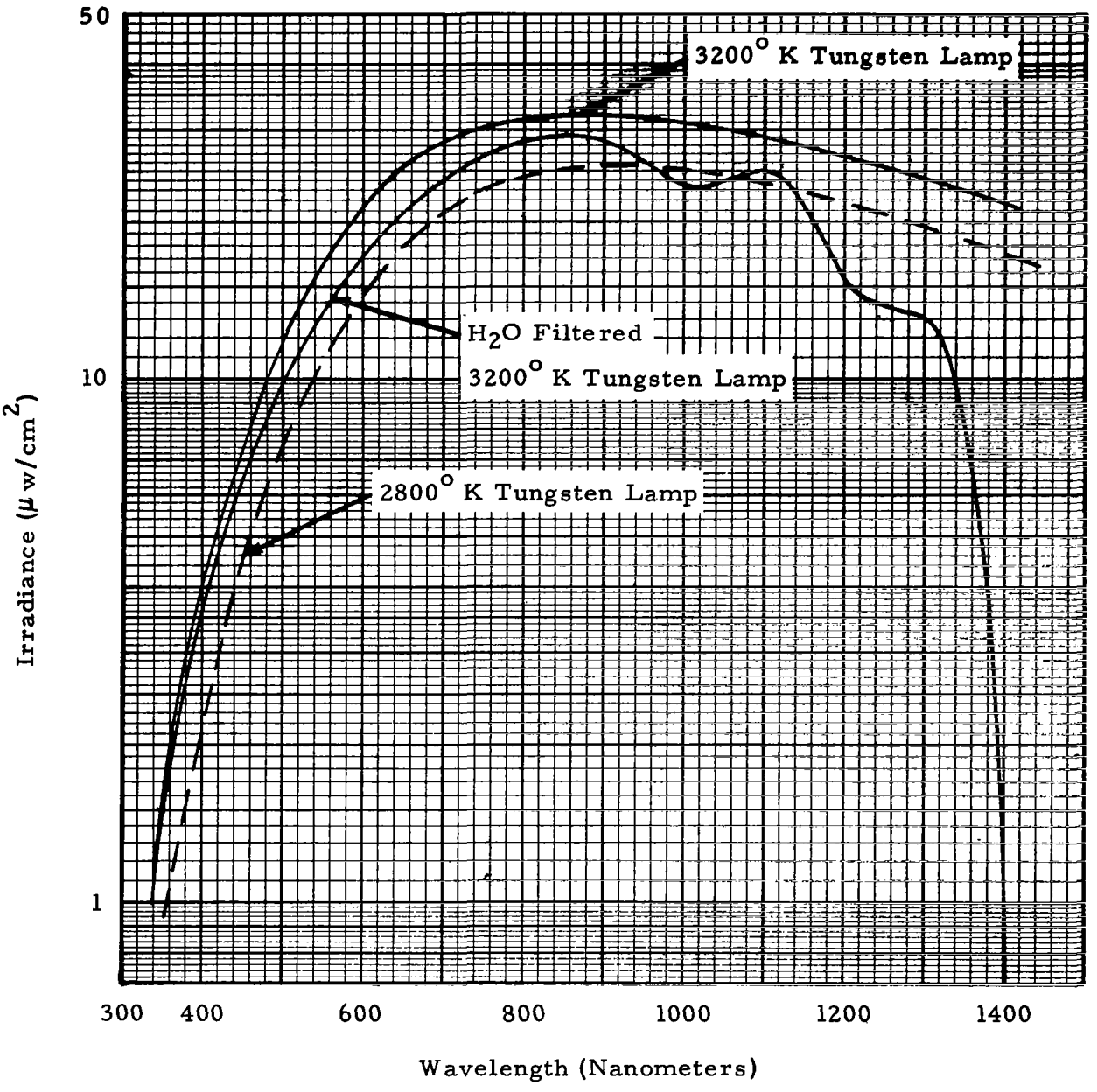

FIGURE 3.6-2 SPECTRAL IRRADIANCE OF 1000 WATT TUNGSTEN FILAMENT LAMPS

container and distilled water. The water was replaced weekly in accordance with a plan of preventive maintenance. b) Neutral density filter. A combination of screen type filters were used. To eliminate the problem of illumination passing straight through the openings in a grouping of multiple screens, each screen was separated from an adjacent screen by a minimum distance of one-half inch. This geometric separation plus non-registration between screens resulted in a capability to series multiplication factors of each screen and arrive at very low filter transmission capabilities. c) Slit aperture. A long narrow slit opening was used to obtain the very low levels of simulated lunar illumination. The use of a pin-hole aperture was rejected because it resulted in the lamp element being focused on the phototube. The slit opening performed satisfactorily and provided uniform illumination over the phototube without any focusing characteristics. d) Quartz window. On the optical entrance port served to further reduce the level of illumination on the phototubes.

A summary of slit aperture and filter values used for different illuminating fluxes is shown in Figure 3.6-3. A thermopile detector located in the test chamber and in the plane of the phototube faces was used to measure illuminating fluxes.

Illuminations of the phototubes were controlled by mechanical choppers operating at a constant speed of three revolutions per minute. Optical alignment was arranged so that earth and moon albedos were phased 180° apart and the following periods of ON and OFF duty cycles were used:

Earth Albedo of the sun (E_s)	8.7 seconds ON
	11.3 seconds OFF
Earth Albedo of the moon (E_m)	8.7 seconds ON
	11.3 seconds OFF
Moon Albedo of the sun (M & M_a)	
Direct Viewing (M)	1.1 seconds ON
	18.9 seconds OFF
Sunshield Attenuated (M_a)	2.8 seconds ON
	17.2 seconds OFF

Theoretical Flux Values	Test Flux On Phototube W/cm^2	Simulation	Filter %τ	Slit Size
1.57×10^{-4}	1.6×10^{-4}	$S + E_s$	3	Slit not used
1.8×10^{-8}	1.8×10^{-8}	M	1	0.004" Slit
6.75×10^{-10}	5.4×10^{-10}	M_a	.03	0.004" Slit
5×10^{-12}	5.4×10^{-12}	E_m	.0003	0.004" Slit

FIGURE 3.6-3 OPTICAL ATTENUATION OF ILLUMINATING FLUXES

The 90 minute spacecraft orbit period was simulated by controlling power to the illuminating lamps at duty cycles of 54 minutes and 36 minutes. The lamps have a rise time to total stable power in less than 30 seconds, so therefore, no compensation in duty cycles was made. When the $S + E_s$ lamp was "ON" the M, M_a, E_m lamp was "OFF" and vice-versa.

The illuminating flux levels on the phototubes are sufficient, in some cases, to be beyond the phototube capability. Therefore, electrical power to the phototubes was supplied at the following periods only:

$S + E_s$	:	54 minutes OFF and 36 minutes ON and phased so that when power was on the phototubes, the illuminating flux was OFF and vice-versa.
M and M_a	:	Power was OFF during these illuminating periods.
E_m	:	Power was ON during this period of illumination.

The period of illumination for lunar fluxes was arranged for compatibility with the 28 day period of lunar phases. A total period of illumination for 205 hours and 20 minutes out of each 672 hours (28 days) was accomplished.

3.7 ELECTRICAL ARRANGEMENT

Electrical circuits were provided in the test facility to control the albedo light levels, orbit sequences, and measurements of phototube properties. Automatic timing switches and choppers were arranged to provide power to the phototubes and albedo lamps at simulated real time orbit conditions. An adjustable 90 minute timer with multiple stations was used to control power to the phototubes and albedo lamps at a duty cycle of 54 and 36 minutes. A mechanical chopper which was synchronized at a constant speed of three rpm had a duty cycle of 7.7 seconds and was used to simulate spacecraft rotation by chopping the albedo lamps. The 90 minute timer and three rpm chopper were not synchronized together to more closely duplicate the real time spacecraft conditions.

3.7.1 Electrical circuits of the primary controls were arranged to control and measure each phototube. The gain of each dynode stage and the overall phototube was measured with an accurate battery operated Keithley Electrometer capable to 10^{-13} amperes and a variable high voltage power supply. Each stage of the phototube was selected with specially constructed, low contact resistance, jacks.

3.7.2 The albedo light sources were arranged and controlled so that when the lights were on the phototubes the power supply was off. The periodic timer for "ON" - "OFF" periods of 54 and 36 minutes was accurate to 1/2 percent of any setting, Figure 3.7.2-1.

3.7.3 Quantum efficiency measurements, associated light sources, and filters were controlled manually during each measurement period. The light levels were controlled by two variable autotransformers and a filament transformer used for coarse and fine control of lamp current and an accurate A.C. current meter, Figure 3.7.3-1.

3.7.4 Since the experimental program was scheduled to run continuously for a minimum period of three months, an emergency shut-off system was required during failure of an irradiating lamp. The emergency shut-off was obtained by controlling power to the orbit timer through a current sensing transformer. (Figure 3.7.4-1). When the lamps are actuated and operating, the relay switch maintains power on the orbit timer; if a lamp fails, current stops flowing and the orbit timer is automatically stopped. A total hour meter in parallel with the orbit timer was used to record the time of failure and total exposure time. The lamp L_3 acts as a simulated load to energize the emergency shut-off system when the moon albedo L_2 is turned off.

SECTION 4.0

MULTIPLIER PHOTOTUBE

The phototube used in the evaluation consisted of a model 541, type N manufactured by EMR, Princeton, New Jersey. In summary, the EMR model 541N phototube had an end-on-window with a one inch diameter photocathode. The window material was 7056 glass and the phototube was spectrally sensitive from approximately 250 to 700 nanometers. The phototube was fabricated with beryllium copper dynodes

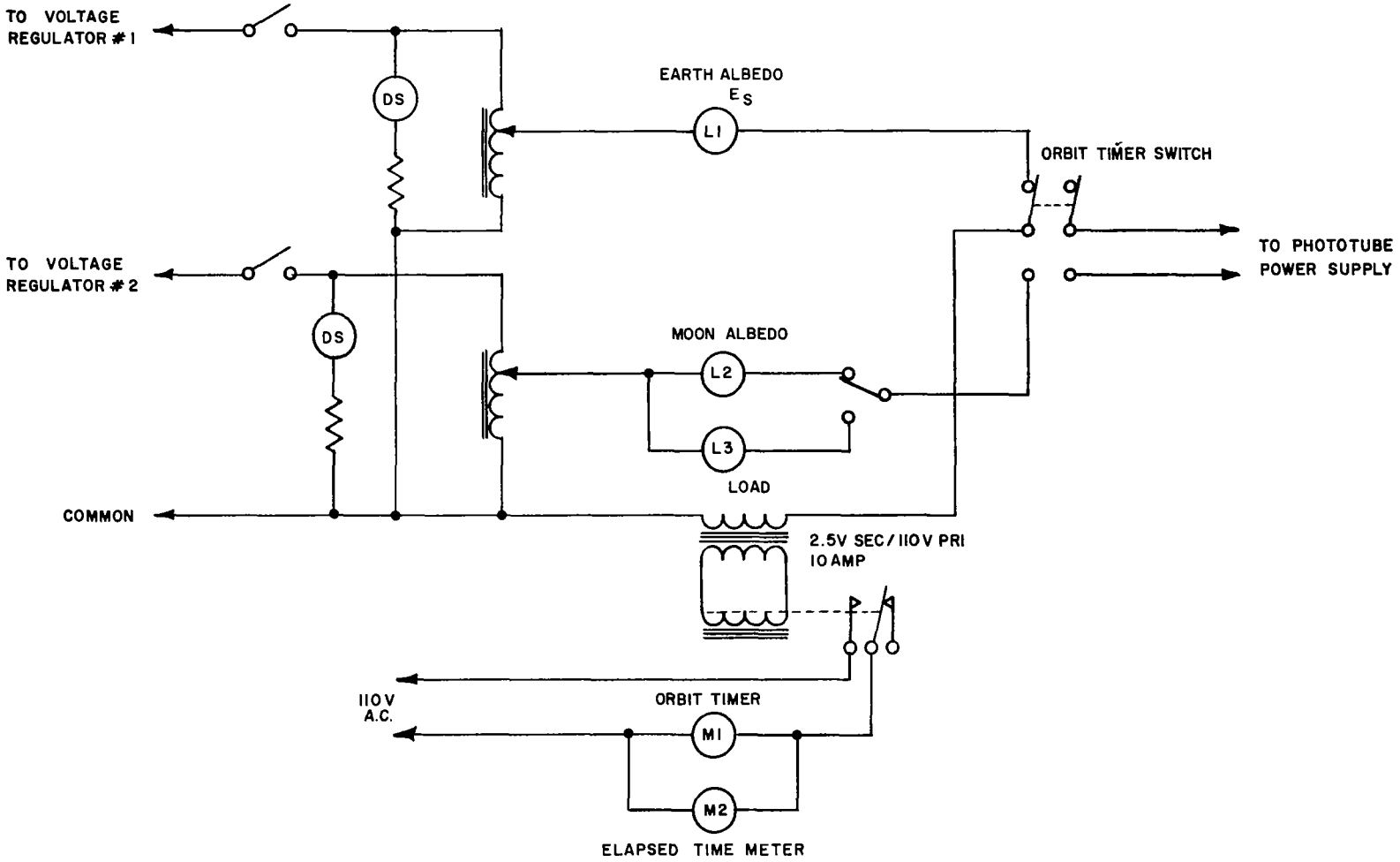

FIGURE 3.7.2-1 CONTROL OF ALBEDO LIGHT SOURCES

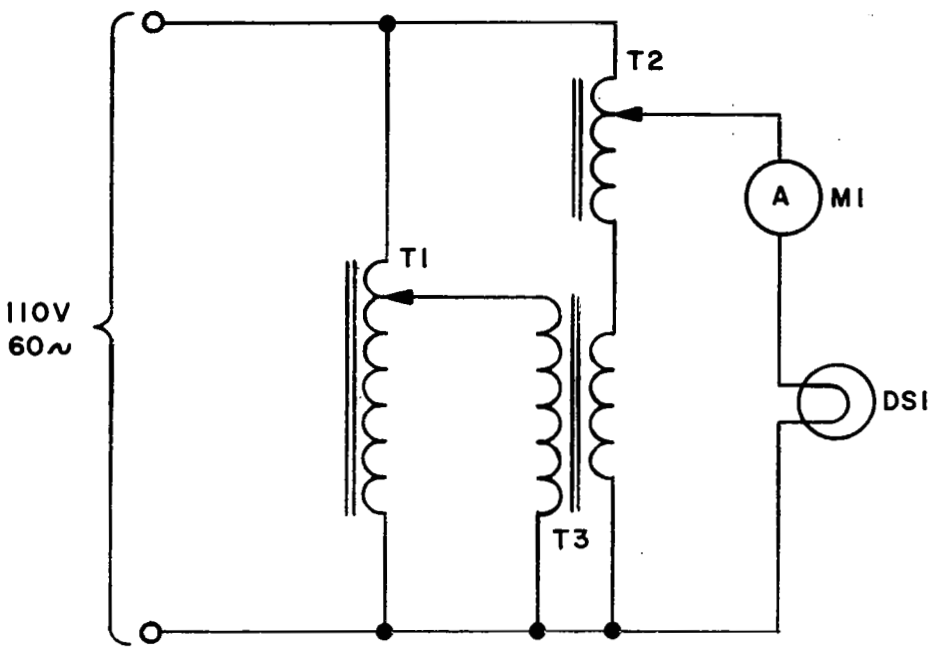

T1 -- 5 AMP AUTOTRANSFORMER FOR FINE CONTROL.

T2 -- 10 AMP AUTOTRANSFORMER FOR COURSE CONTROL.

T3 -- 120V PRIMARY/5 V SECONDARY, 10 AMP FILAMENT TRANSFORMER.

M1 -- 10 AMP ALTERNATING CURRENT METER.

DS1 -- 1000W TUNGSTAN LAMP FOR QUANTUM EFFICIENCY AND VOLTAGE-GAIN LIGHT SOURCE.

FIGURE 3.7.3-1 CONTROL OF MEASUREMENT LIGHT SOURCES

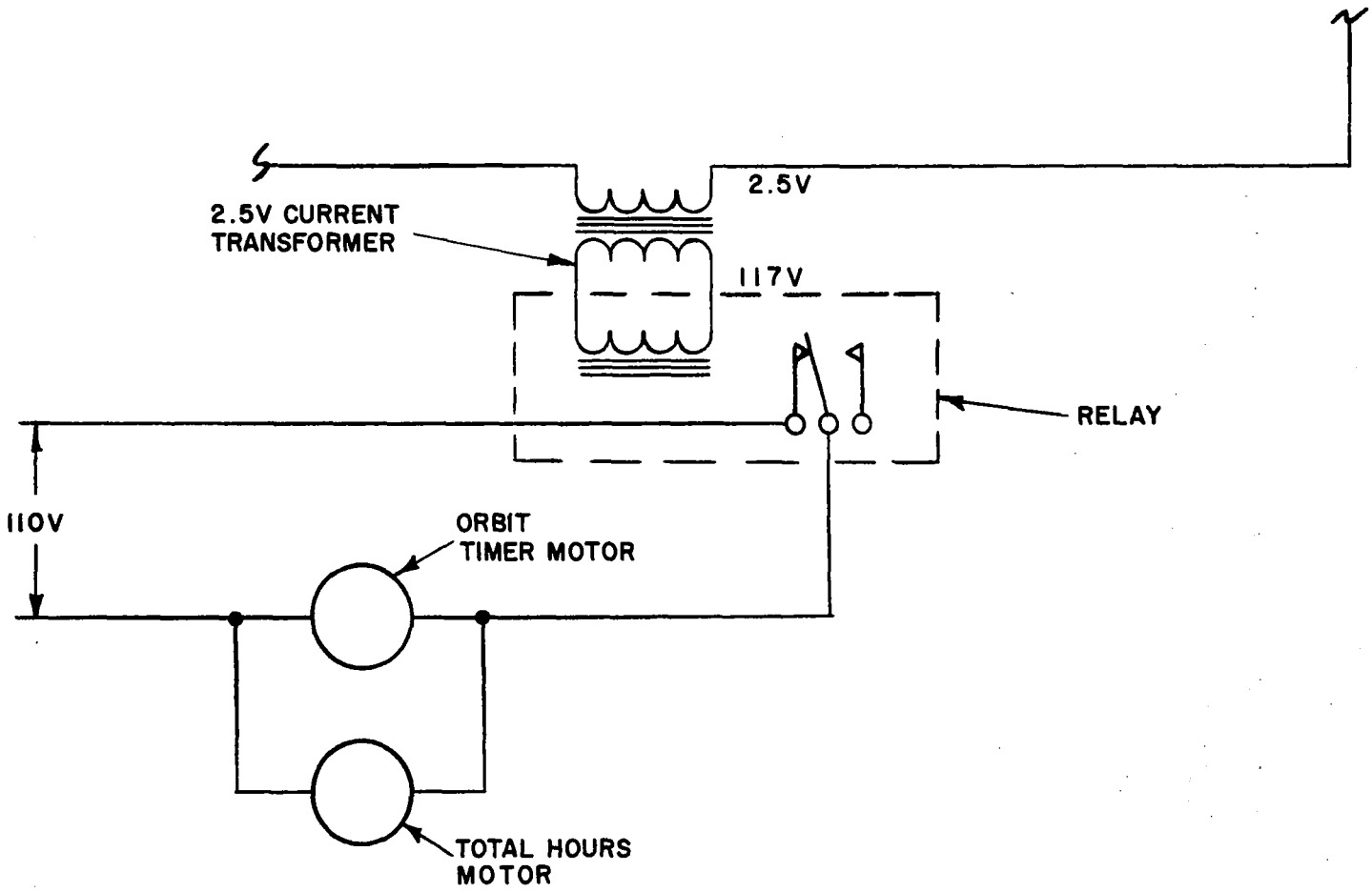

FIGURE 3.7.4-1 AUTOMATIC EMERGENCY SHUT-OFF DURING FAILURE OF ILLUMINATING LAMPS

preconditioned by a period of operational burn-in. A total of four phototubes were purchased to the following specification:

Model: EMR 541 N-01-14-03900 multiplier phototube.

Number and type of Dynodes: 14, Venetian blind, beryllium copper.

Window Material: 7056 glass.

Cathode sensitive area: one inch diameter.

Quantum efficiency at 4100 $\mathring{A}$: 18 percent minimum.

Voltage required for gain of 10^6: 3400 volts maximum after burn-in.

Dark current at gain of 10^6: 1×10^{-10} amperes maximum after burn in.

Burn-in: 100 ± 2 hours at a gain of 10^6 and an anode current of 5×10^{-6} amperes.

Packaging: Fiberglass housing, 1-3/8 inches O.D. by 4-1/4 inches long.

Shock Capability: 100 g for an 11 millisecond duration.

Vibration: 30 g at 20 to 3000 cycles per second.

Temperature: $150^{\circ}C$ to $-55^{\circ}C$.

Lead Length: 18 inches minimum.

Following leads to be brought out: Cathode, Anode, and Dynodes number 1, 12, 13 and 14.

NOTE: Calibration curves, spectral data, and all performance data (including burn-in) to be supplied with delivered phototubes.

Each of the four phototubes satisfactorily met the preceding specifications as shown in Figure 4.0-1. The usual change in properties after a burn-in period was obtained on all phototubes with the least change noted for phototube No. 11762. Phototube No. 11762 appeared to be highly stable and was capable of a 10^6 gain at the lowest voltage.

Prior to testing, the phototubes were selected at random for their respective location in the test array.

Measurement	Test Period	Specification	TEST RESULTS Phototube Identification			
			A	B	C	D
			# 11644	# 11762	# 11647	# 11664
Dark Current	Before Burn-in		5.1×10^{-11} amperes	5.0×10^{-11} amperes	1.7×10^{-11} amperes	1.6×10^{-11} amperes
	After Burn-in	1×10^{-10} amperes max. 10^6 gain	2.8×10^{-11} amperes	4.3×10^{-11} amperes	2.8×10^{-11} amperes	1.4×10^{-11} amperes
Voltage Gain	Before Burn-in		2565 volts	2485 volts	2820 volts	2925 volts
	After Burn-in	3400 Volts max. 10^6 gain	3115 volts	2580 volts	3290 volts	3400 volts
Quantum Efficiency	Before Burn-in		21.5%	20.6%	23.5%	21.5%
	After Burn-in	18% Minimum 4100 Å	21.5%	20.6%	20.3%	18.7%

FIGURE 4.0-1 INITIAL PHOTOTUBE PROPERTIES

SECTION 5.0
TEST SCHEDULE

The schedule of irradiating each phototube was conducted continuously over a seven month period of real time events. Each tube received its particular schedule of events (Figure 5.0-1) at the same time that the other three phototubes received theirs. Therefore, the entire program of exposing four phototubes to various fluxes of irradiation was accomplished in slightly more than seven months. Each parameter of irradiation as shown in Figure 5.0-2 was controlled independent of the other parameters which resulted in an orientation that was typical of spacecraft conditions.

5.1 TEST SPECIFICATIONS

At the conclusion of an analysis of spacecraft orbit environment, the following test specifications were established to test the four phototubes and approved by the technical monitor.

5.1.1 Pressure

A low pressure vacuum environment was maintained continually throughout the periods of exposure and measurement. The test chamber will remain closed until the conclusion of the test program. A pressure below 1×10^{-6} torr will be maintained.

5.1.2 Temperature

The phototubes will be tested at room temperature ($22^{\circ}C$). Temperature of the phototubes will not be controlled during the test program but will be allowed to stabilize at the ambient level.

5.1.3 Illuminating Fluxes

Illumination of the phototubes will be accomplished to simulate the following:

a. Solar Radiation (S)

b. Earth Albedo of the Sun (E_s)

c. Direct Lunar Viewing (M)

d. Sunshield Attenuation of Lunar Viewing (M_a)

e. Earth Albedo of Lunar Illumination (E_m)

PHOTOTUBE	SERIAL NUMBER	IRRADIATION
A	11644	Electrons and protons
B	11762	Electrons, protons, solar, and Earth Albedo
C	11647	Electrons, protons, solar, Earth Albedo, and Lunar irradiances
D	11664	Solar and Earth Albedo

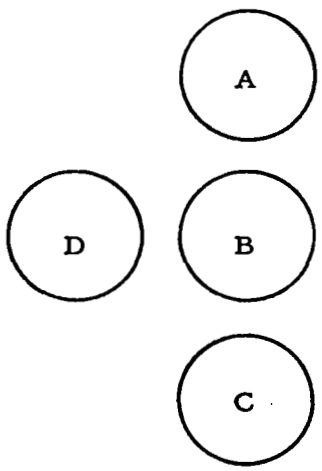

FIGURE 5.0-1 SCHEDULE OF IRRADIATION ON THE PHOTOTUBES

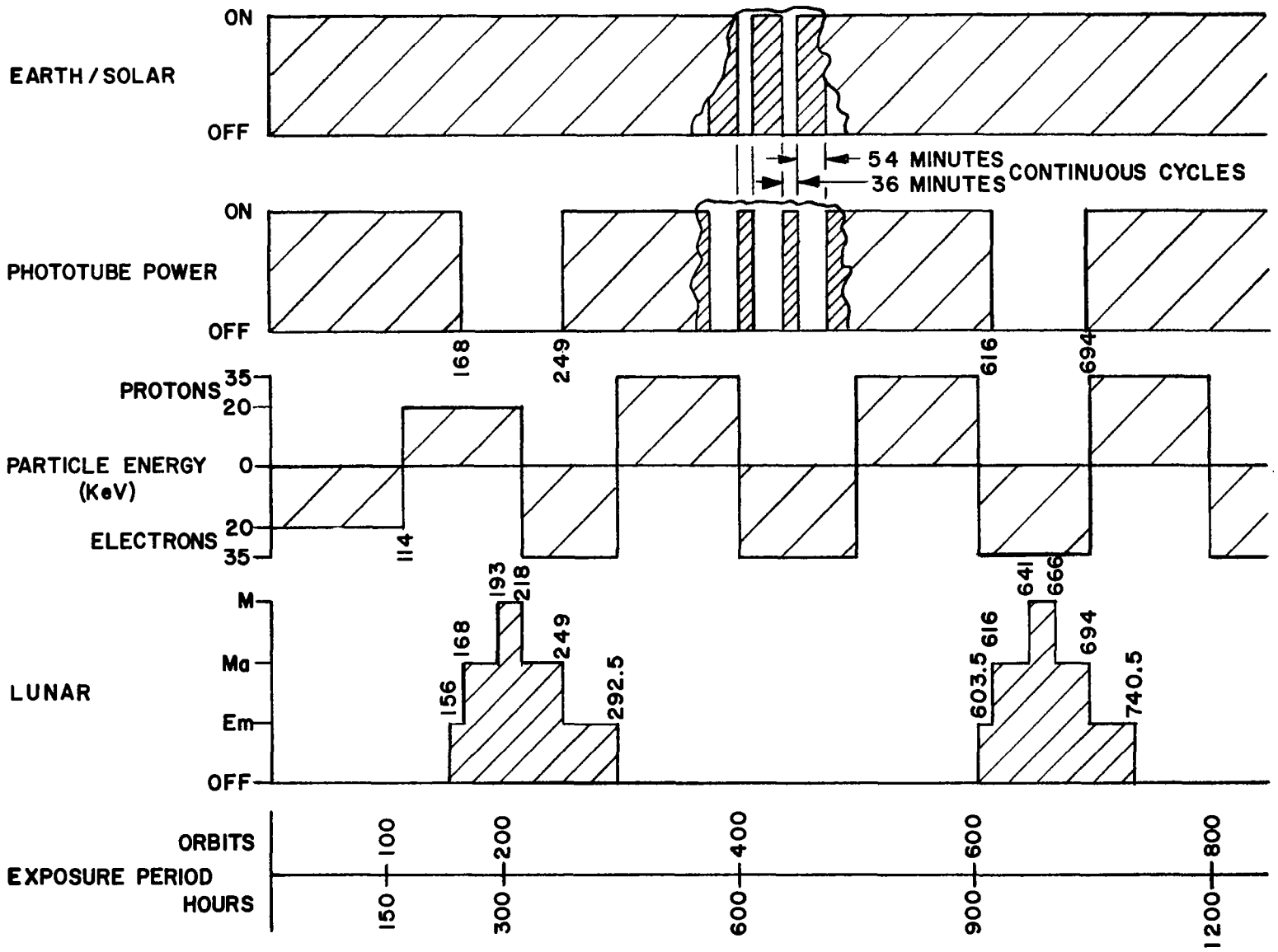

FIGURE 5.0-2 SCHEDULE OF IRRADIATING FLUXES

5.1.3.1 Flux Levels

Flux levels as measured at the phototube face will be as follows:

$S + E_s$: 1.57×10^{-4} W/cm^2

M : 1.8×10^{-8} W/cm^2

M_a : 6.75×10^{-10} W/cm^2

E_m : 5×10^{-12} W/cm^2

5.1.3.2 Flux Source and Measurement

Illuminating fluxes will be simulated with tungsten filament, quartz lamps arranged with water filters and neutral density attenuators.

5.1.3.3 Duty Cycles

Illumination of the phototubes will be controlled by mechanical choppers operating at a constant speed of three rpm. Optical alignment will be arranged so that the earth and moon albedos are phased 180° apart. The following periods of ON and OFF duties will be used:

Earth Albedo of the sun (E_s)	8.7 seconds ON 11.3 seconds OFF
Earth Albedo of the Moon (E_m)	8.7 seconds ON 11.3 seconds OFF
Moon Albedo of the sun (M)	
Direct Viewing	1.1 seconds ON 18.9 seconds OFF
Sunshield Attenuated (M_a)	2.8 seconds ON 17.2 seconds OFF

5.1.3.4 Orbit Simulation

The 90 minute spacecraft orbit period will be simulated by controlling power to the illuminating lamps at duty cycles of 54 minutes and 36 minutes. The lamps have a rise time to stable total power in less than 30 seconds, so therefore, no compensation in duty cycles

will be used. When the S + E_s lamp is "ON", the M, M_a, E_m lamp will be "OFF" and vice-versa.

5.1.3.5 Phototube Power

Illuminating flux levels on the phototubes are sufficient, in some cases, to be beyond the phototube capability. Therefore, electrical power to the phototubes will be supplied at the following periods only:

S + E_s	:	54 minutes OFF and 36 minutes ON and phased so that when power is on the phototubes, the illuminating flux is OFF and vice-versa.
M and M_a	:	Power is OFF during these illuminating periods.
E_m	:	Power is ON during this period of illumination

5.1.3.6 Time Periods for Lunar Illumination

The period of illumination for lunar fluxes will be arranged for compatibility with the 28 day period of lunar phases. A total period of illumination for 205 hours and 20 minutes out of each 672 hours (28 days) will be accomplished in accordance with the following schedule:

1.	E_m	:	18 hours 40 minutes $\approx$ 12.5 orbits
2.	M_a	:	37 hours 20 minutes $\approx$ 25 orbits
3.	M	:	37 hours 20 minutes $\approx$ 25 orbits
4.	M_a	:	46 hours 40 minutes $\approx$ 31 orbits
5.	E_m	:	65 hours 20 minutes $\approx$ 43.5 orbits
6.	Dark	:	466 hours 40 minutes $\approx$ 311 orbits
	Total	:	448 orbits
7.		:	Repeat steps 1 through 6

5.1.4 Proton-Electron Fluxes

Irradiation of the phototubes with protons and electrons will

be accomplished with a low energy Van de Graaff accelerator. The program of exposure will be arranged so that the phototubes are irradiated with protons (H^+) for a one week period and then with electrons (e^-) for a one week period. The irradiation schedule will be continuous throughout the test period. During the first two weeks of exposure, the proton and electron particles will be accelerated at an energy level of 20 KeV. During the remainder of the test program, an energy level of 35 KeV will be utilized (Figure 5.1.4-1). The flux rates will be:

Protons: 4×10^7 particles/cm^2 - day

Electrons: 10^{10} particles/cm^2 - day

5.1.5 Phototube Exposure

The four phototubes will be arranged so that each one has a different history of irradiation as follows:

Phototube A:	Protons/Electrons
Phototube B:	Protons/Electrons $S + E_s$
Phototube C:	$S + E_s$ M M_a E_m Protons/Electrons
Phototube D:	$S + E_s$

5.1.6 Test Measurements

Measurements of phototube characteristics will be made periodically throughout the test period and consist of the following:

1. Spectral Quantum Efficiency
2. Gain - Voltage Characteristics
3. Gain per Dynode Stage

Measurements periods will be selected to be compatible with the rates of degradation experienced by the phototubes. All measurements will be made in situ and individually on each

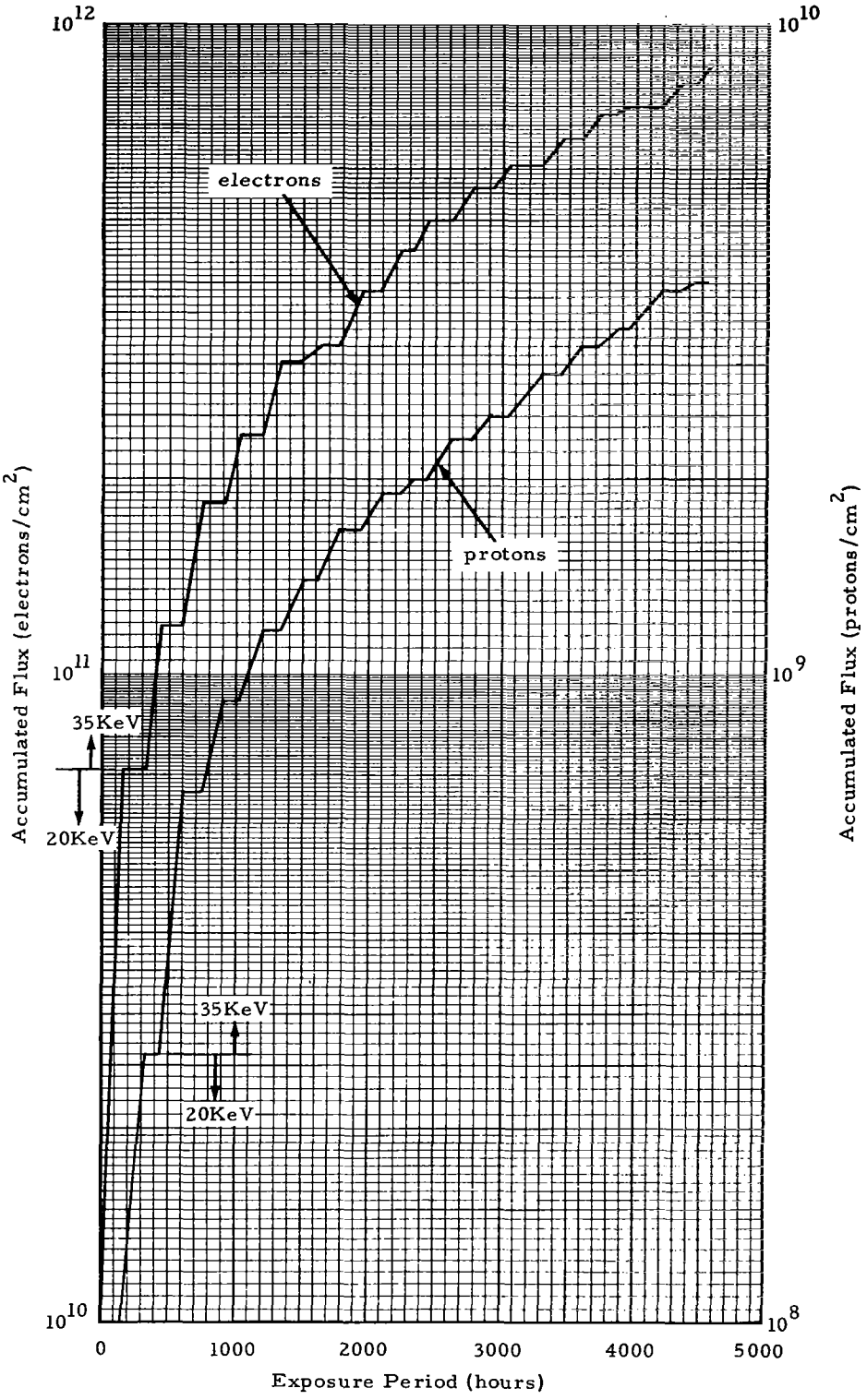

FIGURE 5.1.4-1 ACCUMULATED FLUX OF HIGH ENERGY PARTICLE IRRADIATION

phototube. During the period of measurement, all irradiating fluxes will be stopped.

5.1.6.1 Spectral Quantum Efficiency

Measurements will be made at 12 specific wavelength points between 310 and 694 nanometers.

5.1.6.2 Gain-Voltage Characteristics

Gain-Voltage properties of each phototube will be obtained from 1600 to 3200 volts during illumination by a tungsten lamp.

5.1.6.3 Gain per Dynode Stage

Measurements will be made to establish the values in gain between:

a. Anode and 14th dynode
b. 14th dynode and 13th dynode

5.1.6.4 Time

A running time meter and orbit counter will be used to relate all measurements and testing periods.

SECTION 6.0

TEST RESULTS

Test data obtained on each phototube during a seven month period of exposure to spatial radiations are presented in the appendices, sections 9.3 and 9.4. As with most studies that generate a voluminous quantity of data, the results can be summarized in a variety of ways, usually dependent upon the desires of the investigator. The following discussion of the test results is an attempt to present and summarize the findings based on the data obtained during testing. In summary, changes noted are not of significant magnitude.

6.1 DARK CURRENT

The values of dark current appeared to remain stable throughout the period of testing for all the phototubes except No. 11647 which was exposed to lunar illumination. The effect of illuminating a phototube with a high light level can be seen in Figure 6.1-1. Prior to lunar illumination the phototube dark current remains somewhat stable at a minimum value but then increases during the period of simulated lunar viewing (dark current measured after a dark adaption period of four hours).

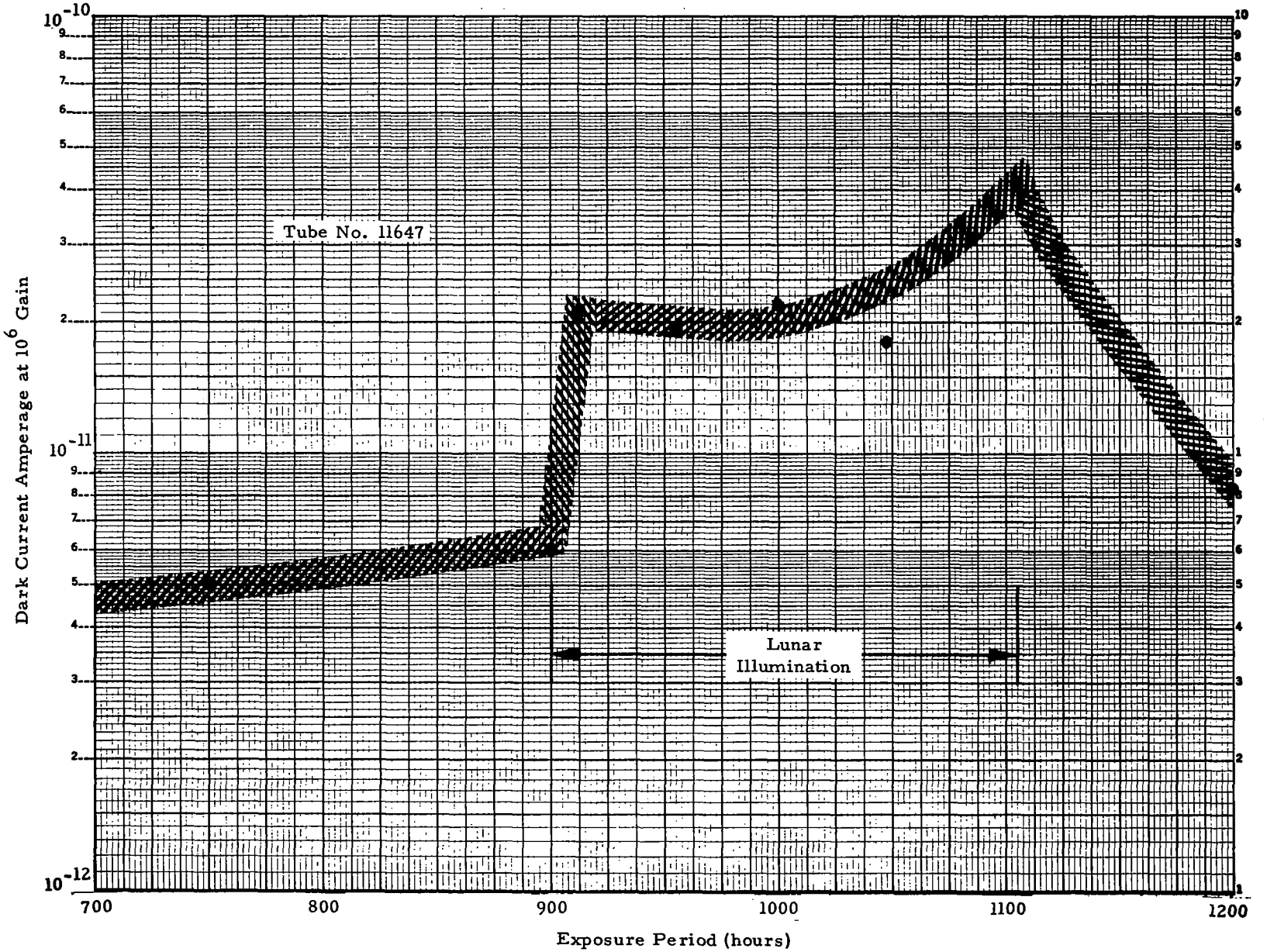

FIGURE 6.1-1 RECOVERY OF DARK CURRENT AFTER LUNAR ILLUMINATION

The dark current remains at this increased value throughout the lunar period but then decreases when the phototube is cycled back into a dark lunar phase. (Adequate data was not taken to accurately detail the dark current decay function). During the dark lunar period, the phototube recovers its initial fully dark adapted value. The other three phototubes appear to be unaffected in dark current properties and indicated very little change. The slight fluctuations in data are due to measurement capability and changes in the period of time that the phototubes were allowed to recover prior to measuring.

6.2 SPECTRAL RESPONSE

Data of spectral response and quantum efficiency are summarized in Figures 6.2-1 through 6.2-12.

Phototube No. 11644 which was irradiated by charged particles (electrons and protons) only, exhibits an increase in spectral response at 3990 Å (Figure 6.2-1). This increase occurred rapidly within the initial 1000 hours of exposure and then remained somewhat constant for the remaining period of exposure as shown in Figure 6.2-5. The slight decrease in spectral response at 5000 Å (Figure 6.2-1) is not significant and values of quantum efficiency remain essentially unchanged throughout the entire test period.

Phototube Nos. 11762 and 11647 both show an overall decrease in spectral response (Figures 6.2-2 and 6.2-3) and quantum efficiency (Figures 6.2-6, 7, 10 and 11). The decrease in properties occurred during the initial 1500 hours of exposure and then stabilized at the lower values. The effect of combined irradiation for each of these two tubes appears to be of the same order of magnitude indicating that illumination plus charged particles is more degrading than either one alone.

Phototube No. 11664 which was irradiated with simulated Earth albedo and stray sunlight only, appeared to benefit from the exposure. An overall increase in spectral response (Figure 6.2-4) and enhancement of quantum efficiency (Figures 6.2-8 and 6.2-12) were in the range of significant measurements.

6.3 ANODE VOLTAGE AT FIXED GAIN

Data of anode voltage at 10^6 gain are summarized in Figures 6.3-1 through 6.3-4.

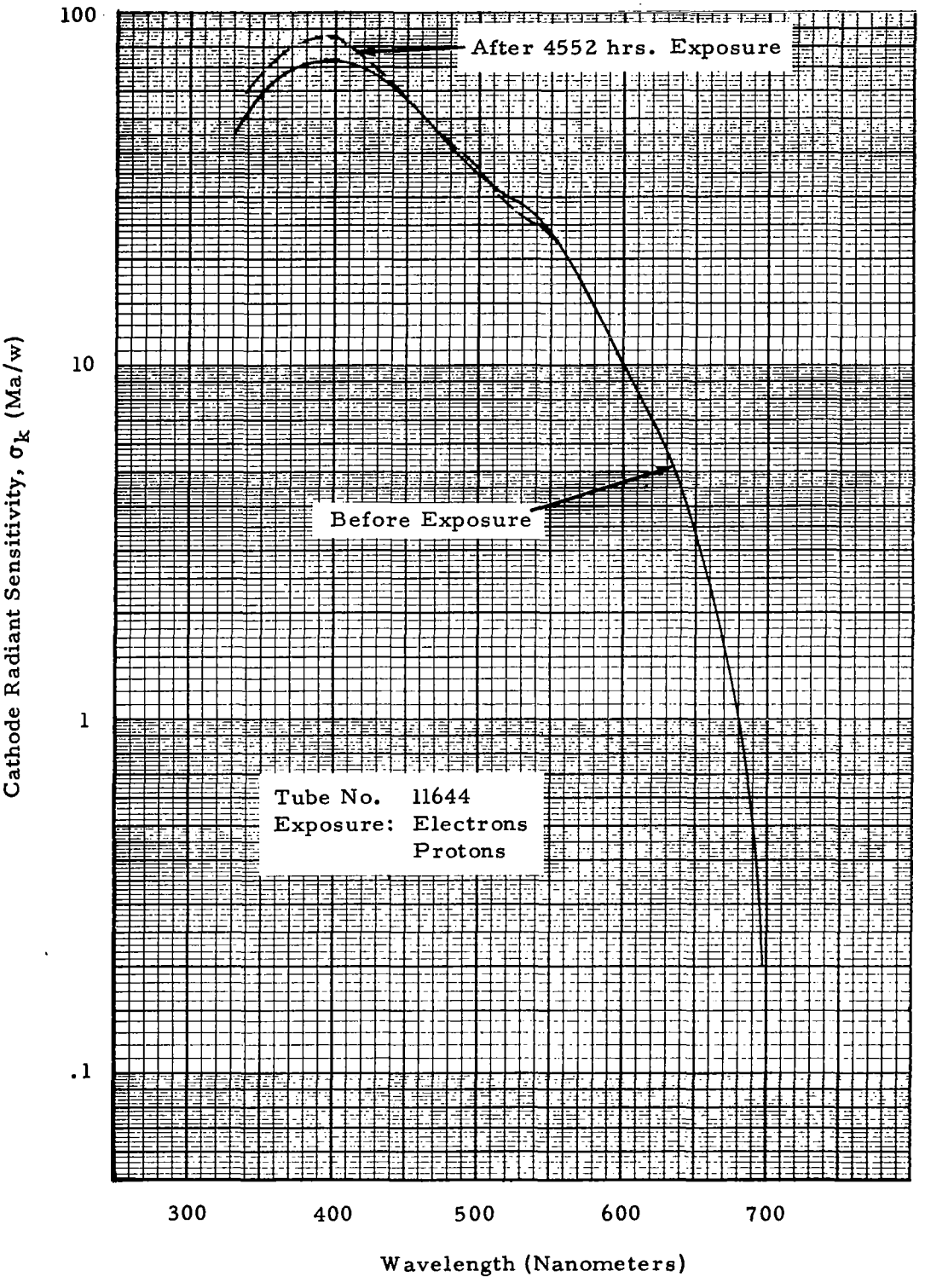

FIGURE 6.2-1 MEASUREMENTS OF SPECTRAL RESPONSE

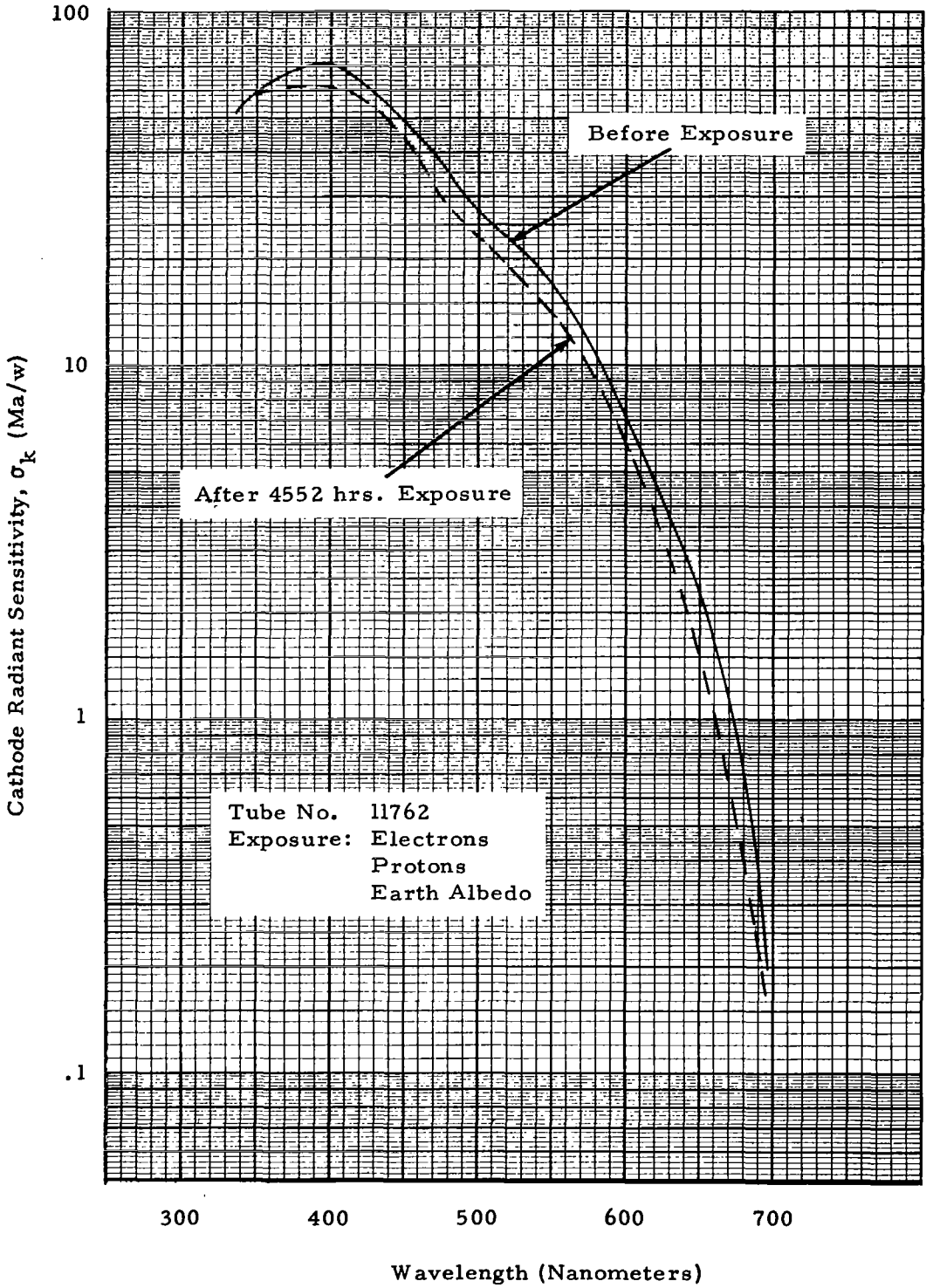

FIGURE 6.2-2 MEASUREMENTS OF SPECTRAL RESPONSE

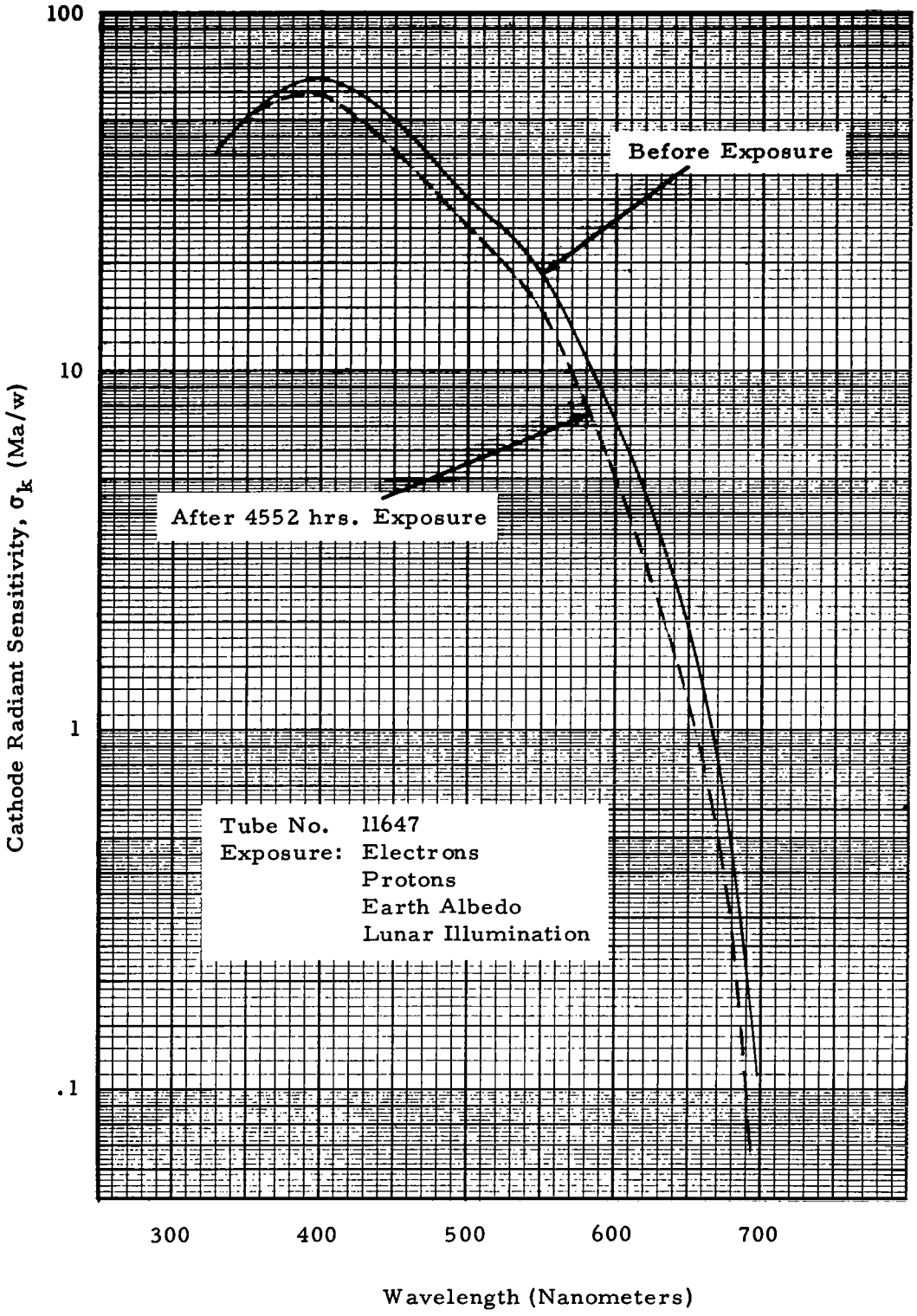

FIGURE 6.2-3 MEASUREMENTS OF SPECTRAL RESPONSE

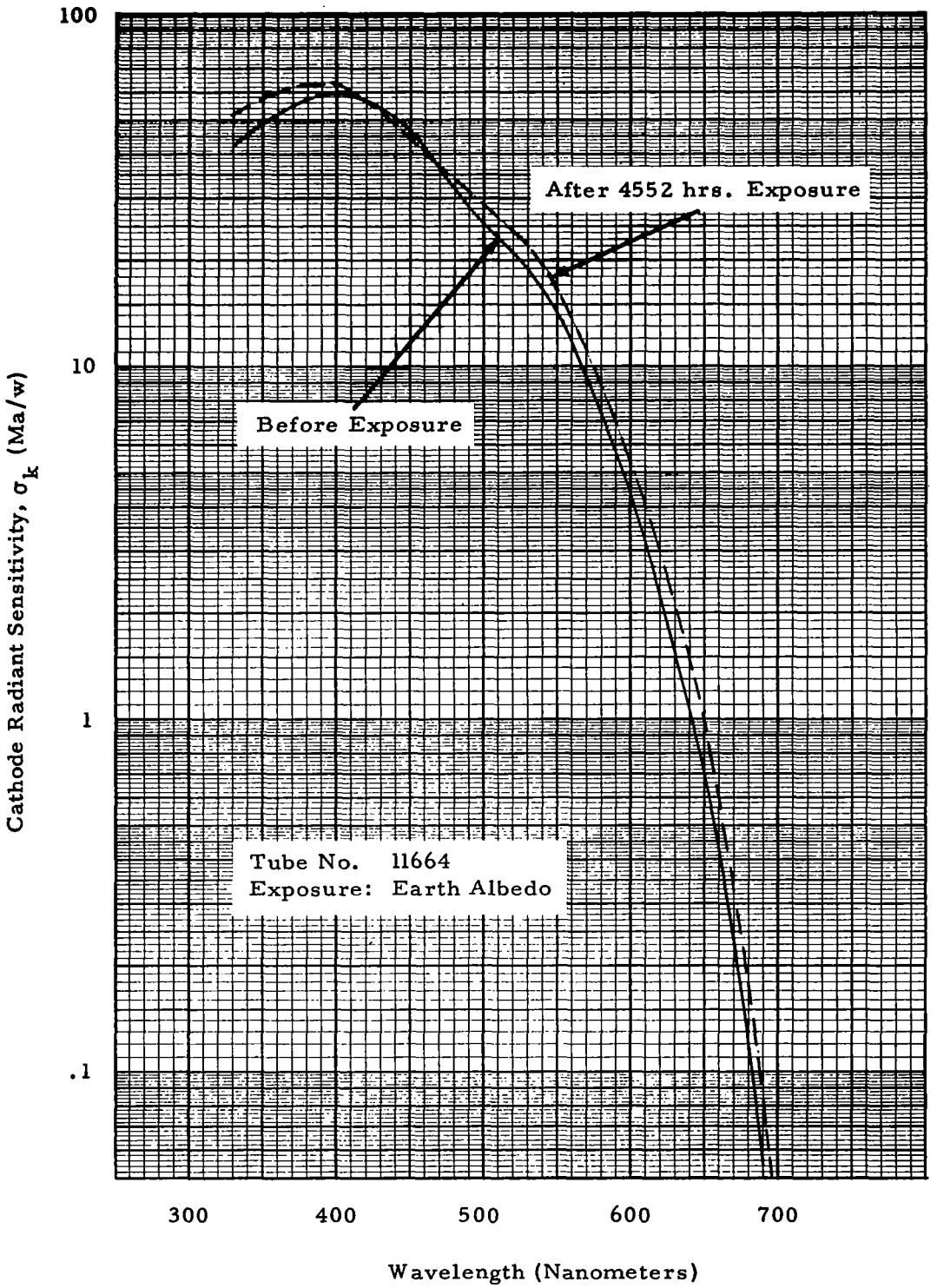

FIGURE 6.2-4 MEASUREMENTS OF SPECTRAL RESPONSE

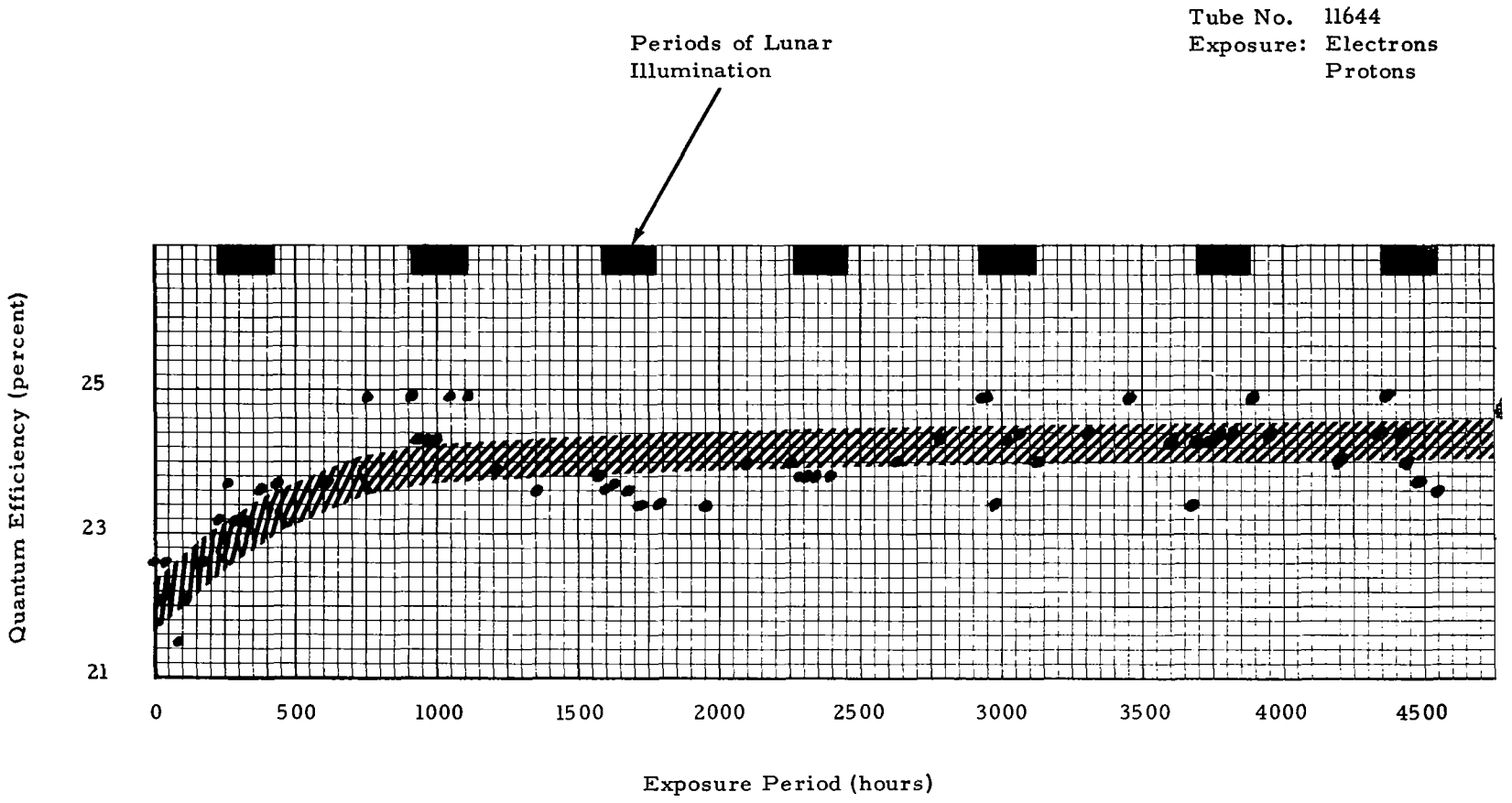

FIGURE 6.2-5 CHANGES IN QUANTUM EFFICIENCY AT 3990 Å WAVELENGTH

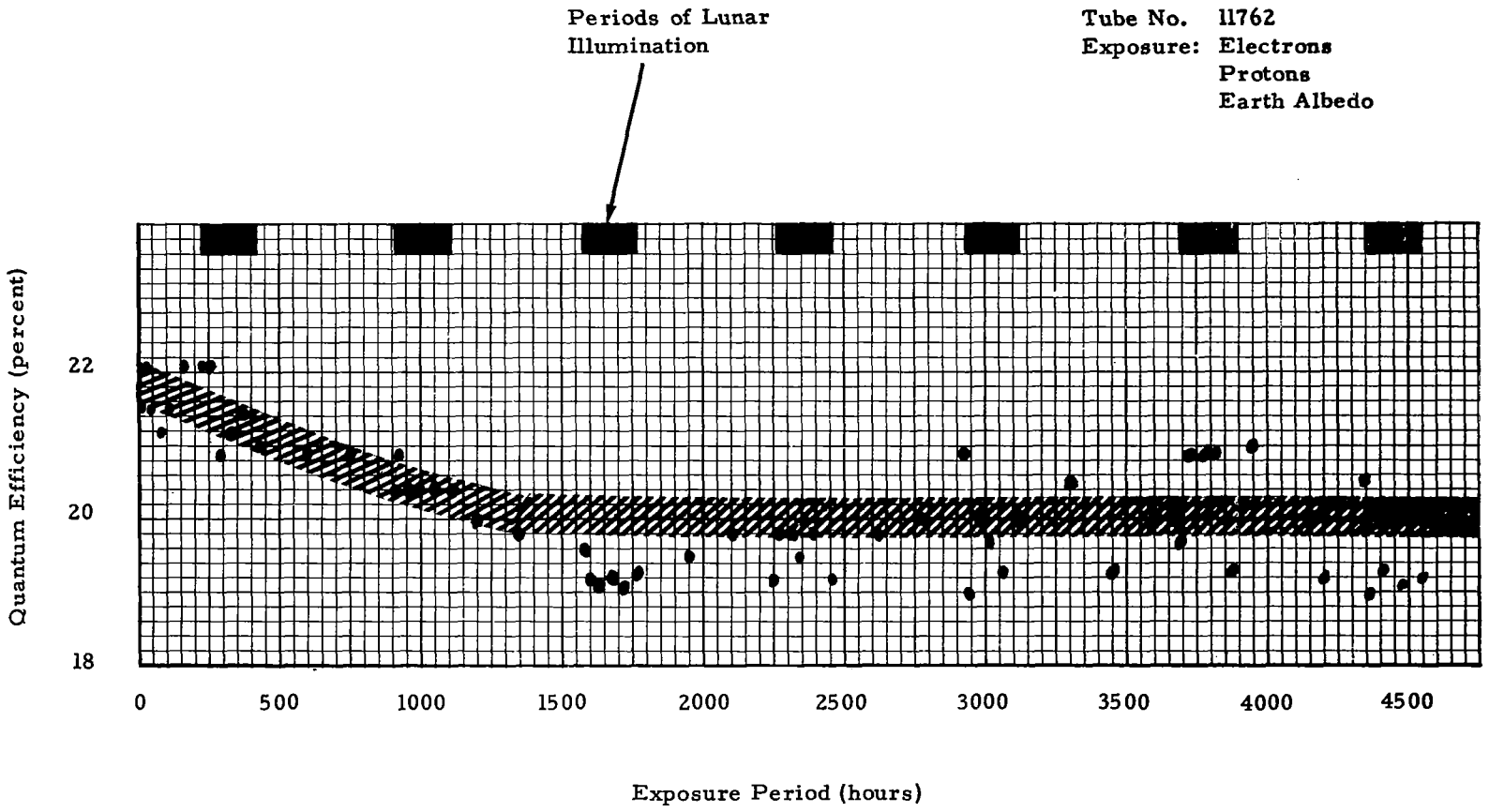

FIGURE 6.2-6 CHANGES IN QUANTUM EFFICIENCY AT 3990 Å WAVELENGTH

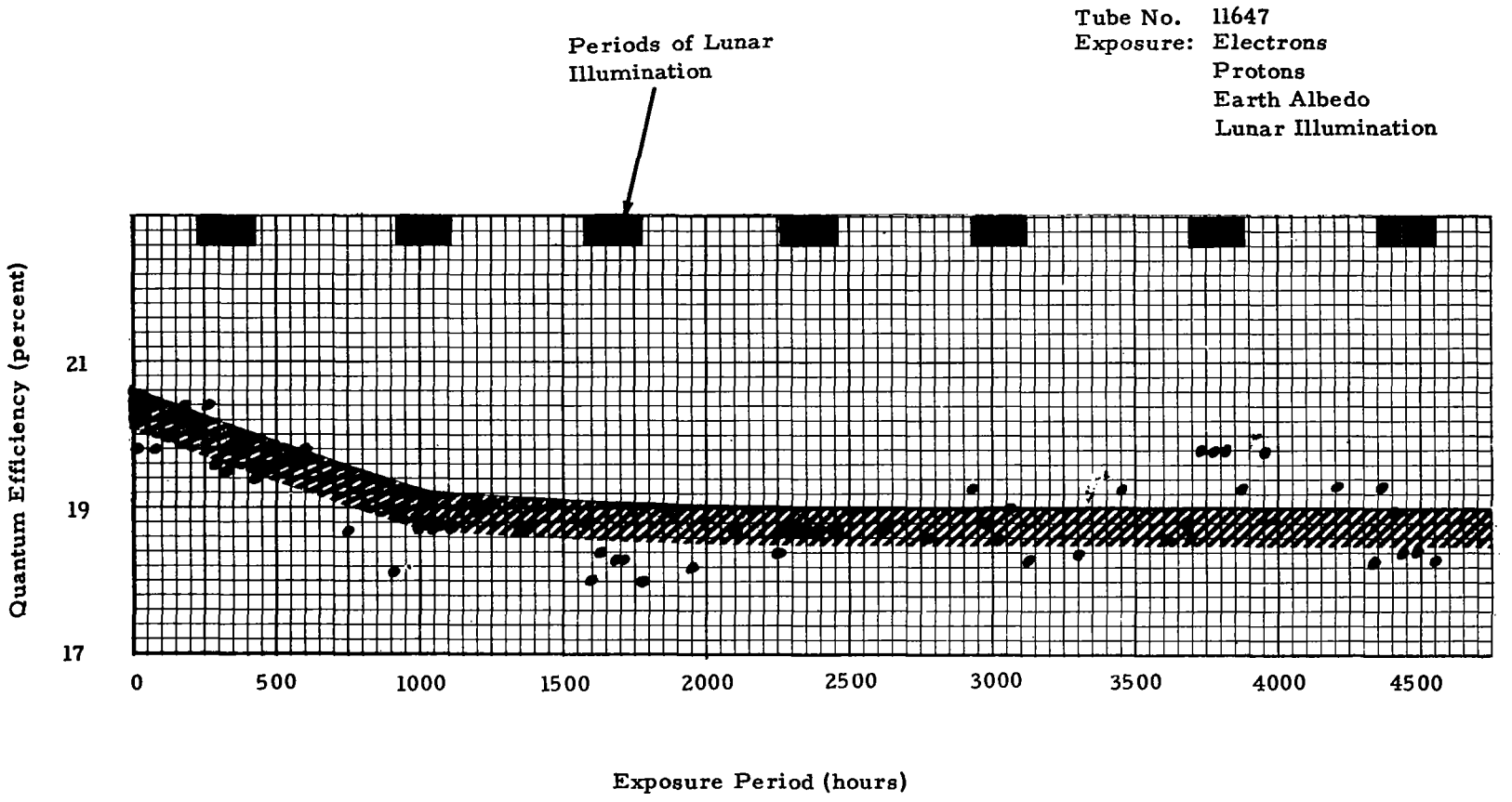

FIGURE 6.2-7 CHANGES IN QUANTUM EFFICIENCY AT 3990 Å WAVELENGTH

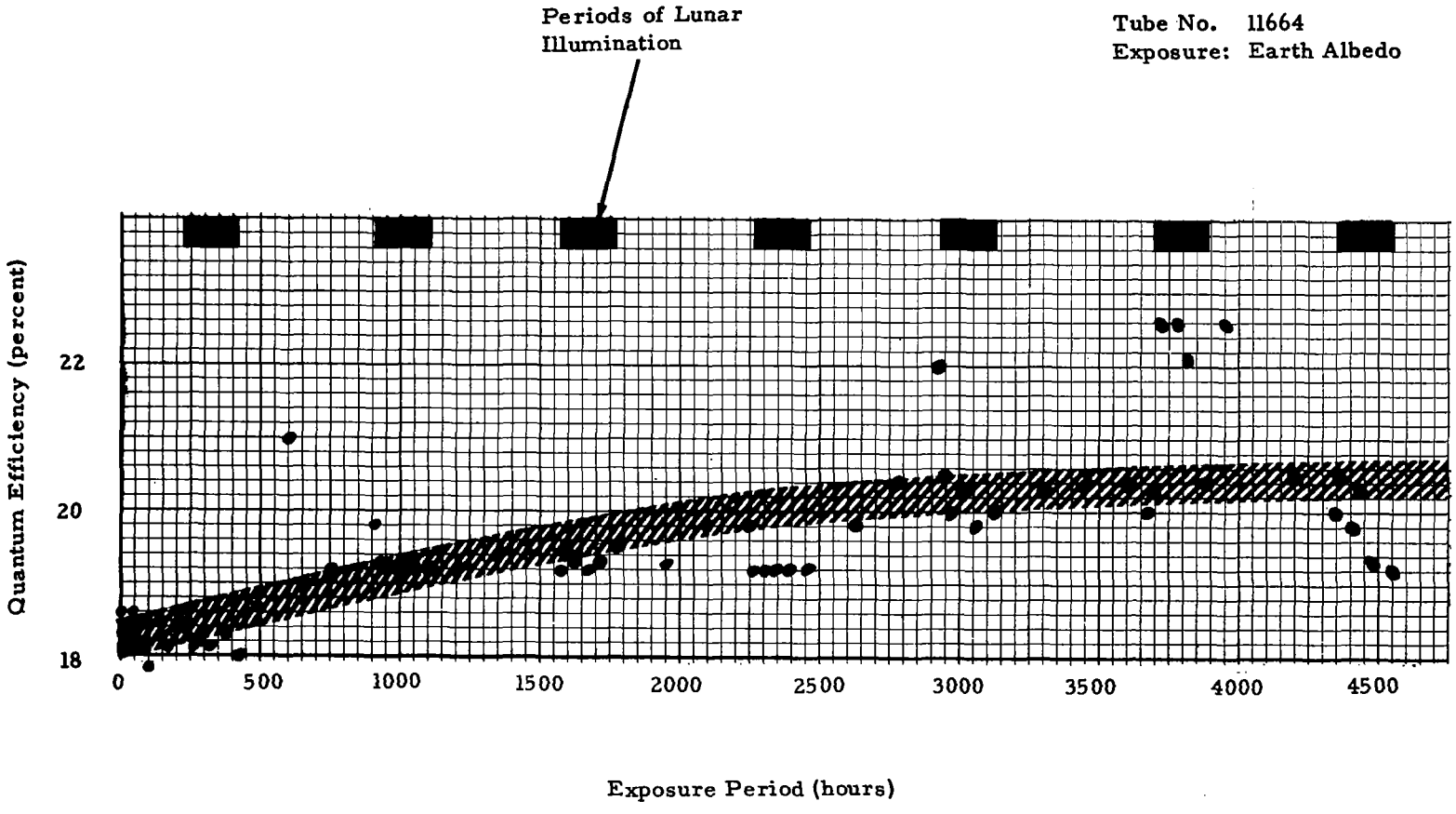

FIGURE 6.2-8 CHANGES IN QUANTUM EFFICIENCY AT 3990 Å WAVELENGTH

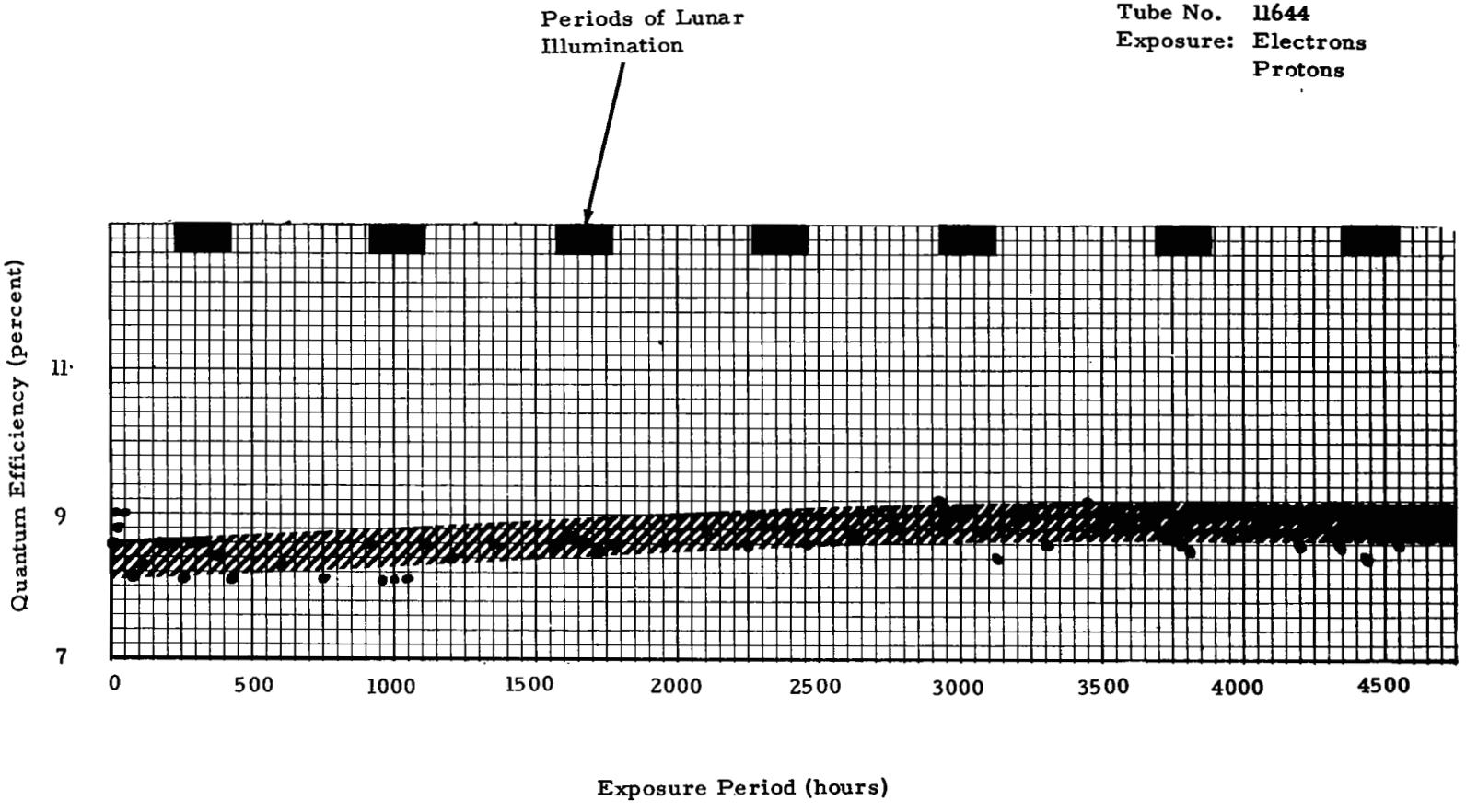

FIGURE 6.2-9 CHANGES IN QUANTUM EFFICIENCY AT 5000 Å WAVELENGTH

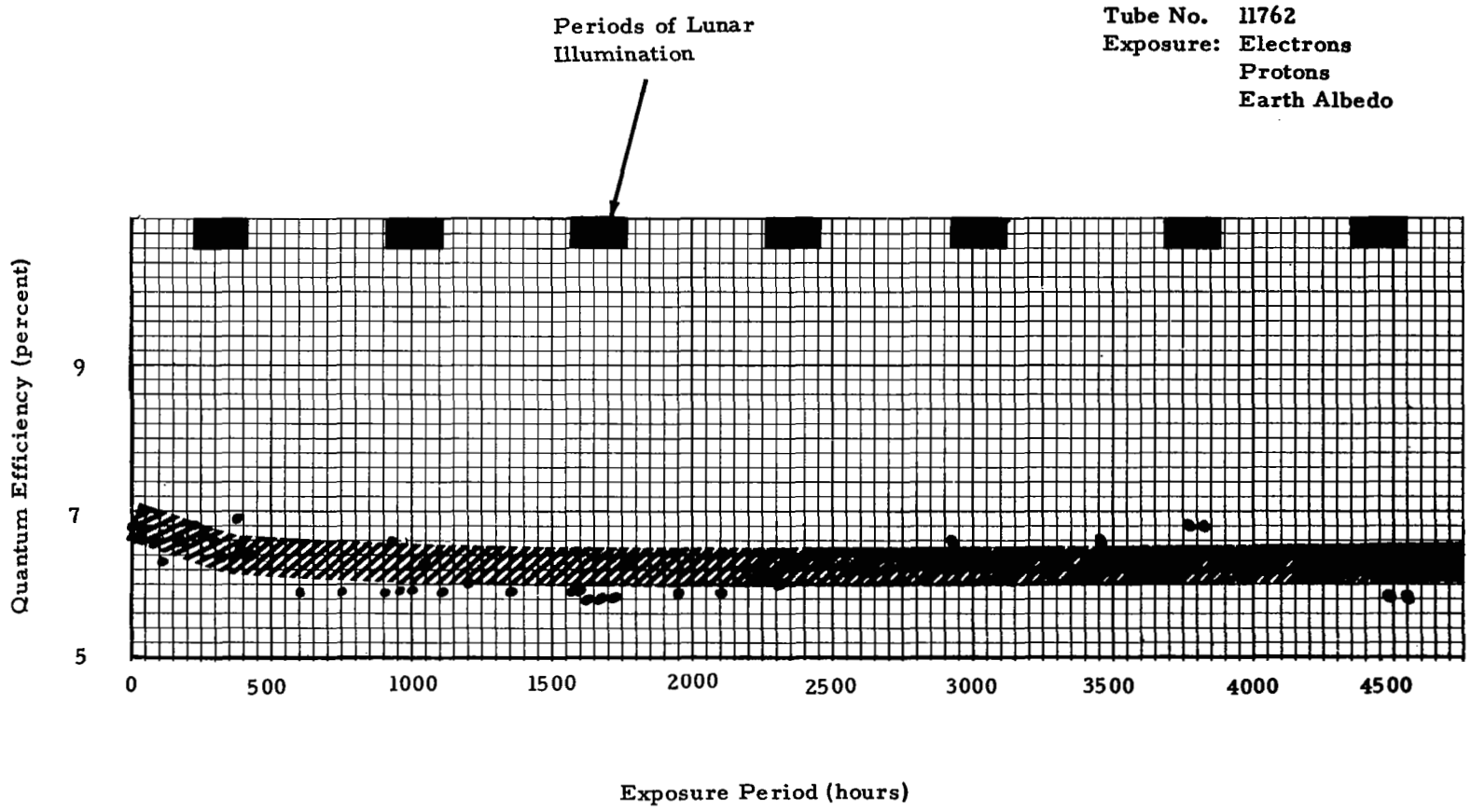

FIGURE 6.2-10 CHANGES IN QUANTUM EFFICIENCY AT 5000 Å WAVELENGTH

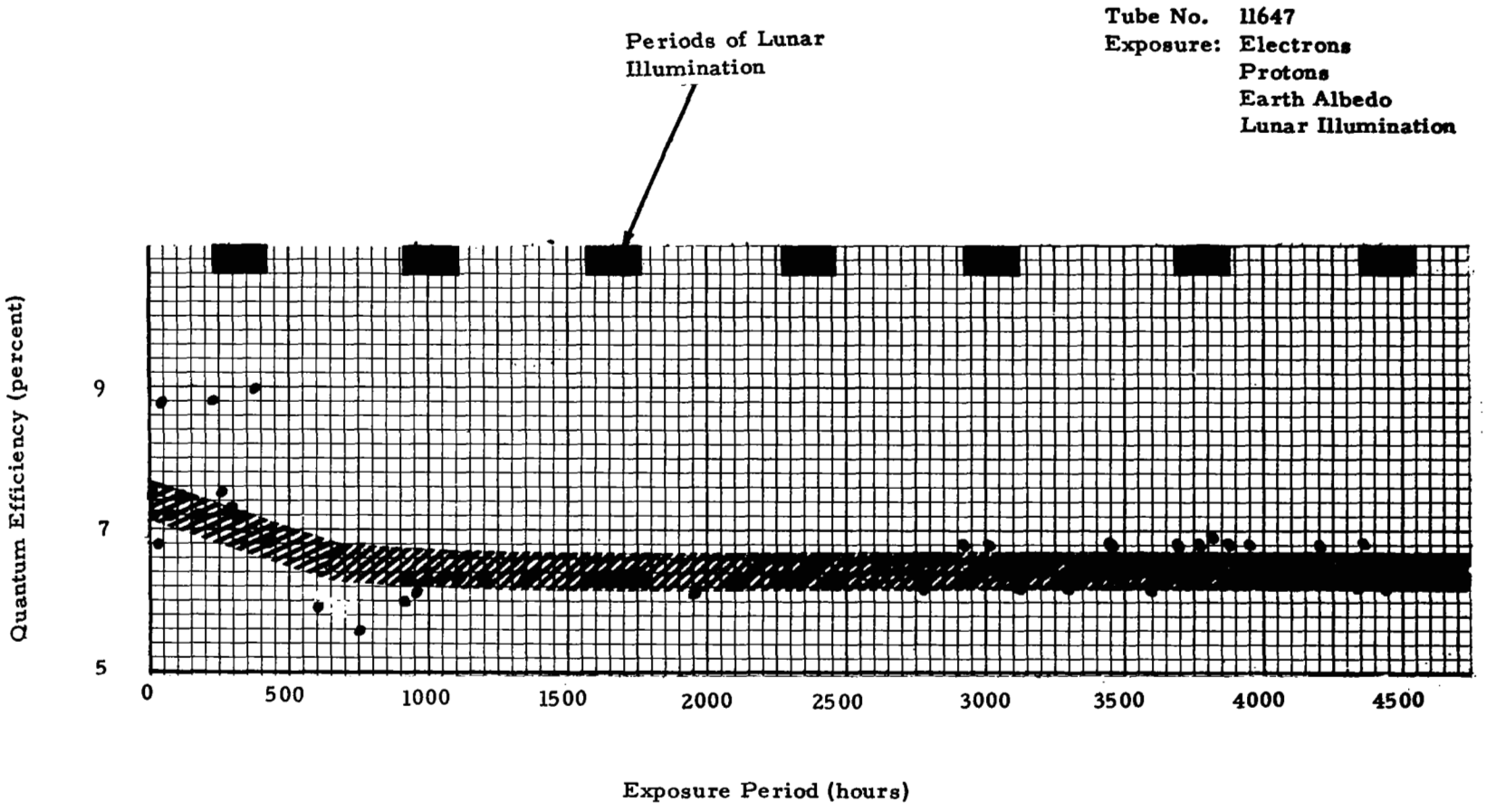

FIGURE 6.2-11 CHANGES IN QUANTUM EFFICIENCY AT 5000 Å WAVELENGTH

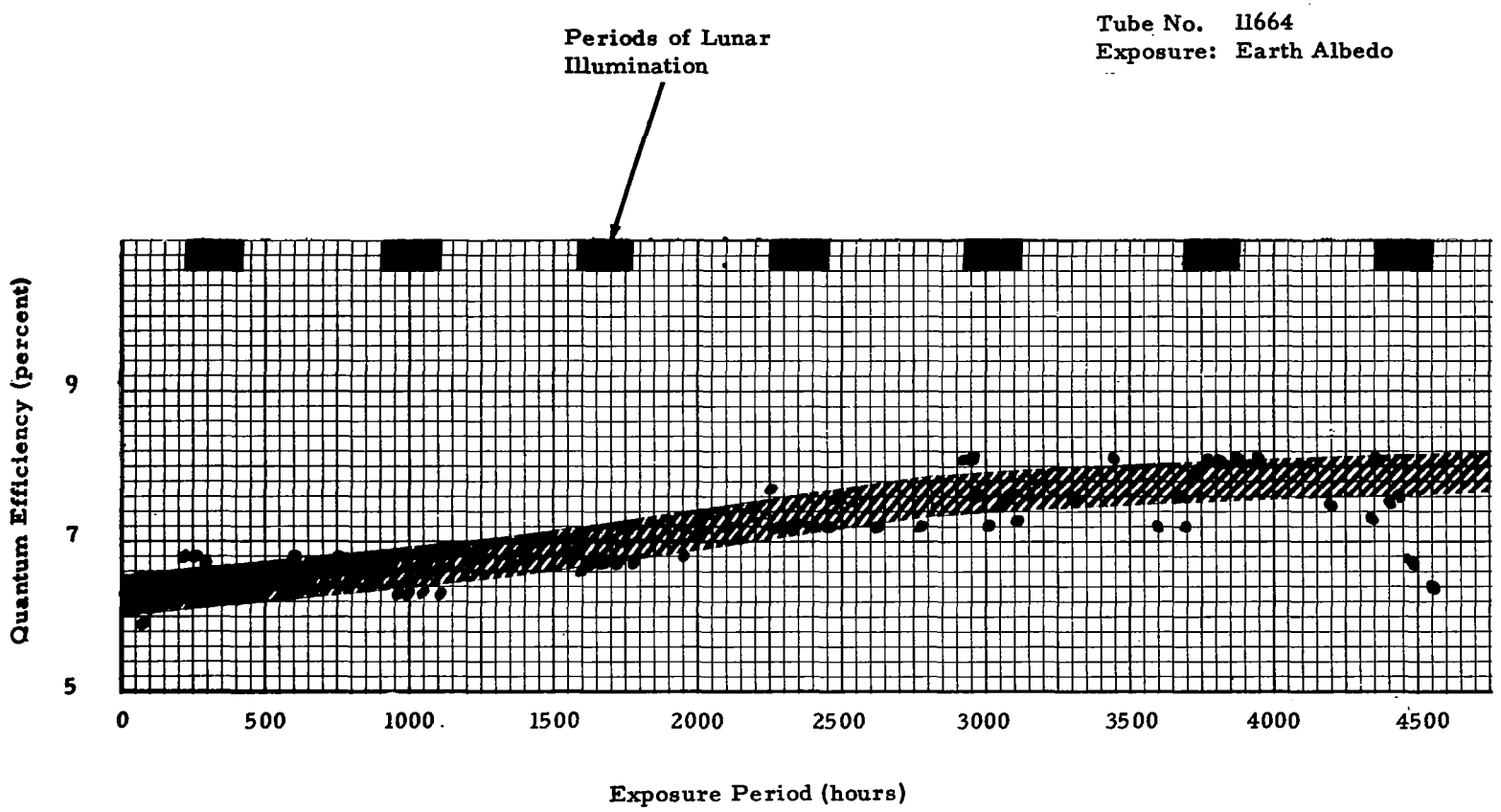

FIGURE 6.2-12 CHANGES IN QUANTUM EFFICIENCY AT 5000 Å WAVELENGTH

Phototube nos. 11644 and 11664 show essentially no change in gain throughout the entire test period (Figures 6.3-1 and 6.3-4). The small increase during the initial 500 hours of exposure returned quickly to the pre-exposure values.

Phototube No. 11762 appears to have suffered a minor increase in voltage required for a gain of 10^6 (Figure 6.3-2). This increase in voltage would indicate a moderate effect from combined irradiation.

Phototube No. 11647 has suffered a substantial amount of degradation in gain (Figure 6.3-3). The increase in voltage which portrays a decrease in phototube gain capability occurred mainly in the initial 500 hours of exposure and then appeared to stabilize for the remaining test period. The primary cause of phototube degradation is the high level of illumination which results in a high anode current during simulated lunar viewing. Had the phototube been pre-conditioned at this anode current, this effect would have been minimized.

6.4 DYNODE STAGES

Measurements of gain between dynode stages were made to assist the manufacturer in assessing the stability of materials used in fabricating the dynodes. But since the test program was arranged to concentrate on measuring overall phototube properties and additional information obtained only where possible without extra cost and complexity, a complete analysis of these data was not accomplished.

During the test program the anode voltage was changed at each measurement to maintain the anode current constant at 2×10^{-6} amps. This adjustment in voltage was required to maintain a constant gain of 10^6 in the phototube and also resulted in maintaining the gain constant in the dynode stages, similarly for 10^4 and 10^5 gains.

6.5 CHARGED PARTICLES

Initial exposure to charged particles was conducted at 20KeV electrons and protons. When the energy level was increased to 35KeV for the remaining test period, there was no significant change. The cycling of electrons and protons throughout the test period did not reveal any corresponding changes in phototube properties.

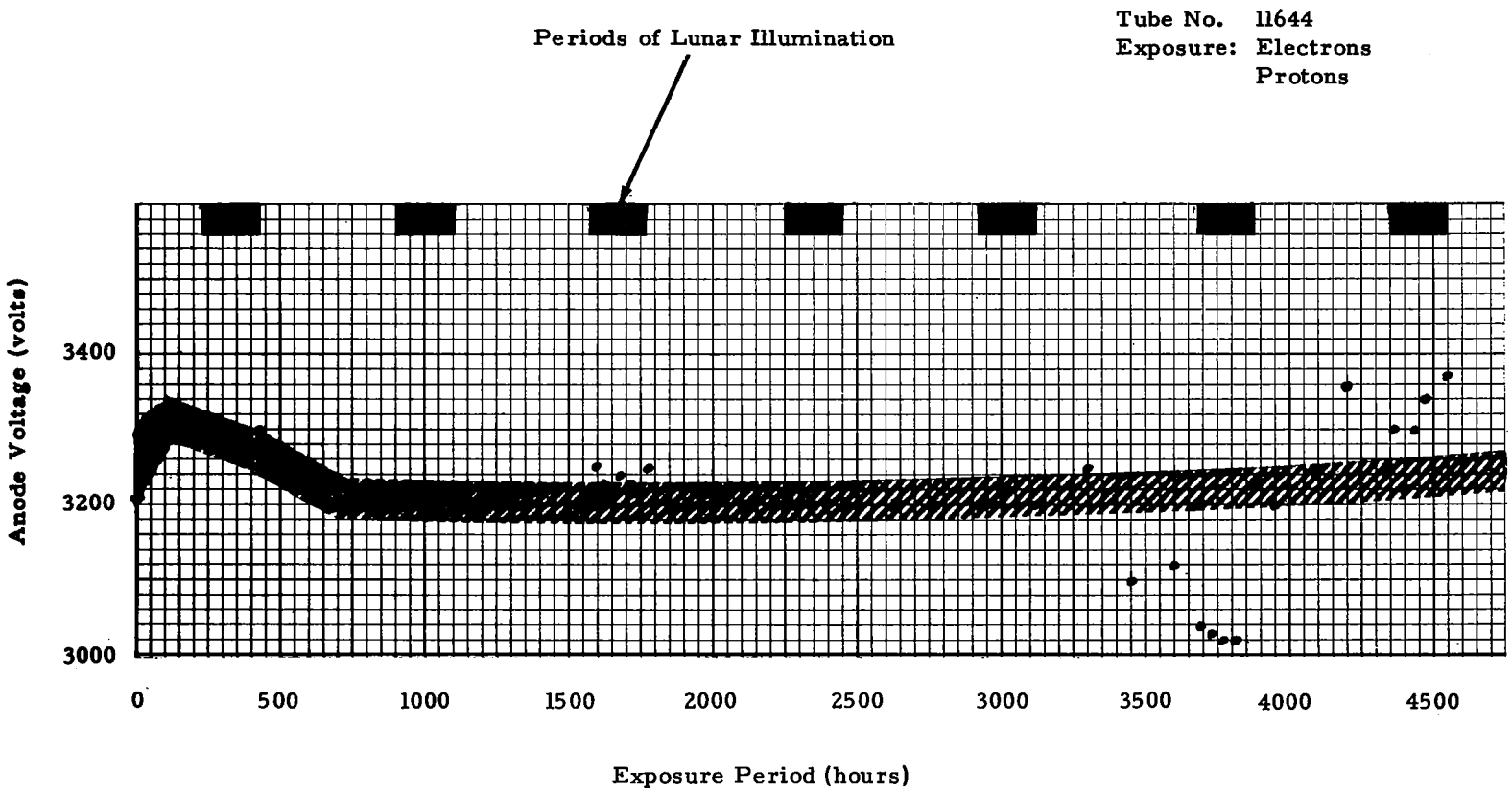

FIGURE 6.3-1 CHANGES IN VOLTAGE AMPLIFICATION AT 10^6 GAIN

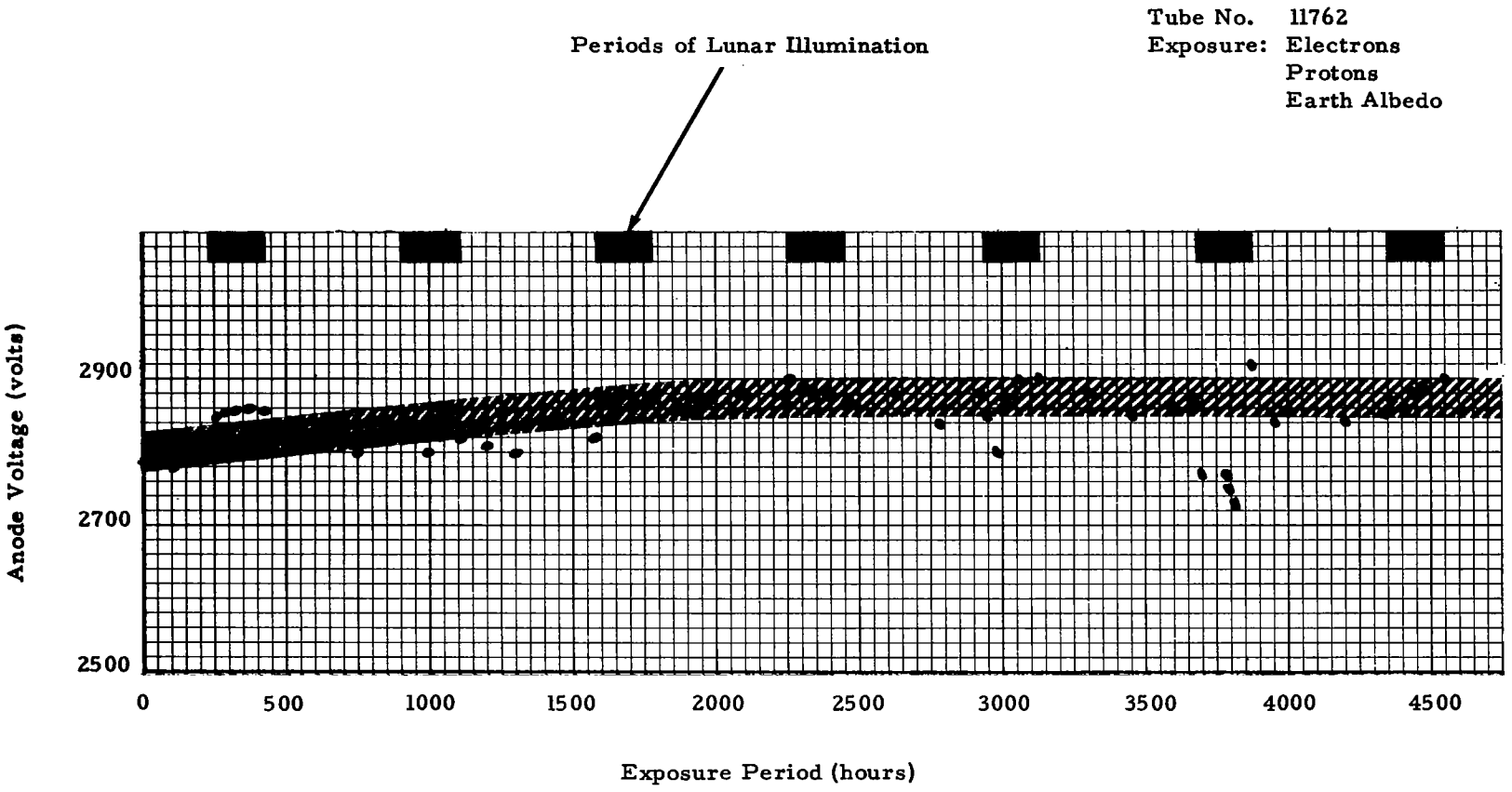

FIGURE 6.3-2 CHANGES IN VOLTAGE AMPLIFICATION AT 10^6 GAIN

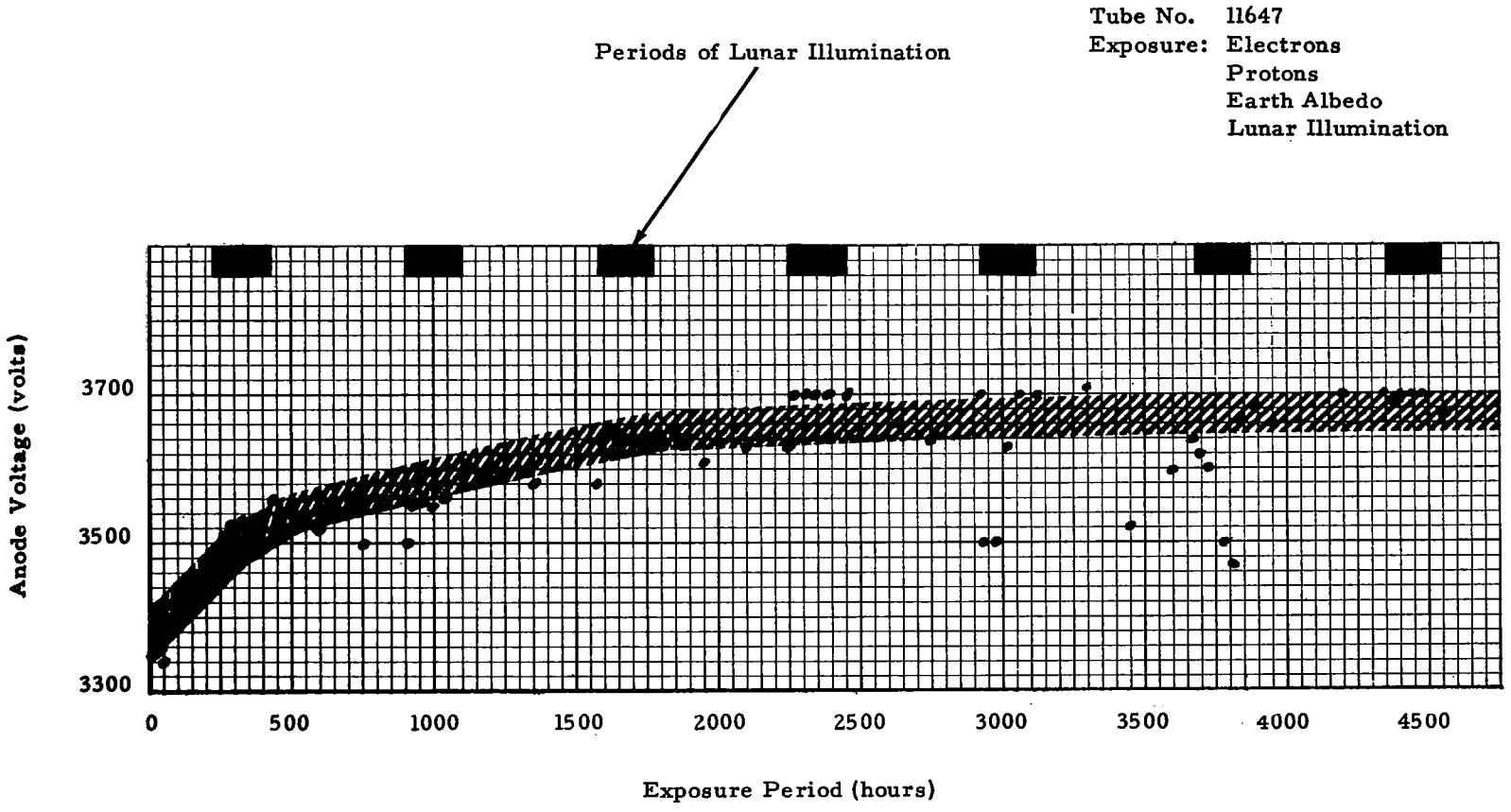

FIGURE 6.3-3 CHANGES IN VOLTAGE AMPLIFICATION AT 10^6 GAIN

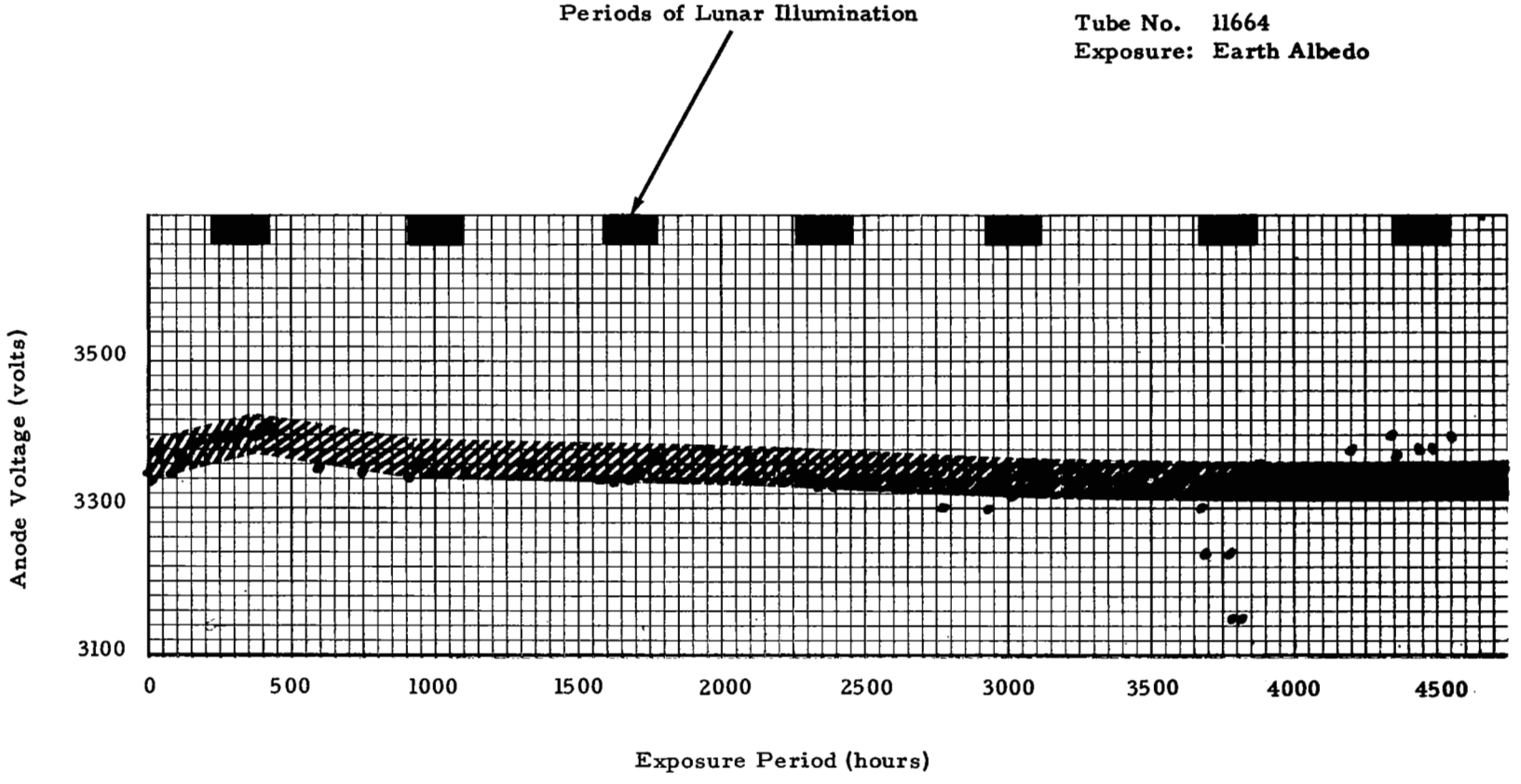

FIGURE 6.3-4 CHANGES IN VOLTAGE AMPLIFICATION AT 10^6 GAIN

6.6 ILLUMINATION EFFECTS

There is a definite increase in degradation when the phototube is exposed to a high level of illumination. Exposure to simulated lunar viewing produced a degradation that appears to be quasi-permanent. The change in dark current which occurred during lunar illumination appears to recover when the phototube is allowed to rest in the dark.

6.7 VISUAL OBSERVATIONS

Inspection of the phototubes after removal from the test apparatus revealed no change in their physical appearance.

SECTION 7.0
CONCLUSIONS

7.1 ELECTRICAL ANALYSIS OF PHOTOTUBE BIASING TECHNIQUES

During operation of the multiplier phototube, the positive side of the high voltage power supply was grounded in order to maintain a low static voltage level with respect to ground and to minimize power supply fluctuations at the phototube output. It was important that the supply voltage be regulated precisely to prevent variations in output from fluctuations in the power supply. A Fluke variable high voltage power supply with regulation of ± .001% and maximum ripple of one mV rms was used for measurements of phototube properties.

For economic reasons, voltage divider resistors were used for the dynode supply voltages rather than individual power supplies. These resistors should be of the low noise type. Since the phototubes were not to be operated under pulse conditions, no capacitors were used with the voltage divider resisters. By eliminating capacitors in the network, variations in the dynode bias voltages due to leakage currents in a capacitor were prevented.

7.2 PHOTOTUBE UTILIZATION

The successful usage of phototubes appears to be greatly dependent upon the level of illumination focused on the photocathode; whereas, exposure to charged particles in the energy range of 35 KeV did not seem to influence their behavior. When both of these radiation sources were combinedsimultaneously, there appeared to be an enhancement in degradation of electrical properties. These changes in properties occurred during the

initial two months of operation and then stabilized at the new value for the remainder of time. If an investigator was interested in long term performance, the phototube should be preconditioned at levels equivalent to expected operational levels. After such preconditioning he could be confident of achieving a successful mission.

SECTION 8.0

RECOMMENDATIONS FOR FUTURE STUDY

8.1 SELF LIMITING PROPERTIES OF PHOTOTUBE

The EMR 541 N multiplier phototube and resistor network exhibits a capability of limiting the anode current relative to input power and cathode illumination. Limiting level appears to be dependent upon resistors selected for the dynode stages. A limiting phototube assembly is desirable to permit operation over a wide range of illumination and to decrease the complexity of operating power supplies. It is proposed that this characteristic of multiplier phototubes assembly be evaluated to define ranges of operation and degree of linearity.

There are four possible sources of saturation in a multiplier phototube. These are:

1.) saturation of the photosensitive cathode
2.) saturation of the secondary emissive surfaces
3.) saturation attributed to "space-charge" effects between electrodes (theoretical consideration)
4.) resistor string effect

In general, of the four possible saturation sources, saturation attributable to space-charge limitations takes place theoretically before the other effects become pronounced.

Because of the construction of the secondary emissive surfaces and the maximum allowable potentials between electrodes, space-charge limitation occurs before the secondary emissive surfaces become saturated. Also, unless an extremely large radiative flux is concentrated on a very small photocathode area, saturation of the photosensitive cathode is not likely to occur before space-charge limitation occurs. The output current at which saturation (as a result of space-charge) occurs is given by the 3/2 power law:

$$I_{o(s)} = K_2(E/10)^{3/2}$$

where $I_{o(s)}$ = Output (anode) current at which saturation occurs

K_2 = Constant of proportionality, amperes per $(\text{Volt})^{3/2}$

E = Overall cathode-to-anode voltage, Volts

In item (4) on the previous page, the effect of a resistor string in the phototube should be evaluated for practical applications. Consideration of equal and unequal resistor values in the resistor string and their effect upon phototube characteristics should be studied to select those resistors which produce optimum performance of the overall phototube.

8.2 PHOTOTUBE OPERATION AT HIGH LEVELS OF ILLUMINATION

In many instances of using multiplier phototubes for measurements from orbiting spacecraft, it is desirable that the phototube withstand exposure to a high level of illumination. Levels of illumination that go beyond the normal operation of a phototube will precipitate new problems for adequate utilization. Some areas which will require further definition include the following:

Stability of dark current properties.
Ability to recover properties after exposure.
Min.-Max. limits of acceptable operation.

8.3 HIGH ENERGY RADIATION EFFECTS

Space radiation effects observed for electronic components due to absorption of energy from the radiation causes either ionization of the target atoms or displacement of those atoms. The ionization effects are generally considered to be temporary within a relatively short time after irradiation ceases. Permanent effects are associated with atomic displacements, which result in disordering of crystal lattices in the component materials. Electron, proton, and bremsstrahlung radiation constitute the three types of radiation that are of primary concern for space electronic applications. The protons and high energy electrons cause significant numbers of atomic displacements. The impingement of high electrons and protons on spacecraft materials is the source of bremsstrahlung radiation which produces primary ionization effects.

The charged particles consisting of electron and proton belts around the Earth are especially degrading to electronic type equipment. Like many electronic devices, the operating characteristics of a multiplier phototube are dependent upon the indigenous environment. Measurements of the operating characteristics of multiplier phototubes during exposure to high energy charged particle irradiation above one MeV are required to further define their stability.

8.4 WRAP AROUND POWER SUPPLY

The use of a power supply integral with the multiplier phototube introduces another consideration in the stability of a detector system. The wrap around type power supply will be susceptible to spatial irradiations and suffer degradation in its characteristics like most electronic components. The net changes that might occur in a phototube - power supply combination needs further evaluation.

SECTION 9.0

APPENDICES

Appendices presented in this section were derived during the period of analysis and testing of four multiple phototubes. Mathematical derivations of two primary constants used in calculating phototube properties are presented in sections 9.1 and 9.2 Data obtained during each period of evaluation are summarized in tabular form in sections 9.3 and 9.4. The time scale reference on the data sheets is in orbits and can be converted to real time by a factor of 1.5, i.e., 1 orbit equals 1.5 hours.

9.1 DERIVATION OF CATHODE RADIANT SENSITIVITY (σ_k)

$$\sigma_k \text{ (Amp/watt)} = \lambda(\mathring{A}) \times \text{Q.E. (\%)} \times 8.0658 \times 10^{-7}$$

$$\sigma_k = \frac{\text{Total Cathode Current}}{\text{Total Incident Power of Photon}} = \frac{A}{B}$$

A = Number of electrons created per unit time (Ne/sec) times charge of one electron (1.6021×10^{-19} coulomb)

B = Number of photons incident per unit time (Nph/sec) times energy of each photon ($E_\lambda = h\nu$)

$$E_\lambda = h\nu = \frac{hc}{\lambda}$$

$h = 6.625 \times 10^{-34}$ Joule-sec

$c = 3 \times 10^{10}$ cm/sec

$\lambda = \lambda\,(\mathring{A}) \times 10^{-8}$ cm

therefore:

$$E_\lambda = \frac{1.9875}{\lambda\,(\mathring{A})} \times 10^{-15} \text{ Watt-sec}$$

(Joule = Watt-sec)

$$\sigma_k = \frac{Ne}{Nph} \times \frac{\lambda(\mathring{A}) \times 1.6021 \times 10^{-19} \text{ (coul/sec)}}{1.9875 \times 10^{-15} \text{ Watt}}$$

(coul/sec = Amp)

However, $\text{Q.E. (\%)} = \frac{Ne}{Nph} \times 100$

Therefore: $\sigma_k = \lambda(\mathring{A}) \times \text{Q.E. (\%)} \times 8.0658 \times 10^{-7} \left(\frac{\text{Amp}}{\text{Watt}}\right)$

For white light:

σ_k is an averaged value for the entire Q. E. spectrum.

9.2 ANODE CURRENT EQUATION

$$Ia = \sigma a \times p \times A$$

p = incident power at the photocathode (W/cm^2)

A = photocathode area (cm^2)

σ_a = anode radiant sensitivity (Amp/W)

$= \sigma_k \times G$

G = Gain

σ_k = cathode radiant sensitivity (see Appendix 9.1)

$$Ia = p \times G \times \sigma_k \times A$$

For the type 541N phototube

$G = 10^6$

$A = 5\ cm^2$

$\sigma_k = 3.2 \times 10^{-2}$ Amp/W for white light

$Ia = p \times 10^6 \times 3.2 \times 10^{-2} \times 5$

$= p\ (W/cm^2) \times 1.6 \times 10^5$ Amp

λ (Å)	11644		11762		11647		11664	
	σ_K (ma/w)	QE (%)	σ_K (ma/w)	QE (%)	σ_K (ma/w)	QE (%)	σ_K (ma/w)	QE (%)
3490	58.2	20.7	58.2	20.7	51	18.1	49	17.4
3990	72.7	22.6	71	22.1	65.5	20.4	60	18.6
4540	54.5	14.9	45.5	12.4	47.5	13.0	45.4	12.4
4720	45.5	12.0	38.2	10.1	40	10.5	34.6	9.1
5000	34.6	8.6	27.4	6.77	30	7.5	25.5	6.33
5260	29.1	6.9	21.8	5.14	24.5	5.8	20	4.72
5520	22.7	5.1	16.4	3.7	18	4.05	13.5	3.04
5970	10.9	2.27	7.64	1.59	7.82	1.63	4.92	1.02
6220	6.5	1.3	4.36	0.87	4.37	0.87	2.0	0.4
6440	4.0	0.77	2.74	0.53	2.36	0.46	0.9	0.176
6940	0.35	0.063	0.25	0.046	0.15	0.027	0.04	0.0072

FIGURE 9.3-1 MEASUREMENTS OF QUANTUM EFFICIENCY

ORBIT 1

λ (Å)	11644		11762		11647		11664	
	σ_K (ma/w)	QE (%)	σ_K (ma/w)	QE (%)	σ_K (ma/w)	QE (%)	σ_K (ma/w)	QE (%)
3490	56.3	20.0	58.2	20.7	49	17.4	49	17.4
3990	72.7	22.6	71	22.1	65.5	20.4	60	18.6
4540	52.7	14.4	45.5	12.4	47.5	13.0	45.4	12.4
4720	45.5	12.0	39.1	10.3	40	10.5	34.6	9.1
5000	34.6	8.6	27.4	6.77	30	7.5	25.5	6.33
5260	28.2	6.65	20.9	4.94	24.5	5.8	20	4.72
5520	22.7	5.1	16.2	3.65	18.2	4.1	13.6	3.06
5970	10.9	2.27	7.47	1.55	7.63	1.53	5.0	1.04
6220	6.4	1.28	4.2	0.84	4.0	0.8	2.0	0.4
6440	3.8	0.73	2.74	0.53	2.18	0.42	0.9	0.176
6940	0.36	0.064	0.24	0.043	0.115	0.023	0.035	0.0063

FIGURE 9.3-2 MEASUREMENTS OF QUANTUM EFFICIENCY

ORBIT 5

λ (Å)	11644		11762		11647		11664	
	σ_K (ma/w)	QE (%)	σ_K (ma/w)	QE (%)	σ_K (ma/w)	QE (%)	σ_K (ma/w)	QE (%)
3490	58.2	20.7	56.3	20.0	51	18.1	47.3	16.8
3990	72.7	22.6	70.0	21.8	64.6	20.2	60	18.6
4540	52.7	14.4	45.5	12.4	46.4	12.7	45	12.3
4720	43.6	11.5	38.2	10.1	38.2	10.05	34	8.9
5000	36.4	9.0	26.4	6.55	29.1	7.22	25	6.2
5260	29.1	6.9	21.8	5.14	23.7	5.6	20	4.72
5520	22.7	5.1	16.2	3.65	17.4	3.93	13.1	2.95
5970	10.5	2.19	7.64	1.59	8.0	1.66	4.5	0.94
6220	6.5	1.3	4.2	0.84	4.37	0.87	1.9	0.38
6440	3.6	0.7	2.5	0.48	2.0	0.39	0.89	0.172
6940	0.35	0.063	0.25	0.046	0.109	0.02	0.04	0.0072

FIGURE 9.3-3 MEASUREMENTS OF QUANTUM EFFICIENCY

ORBIT 10

λ (Å)	11644		11762		11647		11664	
	σ_K (ma/w)	QE (%)	σ_K (ma/w)	QE (%)	σ_K (ma/w)	QE (%)	σ_K (ma/w)	QE (%)
3490	58.2	20.7	56.3	20.0	40	14.2	48.2	17.2
3990	71	22.1	69.1	21.5	63.6	19.8	58.3	18.1
4540	54.5	14.9	44.6	12.2	45.5	12.4	43.6	11.9
4720	47.3	12.4	38.2	10.1	38.2	10.05	34.6	9.1
5000	36.4	9.0	26.4	6.55	29.1	7.22	25.5	6.33
5260	27.4	6.5	20.9	4.94	21.8	5.15	19.6	4.63
5520	21.8	4.9	16.4	3.7	17.2	3.87	13.6	3.06
5970	10.7	2.23	7.27	1.5	7.82	1.63	5.0	1.04
6220	6.2	1.22	4.27	0.85	4.2	0.84	1.82	0.36
6440	3.5	0.67	2.64	0.51	2.18	0.42	0.87	0.168
6940	0.31	0.56	0.24	0.043	0.133	0.024	0.036	0.0065

FIGURE 9.3-4 MEASUREMENTS OF QUANTUM EFFICIENCY

λ (Å)	11644		11762		11647		11664	
	σ_K (ma/w)	QE (%)	σ_K (ma/w)	QE (%)	σ_K (ma/w)	QE (%)	σ_K (ma/w)	QE (%)
3490	56.3	20.0	56.3	20.0	40	14.2	45.5	16.2
3990	72.7	22.6	71	22.1	65.5	20.4	59	18.4
4540	52.7	14.4	44.6	12.2	46.4	12.7	45	12.3
4720	46.4	12.2	38.2	10.1	40	10.5	35	9.2
5000	35.4	8.8	27.4	6.77	27.3	6.77	25	6.2
5260	26.4	6.24	21.8	5.14	20	4.70	20	4.72
5520	20.9	4.7	16.4	3.7	18	4.05	13.4	3.01
5970	10.7	2.23	7.47	1.55	7.63	1.53	5.0	1.04
6220	6.4	1.28	4.2	0.84	4.0	0.8	1.9	0.38
6440	3.54	0.68	2.74	0.53	2.0	0.39	0.9	0.176
6940	0.33	0.059	0.24	0.043	0.142	0.025	0.04	0.0072

FIGURE 9.3-5 MEASUREMENTS OF QUANTUM EFFICIENCY

ORBIT 30

λ (Å)	11644		11762		11647		11664	
	σ_K (ma/w)	QE (%)	σ_K (ma/w)	QE (%)	σ_K (ma/w)	QE (%)	σ_K (ma/w)	QE (%)
3490	58.2	20.7	56.3	20.0	41.8	14.9	45.5	16.2
3990	72.7	22.6	69.1	21.5	65.5	20.4	60	18.6
4540	54.5	14.9	43.6	11.9	45.5	12.4	43.6	11.9
4720	44.5	11.7	36.4	9.6	42.0	11.0	34.6	9.1
5000	36.4	9.0	26.4	6.55	35.5	8.8	25.5	6.33
5260	28.2	6.65	20.0	4.72	21.8	5.15	19.0	4.48
5520	21.8	4.9	16.0	3.6	18.6	4.2	13.3	2.99
5970	10.4	2.16	7.27	1.5	7.82	1.63	4.37	0.91
6220	6.4	1.28	4.0	0.8	4.0	0.8	2.0	0.40
6440	3.36	0.65	2.5	0.48	2.18	0.42	0.89	0.172
6940	0.32	0.057	0.24	0.043	0.155	0.028	0.035	0.0063

FIGURE 9.3-6 MEASUREMENTS OF QUANTUM EFFICIENCY

λ (Å)	11644		11762		11647		11664	
	σ_K (ma/w)	QE (%)	σ_K (ma/w)	QE (%)	σ_K (ma/w)	QE (%)	σ_K (ma/w)	QE (%)
3490	54.5	19.4	54.5	19.4	36.7	13.1	43.6	15.5
3990	69.1	21.5	68.1	21.2	63.6	19.8	58.3	18.1
4540	51.8	14.1	43.6	11.9	46.4	12.7	42.7	11.7
4720	45.5	12.0	36.4	9.6	38.2	10.05	32.7	8.6
5000	32.7	8.1	26.4	6.55	29.1	7.22	23.6	5.85
5260	27.4	6.5	20.0	4.72	23.7	5.6	18.0	4.25
5520	20.9	4.7	16.2	3.65	18.2	4.1	12.8	2.88
5970	10.2	2.12	7.1	1.48	8.0	1.66	4.37	0.91
6220	6.2	1.24	4.0	0.8	4.0	0.8	2.0	0.4
6440	3.27	0.63	2.45	0.47	2.18	0.42	0.9	0.176
6940	0.31	0.056	0.25	0.046	0.145	0.026	0.033	0.006

FIGURE 9.3-7 MEASUREMENTS OF QUANTUM EFFICIENCY

ORBIT 73

λ (Å)	11644		11762		11647		11664	
	σ_K (ma/w)	QE (%)	σ_K (ma/w)	QE (%)	σ_K (ma/w)	QE (%)	σ_K (ma/w)	QE (%)
3490	56.3	20.0	56.3	20.0	36.7	13.1	40	14.2
3990	71	22.1	69.1	21.5	64.6	20.2	57.3	17.8
4540	52.7	14.4	44.6	12.2	47.5	13.0	42.0	11.5
4720	45.5	12.0	37.3	9.8	39	10.3	34.6	9.1
5000	33.6	8.3	25.4	6.3	30	7.5	24.5	6.1
5260	27.4	6.5	20.9	4.94	24.5	5.8	18.6	4.4
5520	21.8	4.9	16.4	3.7	18.0	4.05	12.4	2.8
5970	10.0	2.08	7.47	1.55	7.8	1.62	4.2	0.87
6220	6.4	1.28	4.1	0.82	4.2	0.84	2.09	0.42
6440	3.5	0.67	2.64	0.51	2.18	0.42	1.0	0.193
6940	0.33	0.059	0.26	0.047	0.153	0.027	0.038	0.0068

FIGURE 9.3-8 MEASUREMENTS OF QUANTUM EFFICIENCY

ORBIT 114

λ (Å)	11644		11762		11647		11664	
	σ_K (ma/w)	QE (%)	σ_K (ma/w)	QE (%)	σ_K (ma/w)	QE (%)	σ_K (ma/w)	QE (%)
3490	56.3	20.0	54.5	19.4	43.6	15.5	42.7	15.2
3990	72.7	22.6	71	22.1	65.5	20.4	58.3	18.1
4540	52.7	14.4	45.5	12.4	46.4	12.7	43.6	11.9
4720	45.5	12.0	38.2	10.1	40.0	10.5	36.4	9.6
5000	34.6	8.6	26.4	6.55	29.1	7.22	25.5	6.33
5260	28.2	6.65	20.9	4.94	23.7	5.6	18.0	4.25
5520	21.8	4.9	15.4	3.47	18.6	4.2	13.1	2.95
5970	10.9	2.27	7.1	1.48	7.63	1.53	4.5	.94
6220	6.5	1.3	4.2	.84	4.1	.82	2.18	.42
6440	3.8	.73	2.5	.48	2.18	.42	.9	.176
6940	.33	.059	.27	.047	.15	.027	.036	.0065

FIGURE 9.3-9 MEASUREMENTS OF QUANTUM EFFICIENCY

ORBIT 155.5

λ (Å)	11644		11762		11647		11664	
	σ_K (ma/w)	QE (%)	σ_K (ma/w)	QE (%)	σ_K (ma/w)	QE (%)	σ_K (ma/w)	QE (%)
3490	54.5	19.4	58.2	20.7	47.3	16.8	40	14.2
3990	74.5	23.2	71	22.1	64.6	20.2	59	18.4
4540	54.5	14.9	45.5	12.4	47.5	13.0	43.6	11.9
4720	45.5	12.0	36.4	9.6	39	10.3	36.4	9.6
5000	34.6	8.6	27.4	6.77	35.5	8.8	27.3	6.77
5260	29.1	6.9	21.8	5.14	24.5	5.8	20	4.72
5520	22.7	5.1	16.4	3.7	18.2	4.1	12.8	2.88
5970	10.9	2.27	7.27	1.5	7.82	1.63	4.92	1.02
6220	6.5	1.3	4.36	.87	4.2	.42	2.36	.44
6440	4.0	.77	2.5	.48	2.36	.46	1.0	.193
6940	.35	.063	.27	.047	.164	.0295	.042	.0075

FIGURE 9.3-10 MEASUREMENTS OF QUANTUM EFFICIENCY

ORBIT 168

λ (Å)	11644		11762		11647		11664	
	σ_K (ma/w)	QE (%)	σ_K (ma/w)	QE (%)	σ_K (ma/w)	QE (%)	σ_K (ma/w)	QE (%)
3490	58.2	20.7	58.2	20.7	51.0	18.1	47.3	16.8
3990	76.4	23.7	71.0	22.1	65.5	20.4	58.3	18.1
4540	52.7	14.4	46.4	12.7	48.2	13.2	41.8	11.4
4720	45.5	12.0	38.2	10.0	39	10.3	36.4	9.6
5000	32.7	8.12	27.3	6.67	30	7.5	27.3	6.77
5260	29.1	6.86	21.8	5.15	24.5	5.8	20.0	4.72
5520	21.8	4.9	11.75	2.64	18.2	4.1	14.3	3.22
5970	10.9	2.27	7.65	1.59	8.18	1.7	4.36	9.09
6220	6.55	1.31	4.36	0.87	4.37	0.87	2.36	0.44
6440	3.81	0.735	2.54	0.49	2.36	0.46	1.03	0.199
6940	0.346	0.062	0.29	0.052	0.165	0.0296	0.0418	0.0075

FIGURE 9.3-11 MEASUREMENTS OF QUANTUM EFFICIENCY

ORBIT 193

λ (Å)	11644		11762		11647		11664	
	σ_K (ma/w)	QE (%)	σ_K (ma/w)	QE (%)	σ_K (ma/w)	QE (%)	σ_K (ma/w)	QE (%)
3490	54.6	19.4	51.0	18.1	47.2	16.8	41.8	14.9
3990	74.5	23.2	67.3	20.9	63.0	19.6	58.5	18.2
4540	54.0	14.7	45.5	12.4	46.0	12.6	43.0	11.8
4720	45.7	12.0	37.8	9.9	38.5	10.2	36.9	9.7
5000	34.6	8.58	26.4	6.55	29.4	7.3	27.1	6.73
5260	28.8	6.8	21.8	5.15	23.6	5.56	21.3	5.3
5520	22.6	5.09	16.7	3.76	18.2	4.1	14.3	3.22
5970	10.9	2.27	7.45	1.55	17.8	3.7	4.9	1.02
6220	6.1	1.22	4.2	.82	4.30	.86	2.33	.47
6440	3.82	.737	2.4	.464	2.25	.434	1.07	.206
6940	.331	.059	.269	.048	.147	.026	.046	.0082

FIGURE 9.3-12 MEASUREMENTS OF QUANTUM EFFICIENCY

ORBIT 218

λ (Å)	11644		11762		11647		11664	
	σ_K (ma/w)	QE (%)	σ_K (ma/w)	QE (%)	σ_K (ma/w)	QE (%)	σ_K (ma/w)	QE (%)
3490	84.5	19.4	52.7	18.8	49	17.4	43.6	15.5
3990	74.5	23.2	68.1	21.2	62.9	19.5	58.3	18.1
4540	52.7	14.4	44.6	12.2	46.4	12.7	42.7	11.7
4720	45.5	12.0	37.3	9.8	39	10.3	34.6	9.1
5000	34.6	8.6	25.8	6.4	29.1	7.22	26.4	6.55
5260	28.0	6.60	21.8	5.14	24.5	5.59	19.0	4.48
5520	22.5	5.08	16.0	3.60	18.2	4.1	13.9	3.13
5970	10.9	2.27	7.37	1.52	7.9	1.64	4.82	1.00
6220	6.2	1.24	4.2	.84	4.29	.85	2.27	.43
6440	3.9	.755	2.36	.456	2.26	.434	1.03	.199
6940	.333	.060	.27	.047	.145	.026	.043	.0077

FIGURE 9.3-13 MEASUREMENTS OF QUANTUM EFFICIENCY

ORBIT 249

λ (Å)	11644		11762		11647		11664	
	σ_K (ma/w)	QE (%)	σ_K (ma/w)	QE (%)	σ_K (ma/w)	QE (%)	σ_K (ma/w)	QE (%)
3490	88.2	20.7	56.1	20.0	51.0	18.1	47.3	16.8
3990	76.0	23.6	68.8	21.4	63.6	19.8	58.7	18.3
4540	51.8	14.1	44.6	12.2	46.2	12.6	43.6	11.9
4720	44.6	12.2	36.4	9.6	38.2	10.05	34.6	9.1
5000	34.0	8.42	26.1	6.9	35.7	9.0	25.5	6.33
5260	27.7	6.56	21.3	5.02	22.8	5.37	20.0	4.72
5520	22.5	5.08	16.6	3.73	18.0	4.05	13.6	3.06
5970	11.0	2.29	7.37	1.52	8.0	1.66	4.7	.98
6220	6.4	1.28	4.2	.84	4.26	.85	2.26	.45
6440	4.0	.77	2.45	.47	2.29	.442	1.02	.197
6940	.34	.611	.27	.047	.145	.026	.0418	.0075

FIGURE 9.3-14 MEASUREMENTS OF QUANTUM EFFICIENCY

ORBIT 292.5

λ (Å)	11644		11762		11647		11664	
	σ_K (ma/w)	QE (%)	σ_K (ma/w)	QE (%)	σ_K (ma/w)	QE (%)	σ_K (ma/w)	QE (%)
3490	60.7	21.6	56.7	20.1	48.2	17.2	51	18.1
3990	76.4	23.7	67.6	21.0	62.8	19.4	57.9	18.0
4540	49.8	13.6	43.9	12.0	44.5	12.1	42.0	11.5
4720	43.2	11.3	35.4	9.33	35.5	9.4	34	8.9
5000	32.7	8.1	25.8	6.4	27.3	6.77	25.5	6.33
5260	27.0	6.39	21.4	5.06	21.8	5.15	19.0	4.48
5520	21.6	4.8	16.4	3.7	18.6	4.2	13.6	3.06
5970	10.8	2.25	7.3	1.51	7.46	1.55	4.71	.98
6220	6.3	1.26	4.1	.82	3.71	7.4	2.22	.43
6440	3.7	.71	2.38	.46	2.04	.43	1.02	.197
6940	.331	.059	.266	.048	.137	.024	.046	.0082

FIGURE 9.3-15 MEASUREMENTS OF QUANTUM EFFICIENCY

ORBIT 400

λ (Å)	11644		11762		11647		11664	
	σ_K (ma/w)	QE (%)	σ_K (ma/w)	QE (%)	σ_K (ma/w)	QE (%)	σ_K (ma/w)	QE (%)
3490	58.2	20.7	54.5	19.4	48.8	17.3	52.7	18.8
3990	76.4	23.7	67.3	20.9	63.6	19.8	58.2	18.1
4540	51.9	14.1	44.6	12.2	42.1	11.4	43.6	11.9
4720	43.0	11.2	32.7	8.6	32.8	8.64	36.4	9.6
5000	33.6	8.3	23.6	5.86	23.6	5.86	27.3	6.77
5260	27.4	6.5	18.2	4.30	20.0	4.72	21.1	5.2
5520	21.8	4.9	14.2	3.20	14.7	3.31	14.3	3.22
5970	10.9	2.27	6.28	1.31	6.0	1.25	4.36	.909
6220	6.55	1.31	3.36	.672	2.91	.582	2.36	.44
6440	4.0	.77	1.91	.369	1.53	.295	1.08	.207
6940	.36	.064	.20	.0358	.0727	.0130	.0473	.0085

FIGURE 9.3-16 MEASUREMENTS OF QUANTUM EFFICIENCY

ORBIT 500

λ (Å)	11644		11762		11647		11664	
	σ_K (ma/w)	QE (%)	σ_K (ma/w)	QE (%)	σ_K (ma/w)	QE (%)	σ_K (ma/w)	QE (%)
3490	64.7	23.1	53.1	18.9	45.8	16.3	49.5	17.6
3990	80.0	24.9	67.3	20.9	60.0	18.7	61.8	19.2
4540	51.0	13.9	40.0	10.9	39.1	10.7	43.6	11.9
4720	42.7	11.2	31.8	8.36	32.8	8.63	36.4	9.57
5000	32.7	8.12	23.6	5.86	22.7	5.63	27.3	6.77
5260	27.3	6.45	18.2	4.30	20.0	4.72	21.1	4.98
5520	21.8	4.9	13.8	3.13	14.6	3.29	14.9	3.35
5970	10.7	2.22	6.0	1.25	6.0	1.25	5.45	1.13
6220	6.36	1.27	3.27	.655	3.09	.62	2.54	.508
6440	4.0	.772	1.91	.369	1.47	.2847	1.28	.247
6940	.37	.0662	.21	.0376	.067	.012	.0555	.0075

FIGURE 9.3-17 MEASUREMENTS OF QUANTUM EFFICIENCY

ORBIT 603.5

λ (Å)	11644		11762		11647		11664	
	σ_K (ma/w)	QE (%)	σ_K (ma/w)	QE (%)	σ_K (ma/w)	QE (%)	σ_K (ma/w)	QE (%)
3490	63.6	22.7	58.2	20.7	47.3	16.8	52.7	18.8
3990	80.0	24.9	65.5	20.4	58.2	18.1	63.6	19.8
4540	52.7	14.4	40.0	10.9	40.0	10.9	44.5	12.2
4720	43.6	11.5	32.7	8.60	31.8	8.36	37.5	9.87
5000	34.6	8.59	23.6	5.85	24.0	5.95	27.3	6.77
5260	27.3	6.45	18.2	4.29	19.1	4.51	21.8	5.14
5520	21.8	4.91	13.6	3.06	14.2	3.30	15.3	3.44
5970	10.9	2.27	6.0	12.5	5.82	1.21	5.45	1.13
6220	6.55	1.31	3.28	6.56	2.82	.564	2.55	.510
6440	4.0	.773	1.91	.369	1.42	.274	1.22	.235
6940	.346	.062	.182	.033	.0655	.012	.073	.008

FIGURE 9.3-18 MEASUREMENTS OF QUANTUM EFFICIENCY

ORBIT 616

λ (Å)	11644		11762		11647		11664	
	σ_K (ma/w)	QE (%)	σ_K (ma/w)	QE (%)	σ_K (ma/w)	QE (%)	σ_K (ma/w)	QE (%)
3490	67.3	24.0	61.8	22.0	50.9	18.1	52.7	18.8
3990	78.1	24.3	67.3	20.9	60.9	18.9	61.9	19.3
4540	54.5	14.9	43.6	11.9	40.0	10.9	46.3	12.7
4720	43.6	11.5	32.7	8.60	33.6	8.85	37.3	9.82
5000	34.6	8.58	26.4	6.55	25.4	6.30	26.4	6.55
5260	29.1	6.87	18.2	4.29	20.0	4.72	21.8	5.14
5520	21.8	4.91	14.0	3.15	14.4	3.24	14.7	3.31
5970	11.3	2.35	6.18	1.29	5.82	1.21	5.45	1.13
6220	6.36	1.27	3.27	.654	2.91	.582	2.73	.546
6440	4.0	.773	1.91	.369	1.47	.284	1.24	.239
6940	.346	.062	.200	.036	.0636	.011	.0455	.008

FIGURE 9.3-19 MEASUREMENTS OF QUANTUM EFFICIENCY

ORBIT 641

λ (Å)	11644		11762		11647		11664	
	σ_K (ma/w)	QE (%)	σ_K (ma/w)	QE (%)	σ_K (ma/w)	QE (%)	σ_K (ma/w)	QE (%)
3490	58.2	20.7	54.5	19.4	90.9	18.1	94.5	19.4
3990	78.2	24.3	69.9	20.4	61.8	19.2	61.8	19.2
4540	52.7	14.4	41.8	11.4	40.0	10.9	44.5	12.2
4720	53.6	14.1	34.6	9.10	34.5	9.08	38.2	10.0
5000	32.7	8.12	23.6	5.86	24.5	6.08	25.4	6.30
5260	29.1	6.87	17.8	4.20	20.0	4.72	20.0	4.72
5520	21.8	4.91	13.6	3.08	14.6	3.29	14.9	3.35
5970	10.9	2.27	5.64	1.17	6.0	1.25	5.49	1.13
6220	6.36	1.27	3.09	.618	3.09	.618	2.18	.436
6440	3.82	.742	1.91	.369	1.91	.292	1.24	.239
6940	.374	.067	.182	.033	.0600	.011	.0436	.008

FIGURE 9.3-20 MEASUREMENTS OF QUANTUM EFFICIENCY

ORBIT 666

λ (Å)	11644		11762		11647		11664	
	σ_K (ma/w)	QE (%)	σ_K (ma/w)	QE (%)	σ_K (ma/w)	QE (%)	σ_K (ma/w)	QE (%)
3490	67.3	24.0	60.0	21.4	90.9	18.1	56.4	20.1
3990	78.2	24.3	65.5	20.4	60.0	18.7	61.8	19.2
4540	52.7	14.4	40.0	10.9	41.0	11.2	43.6	11.9
4720	43.6	11.5	32.7	8.60	32.7	8.60	38.2	10.0
5000	32.7	8.12	23.6	5.86	25.4	6.30	25.4	6.30
5260	29.1	6.87	18.2	4.29	20.0	5.72	22.7	5.36
5520	21.8	4.91	14.2	3.19	14.7	3.31	14.7	3.31
5970	11.3	2.35	6.18	1.29	6.00	1.25	5,64	1.17
6220	6.55	1.31	2.54	.508	2.91	.582	2.73	.546
6440	4.0	.772	1.82	.351	1.53	.295	1.27	.245
6940	.346	.062	.200	.036	.0727	.013	.0491	.009

FIGURE 9.3-21 MEASUREMENTS OF QUANTUM EFFICIENCY

ORBIT 697

λ (Å)	11644		11762		11647		11664	
	σ_K (ma/w)	QE (%)	σ_K (ma/w)	QE (%)	σ_K (ma/w)	QE (%)	σ_K (ma/w)	QE (%)
3490	65.5	23.3	60.0	21.4	54.5	19.4	54.5	19.4
3990	80.0	24.9	65.5	20.4	60.0	18.7	61.8	19.2
4540	52.7	14.4	40.0	10.9	41.8	11.4	45.5	12.4
4720	45.5	12.0	34.6	9.10	33.6	8.85	38.2	10.0
5000	32.7	8.12	29.4	6.30	29.4	6.30	29.4	6.30
5260	29.1	6.87	18.2	4.29	20.0	4.72	21.8	5.14
5520	21.8	4.91	14.4	3.24	15.6	3.51	14.9	3.35
5970	11.3	2.35	6.36	1.32	6.18	1.29	5.45	1.13
6220	6.73	1.35	3.27	.654	3.00	.600	2.64	.528
6440	4.18	.806	2.00	.386	1.51	.292	1.26	.243
6940	.364	.065	.200	.036	.0727	.013	.0491	.009

FIGURE 9.3-22 MEASUREMENTS OF QUANTUM EFFICIENCY

ORBIT 740.5

λ (Å)	11644		11762		11647		11664	
	σ_K (ma/w)	QE (%)	σ_K (ma/w)	QE (%)	σ_K (ma/w)	QE (%)	σ_K (ma/w)	QE (%)
3490	65.5	23.3	60.0	21.4	54.6	19.4	54.6	19.4
3990	80.0	24.9	65.5	20.4	60.0	18.7	61.9	19.3
4540	52.7	14.4	41.8	11.4	40.9	11.2	45.5	12.4
4720	45.5	12.0	32.7	8.60	33.6	8.84	38.9	10.2
5000	34.5	8.55	23.6	5.86	25.5	6.33	29.4	6.30
5260	29.1	6.87	18.2	4.29	20.9	4.93	21.8	5.14
5520	21.8	4.91	14.4	3.24	14.9	3.35	15.1	3.40
5970	11.5	2.39	6.00	1.25	6.0	1.25	5.82	1.21
6220	6.73	1.35	3.45	.690	3.0	.600	2.73	.547
6440	4.18	0.808	1.94	.374	1.57	.303	1.28	.247
6940	.364	.065	.200	.036	.0691	.012	.0473	.008

FIGURE 9.3-23 MEASUREMENTS OF QUANTUM EFFICIENCY

ORBIT 800

λ (Å)	11644		11762		11647		11664	
	σ_K (ma/w)	QE (%)	σ_K (ma/w)	QE (%)	σ_K (ma/w)	QE (%)	σ_K (ma/w)	QE (%)
3490	65.5	23.3	60.0	21.4	50.9	18.1	58.2	20.7
3990	76.8	23.9	64.4	20.0	61.1	19.0	61.9	19.2
4540	52.7	14.4	41.5	11.3	41.8	11.4	43.6	11.9
4720	45.5	12.0	36.4	9.57	34.6	9.1	40.0	10.5
5000	33.9	8.4	24.2	6.0	25.4	6.3	27.3	6.77
5260	27.3	6.45	20.0	4.71	18.2	4.3	23.6	5.57
5520	21.8	4.91	14.5	3.26	14.5	3.26	16.0	3.60
5970	11.5	2.39	6.55	1.36	6.00	1.25	5.82	1.21
6220	6.92	1.38	3.09	0.62	2.91	0.582	2.73	0.546
6440	4.18	0.808	1.82	0.35	1.56	0.3	0.436	0.042
6940	0.364	0.065	0.236	0.042	0.0782	0.014	0.0527	0.0094

FIGURE 9.3-24 MEASUREMENTS OF QUANTUM EFFICIENCY

ORBIT 900

λ (Å)	11644		11762		11647		11664	
	σ_K (ma/w)	QE (%)	σ_K (ma/w)	QE (%)	σ_K (ma/w)	QE (%)	σ_K (ma/w)	QE (%)
3490	66.3	23.6	60.0	21.4	52.7	18.8	56.4	20.1
3990	76.0	23.6	63.6	19.8	60.0	18.7	62.3	19.4
4540	52.7	14.4	41.5	11.3	41.8	11.4	45.2	12.3
4720	45.5	12.0	32.7	8.61	34.6	9.1	40.0	10.5
5000	34.6	8.58	23.6	5.86	25.4	6.3	26.8	6.65
5260	29.1	6.87	18.2	4.30	20.0	4.72	23.6	5.57
5520	22.7	5.11	14.2	3.19	14.9	3.35	16.0	3.60
5970	11.5	2.39	5.82	1.21	6.0	1.25	5.82	1.21
6220	6.91	1.38	3.18	0.636	2.91	0.58	2.91	0.582
6440	4.18	0.808	1.29	0.249	1.45	0.28	1.36	0.262
6940	0.364	0.005	0.182	0.032	0.0727	0.013	0.0545	0.0098

FIGURE 9.3-25 MEASUREMENTS OF QUANTUM EFFICIENCY

ORBIT 1051.5

λ (Å)	11644		11762		11647		11664	
	σ_K (ma/w)	QE (%)	σ_K (ma/w)	QE (%)	σ_K (ma/w)	QE (%)	σ_K (ma/w)	QE (%)
3490	66.3	23.6	58.2	20.7	58.2	20.7	54.5	19.4
3990	76.5	23.8	63.0	19.6	60.5	18.8	61.8	19.2
4540	52.4	14.3	41.8	11.4	41.8	11.4	45.5	12.4
4720	43.6	11.5	32.7	8.61	34.5	9.08	38.2	10.1
5000	34.7	8.63	23.6	5.86	25.4	6.3	27.5	6.8
5260	29.1	6.87	20.0	4.72	21.8	5.14	20.0	4.72
5520	21.8	4.9	14.5	3.26	14.9	3.35	15.3	3.45
5970	11,5	2.39	5.82	1.21	5.64	1.7	6.0	1.25
6220	6.73	1.35	3.45	0.69	2.91	0.582	2.91	0.582
6440	4.18	0.808	2.0	0.386	1.55	0.3	1.29	0.25
6940	0.273	0.049	0.182	0.033	0.727	0.013	0.0545	0.01

FIGURE 9.3-26 MEASUREMENTS OF QUANTUM EFFICIENCY

ORBIT 1064

λ (Å)	11644		11762		11647		11664	
	σ_K (ma/w)	QE (%)	σ_K (ma/w)	QE (%)	σ_K (ma/w)	QE (%)	σ_K (ma/w)	QE (%)
3490	64.4	22.9	58.2	20.7	50.9	18.1	56.0	19.9
3990	76.0	23.6	61.8	19.2	58.0	18.0	62.3	19.4
4540	52.7	14.4	41.8	11.4	40.9	11.2	45.5	12.4
4720	45.5	12.0	32.7	8.61	34.6	9.1	38.2	10.1
5000	34.5	8.56	23.6	5.86	25.4	6.30	25.6	6.6
5260	29.1	6.87	18.2	4.30	20.0	4.72	21.8	5.14
5520	21.6	5.0	13.8	3.11	14.6	3.29	15.8	3.55
5970	11.6	2.41	6.0	1.25	5.82	1.21	5.82	1.21
6220	6.92	1.38	3.27	0.654	2.91	0.582	2.73	0.546
6440	4.18	0.808	1.82	0.351	1.46	0.282	1.35	0.261
6940	0.373	0.067	0.200	0.036	0.062	0.011	0.0545	0.01

FIGURE 9.3-27 MEASUREMENTS OF QUANTUM EFFICIENCY

ORBIT 1089

λ (Å)	11644		11762		11647		11664	
	σ_K (ma/w)	QE (%)	σ_K (ma/w)	QE (%)	σ_K (ma/w)	QE (%)	σ_K (ma/w)	QE (%)
3490	64.9	23.1	57.9	20.6	50.7	18.0	57.9	20.6
3990	76.3	23.7	61.5	19.1	59.1	18.4	61.9	19.3
4540	52.7	14.4	41.6	11.4	41.6	11.4	45.2	12.3
4720	45.4	11.9	32.6	8.6	32.6	8.6	38.0	10.0
5000	36.3	8.7	23.5	5.8	25.3	6.3	27.0	6.7
5260	29.0	6.8	18.1	4.3	19.9	4.7	23.6	5.6
5520	22.7	5.1	13.7	3.1	14.5	3.3	15.9	3.6
5970	11.2	2.3	5.8	1.2	5.8	1.2	5.8	1.2
6220	6.7	1.3	3.3	0.66	2.9	0.58	2.9	0.58
6440	4.1	0.8	1.8	0.35	1.5	0.29	1.3	0.25
6940	0.362	0.065	0.18	0.032	0.063	0.011	0.054	0.0097

FIGURE 9.3-28 MEASUREMENTS OF QUANTUM EFFICIENCY

ORBIT 1114

λ (Å)	11644		11762		11647		11664	
	σ_K (ma/w)	QE (%)	σ_K (ma/w)	QE (%)	σ_K (ma/w)	QE (%)	σ_K (ma/w)	QE (%)
3490	64.9	23.1	57.9	20.6	50.7	18.0	57.9	20.6
3990	76.0	23.6	61.5	19.2	58.8	18.3	61.9	19.2
4540	52.0	14.2	41.6	11.4	39.8	10.9	45.3	12.4
4720	45.3	11.9	30.8	8.1	32.6	8.6	36.2	9.5
5000	34.6	8.6	23.5	5.8	25.3	6.3	27.0	6.7
5260	27.2	6.4	18.1	4.3	19.9	4.7	23.5	5.5
5520	22.7	5.1	13.8	3.1	14.5	3.3	15.7	3.5
5970	11.0	2.3	5.8	1.2	5.6	1.2	5.8	1.2
6220	6.5	1.3	3.1	0.62	2.7	0.54	2.7	0.54
6440	4.0	0.77	1.8	0.35	1.5	0.3	1.3	0.25
6940	0.36	0.065	0.10	0.032	0.07	0.013	0.054	.0097

FIGURE 9.3-29 MEASUREMENTS OF QUANTUM EFFICIENCY

ORBIT 1145

λ (Å)	11644		11762		11647		11664	
	σ_K (ma/w)	QE (%)	σ_K (ma/w)	QE (%)	σ_K (ma/w)	QE (%)	σ_K (ma/w)	QE (%)
3490	66.0	23.5	57.9	20.6	50.7	18.0	54.3	19.3
3990	75.2	23.4	61.5	19.1	58.8	18.3	61.9	19.3
4540	52.4	14.3	41.6	11.4	41.6	11.4	45.3	12.4
4720	45.3	11.9	32.6	8.6	32.6	8.6	38.0	10.0
5000	34.3	8.5	23.5	5.8	25.3	6.3	27.0	6.7
5260	29.0	6.8	18.1	4.3	20.0	4.7	23.5	5.5
5520	22.7	5.1	13.8	3.1	14.5	3.3	15.6	3.5
5970	11.6	2.4	6.0	1.3	6.0	1.3	5.8	1.2
6220	6.7	1.3	3.1	0.62	2.9	0.58	2.9	0.58
6440	4.2	0.81	1.8	0.35	1.4	0.27	1.3	0.25
6940	0.36	0.065	0.18	0.032	0.072	0.013	0.06	0.011

FIGURE 9.3-30 MEASUREMENTS OF QUANTUM EFFICIENCY

ORBIT 1188.5

λ (Å)	11644		11762		11647		11664	
	σ_K (ma/w)	QE (%)	σ_K (ma/w)	QE (%)	σ_K (ma/w)	QE (%)	σ_K (ma/w)	QE (%)
3490	66.0	23.5	61.54	21.9	52.5	18.7	54.3	19.3
3990	75.2	23.4	61.9	19.3	58.0	18.0	62.7	19.5
4540	52.4	14.3	42.1	11.5	39.8	10.9	43.4	11.8
4720	45.3	11.9	34.4	9.0	32.6	8.6	38.0	10.0
5000	34.6	8.6	25.3	6.3	25.3	6.3	27.2	6.7
5260	27.2	6.4	18.1	4.3	20.0	4.7	21.7	5.1
5520	21.8	4.9	14.5	3.3	14.5	3.3	15.6	3.5
5970	11.8	2.5	6.2	1.3	6.2	1.3	5.6	1.2
6220	6.9	1.4	3.3	0.66	2.9	0.58	2.7	0.54
6440	4.3	0.83	2.0	0.39	1.5	0.29	1.2	0.23
6940	0.38	0.068	0.18	0.033	0.07	0.013	.06	0.011

FIGURE 9.3-31 MEASUREMENTS OF QUANTUM EFFICIENCY

ORBIT 1300

λ (Å)	11644		11762		11647		11664	
	σ_K (ma/w)	QE (%)	σ_K (ma/w)	QE (%)	σ_K (ma/w)	QE (%)	σ_K (ma/w)	QE (%)
3490	65.1	23.4	60.1	21.4	52.8	18.8	56.4	20.1
3990	75.2	23.4	62.7	19.5	58.6	18.2	61.9	19.3
4540	52.0	14.2	41.9	11.4	41.9	11.4	43.6	11.9
4720	45.5	12.0	32.8	8.6	32.8	8.6	40.0	10.5
5000	34.6	8.6	23.7	5.9	24.6	6.1	27.5	6.8
5260	29.1	6.9	18.2	4.3	20.0	4.7	23.7	5.6
5520	21.8	4.9	14.2	3.2	14.7	3.3	15.9	3.6
5970	11.5	2.4	5.82	1.2	5.8	1.2	6.0	1.3
6220	6.7	1.3	3.3	0.66	3.1	0.62	3.0	0.6
6440	4.2	0.81	2.0	0.39	1.5	0.29	1.4	0.27
6940	0.36	0.064	0.19	0.034	0.07	0.013	0.055	0.0098

FIGURE 9.3-32 MEASUREMENTS OF QUANTUM EFFICIENCY

ORBIT 1400

λ (Å)	11644		11762		11647		11664	
	σ_K (ma/w)	QE (%)	σ_K (ma/w)	QE (%)	σ_K (ma/w)	QE (%)	σ_K (ma/w)	QE (%)
3490	65.5	23.3	59.6	21.2	51.6	18.4	56	19.9
3990	77.4	24.0	63.6	19.8	60.0	18.7	63.6	19.8
4540	56.4	15.4	41.8	11.4	41.8	11.4	47.3	12.9
4720	45.5	12.0	32.7	8.6	34.5	9.06	39.2	10.3
5000	35.2	8.77	23.6	5.85	25.4	6.3	29.1	7.22
5260	29.1	6.9	18.2	4.3	20.0	4.72	22.7	5.36
5520	23.6	5.3	14.0	3.15	14.9	3.35	16.0	3.6
5970	11.6	2.41	6.0	1.25	6.0	1.25	6.0	1.25
6220	6.9	1.38	3.18	0.64	3.1	0.62	2.9	0.58
6440	4.2	0.81	1.82	0.35	1.56	0.301	1.4	0.27
6940	0.38	0.068	0.18	0.032	0.07	0.0125	0.058	0.0104

FIGURE 9.3-33 MEASUREMENTS OF QUANTUM EFFICIENCY

ORBIT 1499.5

λ (Å)	11644		11762		11647		11664	
	σ_K (ma/w)	QE (%)	σ_K (ma/w)	QE (%)	σ_K (ma/w)	QE (%)	σ_K (ma/w)	QE (%)
3490	69.1	24.6	59.6	21.2	52.4	18.6	55.0	19.7
3990	77.4	24.0	61.9	19.2	59.0	18.4	63.6	19.8
4540	54.6	14.9	41.8	11.4	41.8	11.4	48.1	13.1
4720	45.5	12.0	32.7	8.6	34.5	9.06	40.0	10.5
5000	34.6	8.58	24.5	6.06	25.4	6.3	31	7.7
5260	29.1	6.9	18.2	4.3	20.0	4.72	23.6	5.57
5520	23.6	5.3	13.8	3.1	14.9	3.35	16.3	3.07
5970	11.6	2.41	5.8	1.2	6.0	1.25	6.2	1.29
6220	6.73	1.35	3.18	0.64	3.1	0.62	2,9	0.58
6440	4.2	0.81	1.82	0.35	1.56	0.301	1.38	0.266
6940	0.36	0.064	0.18	0.032	0.07	0.0125	0.054	0.0097

FIGURE 9.3-34 MEASUREMENTS OF QUANTUM EFFICIENCY

ORBIT 1512

λ (Å)	11644		11762		11647		11664	
	σ_K (ma/w)	QE (%)	σ_K (ma/w)	QE (%)	σ_K (ma/w)	QE (%)	σ_K (ma/w)	QE (%)
3490	69.1	24.6	61.9	22.0	53.9	19.2	58.2	20.7
3990	76.4	23.8	63.6	19.8	60.0	18.7	61.9	19.2
4540	56.4	15.4	42.7	11.7	42.7	11.7	47.3	12.9
4720	46.4	12.2	33.6	8.84	34.5	9.06	41.8	11
5000	36.4	9.02	24.5	6.06	26.4	6.55	29.1	7.22
5260	29.1	6.9	19.1	4.5	20.9	4.94	24.5	5.55
5520	23.6	5.3	14.3	3.22	15.3	3.44	16.3	3.07
5970	11.8	2.45	6.18	1.28	6.36	1.32	6.36	1.32
6220	7.1	1.42	3.36	0.67	3.09	0.62	3.09	0.62
6440	4.54	0.88	1.96	0.38	1.64	0.316	1.51	0.291
6940	0.29	0.07	0.2	0.036	0.078	0.014	0.06	0.0107

FIGURE 9.3-35 MEASUREMENTS OF QUANTUM EFFICIENCY

ORBIT 1537

λ (Å)	11644		11762		11647		11664	
	σ_K (ma/w)	QE (%)	σ_K (ma/w)	QE (%)	σ_K (ma/w)	QE (%)	σ_K (ma/w)	QE (%)
3490	69.1	24.6	58	20.6	50.1	17.9	56	19.9
3990	76.4	23.8	63.6	19.8	60.0	18.7	61.9	19.2
4540	56.4	15.4	41.8	11.4	42	11.5	47.3	12.9
4720	46.1	12.1	33.1	8.7	34	8.94	40.3	10.6
5000	35.6	8.82	24.2	6.0	25.3	6.27	29.1	7.22
5260	29.1	6.9	18.7	4.4	19.8	4.67	23.8	5.38
5520	23.6	5.3	14.0	3.15	14.9	3.35	16.3	3.67
5970	11.8	2.45	6.0	1.25	6.0	1.25	6.19	1.29
6220	6.9	1.38	3.27	0.65	3.1	0.62	3.02	0.604
6440	4.2	0.81	1.85	0.36	1.51	0.291	1.47	0.284
6940	0.38	0.068	0.18	0.032	0.07	0.0125	0.06	0.0107

FIGURE 9.3-36 MEASUREMENTS OF QUANTUM EFFICIENCY

ORBIT 1562

λ (Å)	11644		11762		11647		11664	
	σ_K (ma/w)	QE (%)	σ_K (ma/w)	QE (%)	σ_K (ma/w)	QE (%)	σ_K (ma/w)	QE (%)
3490	69.1	24.6	60.4	21.5	52.4	18.6	57.5	20.4
3990	76.4	23.8	62.8	19.5	60.0	18.7	61.9	19.2
4540	56.4	15.4	41.8	11.4	41.8	11.4	48.4	13.2
4720	45.5	12.0	34.5	9.07	34.5	9.06	40.9	10.7
5000	35.2	8.77	25.4	6.3	25.4	6.3	29.1	7.22
5260	29.1	6.9	19.5	4.6	20.0	4.72	23.6	5.57
5520	23.6	5.3	14.5	3.26	14.9	3.35	16.3	3.67
5970	11.7	2.43	6.2	1.29	6.0	1.25	6.0	1.25
6220	6.9	1.38	3.4	0.68	3.1	0.62	3.04	0.608
6440	4.27	0.82	1.93	0.37	1.54	0.297	1.49	0.288
6940	0.38	0.068	0.19	0.034	0.076	0.0136	0.065	0.0116

FIGURE 9.3-37 MEASUREMENTS OF QUANTUM EFFICIENCY

ORBIT 1593

λ (Å)	11644		11762		11647		11664	
	σ_K (ma/w)	QE (%)	σ_K (ma/w)	QE (%)	σ_K (ma/w)	QE (%)	σ_K (ma/w)	QE (%)
3490	65.5	23.3	61.9	22.0	53.9	19.2	59.6	21.2
3990	76.4	23.8	63.6	19.8	60.0	18.7	61.9	19.2
4540	56.4	15.4	41.8	11.4	43.6	11.9	47.3	12.9
4720	45.5	12.0	34.5	9.07	35.5	9.32	40.0	10.5
5000	35.2	8.77	25.4	6.3	26.5	6.57	29.1	7.22
5260	29.1	6.9	19.6	4.62	21.8	5.15	23.6	5.57
5520	23.6	5.3	14.7	3.3	15.3	3.44	16.3	3.07
5970	11.6	2.41	6.55	1.36	6.36	1.32	6.0	1.25
6220	7.1	1.42	3.52	0.7	3.24	0.648	3.09	0.62
6440	4.45	0.86	2.45	0.47	1.65	0.318	1.49	0.288
6940	0.38	0.068	0.25	0.045	0.084	0.015	0.065	0.0116

FIGURE 9.3-38 MEASUREMENTS OF QUANTUM EFFICIENCY

ORBIT 1636.5

λ (Å)	11644		11762		11647		11664	
	σ_K (ma/w)	QE (%)	σ_K (ma/w)	QE (%)	σ_K (ma/w)	QE (%)	σ_K (ma/w)	QE (%)
3490	65.5	23.3	60.4	21.5	52.4	18.6	58.2	20.7
3990	76.4	23.8	61.9	19.2	60.0	18.7	61.9	19.2
4540	52.7	14.4	41.8	11.4	41.8	11.4	47.3	12.9
4720	45.5	12.0	32.7	8.6	36.4	9.56	40.0	10.5
5000	34.6	8.58	25.4	6.3	25.4	6.3	29.1	7.22
5260	29.1	6.9	19.1	4.5	20.0	4.72	23.6	5.57
5520	23.6	5.3	13.8	3.1	15.1	3.4	16.3	3.67
5970	11.4	2.37	5.8	1.2	6.0	1.25	6.2	1.29
6220	6.73	1.35	3.27	0.65	3.09	0.62	2.9	0.58
6440	4.0	0.77	1.9	0.37	1.56	0.301	1.38	0.266
6940	0.36	0.064	0.2	0.036	0.07	0.0125	0.062	0.0111

FIGURE 9.3-39 MEASUREMENTS OF QUANTUM EFFICIENCY

ORBIT 1750

λ (Å)	11644		11762		11647		11664	
	σ_K (ma/w)	QE (%)	σ_K (ma/w)	QE (%)	σ_K (ma/w)	QE (%)	σ_K (ma/w)	QE (%)
3490	65.5	23.3	60.4	21.5	53.9	19.2	55.0	19.7
3990	77.4	24.0	63.6	19.8	60.0	18.7	63.6	19.8
4540	54.6	14.9	41.8	11.4	41.8	11.4	48.5	13.2
4720	45.5	12.0	34.5	9.07	34.5	9.06	40.0	10.5
5000	35.1	8.72	24.9	6.17	26.0	6.45	31.0	7.7
5260	27.3	6.45	18.9	4.46	20.4	4.81	23.6	5.57
5520	22.7	5.1	14.5	3.26	15.3	3.44	16.5	3.71
5970	11.4	2.37	6.36	1.32	6.19	1.29	6.36	1.32
6220	6.73	1.35	3.36	0.67	3.18	0.636	3.16	0.632
6440	4.15	0.8	1.95	0.38	1.64	0.316	1.53	0.295
6940	0.36	0.064	0.2	0.036	0.076	0.0136	0.065	0.0116

FIGURE 9.3-40 MEASUREMENTS OF QUANTUM EFFICIENCY

ORBIT 1850

λ (Å)	11644		11762		11647		11664	
	σ_K (ma/w)	QE (%)	σ_K (ma/w)	QE (%)	σ_K (ma/w)	QE (%)	σ_K (ma/w)	QE (%)
3490	68.1	24.6	58.0	20.7	.55	19.7	59.6	21.2
3990	78.3	24.3	64.3	20.0	59.8	18.6	65.6	20.4
4540	56.4	15.4	43.5	11.9	43.5	11.9	47.3	13.0
4720	45.6	12.0	36.4	9.58	32.8	8.6	40.0	10.6
5000	35.4	8.76	25.5	6.32	25.1	6.23	29.1	7.2
5260	29.1	6.9	20.0	4.72	21.7	5.13	23.6	5.55
5520	23.7	5.33	15.2	3.41	15.0	3.37	17.1	3.8
5970	11.5	2.38	6.34	1.31	6.34	1.34	6.4	1.33
6220	6.8	1.35	6.64	1.71	3.31	.66	3.1	.62
6440	4.14	.8	2.0	.387	1.73	.344	1.5	.29
6940	.364	.063	.2	.0357	.095	.017	.073	.013

FIGURE 9.3-41 MEASUREMENTS OF QUANTUM EFFICIENCY

ORBIT 1947.5

λ (Å)	11644		11762		11647		11664	
	σ_K (ma/w)	QE (%)	σ_K (ma/w)	QE (%)	σ_K (ma/w)	QE (%)	σ_K (ma/w)	QE (%)
3490	72.44	25.79	63.3	22.5	54.7	19.5	59.68	21.3
3990	80.08	24.90	67.34	20.9	61.9	19.3	71.0	22.0
4540	58.24	15.9	44.6	12.2	43.7	11.9	51.0	13.9
4720	47.32	12.4	35.5	9.34	35.5	9.3	41.86	11.0
5000	36.40	9.2	26.4	6.55	27.3	6.8	32.80	8.1
5260	29.12	6.87	20.02	4.72	20.9	4.9	24.6	5.8
5520	23.66	5.32	15.1	3.4	15.7	3.5	18.2	4.1
5970	12.00	2.5	6.7	1.4	6.5	1.35	6.55	1.4
6220	8.0	1.6	3.64	.73	3.4	.68	3.3	.66
6440	4.5	.87	2.2	.42	1.75	.34	1.62	.31
6940	.40	.072		.039	.093	.0166	.073	.013

FIGURE 9.3-42 MEASUREMENTS OF QUANTUM EFFICIENCY

ORBIT 1960

λ (Å)	11644		11762		11647		11664	
	σ_K (ma/w)	QE (%)	σ_K (ma/w)	QE (%)	σ_K (ma/w)	QE (%)	σ_K (ma/w)	QE (%)
3490	66.4	23.6	58.1	20.7	56.8	20.2	59.6	21.2
3990	80.1	24.9	61.1	19.0	61.9	19.3	6.6	20.5
4540	56.4	15.4	45.5	12.4	43.7	11.9	51.0	13.9
4720	46.4	12.2	36.4	9.6	36.4	9.6	41.9	11.0
5000	35.5	8.8	25.5	6.3	27.3	6.3	32.8	8.1
5260	27.3	6.4	19.1	4.5	21.8	5.1	25.5	6.0
5520	22.8	5.1	14.9	3.4	15.7	3.5	19.1	4.3
5970	11.7	2.4	6.6	1.4	6.6	1.4	6.6	1.37
6220	6.7	1.34	3.5	.70	3.5	.70	3.5	.7
6440	3.8	.73	2.0	.386	1.8	.35	1.6	.31
6940	.42	.075	.22	.039	.095	.017	.076	.014

FIGURE 9.3-43 MEASUREMENTS OF QUANTUM EFFICIENCY

λ (Å)	11644		11762		11647		11664	
	σ_K (ma/w)	QE (%)	σ_K (ma/w)	QE (%)	σ_K (ma/w)	QE (%)	σ_K (ma/w)	QE (%)
3490	71.3	25.4	67.3	20.9	53.1	18.9	58.2	20.7
3990	76.4	23.4	64.3	20.0	60.6	18.8	64.3	20.0
4540	54.6	14.9	43.5	12.0	40.8	11.1	48.3	13.2
4720	45.5	12.0	35.3	13.4	34.4	9.0	41.0	10.75
5000	36.4	9.0	25.4	6.3	26.0	6.5	30.5	7.57
5260	29.1	6.9	20.0	4.73	20.2	4.8	23.3	5.5
5520	22.8	5.1	14.7	3.3	15.7	3.5	17.1	3.8
5970	11.6	2.4	6.53	1.35	6.4	1.33	6.42	1.34
6220	6.7	1.34	3.5	.7	3.2	.64	3.02	.604
6440	4.4	.85	2.1	.385	1.72	.33	1.53	.294
6940	.39	.069	.21	.037	.089	.015	.063	.0115

FIGURE 9.3-44 MEASUREMENTS OF QUANTUM EFFICIENCY

ORBIT 2010

λ (Å)	11644		11762		11647		11664	
	σ_K (ma/w)	QE (%)	σ_K (ma/w)	QE (%)	σ_K (ma/w)	QE (%)	σ_K (ma/w)	QE (%)
3490	69.6	24.8	57.0	20.3	.55	19.7	59.6	21.2
3990	78.3	24.3	63.4	19.7	59.8	18.6	65.50	20.3
4540	56.4	15.4	41.8	11.4	43.5	11.9	47.3	13.0
4720	47.3	12.45	36.4	9.58	36.4	9.6	40.0	10.6
5000	36.4	9.00	25.5	6.32	27.2	6.75	29.1	7.2
5260	29.1	6.9	20.0	4.72	21.7	5.13	23.6	5.55
5520	23.7	5.33	15.2	3.42	15.0	3.38	16.4	3.7
5970	11.65	2.43	7.3	1.52	6.34	1.34	6.0	1.25
6220	7.28	1.456	3.64	.71	3.3	.655	3.1	.62
6440	4.55	.878	2.0	.387	1.6	.32	1.5	.29
6940	.364	.063	.20	.0357	.091	.0163	.073	.013

FIGURE 9.3-45 MEASUREMENTS OF QUANTUM EFFICIENCY

ORBIT 2041

λ (Å)	11644		11762		11647		11664	
	σ_K (ma/w)	QE (%)	σ_K (ma/w)	QE (%)	σ_K (ma/w)	QE (%)	σ_K (ma/w)	QE (%)
3490	71.0	26	60.0	21.2	54.5	19.4	56.7	20.2
3990	78.5	24.4	62.0	19.3	61.0	19.0	63.7	19.8
4540	54.7	15.0	43.5	11.9	43.0	11.8	48.0	13.1
4720	45.6	12.0	34.4	9.05	35.0	9.2	39.7	10.8
5000	35.4	8.76	25.4	6.27	26.2	6.5	30.2	7.5
5260	29.0	6.83	19.8	4.67	21.0	4.95	23.7	5.6
5520	23.3	5.23	15.0	3.4	15.7	3.53	17.2	3.87
5970	11.7	2.44	6.55	1.36	6.5	1.35	6.5	1.34
6220	6.9	1.38	3.57	.71	3.26	.65	3.14	.625
6440	4.35	.84	2.11	.407	1.73	.34	1.55	.30
6940	.39	.069	.211	.038	.09	.017	.062	.011

FIGURE 9.3-46 MEASUREMENTS OF QUANTUM EFFICIENCY

ORBIT 2084.5

λ (Å)	11644		11762		11647		11664	
	σ_K (ma/w)	QE (%)	σ_K (ma/w)	QE (%)	σ_K (ma/w)	QE (%)	σ_K (ma/w)	QE (%)
3490	70.0	24.8	61.0	21.8	56.7	20.2	57.3	20.4
3990	77.3	24.0	64.5	20.0	59.0	18.3	64.3	20.0
4540	53.5	14.6	42.4	11.6	39.7	10.8	47.4	13.0
4720	44.4	11.4	33.7	8.85	32.0	8.4	39.6	10.4
5000	34.0	8.43	24.6	6.1	25.0	6.18	29.5	7.3
5260	28.0	6.6	19.3	4.55	19.5	4.6	23.7	5.58
5520	22.6	5.08	14.5	3.27	14.4	3.23	17.0	3.8
5970	11.4	2.38	6.32	1.31	6.1	1.27	6.28	1.3
6220	6.75	1.35	3.47	.694	3.15	.63	3.07	.615
6440	4.15	.8	2.00	.386	1.68	.322	1.5	.29
6940	.37	.66	.20	.0358	.091	.0163	.059	.0105

FIGURE 9.3-47 MEASUREMENTS OF QUANTUM EFFICIENCY

ORBIT 2200

λ (Å)	11644		11762		11647		11664	
	σ_K (ma/w)	QE (%)	σ_K (ma/w)	QE (%)	σ_K (ma/w)	QE (%)	σ_K (ma/w)	QE (%)
3490	68.4	24.3	61.6	21.9	57.5	20.5	58.7	20.9
3990	78.5	24.4	66.0	20.5	59.4	18.4	65.5	20.3
4540	54.8	15.0	43.5	11.9	40.0	10.9	48.6	13.5
4720	45.3	11.9	34.2	9.0	32.8	8.6	40.0	10.6
5000	34.8	8.6	25.7	6.37	25.1	6.23	30.7	7.6
5260	28.7	6.77	20.4	4.8	20.0	4.76	23.7	5.57
5520	23.1	5.2	15.2	3.41	14.6	3.27	17.0	3.83
5970	11.5	2.38	6.35	1.32	6.2	1.29	6.5	1.35
6220	6.8	1.36	3.53	.705	3.31	.66	3.17	.632
6440	4.13	.798	2.08	.40	1.73	.344	1.53	.295
6940	.37	.066	.215	.0384	.095	.017	.068	.012

FIGURE 9.3-48 MEASUREMENTS OF QUANTUM EFFICIENCY

ORBIT 2300

λ (Å)	11644		11762		11647		11664	
	σ_K (ma/w)	QE (%)	σ_K (ma/w)	QE (%)	σ_K (ma/w)	QE (%)	σ_K (ma/w)	QE (%)
3490	72.44	25.79	59.7	21.3	54.7	19.5	59.68	21.3
3990	80.08	24.90	62.0	19.3	61.9	19.3	65.6	20.4
4540	58.24	15.9	44.6	12.2	43.7	11.9	51.0	13.9
4720	47.32	12.4	35.5	9.34	35.5	9.3	41.86	11.0
5000	36.40	9.2	26.4	6.55	27.3	6.8	32.80	8.1
5260	29.12	6.87	20.02	4.72	20.9	4.9	24.6	5.8
5520	23.66	5.32	15.1	3.4	15.7	3.5	18.2	4.1
5970	12.00	2.5	6.7	1.4	6.5	1.35	6.55	1.4
6220	8.0	1.6	3.64	.73	3.4	.68	3.3	.66
6440	4.5	.87	2.2	.42	1.75	.34	1.62	.31
6940	.40	.072	.22	.039	.093	.0166	.073	.013

FIGURE 9.3-49 MEASUREMENTS OF QUANTUM EFFICIENCY

ORBIT 2400

λ (Å)	11644		11762		11647		11664	
	σ_K (ma/w)	QE (%)	σ_K (ma/w)	QE (%)	σ_K (ma/w)	QE (%)	σ_K (ma/w)	QE (%)
3490	68.1	24.6	58.0	20.7	55	19.7	59.6	21.2
3990	78.3	24.3	64.3	20.0	59.8	18.6	65.6	20.4
4540	56.4	15.4	43.5	11.9	43.5	11.9	47.3	13.0
4720	45.6	12.0	36.4	9.58	32.8	8.6	40.0	10.6
5000	35.4	8.76	25.5	6.32	25.1	6.23	29.1	7.2
5260	29.1	6.9	20.0	4.72	21.7	5.13	23.6	5.55
5520	23.7	5.33	15.2	3.41	15.0	3.37	17.1	3.8
5970	11.5	2.38	6.34	1.31	6.34	1.34	6.4	1.33
6220	6.8	1.35	3.64	.71	3.31	.66	3.1	.62
6440	4.14	.8	2.0	.387	1.73	.344	1.5	.29
6940	.364	.063	.2	.0357	.095	.017	.073	.013

FIGURE 9.3-50 MEASUREMENTS OF QUANTUM EFFICIENCY

ORBIT 2451.5

λ (Å)	11644		11762		11647		11664	
	σ_K (ma/w)	QE (%)	σ_K (ma/w)	QE (%)	σ_K (ma/w)	QE (%)	σ_K (ma/w)	QE (%)
3490	71.3	25.4	67.3	20.9	53.1	18.9	58.2	20.7
3990	76.4	23.4	64.3	20.0	60.6	18.8	64.3	20.0
4540	54.6	14.9	43.5	12.0	40.8	11.1	48.3	13.2
4720	45.5	12.0	35.3	13.4	34.4	9.0	41.0	10.75
5000	36.4	9.0	25.4	6.3	26.0	6.5	30.5	7.57
5260	29.1	6.9	20.0	4.73	20.2	4.8	23.3	5.5
5520	22.8	5.1	14.7	3.3	15.7	3.5	17.1	3.8
5970	11.6	2.4	6.53	1.35	6.4	1.33	6.42	1.34
6220	6.7	1.34	3.5	.7	3.2	.64	3.02	.604
6440	4.4	.85	2.1	.385	1.72	.33	1.53	.294
6940	.39	.069	.21	.037	.089	.0159	.063	.0115

FIGURE 9.3-51 MEASUREMENTS OF QUANTUM EFFICIENCY

ORBIT 2464.5

λ (Å)	11644		11762		11647		11664	
	σ_K (ma/w)	QE (%)	σ_K (ma/w)	QE (%)	σ_K (ma/w)	QE (%)	σ_K (ma/w)	QE (%)
3490	69.6	24.8	57.0	20.3	.55	19.7	59.6	21.2
3990	78.3	24.3	63.4	19.7	59.8	18.6	65.50	20.3
4540	56.4	15.4	41.8	11.4	43.5	11.9	47.3	13.0
4720	47.3	12.45	36.4	9.58	36.4	9.6	40.0	10.6
5000	36.4	9.00	25.5	6.32	27.2	6.75	29.1	7.2
5260	29.1	6.9	20.0	4.72	21.7	5.13	23.6	5.55
5520	23.7	5.33	15.2	3.42	15.0	3.38	16.4	3.7
5970	11.65	2.43	7.3	1.52	6.34	1.34	6.0	1.25
6220	7.28	1.456	3.64	.71	3.3	.655	3.1	.62
6440	4.55	.878	2.0	.387	1.6	.32	1.5	.29
6940	.364	.063	.20	.0357	.091	.0163	.073	.013

FIGURE 9.3-52 MEASUREMENTS OF QUANTUM EFFICIENCY

ORBIT 2489.5

λ (Å)	11644		11762		11647		11664	
	σ_K (ma/w)	QE (%)	σ_K (ma/w)	QE (%)	σ_K (ma/w)	QE (%)	σ_K (ma/w)	QE (%)
3490	70.1	25.0	63.7	22.7	54.6	19.4	61.2	21.8
3990	78.3	24.3	67.3	20.9	63.7	19.8	72.8	22.6
4540	54.6	14.9	43.7	11.9	43.7	11.9	50.6	13.8
4720	45.5	11.9	34.6	9.1	35.9	9.4	42.4	11.5
5000	34.9	8.7	25.5	6.3	26.8	6.6	31.9	7.9
5260	28.57	6.7	20.0	4.7	21.3	5.0	24.6	5.8
5520	22.8	5.1	14.8	3.3	16.2	3.6	17.5	3.9
5970	11.5	2.4	6.6	1.4	6.9	1.4	6.7	1.4
6220	6.8	1.4	3.6	.72	3.5	.7	3.3	.66
6440	4.3	.83	2.1	.41	1.6	.3	1.7	.33
6940	.38	.068	.21	.038	.104	.018	.023	.04

FIGURE 9.3-53 MEASUREMENTS OF QUANTUM EFFICIENCY

ORBIT 2514.5

λ (Å)	11644		11762		11647		11664	
	σ_K (ma/w)	QE (%)	σ_K (ma/w)	QE (%)	σ_K (ma/w)	QE (%)	σ_K (ma/w)	QE (%)
3490	69.4	24.7	62.6	22.3	54.6	19.4	61.2	21.8
3990	78.3	24.4	67.3	20.9	63.7	19.8	72.8	22.6
4540	56.4	15.4	43.7	11.9	43.7	11.9	52.8	14.4
4720	43.7	11.5	38.2	10.0	36.4	9.6	41.9	11.1
5000	34.6	8.6	27.3	6.8	27.3	6.8	32.8	8.1
5260	29.1	6.9	21.8	5.1	20.0	4.7	24.6	5.8
5520	23.7	5.3	14.9	3.4	16.4	3.7	17.5	3.9
5970	11.5	2.4	6.7	1.4	6.9	1.4	6.7	1.4
6220	6.7	1.3	3.8	.76	3.5	.7	3.3	.66
6440	4.2	.81	2.2	.43	1.6	.31	1.7	.33
6940	.38	.068	.20	.036	.104	.018	.022	.039

FIGURE 9.3-54 MEASUREMENTS OF QUANTUM EFFICIENCY

ORBIT 2545.5

λ (Å)	11644		11762		11647		11664	
	σ_K (ma/w)	QE (%)	σ_K (ma/w)	QE (%)	σ_K (ma/w)	QE (%)	σ_K (ma/w)	QE (%)
3490	70.1	25.0	61.9	22.0	57.5	20.5	61.2	21.8
3990	78.3	24.4	67.3	20.9	63.7	19.8	71.0	22.1
4540	54.6	14.9	43.7	11.7	44.8	12.2	51.0	13.9
4720	43.7	11.5	36.0	9.5	36.9	9.7	42.4	11.2
5000	34.4	8.5	27.3	6.8	27.8	6.9	32.8	8.1
5260	28.8	6.8	20.9	4.9	22.4	5.3	25.5	6.0
5520	23.7	5.3	15.0	3.4	16.1	3.6	18.0	4.1
5970	11.5	2.4	6.7	1.4	6.9	1.4	7.1	1.5
6220	6.7	1.34	3.6	.72	3.6	.72	2.5	.5
6440	4.3	.83	2.2	.42	1.8	.35	1.7	.33
6940	.36	.064	.22	.039	.011	.019	0.082	.014

FIGURE 9.3-55 MEASUREMENTS OF QUANTUM EFFICIENCY

ORBIT 2589

λ (Å)	11644		11762		11647		11664	
	σ_K (ma/w)	QE (%)	σ_K (ma/w)	QE (%)	σ_K (ma/w)	QE (%)	σ_K (ma/w)	QE (%)
3490	66.2	23.6	58.9	21.0	58.0	20.6	60.1	21.4
3990	80.1	24.9	61.9	19.3	61.9	19.3	65.5	20.4
4540	56.4	15.4	45.5	12.4	43.7	11.9	51.0	13.9
4720	47.3	12.4	36.4	9.6	38.2	10.0	41.9	11.1
5000	36.4	9.0	25.5	6.3	27.3	6.8	32.8	8.1
5260	27.3	6.4	19.1	4.5	21.8	5.1	25.5	6.0
5520	23.7	5.3	15.1	3.4	15.7	3.5	20.0	4.5
5970	11.5	2.4	6.6	1.4	6.6	1.4	6.6	1.4
6220	6.7	1.34	3.6	.72	3.5	.7	3.6	.3
6440	3.8	.73	2.0	.37	1.8	.35	1.6	.3
6940	.42	.075	.022	.039	.094	.017	.076	.014

FIGURE 9.3-56 MEASUREMENTS OF QUANTUM EFFICIENCY

ORBIT 2700

λ (Å)	11644		11762		11647		11664	
	σ_K (ma/w)	QE (%)	σ_K (ma/w)	QE (%)	σ_K (ma/w)	QE (%)	σ_K (ma/w)	QE (%)
3490	69.9	24.9	48.8	17.4	56.8	20.2	61.9	22.0
3990	78.3	24.4	67.5	21.0	63.7	19.8	72.8	22.6
4540	56.4	15.4	43.9	12.0	44.0	12.0	51.0	13.9
4720	45.5	12.0	36.4	9.6	38.2	10.0	41.9	11.0
5000	34.9	8.7	25.5	6.3	27.3	6.8	32.8	8.1
5260	29.1	6.8	23.7	5.6	21.7	5.1	25.5	6.0
5520	23.8	5.4	14.9	3.4	16.4	3.7	18.2	4.1
5970	11.5	2.4	6.6	1.4	6.9	1.4	6.7	1.4
6220	6.8	1.4	3.8	.76	3.5	.7	.33	.66
6440	4.4	.84	2.0	.39	.54	.1	1.7	.33
6940	.38	.07	.20	.036	.1	.018	.21	.038

FIGURE 9.3-57 MEASUREMENTS OF QUANTUM EFFICIENCY

ORBIT 2800

λ (Å)	11644		11762		11647		11664	
	σ_K (ma/w)	QE (%)	σ_K (ma/w)	QE (%)	σ_K (ma/w)	QE (%)	σ_K (ma/w)	QE (%)
3490	65.5	23.3	59.6	21.2	56.8	20.2	57.3	20.4
3990	77.6	24.0	61.9	19.2	61.9	19.3	66.0	20.5
4540	56.4	15.4	41.8	11.4	43.0	11.8	47.4	13.0
4720	45.5	12.0	32.7	8.6	35.0	9.2	39.7	10.8
5000	34.6	8.58	24.5	6.1	27.3	6.8	30.2	7.5
5260	29.1	6.9	18.2	4.3	19.5	4.6	23.7	5.58
5520	23.6	5.3	14.0	3.5	.44	3.23	17.0	3.8
5970	11.6	2.41	5.8	1.2	6.1	1.27	6.6	1.4
6220	6.9	1.38	3.18	0.64	3.5	.7	3.5	.7
6440	4.2	0.81	1.82	0.35	1.8	.37	1.55	.3
6940	.36	.064	0.18	.032	.09	.016	.062	.011

FIGURE 9.3-58 MEASUREMENTS OF QUANTUM EFFICIENCY

ORBIT 2897.5

λ (Å)	11644		11762		11647		11664	
	σ_K (ma/w)	QE (%)	σ_K (ma/w)	QE (%)	σ_K (ma/w)	QE (%)	σ_K (ma/w)	QE (%)
3490	68.4	24.3	61.6	21.9	56.7	20.2	57.3	20.4
3990	78.5	24.4	66.0	20.5	59.0	18.3	64.3	20.0
4540	54.8	15.0	43.5	11.9	39.7	10.8	47.4	13.0
4720	45.3	11.9	34.2	9.0	32.0	8.4	40.0	11.2
5000	34.8	8.6	25.7	6.37	25.0	6.18	29.5	7.3
5260	28.7	6.77	20.4	4.8	19.5	4.6	23.7	5.58
5520	23.1	5.2	15.2	3.41	14.4	3.23	17.0	3.8
5970	11.5	2.38	6.35	1.32	6.1	1.27	6.28	1.3
6220	6.8	1.36	3.53	.705	3.15	.63	3.07	.615
6440	4.13	.798	2.08	.40	1.68	.322	1.5	.29
6940	.37	.066	.215	.0384	.091	.0163	.059	.0105

FIGURE 9.3-59 MEASUREMENTS OF QUANTUM EFFICIENCY

ORBIT 2910

λ (Å)	11644		11762		11647		11664	
	σ_K (ma/w)	QE (%)	σ_K (ma/w)	QE (%)	σ_K (ma/w)	QE (%)	σ_K (ma/w)	QE (%)
3490	66.4	23.6	58.1	20.7	56.8	20.2	59.6	21.2
3990	80.1	24.9	61.1	19.0	61.9	19.3	.66	20.5
4540	56.4	15.4	45.5	12.4	43.7	11.9	51.0	43.9
4720	46.4	12.2	36.4	9.6	36.4	9.6	39.6	10.4
5000	35.5	8.8	25.5	6.3	27.3	6.8	32.8	8.7
5260	27.3	6.4	19.1	4.5	21.8	5.1	25.5	6.0
5520	22.8	5.1	14.9	3.4	15.7	3.5	19.1	4.3
5970	11.7	2.4	6.6	1.4	6.6	1.4	6.6	1.37
6220	6.7	1.34	3.5	.70	3.5	.70	3.5	.7
6440	3.8	.73	2.0	.386	1.8	.35	1.6	.31
6940	.42	.075	.22	.039	.095	.017	.076	.014

FIGURE 9.3-60 MEASUREMENTS OF QUANTUM EFFICIENCY

ORBIT 2935

λ (Å)	11644		11762		11647		11664	
	σ_K (ma/w)	QE (%)	σ_K (ma/w)	QE (%)	σ_K (ma/w)	QE (%)	σ_K (ma/w)	QE (%)
3490	71.0	26	60.0	21.2	54.5	19.4	56.7	20.2
3990	78.5	24.4	62.0	19.3	61.0	19.0	63.7	19.8
4540	54.7	15.0	43.5	11.9	43.0	11.8	48.0	13.1
4720	45.6	12.0	34.4	9.05	35.0	9.2	39.7	10.8
5000	35.4	8.76	25.4	6.27	26.2	6.5	30.2	7.5
5260	29.0	6.83	19.8	4.67	21.0	4.95	23.7	5.6
5520	23.3	5.23	15.0	3.4	15.7	3.53	17.2	3.87
5970	11.7	2.44	6.55	1.36	6.5	1.35	6.5	1.34
6220	6.9	1.38	3.57	.71	3.26	.65	3.14	.625
6440	4.35	.84	2.11	.407	1.73	.34	1.55	.30
6940	.39	.069	.211	.038	.09	.017	.062	.011

FIGURE 9.3-61 MEASUREMENTS OF QUANTUM EFFICIENCY

ORBIT 2960.0

λ (Å)	11644		11762		11647		11664	
	σ_K (ma/w)	QE (%)	σ_K (ma/w)	QE (%)	σ_K (ma/w)	QE (%)	σ_K (ma/w)	QE (%)
3490	70.0	24.8	61.0	21.8	57.5	20.5	58.7	20.9
3990	77.3	24.0	64.5	20.0	59.4	18.4	65.5	20.3
4540	53.5	14.6	42.4	11.6	40.0	10.9	48.6	13.5
4720	44.4	11.4	33.7	8.85	32.8	8.6	40.0	10.6
5000	34.0	8.43	24.6	6.1	25.1	6.23	30.7	7.6
5260	28.0	6.6	19.3	4.55	20.0	4.76	23.7	5.57
5520	22.6	5.08	14.5	3.27	14.6	3.27	17.0	3.83
5970	11.4	2.38	6.32	1.31	6.2	1.29	6.5	1.35
6220	6.75	1.35	3.47	.694	3.31	.66	3.17	.632
6440	4.15	.8	2.00	.386	1.73	.344	1.53	.295
6940	.37	.66	.20	.0358	.095	.017	.068	.012

FIGURE 9.3-62 MEASUREMENTS OF QUANTUM EFFICIENCY

ORBIT 2991.0

λ (Å)	11644		11762		11647		11664	
	σ_K (ma/w)	QE (%)	σ_K (ma/w)	QE (%)	σ_K (ma/w)	QE (%)	σ_K (ma/w)	QE (%)
3490	67.6	23.1	57.9	20.6	50.7	18.0	57.9	20.6
3990	76.3	23.7	61.5	19.1	59.7	18.4	65.2	19.3
4540	52.7	14.4	41.6	11.4	41.6	11.4	47.1	12.3
4720	45.4	11.9	32.6	8.6	32.6	8.6	38.0	10.0
5000	36.3	8.7	23.5	5.8	25.3	6.3	29.0	6.7
5260	29.0	6.8	18.1	4.3	19.9	4.7	23.5	5.6
5520	23.6	5.1	13.7	3.1	14.5	3.3	15.9	3.6
5970	11.2	2.3	5.8	1.2	5.8	1.2	5.8	1.2
6220	6.7	1.3	3.3	.66	2.9	.58	2.9	.58
6440	4.1	.8	1.8	.35	1.5	.29	1.3	.25
6940	.362	.065	.18	.032	.063	.011	.054	.0097

FIGURE 9.3-63 MEASUREMENTS OF QUANTUM EFFICIENCY

ORBIT 3034.5

λ (Å)	11644		11762		11647		11664	
	σ_K (ma/w)	QE (%)	σ_K (ma/w)	QE (%)	σ_K (ma/w)	QE (%)	σ_K (ma/w)	QE (%)
3490	67.0	23.1	57.9	20.6	50.7	18.0	57.9	20.6
3990	76.0	23.6	61.5	19.2	59.7	18.3	63.4	19.2
4540	54.3	14.2	41.6	11.4	39.8	10.9	45.3	12.4
4720	45.3	11.9	30.8	8.1	32.6	8.6	36.2	9.5
5000	36.2	8.6	23.5	5.8	25.3	6.3	29.0	6.7
5260	27.2	6.4	18.1	4.3	19.9	4.7	23.5	5.5
5520	23.5	5.1	13.8	3.1	14.5	3.3	15.7	3.5
5970	11.0	2.3	5.8	1.2	5.6	1.2	5.8	1.2
6220	6.5	1.3	3.1	.62	2.7	.54	2.7	.54
6440	4.0	.77	1.8	.35	1.5	.3	1.3	.25
6940	.36	.065	.18	.032	.07	.013	.054	.0097

FIGURE 9.3-64 MEASUREMENTS OF QUANTUM EFFICIENCY

	11644				11762			
Gain	V_A (volt)	I_A (amps)	I_{13} (amps)	I_{14} (amps)	V_A (volt)	I_A (amps)	I_{13} (amps)	I_{14} (amps)
10^4	1530	10^{-8}	3.7×10^{-8}	6.5×10^{-8}	1380	10^{-8}	3.0×10^{-8}	5.6×10^{-8}
10^5	2150	10^{-7}	3.0×10^{-7}	6.0×10^{-7}	1950	10^{-7}	2.9×10^{-7}	5.5×10^{-7}
10^6	3210	10^{-6}	2.8×10^{-6}	5.8×10^{-6}	2790	10^{-6}	2.9×10^{-6}	5.8×10^{-6}
I_D	3210	6.5×10^{-11} Amp @ G = 10^6			2790	9.3×10^{-11} Amp @ G = 10^6		

	11647				11664			
Gain	V_A (volt)	I_A (amps)	I_{13} (amps)	I_{14} (amps)	V_A (volt)	I_A (amps)	I_{13} (amps)	I_{14} (amps)
10^4	1610	10^{-8}	3.8×10^{-8}	6.3×10^{-8}	1590	10^{-8}	3.5×10^{-8}	6.2×10^{-8}
10^5	2250	10^{-7}	3.1×10^{-7}	6.1×10^{-7}	2410	10^{-7}	2.4×10^{-7}	5.8×10^{-7}
10^6	3360	10^{-6}	2.8×10^{-6}	6.2×10^{-6}	3350	10^{-6}	2.6×10^{-6}	6.0×10^{-6}
I_D	3360	4.8×10^{-11} Amp @ G = 10^6			3350	4.2×10^{-11} Amp @ G = 10^6		

FIGURE 9.4-1 MEASUREMENTS OF CURRENT VOLTAGE GAIN AND DARK CURRENT

ORBIT 1

	11644				11762			
Gain	V_A (volt)	I_A (amps)	I_{13} (amps)	I_{14} (amps)	V_A (volt)	I_A (amps)	I_{13} (amps)	I_{14}(amps)
10^4	1530	10^{-8}	3.8×10^{-8}	6.2×10^{-8}	1380	10^{-8}	3.0×10^{-8}	5.5×10^{-8}
10^5	2150	10^{-7}	3.2×10^{-7}	6.0×10^{-7}	1950	10^{-7}	2.8×10^{-7}	5.2×10^{-7}
10^6	3220	10^{-6}	3.0×10^{-6}	5.9×10^{-6}	2805	10^{-6}	2.7×10^{-6}	5.0×10^{-6}
I_D	3220	6.5×10^{-11} Amp @ G = 10^6			2805	9.3×10^{-11} Amp @ G = 10^6		

	11647				11664			
Gain	V_A (volt)	I_A (amps)	I_{13} (amps)	I_{14} (amps)	V_A (volt)	I_A (amps)	I_{13} (amps)	I_{14} (amps)
10^4	1610	10^{-8}	3.3×10^{-8}	6.0×10^{-8}	1590	10^{-8}	2.9×10^{-8}	6.5×10^{-8}
10^5	2240	10^{-7}	3.0×10^{-7}	5.8×10^{-7}	2425	10^{-7}	2.6×10^{-7}	6.0×10^{-7}
10^6	3355	10^{-6}	3.2×10^{-6}	5.9×10^{-6}	3350	10^{-6}	3.2×10^{-6}	6.0×10^{-6}
I_D	3355	4.8×10^{-11} Amp @ G = 10^6			3350	4.2×10^{-11} Amp @ G = 10^6		

FIGURE 9.4-2 MEASUREMENTS OF CURRENT VOLTAGE GAIN AND DARK CURRENT

	11644				11762			
Gain	V_A (volt)	I_A (amps)	I_{13} (amps)	I_{14} (amps)	V_A (volt)	I_A (amps)	I_{13} (amps)	I_{14} (amps)
10^4	1530	10^{-8}	3.9×10^{-8}	6.2×10^{-8}	1380	10^{-8}	2.9×10^{-8}	5.6×10^{-8}
10^5	2170	10^{-7}	3.4×10^{-7}	5.9×10^{-7}	1945	10^{-7}	2.6×10^{-7}	5.3×10^{-7}
10^6	3200	10^{-6}	2.6×10^{-6}	5.6×10^{-6}	2780	10^{-6}	2.5×10^{-6}	5.5×10^{-6}
I_D	3200	6.5×10^{-11} Amp @ G = 10^6			2780	9.3×10^{-11} Amp @ G = 10^6		

	11647				11664			
Gain	V_A (volt)	I_A (amps)	I_{13} (amps)	I_{14} (amps)	V_A (volt)	I_A (amps)	I_{13} (amps)	I_{14} (amps)
10^4	1600	10^{-8}	3.2×10^{-8}	6.2×10^{-8}	1600	10^{-8}	3.5×10^{-8}	6.3×10^{-8}
10^5	2220	10^{-7}	2.8×10^{-7}	5.8×10^{-7}	2410	10^{-7}	3.0×10^{-7}	5.7×10^{-7}
10^6	3335	10^{-6}	3.0×10^{-6}	6.0×10^{-6}	3360	10^{-6}	3.2×10^{-6}	5.9×10^{-6}
I_D	3335	4.8×10^{-11} Amp @ G = 10^6			3360	4.2×10^{-11} Amp @ G = 10^6		

FIGURE 9.4-3 MEASUREMENTS OF CURRENT VOLTAGE GAIN AND DARK CURRENT

ORBIT 10

11644					11762			
Gain	V_A (volt)	I_A (amps)	I_{13} (amps)	I_{14} (amps)	V_A (volt)	I_A (amps)	I_{13} (amps)	I_{14} (amps)
10^4	1540	10^{-8}	3.3×10^{-8}	5.9×10^{-8}	1390	10^{-8}	2.9×10^{-8}	5.4×10^{-8}
10^5	2170	10^{-7}	2.9×10^{-7}	5.5×10^{-7}	1950	10^{-7}	2.6×10^{-7}	5.4×10^{-7}
10^6	3250	10^{-6}	2.5×10^{-6}	5.7×10^{-6}	2800	10^{-6}	2.6×10^{-6}	5.5×10^{-6}
I_D	3250	6.5×10^{-11} Amp @ G = 10^6			2800	1.02×10^{-10} Amp @ G = 10^6		

11647					11664			
Gain	V_A (volt)	I_A (amps)	I_{13} (amps)	I_{14} (amps)	V_A (volt)	I_A (amps)	I_{13} (amps)	I_{14} (amps)
10^4	1610	10^{-8}	3.3×10^{-8}	6.0×10^{-8}	1650	10^{-8}	3.3×10^{-8}	6.2×10^{-8}
10^5	2250	10^{-7}	2.9×10^{-7}	5.7×10^{-7}	2450	10^{-7}	2.6×10^{-7}	5.7×10^{-7}
10^6	3350	10^{-6}	3.1×10^{-6}	5.9×10^{-6}	3340	10^{-6}	2.9×10^{-6}	5.8×10^{-6}
I_D	3350	4.7×10^{-11} Amp @ G = 10^6			3340	4.3×10^{-11} Amp @ G = 10^6		

FIGURE 9.4-4 MEASUREMENTS OF CURRENT VOLTAGE GAIN AND DARK CURRENT

11644					11762			
Gain	V_A (volt)	I_A (amps)	I_{13} (amps)	I_{14} (amps)	V_A (volt)	I_A (amps)	I_{13} (amps)	I_{14}(amps)
10^4	1570	10^{-8}	2.9×10^{-8}	5.7×10^{-8}	1400	10^{-8}	2.8×10^{-8}	5.5×10^{-8}
10^5	2200	10^{-7}	2.8×10^{-7}	5.3×10^{-7}	1990	10^{-7}	2.2×10^{-7}	4.9×10^{-7}
10^6	3300	10^{-6}	2.7×10^{-6}	5.5×10^{-6}	2815	10^{-6}	2.2×10^{-6}	4.8×10^{-6}
I_D	3300	6.0×10^{-11} Amp @ G = 10^6			2815	9.8×10^{-11} Amp @ G = 10^6		

11647					11664			
Gain	V_A (volt)	I_A (amps)	I_{13} (amps)	I_{14} (amps)	V_A (volt)	I_A (amps)	I_{13} (amps)	I_{14} (amps)
10^4	1610	10^{-8}	3.1×10^{-8}	6.0×10^{-8}	1640	10^{-8}	3.2×10^{-8}	5.9×10^{-8}
10^5	2290	10^{-7}	2.2×10^{-7}	5.3×10^{-7}	2400	10^{-7}	2.8×10^{-7}	5.6×10^{-7}
10^6	3360	10^{-6}	2.5×10^{-6}	5.6×10^{-6}	3375	10^{-6}	3.0×10^{-6}	5.8×10^{-6}
I_D	3360	4.9×10^{-11} Amp @ G = 10^6			3375	4.5×10^{-11} Amp @ G = 10^6		

FIGURE 9.4-5 MEASUREMENTS OF CURRENT VOLTAGE GAIN AND DARK CURRENT

	11644				11762			
Gain	V_A (volt)	I_A (amps)	I_{13} (amps)	I_{14} (amps)	V_A (volt)	I_A (amps)	I_{13} (amps)	I_{14} (amps)
10^4	1550	10^{-8}	2.9×10^{-8}	5.5×10^{-8}	1385	10^{-8}	2.8×10^{-8}	5.5×10^{-8}
10^5	2180	10^{-7}	2.7×10^{-7}	5.2×10^{-7}	1890	10^{-7}	2.5×10^{-7}	5.2×10^{-7}
10^6	3280	10^{-6}	2.8×10^{-6}	5.1×10^{-6}	2785	10^{-6}	2.3×10^{-6}	5.0×10^{-6}
I_D	3280	6.3×10^{-11} Amp @ G = 10^6			2785	1.0×10^{-10} Amp @ G = 10^6		

	11647				11664			
Gain	V_A (volt)	I_A (amps)	I_{13} (amps)	I_{14} (amps)	V_A (volt)	I_A (amps)	I_{13} (amps)	I_{14} (amps)
10^4	1600	10^{-8}	3.2×10^{-8}	6.3×10^{-8}	1630	10^{-8}	3.3×10^{-8}	6.0×10^{-8}
10^5	2300	10^{-7}	2.2×10^{-7}	5.5×10^{-7}	2385	10^{-7}	2.3×10^{-7}	5.2×10^{-7}
10^6	3340	10^{-6}	2.6×10^{-6}	5.8×10^{-6}	3380	10^{-6}	2.8×10^{-6}	5.5×10^{-6}
I_D	3340	4.7×10^{-11} Amp @ G = 10^6			3380	4.2×10^{-11} Amp @ G = 10^6		

FIGURE 9.4-6 MEASUREMENTS OF CURRENT VOLTAGE GAIN AND DARK CURRENT

	11644				11762			
Gain	V_A (volt)	I_A (amps)	I_{13} (amps)	I_{14} (amps)	V_A (volt)	I_A (amps)	I_{13} (amps)	I_{14} (amps)
10^4	1540	10^{-8}	3.0×10^{-8}	5.8×10^{-8}	1380	10^{-8}	2.7×10^{-8}	5.2×10^{-8}
10^5	2200	10^{-7}	2.7×10^{-7}	5.2×10^{-7}	1900	10^{-7}	2.4×10^{-7}	5.0×10^{-7}
10^6	3300	10^{-6}	2.6×10^{-6}	5.0×10^{-6}	2815	10^{-6}	2.4×10^{-6}	5.1×10^{-6}
I_D	3300	6.3×10^{-11} Amp @ G = 10^6			2815	9.0×10^{-11} Amp @ G = 10^6		

	11647				11664			
Gain	V_A (volt)	I_A (amps)	I_{13} (amps)	I_{14} (amps)	V_A (volt)	I_A (amps)	I_{13} (amps)	I_{14} (amps)
10^4	1575	10^{-8}	3.1×10^{-8}	6.0×10^{-8}	1590	10^{-8}	3.2×10^{-8}	5.9×10^{-8}
10^5	2275	10^{-7}	2.3×10^{-7}	5.6×10^{-7}	2390	10^{-7}	2.5×10^{-7}	5.6×10^{-7}
10^6	3390	10^{-6}	2.5×10^{-6}	5.8×10^{-6}	3350	10^{-6}	2.7×10^{-6}	5.9×10^{-6}
I_D	3390	4.8×10^{-11} Amp @ G = 10^6			3350	4.4×10^{-11} Amp @ G = 10^6		

FIGURE 9.4-7 MEASUREMENTS OF CURRENT VOLTAGE GAIN AND DARK CURRENT

	11644				11762			
Gain	V_A (volt)	I_A (amps)	I_{13} (amps)	I_{14} (amps)	V_A (volt)	I_A (amps)	I_{13} (amps)	I_{14} (amps)
10^4	1530	10^{-8}	3.2×10^{-8}	5.9×10^{-8}	1380	10^{-8}	2.8×10^{-8}	5.3×10^{-8}
10^5	2180	10^{-7}	2.9×10^{-7}	5.7×10^{-7}	1930	10^{-7}	2.5×10^{-7}	4.9×10^{-7}
10^6	3330	10^{-6}	3.0×10^{-6}	5.8×10^{-6}	2780	10^{-6}	2.5×10^{-6}	4.9×10^{-6}
I_D	3330	6.3×10^{-11} Amp @ G = 10^6			2780	9.2×10^{-11}	Amp @ G = 10^6	

	11647				11664			
Gain	V_A (volt)	I_A (amps)	I_{13} (amps)	I_{14} (amps)	V_A (volt)	I_A (amps)	I_{13} (amps)	I_{14} (amps)
10^4	1560	10^{-8}	3.0×10^{-8}	5.8×10^{-8}	1540	10^{-8}	2.9×10^{-8}	6.0×10^{-8}
10^5	2290	10^{-7}	2.7×10^{-7}	5.5×10^{-7}	2240	10^{-7}	2.5×10^{-7}	5.7×10^{-7}
10^6	3400	10^{-6}	2.6×10^{-6}	5.7×10^{-6}	3370	10^{-6}	2.6×10^{-6}	5.9×10^{-6}
I_D	3400	4.7×10^{-11} Amp @ G = 10^6			3370	4.6×10^{-11}	Amp @ G = 10^6	

FIGURE 9.4-8 MEASUREMENTS OF CURRENT VOLTAGE GAIN AND DARK CURRENT

	11644				11762			
Gain	V_A (volt)	I_A (amps)	I_{13} (amps)	I_{14} (amps)	V_A (volt)	I_A (amps)	I_{13} (amps)	I_{14}(amps)
10^4	1520	10^{-8}	3.3×10^{-8}	5.8×10^{-8}	1405	10^{-8}	2.8×10^{-8}	5.2×10^{-8}
10^5	2150	10^{-7}	3.0×10^{-7}	5.5×10^{-7}	1950	10^{-7}	2.5×10^{-7}	4.9×10^{-7}
10^6	3290	10^{-6}	2.8×10^{-6}	5.7×10^{-6}	2815	10^{-6}	2.2×10^{-6}	4.8×10^{-6}
I_D	3290	6.3×10^{-11} Amp @ G = 10^6			2815	8.5×10^{-11} Amp @ G = 10^6		

	11647				11664			
Gain	V_A (volt)	I_A (amps)	I_{13} (amps)	I_{14} (amps)	V_A (volt)	I_A (amps)	I_{13} (amps)	I_{14} (amps)
10^4	1595	10^{-8}	2.9×10^{-8}	5.9×10^{-8}	1615	10^{-8}	3.2×10^{-8}	5.9×10^{-8}
10^5	2320	10^{-7}	2.5×10^{-7}	5.4×10^{-7}	2405	10^{-7}	2.8×10^{-7}	5.6×10^{-7}
10^6	3450	10^{-6}	2.7×10^{-6}	5.6×10^{-6}	3390	10^{-6}	2.9×10^{-6}	5.8×10^{-6}
I_D	3450	5.0×10^{-11} Amp @ G = 10^6			3390	3.8×10^{-11} Amp @ G = 10^6		

FIGURE 9.4-9 MEASUREMENTS OF CURRENT VOLTAGE GAIN AND DARK CURRENT

ORBIT 155.5

	11644				11762			
Gain	V_A (volt)	I_A (amps)	I_{13} (amps)	I_{14} (amps)	V_A (volt)	I_A (amps)	I_{13} (amps)	I_{14}(amps)
10^4	1520	10^{-8}	3.9×10^{-8}	6.0×10^{-8}	1397	10^{-8}	3.2×10^{-8}	5.5×10^{-8}
10^5	2145	10^{-7}	3.7×10^{-7}	5.7×10^{-7}	1943	10^{-7}	3.1×10^{-7}	5.6×10^{-7}
10^6	3285	10^{-6}	2.7×10^{-6}	5.9×10^{-6}	2810	10^{-6}	2.3×10^{-6}	5.7×10^{-6}
I_D	3285	4.1×10^{-11} Amp @ G = 10^6			2810	7.4×10^{-11}	Amp @ G = 10^6	

	11647				11664			
Gain	V_A (volt)	I_A (amps)	I_{13} (amps)	I_{14} (amps)	V_A (volt)	I_A (amps)	I_{13} (amps)	I_{14} (amps)
10^4	1605	10^{-8}	3.2×10^{-8}	6.2×10^{-8}	1610	10^{-8}	3.3×10^{-8}	5.1×10^{-8}
10^5	2327	10^{-7}	2.8×10^{-7}	6.0×10^{-7}	2404	10^{-7}	2.9×10^{-7}	5.4×10^{-7}
10^6	3460	10^{-6}	2.9×10^{-6}	5.9×10^{-6}	3397	10^{-6}	3.0×10^{-6}	5.8×10^{-6}
I_D	3460	6.4×10^{-11} Amp @ G = 10^6			3397	4.3×10^{-11}	Amp @ G = 10^6	

FIGURE 9.4-10 MEASUREMENTS OF CURRENT VOLTAGE GAIN AND DARK CURRENT

	11644				11762			
Gain	V_A (volt)	I_A (amps)	I_{13} (amps)	I_{14} (amps)	V_A (volt)	I_A (amps)	I_{13} (amps)	I_{14} (amps)
10^4	1520	10^{-8}	3.1×10^{-8}	5.5×10^{-8}	1405	10^{-8}	2.8×10^{-8}	5.2×10^{-8}
10^5	2145	10^{-7}	3.0×10^{-7}	5.7×10^{-7}	1950	10^{-7}	2.6×10^{-7}	5.3×10^{-7}
10^6	3280	10^{-6}	2.9×10^{-6}	5.8×10^{-6}	2850	10^{-6}	2.8×10^{-6}	5.3×10^{-6}
I_D	3280	4.9×10^{-11} Amp @ G = 10^6			2850	7.7×10^{-11} Amp @ G = 10^6		

	11647				11664			
Gain	V_A (volt)	I_A (amps)	I_{13} (amps)	I_{14} (amps)	V_A (volt)	I_A (amps)	I_{13} (amps)	I_{14} (amps)
10^4	1620	10^{-8}	3.5×10^{-8}	6.1×10^{-8}	1615	10^{-8}	3.5×10^{-8}	5.2×10^{-8}
10^5	2350	10^{-7}	2.9×10^{-7}	6.2×10^{-7}	2395	10^{-7}	3.2×10^{-7}	5.6×10^{-7}
10^6	3510	10^{-6}	2.9×10^{-6}	6.3×10^{-6}	3395	10^{-6}	2.7×10^{-6}	5.7×10^{-6}
I_D	3510	1.6×10^{-10} Amp @ G = 10^6			3395	3.5×10^{-11} Amp @ G = 10^6		

FIGURE 9.4-11 MEASUREMENTS OF CURRENT VOLTAGE GAIN AND DARK CURRENT

	11644				11762			
Gain	V_A (volt)	I_A (amps)	I_{13} (amps)	I_{14} (amps)	V_A (volt)	I_A (amps)	I_{13} (amps)	I_{14} (amps)
10^4	1520	10^{-8}	3.3×10^{-8}	5.9×10^{-8}	1400	10^{-8}	2.9×10^{-8}	5.1×10^{-8}
10^5	2140	10^{-7}	2.9×10^{-7}	5.6×10^{-7}	1950	10^{-7}	2.5×10^{-7}	4.9×10^{-7}
10^6	3275	10^{-6}	2.8×10^{-6}	5.8×10^{-6}	2855	10^{-6}	2.5×10^{-6}	5.5×10^{-6}
I_D	3275	4.6×10^{-11} Amp @ G = 10^6			2855	7.5×10^{-11} Amp @ G = 10^6		

	11647				11664			
Gain	V_A (volt)	I_A (amps)	I_{13} (amps)	I_{14} (amps)	V_A (volt)	I_A (amps)	I_{13} (amps)	I_{14} (amps)
10^4	1630	10^{-8}	3.6×10^{-8}	6.1×10^{-8}	1615	10^{-8}	3.4×10^{-8}	5.7×10^{-8}
10^5	2360	10^{-7}	2.7×10^{-7}	5.8×10^{-7}	2405	10^{-7}	3.1×10^{-7}	5.6×10^{-7}
10^6	3525	10^{-6}	2.8×10^{-6}	5.9×10^{-6}	3400	10^{-6}	2.9×10^{-6}	5.6×10^{-6}
I_D	3525	1.7×10^{-10} Amp @ G = 10^6			3400	3.9×10^{-11} Amp @ G = 10^6		

FIGURE 9.4-12 MEASUREMENTS OF CURRENT VOLTAGE GAIN AND DARK CURRENT

	11644				11762			
Gain	V_A (volt)	I_A (amps)	I_{13} (amps)	I_{14} (amps)	V_A (volt)	I_A (amps)	I_{13} (amps)	I_{14}(amps)
10^4	1530	10^{-8}	3.4×10^{-8}	6.2×10^{-8}	1403	10^{-8}	3.0×10^{-8}	5.6×10^{-8}
10^5	2148	10^{-7}	3.3×10^{-7}	6.0×10^{-7}	1950	10^{-7}	2.7×10^{-7}	5.4×10^{-7}
10^6	3285	10^{-6}	2.9×10^{-6}	5.9×10^{-6}	2860	10^{-6}	2.6×10^{-6}	5.4×10^{-6}
I_D	3285	5.1×10^{-11} Amp @ G = 10^6			2860	8.2×10^{-11} Amp @ G = 10^6		

	11647				11664			
Gain	V_A (volt)	I_A (amps)	I_{13} (amps)	I_{14} (amps)	V_A (volt)	I_A (amps)	I_{13} (amps)	I_{14} (amps)
10^4	1625	10^{-8}	3.5×10^{-8}	6.3×10^{-8}	1620	10^{-8}	3.3×10^{-8}	5.2×10^{-8}
10^5	2355	10^{-7}	3.1×10^{-7}	6.3×10^{-7}	2400	10^{-7}	3.0×10^{-7}	5.5×10^{-7}
10^6	3530	10^{-6}	3.0×10^{-6}	6.4×10^{-6}	3405	10^{-6}	3.1×10^{-6}	5.7×10^{-6}
I_D	3530	2.1×10^{-10} Amp @ G = 10^6			3405	4.0×10^{-11} Amp @ G = 10^6		

FIGURE 9.4-13 MEASUREMENTS OF CURRENT VOLTAGE GAIN AND DARK CURRENT

	11644				11762			
Gain	V_A (volt)	I_A (amps)	I_{13} (amps)	I_{14} (amps)	V_A (volt)	I_A (amps)	I_{13} (amps)	I_{14} (amps)
10^4	1530	10^{-8}	3.4×10^{-8}	5.9×10^{-8}	1400	10^{-8}	2.9×10^{-8}	5.4×10^{-8}
10^5	2138	10^{-7}	3.3×10^{-7}	6.1×10^{-7}	1950	10^{-7}	2.8×10^{-7}	5.4×10^{-7}
10^6	3285	10^{-6}	3.5×10^{-6}	6.3×10^{-6}	2860	10^{-6}	3.0×10^{-6}	5.7×10^{-6}
I_D	3285	4.7×10^{-11} Amp @ G = 10^6			2860	7.4×10^{-11} Amp @ G = 10^6		

	11647				11664			
Gain	V_A (volt)	I_A (amps)	I_{13} (amps)	I_{14} (amps)	V_A (volt)	I_A (amps)	I_{13} (amps)	I_{14} (amps)
10^4	1620	10^{-8}	3.3×10^{-8}	6.3×10^{-8}	1615	10^{-8}	3.2×10^{-8}	5.3×10^{-8}
10^5	2350	10^{-7}	3.3×10^{-7}	6.1×10^{-7}	2400	10^{-7}	3.1×10^{-7}	5.7×10^{-7}
10^6	3524	10^{-6}	3.5×10^{-6}	6.4×10^{-6}	3405	10^{-6}	3.3×10^{-6}	5.9×10^{-6}
I_D	3524	1.3×10^{-10} Amp @ G = 10^6			3405	3.7×10^{-11} Amp @ G = 10^6		

FIGURE 9.4-14 MEASUREMENTS OF CURRENT VOLTAGE GAIN AND DARK CURRENT

	11644				11762			
Gain	V_A (volt)	I_A (amps)	I_{13} (amps)	I_{14} (amps)	V_A (volt)	I_A (amps)	I_{13} (amps)	I_{14}(amps)
10^4	1530	10^{-8}	3.2×10^{-8}	5.5×10^{-8}	1403	10^{-8}	2.7×10^{-8}	5.3×10^{-8}
10^5	2147	10^{-7}	3.1×10^{-7}	5.9×10^{-7}	1950	10^{-7}	2.8×10^{-7}	5.5×10^{-7}
10^6	3300	10^{-6}	3.3×10^{-6}	6.3×10^{-6}	2855	10^{-6}	2.8×10^{-6}	5.6×10^{-6}
I_D	3300	4.0×10^{-11} Amp @ G = 10^6			2855	7.2×10^{-11} Amp @ G = 10^6		

	11647				11664			
Gain	V_A (volt)	I_A (amps)	I_{13} (amps)	I_{14} (amps)	V_A (volt)	I_A (amps)	I_{13} (amps)	I_{14} (amps)
10^4	1637	10^{-8}	3.4×10^{-8}	6.5×10^{-8}	1610	10^{-8}	3.5×10^{-8}	5.7×10^{-8}
10^5	2360	10^{-7}	3.3×10^{-7}	6.2×10^{-7}	2400	10^{-7}	3.3×10^{-7}	5.7×10^{-7}
10^6	3560	10^{-6}	3.6×10^{-6}	6.7×10^{-6}	3408	10^{-6}	3.6×10^{-6}	5.9×10^{-6}
I_D	3560	3.5×10^{-10} Amp @ G = 10^6			3408	3.3×10^{-11} Amp @ G = 10^6		

FIGURE 9.4-15 MEASUREMENTS OF CURRENT VOLTAGE GAIN AND DARK CURRENT

11644					11762			
Gain	V_A (volt)	I_A (amps)	I_{13} (amps)	I_{14} (amps)	V_A (volt)	I_A (amps)	I_{13} (amps)	I_{14} (amps)
10^4	1550	2×10^{-8}	5.2×10^{-9}	1.06×10^{-8}	1440	2×10^{-8}	4.5×10^{-9}	1.05×10^{-8}
10^5	2175	2×10^{-7}	3.8×10^{-8}	1.2×10^{-7}	1986	2×10^{-7}	4.2×10^{-8}	1.2×10^{-7}
10^6	3210	2×10^{-6}	3.7×10^{-7}	1.35×10^{-6}	2810	2×10^{-6}	3.9×10^{-7}	1.3×10^{-6}
I_D	3210	4.08×10^{-11} Amp @ G = 10^6			2810	6.03×10^{-11} Amp @ G = 10^6		

11647					11664			
Gain	V_A (volt)	I_A (amps)	I_{13} (amps)	I_{14} (amps)	V_A (volt)	I_A (amps)	I_{13} (amps)	I_{14} (amps)
10^4	1633	2×10^{-8}	4.6×10^{-9}	1.03×10^{-8}	1640	2×10^{-8}	4.0×10^{-9}	1.05×10^{-8}
10^5	2330	2×10^{-7}	4.2×10^{-8}	1.18×10^{-7}	2310	2×10^{-7}	3.8×10^{-8}	1.2×10^{-7}
10^6	3520	2×10^{-6}	3.9×10^{-7}	1.33×10^{-6}	3355	2×10^{-6}	3.7×10^{-7}	1.3×10^{-6}
I_D	3520	3.14×10^{-11} Amp @ G = 10^6			3355	4.97×10^{-11} Amp @ G = 10^6		

FIGURE 9.4-16 MEASUREMENTS OF CURRENT VOLTAGE GAIN AND DARK CURRENT

	11644				11762			
Gain	V_A (volt)	I_A (amps)	I_{13} (amps)	I_{14} (amps)	V_A (volt)	I_A (amps)	I_{13} (amps)	I_{14}(amps)
10^4	1530	2×10^{-8}	4.2×10^{-9}	1.1×10^{-8}	1430	2×10^{-8}	4.6×10^{-9}	1.05×10^{-8}
10^5	2165	2×10^{-7}	4×10^{-8}	1.22×10^{-7}	1980	2×10^{-7}	4.4×10^{-8}	1.2×10^{-7}
10^6	3200	2×10^{-6}	3.8×10^{-7}	1.4×10^{-6}	2800	2×10^{-6}	4.2×10^{-7}	1.36×10^{-6}
I_D	3200	4.6×10^{-11} Amp @ G = 10^6			2800	6.2×10^{-11} Amp @ G = 10^6		

	11647				11664			
Gain	V_A (volt)	I_A (amps)	I_{13} (amps)	I_{14} (amps)	V_A (volt)	I_A (amps)	I_{13} (amps)	I_{14} (amps)
10^4	1610	2×10^{-8}	4.7×10^{-9}	1.05×10^{-8}	1630	2×10^{-8}	3.8×10^{-9}	1×10^{-8}
10^5	2310	2×10^{-7}	4.2×10^{-8}	1.16×10^{-7}	2295	2×10^{-7}	3.8×10^{-8}	1.2×10^{-7}
10^6	3500	2×10^{-6}	4.1×10^{-7}	1.36×10^{-6}	3350	2×10^{-6}	3.6×10^{-7}	1.3×10^{-6}
I_D	3500	5×10^{-11} Amp @ G = 10^6			3350	5.5×10^{-11} Amp @ G = 10^6		

FIGURE 9.4-17 MEASUREMENTS OF CURRENT VOLTAGE GAIN AND DARK CURRENT

11644					11762			
Gain	V_A (volt)	I_A (amps)	I_{13} (amps)	I_{14} (amps)	V_A (volt)	I_A (amps)	I_{13} (amps)	I_{14} (amps)
10^4	1540	2×10^{-8}	4.0×10^{-9}	1.1×10^{-8}	1445	2×10^{-8}	4.4×10^{-9}	1.1×10^{-8}
10^5	2170	2×10^{-7}	3.83×10^{-8}	1.23×10^{-7}	1990	2×10^{-7}	4.2×10^{-8}	1.25×10^{-7}
10^6	3200	2×10^{-6}	3.8×10^{-7}	1.42×10^{-6}	2830	2×10^{-6}	3.9×10^{-7}	1.34×10^{-6}
I_D	3200	5.5×10^{-11} Amp @ G = 10^6			2830	7.4×10^{-11} Amp @ G = 10^6		

11647					11664			
Gain	V_A (volt)	I_A (amps)	I_{13} (amps)	I_{14} (amps)	V_A (volt)	I_A (amps)	I_{13} (amps)	I_{14} (amps)
10^4	1600	2×10^{-8}	4.3×10^{-9}	1×10^{-8}	1630	2×10^{-8}	3.7×10^{-9}	1.0×10^{-8}
10^5	2305	2×10^{-7}	4.1×10^{-8}	1.2×10^{-7}	2300	2×10^{-7}	3.8×10^{-8}	1.18×10^{-7}
10^6	3500	2×10^{-6}	3.8×10^{-7}	1.31×10^{-6}	3345	2×10^{-6}	3.63×10^{-7}	1.3×10^{-6}
I_D	3500	6.1×10^{-11} Amp @ G = 10^6			3345	6.0×10^{-11} Amp @ G = 10^6		

FIGURE 9.4-18 MEASUREMENTS OF CURRENT VOLTAGE GAIN AND DARK CURRENT

11644					11762			
Gain	V_A (volt)	I_A (amps)	I_{13} (amps)	I_{14} (amps)	V_A (volt)	I_A (amps)	I_{13} (amps)	I_{14}(amps)
10^4	1550	2×10^{-8}	4.0×10^{-9}	1.07×10^{-8}	1450	2×10^{-8}	4.3×10^{-9}	1.05×10^{-8}
10^5	2185	2×10^{-7}	3.9×10^{-8}	1.23×10^{-7}	1995	2×10^{-7}	4.2×10^{-8}	1.25×10^{-7}
10^6	3210	2×10^{-6}	3.6×10^{-7}	1.36×10^{-6}	2840	2×10^{-6}	4×10^{-7}	1.36×10^{-6}
I_D	3210	5.1×10^{-11} Amp @ G = 10^6			2840	7.3×10^{-11} Amp @ G = 10^6		

11647					11664			
Gain	V_A (volt)	I_A (amps)	I_{13} (amps)	I_{14} (amps)	V_A (volt)	I_A (amps)	I_{13} (amps)	I_{14} (amps)
10^4	1650	2×10^{-8}	4.4×10^{-9}	1×10^{-8}	1650	2×10^{-8}	3.8×10^{-9}	1.03×10^{-8}
10^5	2350	2×10^{-7}	4.2×10^{-8}	1.2×10^{-7}	2320	2×10^{-7}	3.8×10^{-8}	1.18×10^{-7}
10^6	3550	2×10^{-6}	3.8×10^{-7}	1.3×10^{-6}	3360	2×10^{-6}	3.6×10^{-7}	1.28×10^{-6}
I_D	3550	2.1×10^{-10} Amp @ G = 10^6			3360	5.4×10^{-11} Amp @ G = 10^6		

FIGURE 9.4-19 MEASUREMENTS OF CURRENT VOLTAGE GAIN AND DARK CURRENT

ORBIT 641

	11644				11762			
Gain	V_A (volt)	I_A (amps)	I_{13} (amps)	I_{14} (amps)	V_A (volt)	I_A (amps)	I_{13} (amps)	I_{14} (amps)
10^4	1530	2×10^{-8}	4.2×10^{-9}	1.1×10^{-8}	1450	2×10^{-8}	4.4×10^{-9}	1.05×10^{-8}
10^5	2175	2×10^{-7}	3.9×10^{-8}	1.2×10^{-7}	1990	2×10^{-7}	4.1×10^{-8}	1.3×10^{-7}
10^6	3210	2×10^{-6}	3.8×10^{-7}	1.4×10^{-6}	2820	2×10^{-6}	3.9×10^{-7}	1.35×10^{-6}
I_D	3210	4.9×10^{-11} Amp @ G = 10^6			2820	7.02×10^{-11} Amp @ G = 10^6		

	11647				11664			
Gain	V_A (volt)	I_A (amps)	I_{13} (amps)	I_{14} (amps)	V_A (volt)	I_A (amps)	I_{13} (amps)	I_{14} (amps)
10^4	1650	2×10^{-8}	4.5×10^{-9}	1.0×10^{-8}	1640	2×10^{-8}	4×10^{-9}	1.03×10^{-8}
10^5	2355	2×10^{-7}	4.2×10^{-8}	1.2×10^{-7}	2320	2×10^{-7}	3.8×10^{-8}	1.2×10^{-7}
10^6	3555	2×10^{-6}	3.8×10^{-7}	1.3×10^{-6}	3360	2×10^{-6}	3.7×10^{-7}	1.3×10^{-6}
I_D	3555	1.9×10^{-11} Amp @ G = 10^6			3360	4.9×10^{-11} Amp @ G = 10^6		

FIGURE 9.4-20 MEASUREMENTS OF CURRENT VOLTAGE GAIN AND DARK CURRENT

	11644				11762			
Gain	V_A (volt)	I_A (amps)	I_{13} (amps)	I_{14} (amps)	V_A (volt)	I_A (amps)	I_{13} (amps)	I_{14}(amps)
10^4	1540	2×10^{-8}	4.1×10^{-9}	1.1×10^{-8}	1440	2×10^{-8}	4.4×10^{-9}	1.06×10^{-8}
10^5	2170	2×10^{-7}	3.8×10^{-8}	1.23×10^{-7}	1980	2×10^{-7}	4.2×10^{-8}	1.2×10^{-7}
10^6	3200	2×10^{-6}	3.7×10^{-7}	1.4×10^{-6}	2800	2×10^{-6}	4×10^{-7}	1.33×10^{-6}
I_D	3200	4.2×10^{-11} Amp @ G = 10^6			2800	7.5×10^{-11} Amp @ G = 10^6		

	11647				11664			
Gain	V_A (volt)	I_A (amps)	I_{13} (amps)	I_{14} (amps)	V_A (volt)	I_A (amps)	I_{13} (amps)	I_{14} (amps)
10^4	1645	2×10^{-8}	4.4×10^{-9}	1×10^{-8}	1640	2×10^{-8}	3.7×10^{-9}	1.03×10^{-8}
10^5	2340	2×10^{-7}	4.2×10^{-8}	1.2×10^{-7}	2300	2×10^{-7}	3.6×10^{-8}	1.15×10^{-7}
10^6	3550	2×10^{-6}	4.1×10^{-7}	1.4×10^{-6}	3350	2×10^{-6}	3.6×10^{-7}	1.3×10^{-6}
I_D	3550	2.2×10^{-10} Amp @ G = 10^6			3350	5.2×10^{-11} Amp @ G = 10^6		

FIGURE 9.4-21 MEASUREMENTS OF CURRENT VOLTAGE GAIN AND DARK CURRENT

	11644				11762			
Gain	V_A (volt)	I_A (amps)	I_{13} (amps)	I_{14} (amps)	V_A (volt)	I_A (amps)	I_{13} (amps)	I_{14} (amps)
10^4	1540	2×10^{-8}	4×10^{-9}	1.06×10^{-8}	1450	2×10^{-8}	4.6×10^{-9}	1.1×10^{-8}
10^5	2170	2×10^{-7}	3.9×10^{-8}	1.25×10^{-7}	1990	2×10^{-7}	4.2×10^{-8}	1.2×10^{-7}
10^6	3200	2×10^{-6}	3.8×10^{-7}	1.4×10^{-6}	2820	2×10^{-6}	4×10^{-7}	1.35×10^{-6}
I_D	3200	4.3×10^{-11} Amp @ G = 10^6			2820	7.6×10^{-11} Amp @ G = 10^6		

	11647				11664			
Gain	V_A (volt)	I_A (amps)	I_{13} (amps)	I_{14} (amps)	V_A (volt)	I_A (amps)	I_{13} (amps)	I_{14} (amps)
10^4	1650	2×10^{-8}	4.4×10^{-9}	1.03×10^{-8}	1635	2×10^{-8}	3.8×10^{-9}	1.05×10^{-8}
10^5	2350	2×10^{-7}	4.2×10^{-8}	1.2×10^{-7}	2300	2×10^{-7}	3.8×10^{-8}	1.2×10^{-7}
10^6	3560	2×10^{-6}	3.9×10^{-7}	1.35×10^{-6}	3350	2×10^{-6}	3.7×10^{-7}	1.3×10^{-6}
I_D	3560	1.8×10^{-10} Amp @ G = 10^6			3350	4.4×10^{-11} Amp @ G = 10^6		

FIGURE 9.4-22 MEASUREMENTS OF CURRENT VOLTAGE GAIN AND DARK CURRENT

	11644				11762			
Gain	V_A (volt)	I_A (amps)	I_{13} (amps)	I_{14} (amps)	V_A (volt)	I_A (amps)	I_{13} (amps)	I_{14} (amps)
10^4	1540	2×10^{-8}	4×10^{-9}	1.1×10^{-8}	1455	2×10^{-8}	4.3×10^{-9}	1.05×10^{-8}
10^5	2175	2×10^{-7}	3.9×10^{-8}	1.25×10^{-7}	2003	2×10^{-7}	4.2×10^{-8}	1.2×10^{-7}
10^6	3200	2×10^{-6}	3.6×10^{-7}	1.37×10^{-6}	2820	2×10^{-6}	3.9×10^{-7}	1.3×10^{-6}
I_D	3200	4.7×10^{-11} Amp @ G = 10^6			2820	8.0×10^{-11} Amp @ G = 10^6		

	11647				11664			
Gain	V_A (volt)	I_A (amps)	I_{13} (amps)	I_{14} (amps)	V_A (volt)	I_A (amps)	I_{13} (amps)	I_{14} (amps)
10^4	1670	2×10^{-8}	4.3×10^{-9}	1.02×10^{-8}	1640	2×10^{-8}	3.7×10^{-9}	1.02×10^{-8}
10^5	2380	2×10^{-7}	4.1×10^{-8}	1.16×10^{-7}	2310	2×10^{-7}	3.8×10^{-8}	1.17×10^{-7}
10^6	3605	2×10^{-6}	3.9×10^{-7}	1.35×10^{-6}	3350	2×10^{-6}	3.6×10^{-7}	1.3×10^{-6}
I_D	3605	4.1×10^{-11} Amp @ G = 10^6			3350	4.7×10^{-11} Amp @ G = 10^6		

FIGURE 9.4-23 MEASUREMENTS OF CURRENT VOLTAGE GAIN AND DARK CURRENT

11644					11762			
Gain	V_A (volt)	I_A (amps)	I_{13} (amps)	I_{14} (amps)	V_A (volt)	I_A (amps)	I_{13} (amps)	I_{14}(amps)
10^4	1540	2×10^{-8}	4×10^{-9}	1.1×10^{-8}	1450	2×10^{-8}	4.6×10^{-9}	1.1×10^{-8}
10^5	2200	2×10^{-7}	3.9×10^{-8}	1.25×10^{-7}	1990	2×10^{-7}	4.2×10^{-8}	1.2×10^{-7}
10^6	3210	2×10^{-6}	3.6×10^{-7}	1.4×10^{-6}	2820	2×10^{-6}	4.0×10^{-7}	1.3×10^{-6}
I_D	3210	4.1×10^{-11} Amp @ G = 10^6			2820	7.0×10^{-11} Amp @ G = 10^6		

11647					11664			
Gain	V_A (volt)	I_A (amps)	I_{13} (amps)	I_{14} (amps)	V_A (volt)	I_A (amps)	I_{13} (amps)	I_{14} (amps)
10^4	1610	2×10^{-8}	4.3×10^{-9}	1.02×10^{-8}	1630	2×10^{-8}	3.7×10^{-9}	1.0×10^{-8}
10^5	2370	2×10^{-7}	4.1×10^{-8}	1.2×10^{-7}	2300	2×10^{-7}	3.8×10^{-8}	1.2×10^{-7}
10^6	3580	2×10^{-6}	3.9×10^{-7}	1.4×10^{-6}	3340	2×10^{-6}	3.6×10^{-7}	1.3×10^{-6}
I_D	3580	6.2×10^{-11} Amp @ G = 10^6			3340	6.1×10^{-11} Amp @ G = 10^6		

FIGURE 9.4-26 MEASUREMENTS OF CURRENT VOLTAGE GAIN AND DARK CURRENT

	11644				11762			
Gain	V_A (volt)	I_A (amps)	I_{13} (amps)	I_{14} (amps)	V_A (volt)	I_A (amps)	I_{13} (amps)	I_{14}(amps)
10^4	1550	2×10^{-8}	4.4×10^{-9}	1.1×10^{-8}	1500	2×10^{-8}	4.8×10^{-9}	1.1×10^{-8}
10^5	2210	2×10^{-7}	3.9×10^{-8}	1.2×10^{-7}	2010	2×10^{-7}	4.4×10^{-8}	1.25×10^{-7}
10^6	3250	2×10^{-6}	3.7×10^{-6}	1.4×10^{-6}	2875	2×10^{-6}	4.2×10^{-7}	1.4×10^{-6}
I_D	3250	4.3×10^{-11} Amp @ G = 10^6			2875	7.9×10^{-11} Amp @ G = 10^6		

	11647				11664			
Gain	V_A (volt)	I_A (amps)	I_{13} (amps)	I_{14} (amps)	V_A (volt)	I_A (amps)	I_{13} (amps)	I_{14} (amps)
10^4	1670	2×10^{-8}	4.3×10^{-9}	1.1×10^{-8}	1620	2×10^{-8}	4.1×10^{-9}	1.0×10^{-8}
10^5	2360	2×10^{-7}	4.0×10^{-8}	1.3×10^{-7}	2270	2×10^{-7}	3.9×10^{-8}	1.15×10^{-7}
10^6	3640	2×10^{-6}	3.9×10^{-6}	1.4×10^{-6}	3340	2×10^{-6}	3.7×10^{-7}	1.35×10^{-6}
I_D	3640	2.7×10^{-11} Amp @ G = 10^6			3340	5.8×10^{-11} Amp @ G = 10^6		

FIGURE 9.4-27 MEASUREMENTS OF CURRENT VOLTAGE GAIN AND DARK CURRENT

ORBIT 1089

	11644				11762			
Gain	V_A (volt)	I_A (amps)	I_{13} (amps)	I_{14} (amps)	V_A (volt)	I_A (amps)	I_{13} (amps)	I_{14}(amps)
10^4	1540	2×10^{-8}	4.1×10^{-9}	1.1×10^{-8}	1495	2×10^{-8}	4.8×10^{-9}	1.1×10^{-8}
10^5	2180	2×10^{-7}	3.3×10^{-8}	1.3×10^{-7}	2010	2×10^{-7}	4.4×10^{-8}	1.3×10^{-7}
10^6	3230	2×10^{-6}	3.7×10^{-7}	1.4×10^{-6}	2870	2×10^{-6}	4.2×10^{-7}	1.4×10^{-6}
I_D	3230	4.7×10^{-11} Amp @ G = 10^6			2870	7.7×10^{-11} Amp @ G = 10^6		

	11647				11664			
Gain	V_A (volt)	I_A (amps)	I_{13} (amps)	I_{14} (amps)	V_A (volt)	I_A (amps)	I_{13} (amps)	I_{14} (amps)
10^4	1680	2×10^{-8}	4.3×10^{-9}	1.1×10^{-8}	1620	2×10^{-8}	4.1×10^{-9}	1×10^{-8}
10^5	2370	2×10^{-7}	4.0×10^{-8}	1.3×10^{-7}	2270	2×10^{-7}	3.9×10^{-8}	1.2×10^{-7}
10^6	3650	2×10^{-6}	3.9×10^{-7}	1.4×10^{-6}	3345	2×10^{-6}	3.7×10^{-7}	1.4×10^{-6}
I_D	3650	2.1×10^{-10} Amp @ G = 10^6			3345	6.2×10^{-11} Amp @ G = 10^6		

FIGURE 9.4-28 MEASUREMENTS OF CURRENT VOLTAGE GAIN AND DARK CURRENT

11644					11762			
Gain	V_A (volt)	I_A (amps)	I_{13} (amps)	I_{14} (amps)	V_A (volt)	I_A (amps)	I_{13} (amps)	I_{14}(amps)
10^4	1540	2×10^{-8}	4.1×10^{-9}	1.1×10^{-8}	1500	2×10^{-8}	4.8×10^{-9}	1.1×10^{-8}
10^5	2190	2×10^{-7}	3.8×10^{-8}	1.3×10^{-7}	2000	2×10^{-7}	4.4×10^{-8}	1.3×10^{-7}
10^6	3240	2×10^{-6}	3.7×10^{-7}	1.4×10^{-6}	2880	2×10^{-6}	4.2×10^{-7}	1.4×10^{-6}
I_D	3240	4.9×10^{-11} Amp @ G = 10^6			2880	7.8×10^{-11}	Amp @ G = 10^6	

11647					11664			
Gain	V_A (volt)	I_A (amps)	I_{13} (amps)	I_{14} (amps)	V_A (volt)	I_A (amps)	I_{13} (amps)	I_{14} (amps)
10^4	1680	2×10^{-8}	4.3×10^{-9}	1.1×10^{-8}	1620	2×10^{-8}	4.1×10^{-9}	1×10^{-8}
10^5	2360	2×10^{-7}	4.0×10^{-8}	1.3×10^{-7}	2270	2×10^{-7}	3.9×10^{-8}	1.2×10^{-7}
10^6	3640	2×10^{-6}	3.9×10^{-7}	1.4×10^{-6}	3340	2×10^{-6}	3.7×10^{-7}	1.4×10^{-6}
I_D	3640	1.9×10^{-10} Amp @ G = 10^6			3340	5.9×10^{-11}	Amp @ G = 10^6	

FIGURE 9.4-29 MEASUREMENTS OF CURRENT VOLTAGE GAIN AND DARK CURRENT

	11644				11762			
Gain	V_A (volt)	I_A (amps)	I_{13} (amps)	I_{14} (amps)	V_A (volt)	I_A (amps)	I_{13} (amps)	I_{14} (amps)
10^4	1540	2×10^{-8}	4.1×10^{-9}	1.1×10^{-8}	1495	2×10^{-8}	4.8×10^{-9}	1.1×10^{-8}
10^5	2170	2×10^{-7}	3.8×10^{-8}	1.3×10^{-7}	1990	2×10^{-7}	4.4×10^{-8}	1.3×10^{-7}
10^6	3230	2×10^{-6}	3.7×10^{-7}	1.4×10^{-6}	2870	2×10^{-6}	4.1×10^{-7}	1.4×10^{-6}
I_D	3230	4.7×10^{-11} Amp @ G = 10^6			2870	7.7×10^{-11} Amp @ G = 10^6		

	11647				11664			
Gain	V_A (volt)	I_A (amps)	I_{13} (amps)	I_{14} (amps)	V_A (volt)	I_A (amps)	I_{13} (amps)	I_{14} (amps)
10^4	1680	2×10^{-8}	4.3×10^{-9}	1.1×10^{-8}	1620	2×10^{-8}	4.1×10^{-9}	1×10^{-8}
10^5	2370	2×10^{-7}	4.0×10^{-8}	1.3×10^{-7}	2280	2×10^{-7}	3.9×10^{-8}	1.2×10^{-7}
10^6	3640	2×10^{-6}	3.9×10^{-7}	1.4×10^{-6}	3350	2×10^{-6}	3.7×10^{-7}	1.4×10^{-6}
I_D	3640	2.0×10^{-10} Amp @ G = 10^6			3350	5.7×10^{-11} Amp @ G = 10^6		

FIGURE 9.4-30 MEASUREMENTS OF CURRENT VOLTAGE GAIN AND DARK CURRENT

	11644				11762			
Gain	V_A (volt)	I_A (amps)	I_{13} (amps)	I_{14} (amps)	V_A (volt)	I_A (amps)	I_{13} (amps)	I_{14} (amps)
10^4	1550	2×10^{-8}	4.1×10^{-9}	1.1×10^{-8}	1500	2×10^{-8}	4.8×10^{-9}	1.1×10^{-8}
10^5	2220	2×10^{-7}	3.8×10^{-8}	1.3×10^{-7}	2000	2×10^{-7}	4.4×10^{-8}	1.3×10^{-7}
10^6	3250	2×10^{-6}	3.7×10^{-7}	1.4×10^{-6}	2880	2×10^{-6}	4.0×10^{-7}	1.4×10^{-6}
I_D	3250	5.1×10^{-11} Amp @ G = 10^6			2880	8.1×10^{-11} Amp @ G = 10^6		

	11647				11664			
Gain	V_A (volt)	I_A (amps)	I_{13} (amps)	I_{14} (amps)	V_A (volt)	I_A (amps)	I_{13} (amps)	I_{14} (amps)
10^4	1690	2×10^{-8}	4.4×10^{-9}	1.1×10^{-8}	1640	2×10^{-8}	4.0×10^{-9}	1×10^{-8}
10^5	2390	2×10^{-7}	4.1×10^{-8}	1.3×10^{-7}	2330	2×10^{-7}	3.8×10^{-8}	1.2×10^{-7}
10^6	3650	2×10^{-6}	4.0×10^{-7}	1.4×10^{-6}	3370	2×10^{-6}	3.7×10^{-7}	1.2×10^{-6}
I_D	3650	3.8×10^{-10} Amp @ G = 10^6			3370	5.8×10^{-11} Amp @ G = 10^6		

FIGURE 9.4-31 MEASUREMENTS OF CURRENT VOLTAGE GAIN AND DARK CURRENT

11644					11762			
Gain	V_A (volt)	I_A (amps)	I_{13} (amps)	I_{14} (amps)	V_A (volt)	I_A (amps)	I_{13} (amps)	I_{14} (amps)
10^4	1550	2×10^{-8}	4.5×10^{-9}	1.2×10^{-8}	1460	2×10^{-8}	4.8×10^{-9}	1.1×10^{-8}
10^5	2170	2×10^{-7}	4.1×10^{-8}	1.25×10^{-7}	2020	2×10^{-7}	4.6×10^{-8}	1.2×10^{-7}
10^6	3220	2×10^{-6}	3.9×10^{-7}	1.4×10^{-6}	2870	2×10^{-6}	4.2×10^{-7}	1.36×10^{-6}
I_D	3220	4.8×10^{-11} Amp @ G = 10^6			2870	7.5×10^{-11} Amp @ G = 10^6		

11647					11664			
Gain	V_A (volt)	I_A (amps)	I_{13} (amps)	I_{14} (amps)	V_A (volt)	I_A (amps)	I_{13} (amps)	I_{14} (amps)
10^4	1650	2×10^{-8}	4.7×10^{-9}	1.05×10^{-8}	1660	2×10^{-8}	4.3×10^{-9}	1.05×10^{-8}
10^5	2360	2×10^{-7}	4.3×10^{-8}	1.2×10^{-7}	2330	2×10^{-7}	4.0×10^{-8}	1.2×10^{-7}
10^6	3610	2×10^{-6}	4.1×10^{-7}	1.35×10^{-6}	3380	2×10^{-6}	3.7×10^{-7}	1.3×10^{-6}
I_D	3610	9.1×10^{-11} Amp @ G = 10^6			3380	5.5×10^{-11} Amp @ G = 10^6		

FIGURE 9.4-32 MEASUREMENTS OF CURRENT VOLTAGE GAIN AND DARK CURRENT

	11644				11762			
Gain	V_A (volt)	I_A (amps)	I_{13} (amps)	I_{14} (amps)	V_A (volt)	I_A (amps)	I_{13} (amps)	I_{14} (amps)
10^4	1540	2×10^{-8}	4.5×10^{-9}	1.2×10^{-8}	1480	2×10^{-8}	4.6×10^{-9}	1×10^{-8}
10^5	2160	2×10^{-7}	4.1×10^{-8}	1.25×10^{-7}	2020	2×10^{-7}	4.4×10^{-8}	1.2×10^{-7}
10^6	3200	2×10^{-6}	3.9×10^{-7}	1.4×10^{-6}	2880	2×10^{-6}	4.2×10^{-7}	1.4×10^{-6}
I_D	3200	5.0×10^{-11} Amp @ G = 10^6			2880	7.2×10^{-11} Amp @ G = 10^6		

	11647				11664			
Gain	V_A (volt)	I_A (amps)	I_{13} (amps)	I_{14} (amps)	V_A (volt)	I_A (amps)	I_{13} (amps)	I_{14} (amps)
10^4	1680	2×10^{-8}	4.4×10^{-9}	1.1×10^{-8}	1650	2×10^{-8}	4.0×10^{-9}	1×10^{-8}
10^5	2400	2×10^{-7}	4.3×10^{-8}	1.3×10^{-7}	2320	2×10^{-7}	3.8×10^{-8}	1.1×10^{-7}
10^6	3630	2×10^{-6}	4.1×10^{-7}	1.4×10^{-6}	3370	2×10^{-6}	3.7×10^{-7}	1.2×10^{-6}
I_D	3630	8.8×10^{-11} Amp @ G = 10^6			3370	5.2×10^{-11} Amp @ G = 10^6		

FIGURE 9.4-33 MEASUREMENTS OF CURRENT VOLTAGE GAIN AND DARK CURRENT

	11644				11762			
Gain	V_A (volt)	I_A (amps)	I_{13} (amps)	I_{14} (amps)	V_A (volt)	I_A (amps)	I_{13} (amps)	I_{14}(amps)
10^4	1530	2×10^{-8}	4.5×10^{-9}	1.2×10^{-8}	1480	2×10^{-8}	4.8×10^{-9}	1.1×10^{-8}
10^5	2150	2×10^{-7}	4.1×10^{-8}	1.3×10^{-7}	2020	2×10^{-7}	4.6×10^{-8}	1.2×10^{-7}
10^6	3200	2×10^{-6}	3.9×10^{-7}	1.4×10^{-6}	2880	2×10^{-6}	4.2×10^{-7}	1.4×10^{-6}
I_D	3200	4.9×10^{-11} Amp @ G = 10^6			2880	7.0×10^{-11} Amp @ G = 10^6		

	11647				11664			
Gain	V_A (volt)	I_A (amps)	I_{13} (amps)	I_{14} (amps)	V_A (volt)	I_A (amps)	I_{13} (amps)	I_{14} (amps)
10^4	1680	2×10^{-8}	4.4×10^{-9}	1.1×10^{-8}	1650	2×10^{-8}	4×10^{-9}	1×10^{-8}
10^5	2400	2×10^{-7}	4.3×10^{-8}	1.3×10^{-7}	2310	2×10^{-7}	3.8×10^{-8}	1.1×10^{-7}
10^6	3630	2×10^{-6}	4.1×10^{-7}	1.4×10^{-6}	3360	2×10^{-6}	3.7×10^{-7}	1.2×10^{-6}
I_D	3630	8.9×10^{-11} Amp @ G = 10^6			3360	5.0×10^{-11} Amp @ G = 10^6		

FIGURE 9.4-34 MEASUREMENTS OF CURRENT VOLTAGE GAIN AND DARK CURRENT

	11644				11762			
Gain	V_A (volt)	I_A (amps)	I_{13} (amps)	I_{14} (amps)	V_A (volt)	I_A (amps)	I_{13} (amps)	I_{14} (amps)
10^4	1540	2×10^{-8}	4.5×10^{-9}	1.2×10^{-8}	1500	2×10^{-8}	4.8×10^{-9}	1.1×10^{-8}
10^5	2170	2×10^{-7}	4.1×10^{-8}	1.3×10^{-7}	2040	2×10^{-7}	4.6×10^{-8}	1.2×10^{-7}
10^6	3200	2×10^{-6}	3.9×10^{-7}	1.4×10^{-6}	2900	2×10^{-6}	4.2×10^{-7}	1.4×10^{-6}
I_D	3200	5.1×10^{-11} Amp @ G = 10^6			2900	7.4×10^{-11} Amp @ G = 10^6		

	11647				11664			
Gain	V_A (volt)	I_A (amps)	I_{13} (amps)	I_{14} (amps)	V_A (volt)	I_A (amps)	I_{13} (amps)	I_{14} (amps)
10^4	1700	2×10^{-8}	4.4×10^{-9}	1.1×10^{-8}	1650	2×10^{-8}	4×10^{-9}	1×10^{-8}
10^5	2440	2×10^{-7}	4.3×10^{-8}	1.3×10^{-7}	2310	2×10^{-7}	3.8×10^{-8}	1.1×10^{-7}
10^6	3700	2×10^{-6}	4.1×10^{-7}	1.4×10^{-6}	3340	2×10^{-6}	3.6×10^{-7}	1.2×10^{-6}
I_D	3700	2.7×10^{-11} Amp @ G = 10^6			3340	5.2×10^{-11} Amp @ G = 10^6		

FIGURE 9.4-35 MEASUREMENTS OF CURRENT VOLTAGE GAIN AND DARK CURRENT

	11644				11762			
Gain	V_A (volt)	I_A (amps)	I_{13} (amps)	I_{14} (amps)	V_A (volt)	I_A (amps)	I_{13} (amps)	I_{14}(amps)
10^4	1530	2×10^{-8}	4.5×10^{-9}	1.2×10^{-8}	1470	2×10^{-8}	4.8×10^{-9}	1.1×10^{-8}
10^5	2160	2×10^{-7}	4.1×10^{-8}	1.3×10^{-7}	2030	2×10^{-7}	4.6×10^{-8}	1.2×10^{-7}
10^6	3200	2×10^{-6}	4.0×10^{-7}	1.4×10^{-6}	2890	2×10^{-6}	4.2×10^{-7}	1.4×10^{-6}
I_D	3200	4.8×10^{-11} Amp @ G = 10^6			2890	7.5×10^{-11} Amp @ G = 10^6		

	11647				11664			
Gain	V_A (volt)	I_A (amps)	I_{13} (amps)	I_{14} (amps)	V_A (volt)	I_A (amps)	I_{13} (amps)	I_{14} (amps)
10^4	1680	2×10^{-8}	4.4×10^{-9}	1.1×10^{-8}	1640	2×10^{-8}	4.1×10^{-9}	1.05×10^{-8}
10^5	2400	2×10^{-7}	4.3×10^{-8}	1.3×10^{-7}	2300	2×10^{-7}	3.8×10^{-8}	1.1×10^{-7}
10^6	3700	2×10^{-6}	4.1×10^{-7}	1.4×10^{-6}	3340	2×10^{-6}	3.5×10^{-7}	1.2×10^{-6}
I_D	3700	2.4×10^{-10} Amp @ G = 10^6			3340	5.4×10^{-11} Amp @ G = 10^6		

FIGURE 9.4-36 MEASUREMENTS OF CURRENT VOLTAGE GAIN AND DARK CURRENT

11644					11762			
Gain	V_A (volt)	I_A (amps)	I_{13} (amps)	I_{14} (amps)	V_A (volt)	I_A (amps)	I_{13} (amps)	I_{14} (amps)
10^4	1530	2×10^{-8}	4.5×10^{-9}	1.2×10^{-8}	1480	2×10^{-8}	4.8×10^{-9}	1.1×10^{-8}
10^5	2160	2×10^{-7}	4.1×10^{-8}	1.3×10^{-7}	2040	2×10^{-7}	4.6×10^{-8}	1.2×10^{-7}
10^6	3200	2×10^{-6}	3.9×10^{-7}	1.4×10^{-6}	2880	2×10^{-6}	4.2×10^{-7}	1.4×10^{-6}
I_D	3200	4.9×10^{-11} Amp @ G = 10^6			2880	7.6×10^{-11} Amp @ G = 10^6		

209

11647					11664			
Gain	V_A (volt)	I_A (amps)	I_{13} (amps)	I_{14} (amps)	V_A (volt)	I_A (amps)	I_{13} (amps)	I_{14} (amps)
10^4	1680	2×10^{-8}	4.4×10^{-9}	1.1×10^{-8}	1640	2×10^{-8}	4×10^{-9}	1×10^{-8}
10^5	2410	2×10^{-7}	4.3×10^{-8}	1.3×10^{-7}	2300	2×10^{-7}	3.8×10^{-8}	1.1×10^{-7}
10^6	3700	2×10^{-6}	4.1×10^{-7}	1.4×10^{-6}	3330	2×10^{-6}	3.5×10^{-7}	1.2×10^{-6}
I_D	3700	2.1×10^{-10} Amp @ G = 10^6			3330	5.6×10^{-11} Amp @ G = 10^6		

FIGURE 9.4-37 MEASUREMENTS OF CURRENT VOLTAGE GAIN AND DARK CURRENT

	11644				11762			
Gain	V_A (volt)	I_A (amps)	I_{13} (amps)	I_{14} (amps)	V_A (volt)	I_A (amps)	I_{13} (amps)	I_{14}(amps)
10^4	1530	2×10^{-8}	4.5×10^{-9}	1.2×10^{-8}	1480	2×10^{-8}	4.8×10^{-9}	1.1×10^{-8}
10^5	2150	2×10^{-7}	4.1×10^{-8}	1.3×10^{-7}	2030	2×10^{-7}	4.6×10^{-8}	1.2×10^{-7}
10^6	3200	2×10^{-6}	3.9×10^{-7}	1.4×10^{-6}	2880	2×10^{-6}	4.2×10^{-7}	1.4×10^{-6}
I_D	3200	5.2×10^{-11} Amp @ G = 10^6			2880	7.4×10^{-11} Amp @ G = 10^6		

	11647				11664			
Gain	V_A (volt)	I_A (amps)	I_{13} (amps)	I_{14} (amps)	V_A (volt)	I_A (amps)	I_{13} (amps)	I_{14} (amps)
10^4	1680	2×10^{-8}	4.4×10^{-9}	1.1×10^{-8}	1640	2×10^{-8}	4×10^{-9}	1.05×10^{-8}
10^5	2410	2×10^{-7}	4.3×10^{-8}	1.3×10^{-7}	2300	2×10^{-7}	3.7×10^{-8}	1.08×10^{-7}
10^6	3700	2×10^{-6}	4.1×10^{-7}	1.4×10^{-6}	3330	2×10^{-6}	3×10^{-7}	1.2×10^{-6}
I_D	3700	2.1×10^{-10} Amp @ G = 10^6			3330	5.7×10^{-11} Amp @ G = 10^6		

FIGURE 9.4-38 MEASUREMENTS OF CURRENT VOLTAGE GAIN AND DARK CURRENT

	11644				11762			
Gain	V_A (volt)	I_A (amps)	I_{13} (amps)	I_{14} (amps)	V_A (volt)	I_A (amps)	I_{13} (amps)	I_{14}(amps)
10^4	1540	2×10^{-8}	4.5×10^{-9}	1.2×10^{-8}	1480	2×10^{-8}	4.8×10^{-9}	1.1×10^{-8}
10^5	2170	2×10^{-7}	4.1×10^{-8}	1.3×10^{-7}	2040	2×10^{-7}	4.6×10^{-8}	1.2×10^{-7}
10^6	3200	2×10^{-6}	4.0×10^{-7}	1.4×10^{-6}	2870	2×10^{-6}	4.2×10^{-7}	1.4×10^{-6}
I_D	3200	5.4×10^{-11} Amp @ G = 10^6			2870	7.6×10^{-11} Amp @ G = 10^6		

	11647				11664			
Gain	V_A (volt)	I_A (amps)	I_{13} (amps)	I_{14} (amps)	V_A (volt)	I_A (amps)	I_{13} (amps)	I_{14} (amps)
10^4	1670	2×10^{-8}	4.4×10^{-9}	1.1×10^{-8}	1650	2×10^{-8}	4×10^{-9}	1.05×10^{-8}
10^5	2400	2×10^{-7}	4.3×10^{-8}	1.3×10^{-7}	2300	2×10^{-7}	3.8×10^{-8}	1.1×10^{-7}
10^6	3700	2×10^{-6}	4.1×10^{-7}	1.4×10^{-6}	3340	2×10^{-6}	3.6×10^{-7}	1.2×10^{-6}
I_D	3700	2.4×10^{-10} Amp @ G = 10^6			3340	5.9×10^{-11} Amp @ G = 10^6		

FIGURE 9.4-39 MEASUREMENTS OF CURRENT VOLTAGE GAIN AND DARK CURRENT

ORBIT 1947.5

	11644				11762			
Gain	V_A (volt)	I_A (amps)	I_{13} (amps)	I_{14} (amps)	V_A (volt)	I_A (amps)	I_{13} (amps)	I_{14}(amps)
10^4	1530	2×10^{-8}	4.5×10^{-9}	1.2×10^{-8}	1480	2×10^{-8}	4.8×10^{-9}	1.1×10^{-8}
10^5	2150	2×10^{-7}	4.1×10^{-8}	1.3×10^{-7}	2030	2×10^{-7}	4.6×10^{-8}	1.2×10^{-7}
10^6	3200	2×10^{-6}	3.9×10^{-7}	1.4×10^{-6}	2880	2×10^{-6}	4.2×10^{-7}	1.4×10^{-6}
I_D	3200	4.6×10^{-11} Amp @ G = 10^6			2880	9×10^{-11} Amp @ G = 10^6		

	11647				11664			
Gain	V_A (volt)	I_A (amps)	I_{13} (amps)	I_{14} (amps)	V_A (volt)	I_A (amps)	I_{13} (amps)	I_{14} (amps)
10^4	1680	2×10^{-8}	4.4×10^{-9}	1.1×10^{-8}	1640	2×10^{-8}	4×10^{-9}	1.05×10^{-8}
10^5	2410	2×10^{-7}	4.3×10^{-8}	1.3×10^{-7}	2300	2×10^{-7}	3.7×10^{-8}	1.08×10^{-7}
10^6	3700	2×10^{-6}	4.1×10^{-7}	1.4×10^{-6}	3300	2×10^{-6}	3.5×10^{-7}	1.2×10^{-6}
I_D	3700	7.7×10^{-11} Amp @ G = 10^6			3300	9.4×10^{-11} Amp @ G = 10^6		

FIGURE 9.4-42 MEASUREMENTS OF CURRENT VOLTAGE GAIN AND DARK CURRENT

11644					11762			
Gain	V_A (volt)	I_A (amps)	I_{13} (amps)	I_{14} (amps)	V_A (volt)	I_A (amps)	I_{13} (amps)	I_{14} (amps)
10^4	1530	2×10^{-8}	4.5×10^{-9}	1.2×10^{-8}	1440	2×10^{-8}	4.8×10^{-9}	1.1×10^{-8}
10^5	2160	2×10^{-7}	4.1×10^{-8}	1.3×10^{-7}	2000	2×10^{-7}	4.6×10^{-8}	1.2×10^{-7}
10^6	3200	2×10^{-6}	3.9×10^{-7}	1.4×10^{-6}	2850	2×10^{-6}	4.2×10^{-7}	1.4×10^{-6}
I_D	3200	4.4×10^{-11} Amp @ G = 10^6			2850	8.6×10^{-11} Amp @ G = 10^6		

11647					11664			
Gain	V_A (volt)	I_A (amps)	I_{13} (amps)	I_{14} (amps)	V_A (volt)	I_A (amps)	I_{13} (amps)	I_{14} (amps)
10^4	1620	2×10^{-8}	4.4×10^{-9}	1.1×10^{-8}	1640	2×10^{-8}	4×10^{-9}	1.05×10^{-8}
10^5	2400	2×10^{-7}	4.3×10^{-8}	1.3×10^{-7}	2310	2×10^{-7}	3.7×10^{-8}	1.08×10^{-7}
10^6	3500	2×10^{-6}	4.1×10^{-7}	1.4×10^{-6}	3340	2×10^{-6}	3.5×10^{-7}	1.2×10^{-6}
I_D	3500	7.0×10^{-11} Amp @ G = 10^6			3340	9.5×10^{-11} Amp @ G = 10^6		

FIGURE 9.4-43 MEASUREMENTS OF CURRENT VOLTAGE GAIN AND DARK CURRENT

	11644				11762			
Gain	V_A (volt)	I_A (amps)	I_{13} (amps)	I_{14} (amps)	V_A (volt)	I_A (amps)	I_{13} (amps)	I_{14}(amps)
10^4	1530	2×10^{-8}	4.5×10^{-9}	1.2×10^{-8}	1440	2×10^{-8}	4.8×10^{-9}	1.1×10^{-8}
10^5	2150	2×10^{-7}	4.1×10^{-8}	1.3×10^{-7}	2000	2×10^{-7}	4.6×10^{-8}	1.2×10^{-7}
10^6	3200	2×10^{-6}	3.9×10^{-7}	1.4×10^{-6}	2800	2×10^{-6}	4.2×10^{-7}	1.4×10^{-6}
I_D	3200	4.4×10^{-11} Amp @ G = 10^6			2800	8.6×10^{-11} Amp @ G = 10^6		

	11647				11664			
Gain	V_A (volt)	I_A (amps)	I_{13} (amps)	I_{14} (amps)	V_A (volt)	I_A (amps)	I_{13} (amps)	I_{14} (amps)
10^4	1620	2×10^{-8}	4.4×10^{-9}	1.1×10^{-8}	1630	2×10^{-8}	4×10^{-9}	1.1×10^{-8}
10^5	2400	2×10^{-7}	4.3×10^{-8}	1.3×10^{-7}	2300	2×10^{-7}	3.7×10^{-8}	1.9×10^{-7}
10^6	3500	2×10^{-6}	4.1×10^{-7}	1.4×10^{-6}	3350	2×10^{-6}	3.1×10^{-7}	1.2×10^{-6}
I_D	3500	7.0×10^{-11} Amp @ G = 10^6			3350	9.5×10^{-11} Amp @ G = 10^6		

FIGURE 9.4-44 MEASUREMENTS OF CURRENT VOLTAGE GAIN AND DARK CURRENT

11644					11762			
Gain	V_A (volt)	I_A (amps)	I_{13} (amps)	I_{14} (amps)	V_A (volt)	I_A (amps)	I_{13} (amps)	I_{14} (amps)
10^4	1530	2×10^{-8}	4.1×10^{-9}	1.1×10^{-8}	1495	2×10^{-8}	4.8×10^{-9}	1.1×10^{-8}
10^5	2170	2×10^{-7}	3.8×10^{-8}	1.3×10^{-7}	2010	2×10^{-7}	4.4×10^{-8}	1.3×10^{-7}
10^6	3220	$2 \times 10^{=6}$	3.7×10^{-7}	1.4×10^{-6}	2870	2×10^{-6}	4.2×10^{-7}	1.4×10^{-6}
I_D	3220	4.6×10^{-11} Amp @ G = 10^6			2870	9.2×10^{-11} Amp @ G = 10^6		

11647					11664			
Gain	V_A (volt)	I_A (amps)	I_{13} (amps)	I_{14} (amps)	V_A (volt)	I_A (amps)	I_{13} (amps)	I_{14} (amps)
10^4	1680	2×10^{-8}	4.3×10^{-9}	1.1×10^{-8}	1620	2×10^{-8}	4.1×10^{-9}	1.05×10^{-8}
10^5	2400	2×10^{-7}	4.1×10^{-8}	1.3×10^{-7}	2270	2×10^{-7}	3.9×10^{-8}	1.15×10^{-7}
10^6	3630	2 x10 $^{-6}$	3.9×10^{-7}	1.4×10^{-6}	3320	2×10^{-6}	3.7×10^{-7}	1.4×10^{-6}
I_D	3700	8.0×10^{-11} Amp @ G = 10^6			3320	9.4×10^{-11} Amp @ G = 10^6		

FIGURE 9.4-45 MEASUREMENTS OF CURRENT VOLTAGE GAIN AND DARK CURRENT

11644					11762			
Gain	V_A (volt)	I_A (amps)	I_{13} (amps)	I_{14} (amps)	V_A (volt)	I_A (amps)	I_{13} (amps)	I_{14}(amps)
10^4	1540	2×10^{-8}	4.1×10^{-9}	1.1×10^{-8}	1470	2×10^{-8}	4.8×10^{-9}	1.05×10^{-8}
10^5	2170	2×10^{-7}	3.8×10^{-8}	1.3×10^{-7}	2040	2×10^{-7}	4.4×10^{-8}	1.3×10^{-7}
10^6	3200	2×10^{-6}	3.7×10^{-7}	1.4×10^{-6}	2900	2×10^{-6}	4.2×10^{-7}	1.4×10^{-6}
I_D	3200	4.6×10^{-11} Amp @ G = 10^6			2900	9.2×10^{-11} Amp @ G = 10^6		

11647					11664			
Gain	V_A (volt)	I_A (amps)	I_{13} (amps)	I_{14} (amps)	V_A (volt)	I_A (amps)	I_{13} (amps)	I_{14} (amps)
10^4	1680	2×10^{-8}	4.3×10^{-9}	1.1×10^{-8}	1650	2×10^{-8}	4.1×10^{-9}	1.05×10^{-8}
10^5	2400	2×10^{-7}	4.1×10^{-8}	1.3×10^{-7}	2320	2×10^{-7}	3.9×10^{-8}	1.15×10^{-7}
10^6	3700	2×10^{-6}	3.9×10^{-7}	1.4×10^{-6}	3360	2×10^{-6}	3.7×10^{-7}	1.4×10^{-6}
I_D	3700	8.0×10^{-11} Amp @ G = 10^6			3360	9.4×10^{-11} Amp @ G = 10^6		

FIGURE 9.4-46 MEASUREMENTS OF CURRENT VOLTAGE GAIN AND DARK CURRENT

	11644				11762			
Gain	V_A (volt)	I_A (amps)	I_{13} (amps)	I_{14} (amps)	V_A (volt)	I_A (amps)	I_{13} (amps)	I_{14}(amps)
10^4	1540	2×10^{-8}	4.1×10^{-9}	1.1×10^{-8}	1470	2×10^{-8}	4.8×10^{-9}	1.05×10^{-8}
10^5	2170	2×10^{-7}	3.8×10^{-8}	1.3×10^{-7}	2030	2×10^{-7}	4.4×10^{-8}	1.3×10^{-7}
10^6	3200	2×10^{-6}	3.7×10^{-7}	1.4×10^{-6}	2900	2×10^{-6}	4.2×10^{-7}	1.4×10^{-6}
I_D	3200	4.6×10^{-11} Amp @ G = 10^6			2900	9.2×10^{-11} Amp @ G = 10^6		

	11647				11664			
Gain	V_A (volt)	I_A (amps)	I_{13} (amps)	I_{14} (amps)	V_A (volt)	I_A (amps)	I_{13} (amps)	I_{14} (amps)
10^4	1680	2×10^{-8}	4.3×10^{-9}	1.1×10^{-8}	1640	2×10^{-8}	4.1×10^{-9}	1.05×10^{-8}
10^5	2400	2×10^{-7}	4.1×10^{-8}	1.3×10^{-7}	2310	2×10^{-7}	3.9×10^{-8}	1.2×10^{-7}
10^6	3700	2×10^{-6}	3.9×10^{-7}	1.4×10^{-6}	3350	2×10^{-6}	3.7×10^{-7}	1.4×10^{-6}
I_D	3700	8.0×10^{-11} Amp @ G = 10^6			3350	9.4×10^{-11} Amp @ G = 10^6		

FIGURE 9.4-47 MEASUREMENTS OF CURRENT VOLTAGE GAIN AND DARK CURRENT

11644					11762			
Gain	V_A (volt)	I_A (amps)	I_{13} (amps)	I_{14} (amps)	V_A (volt)	I_A (amps)	I_{13} (amps)	I_{14}(amps)
10^4	1560	2×10^{-8}	4.1×10^{-9}	1.1×10^{-8}	1470	2×10^{-8}	4.75×10^{-9}	1.05×10^{-8}
10^5	2210	2×10^{-7}	3.8×10^{-8}	1.3×10^{-7}	2030	2×10^{-7}	4.4×10^{-8}	1.3×10^{-7}
10^6	3250	2×10^{-6}	3.7×10^{-7}	1.4×10^{-6}	2880	2×10^{-6}	4.2×10^{-7}	1.4×10^{-6}
I_D	3200	4.4×10^{-11} Amp @ G = 10^6			2880	8.6×10^{-11} Amp @ G = 10^6		

11647					11664			
Gain	V_A (volt)	I_A (amps)	I_{13} (amps)	I_{14} (amps)	V_A (volt)	I_A (amps)	I_{13} (amps)	I_{14} (amps)
10^4	1700	2×10^{-8}	4.1×10^{-9}	1.1×10^{-8}	1630	2×10^{-8}	4.75×10^{-9}	1.05×10^{-8}
10^5	2440	2×10^{-7}	3.8×10^{-8}	1.3×10^{-7}	2300	2×10^{-7}	4.4×10^{-8}	1.3×10^{-7}
10^6	3720	2×10^{-6}	3.7×10^{-7}	1.4×10^{-6}	3340	2×10^{-6}	4.2×10^{-7}	1.4×10^{-6}
I_D	3700	9.5×10^{-11} Amp @ G = 10^6			3340	7.0×10^{-11} Amp @ G = 10^6		

FIGURE 9.4-48 MEASUREMENTS OF CURRENT VOLTAGE GAIN AND DARK CURRENT

11644					11762			
Gain	V_A (volt)	I_A (amps)	I_{13} (amps)	I_{14} (amps)	V_A (volt)	I_A (amps)	I_{13} (amps)	I_{14}(amps)
10^4	1510	2×10^{-8}	4.1×10^{-9}	1.1×10^{-8}	1460	2×10^{-8}	4.8×10^{-9}	1.1×10^{-8}
10^5	2140	2×10^{-7}	3.8×10^{-8}	1.3×10^{-7}	2020	2×10^{-7}	4.6×10^{-8}	1.2×10^{-7}
10^6	3100	2×10^{-6}	3.7×10^{-7}	1.4×10^{-6}	2850	2×10^{-6}	4.2×10^{-7}	1.4×10^{-6}
I_D	3100	4.4×10^{-11} Amp @ G = 10^6			2850	8.6×10^{-11} Amp @ G = 10^6		

11647					11664			
Gain	V_A (volt)	I_A (amps)	I_{13} (amps)	I_{14} (amps)	V_A (volt)	I_A (amps)	I_{13} (amps)	I_{14} (amps)
10^4	1630	2×10^{-8}	4.4×10^{-9}	1.1×10^{-8}	1650	2×10^{-8}	4×10^{-9}	1.05×10^{-8}
10^5	2330	2×10^{-7}	3.8×10^{-8}	1.3×10^{-7}	2320	2×10^{-7}	3.7×10^{-8}	1.08×10^{-7}
10^6	3520	2×10^{-6}	4.1×10^{-7}	1.4×10^{-6}	3350	2×10^{-6}	3.5×10^{-7}	1.2×10^{-6}
I_D	3520	7×10^{-11} Amp @ G = 10^6			3300	9.5×10^{-11} Amp @ G = 10^6		

FIGURE 9.4-49 MEASUREMENTS OF CURRENT VOLTAGE GAIN AND DARK CURRENT

	11644				11762			
Gain	V_A (volt)	I_A (amps)	I_{13} (amps)	I_{14} (amps)	V_A (volt)	I_A (amps)	I_{13} (amps)	I_{14}(amps)
10^4	1510	2×10^{-8}	4.1×10^{-9}	1.1×10^{-8}	1460	2×10^{-8}	4.8×10^{-9}	1.1×10^{-8}
10^5	2150	2×10^{-7}	3.8×10^{-8}	1.3×10^{-7}	2030	2×10^{-7}	4.6×10^{-8}	1.2×10^{-7}
10^6	3120	2×10^{-6}	3.7×10^{-7}	1.4×10^{-6}	2860	2×10^{-6}	4.2×10^{-7}	1.4×10^{-6}
I_D	3100	4.4×10^{-11} Amp @ G = 10^6			2860	8.6×10^{-11} Amp @ G = 10^6		

	11647				11664			
Gain	V_A (volt)	I_A (amps)	I_{13} (amps)	I_{14} (amps)	V_A (volt)	I_A (amps)	I_{13} (amps)	I_{14} (amps)
10^4	1630	2×10^{-8}	4.4×10^{-9}	1.1×10^{-8}	1610	2×10^{-8}	4×10^{-9}	1.1×10^{-8}
10^5	2360	2×10^{-7}	3.8×10^{-8}	1.3×10^{-7}	2270	2×10^{-7}	3.7×10^{-8}	1.15×10^{-7}
10^6	3600	2×10^{-6}	4.1×10^{-7}	1.4×10^{-6}	3350	2×10^{-6}	3.5×10^{-7}	1.4×10^{-6}
I_D	3600	8.1×10^{-11} Amp @ G = 10^6			3300	9.0×10^{-11} Amp @ G = 10^6		

FIGURE 9.4-50 MEASUREMENTS OF CURRENT VOLTAGE GAIN AND DARK CURRENT

	11644				11762			
Gain	V_A (volt)	I_A (amps)	I_{13} (amps)	I_{14} (amps)	V_A (volt)	I_A (amps)	I_{13} (amps)	I_{14} (amps)
10^4	1560	2×10^{-8}	4.1×10^{-9}	1.1×10^{-8}	1460	2×10^{-8}	4.8×10^{-9}	1.1×10^{-8}
10^5	2200	2×10^{-7}	3.8×10^{-8}	1.3×10^{-7}	2030	2×10^{-7}	4.4×10^{-8}	1.3×10^{-7}
10^6	3200	2×10^{-6}	3.7×10^{-7}	1.4×10^{-6}	2870	2×10^{-6}	4.2×10^{-7}	1.4×10^{-6}
I_D	3200	4.6×10^{-11} Amp @ G = 10^6			2800	9.0×10^{-11} Amp @ G = 10^6		

	11647				11664			
Gain	V_A (volt)	I_A (amps)	I_{13} (amps)	I_{14} (amps)	V_A (volt)	I_A (amps)	I_{13} (amps)	I_{14} (amps)
10^4	1670	2×10^{-8}	4.3×10^{-9}	1.1×10^{-8}	1640	2×10^{-8}	4.1×10^{-9}	1.1×10^{-8}
10^5	2400	2×10^{-7}	4.1×10^{-8}	1.3×10^{-7}	2300	2×10^{-7}	3.9×10^{-8}	1.2×10^{-7}
10^6	3640	2×10^{-6}	3.9×10^{-7}	1.4×10^{-6}	3300	2×10^{-6}	3.7×10^{-7}	1.4×10^{-6}
I_D	3600	8×10^{-11} Amp @ G = 10^6			3300	9.6×10^{-11} Amp @ G = 10^6		

FIGURE 9.4-51 MEASUREMENTS OF CURRENT VOLTAGE GAIN AND DARK CURRENT

ORBIT 2464.5

	11644				11762			
Gain	V_A (volt)	I_A (amps)	I_{13} (amps)	I_{14} (amps)	V_A (volt)	I_A (amps)	I_{13} (amps)	I_{14}(amps)
10^4	1490	2×10^{-8}	4.1×10^{-9}	1.2×10^{-8}	1430	2×10^{-8}	4.8×10^{-9}	1.1×10^{-8}
10^5	2100	2×10^{-7}	3.8×10^{-8}	1.3×10^{-7}	1970	2×10^{-7}	4.6×10^{-8}	1.2×10^{-7}
10^6	3040	2×10^{-6}	3.7×10^{-7}	1.4×10^{-6}	2770	2×10^{-6}	4.2×10^{-7}	1.4×10^{-6}
I_D	3100	4.8×10^{-11} Amp @ G = 10^6			2800	8×10^{-11} Amp @ G = 10^6		

	11647				11664			
Gain	V_A (volt)	I_A (amps)	I_{13} (amps)	I_{14} (amps)	V_A (volt)	I_A (amps)	I_{13} (amps)	I_{14} (amps)
10^4	1640	2×10^{-8}	4.7×10^{-9}	1.05×10^{-8}	1610	2×10^{-8}	4.3×10^{-9}	1.1×10^{-8}
10^5	2350	2×10^{-7}	4.3×10^{-8}	1.2×10^{-7}	2250	2×10^{-7}	4×10^{-8}	1.2×10^{-7}
10^6	3620	2×10^{-6}	4.1×10^{-7}	1.4×10^{-6}	3240	2×10^{-6}	3.7×10^{-7}	1.3×10^{-6}
I_D	3600	9.1×10^{-11} Amp @ G = 10^6			3300	5.5×10^{-11} Amp @ G = 10^6		

FIGURE 9.4-52 MEASUREMENTS OF CURRENT VOLTAGE GAIN AND DARK CURRENT

11644					11762			
Gain	V_A (volt)	I_A (amps)	I_{13} (amps)	I_{14} (amps)	V_A (volt)	I_A (amps)	I_{13} (amps)	I_{14} (amps)
10^4	1490	2×10^{-8}	4.5×10^{-9}	1.2×10^{-8}	1430	2×10^{-8}	4.8×10^{-9}	1.1×10^{-8}
10^5	2100	2×10^{-7}	4.1×10^{-8}	1.25×10^{-7}	1970	2×10^{-7}	4.6×10^{-8}	1.2×10^{-7}
10^6	3030	2×10^{-6}	3.9×10^{-7}	1.4×10^{-6}	2770	2×10^{-6}	4.2×10^{-7}	1.4×10^{-6}
I_D	3000	4×10^{-11} Amp @ G = 10^6			2700	9×10^{-11} Amp @ G = 10^6		

11647					11664			
Gain	V_A (volt)	I_A (amps)	I_{13} (amps)	I_{14} (amps)	V_A (volt)	I_A (amps)	I_{13} (amps)	I_{14} (amps)
10^4	1640	2×10^{-8}	4.4×10^{-9}	1.1×10^{-8}	1610	2×10^{-8}	4.3×10^{-9}	1.1×10^{-8}
10^5	2360	2×10^{-7}	4.3×10^{-8}	1.2×10^{-7}	2250	2×10^{-7}	4×10^{-8}	1.2×10^{-7}
10^6	3600	2×10^{-6}	4.1×10^{-7}	1.4×10^{-6}	3240	2×10^{-6}	3.7×10^{-7}	1.3×10^{-6}
I_D	3600	9.1×10^{-11} Amp @ G = 10^6			3300	5.5×10^{-11} Amp @ G = 10^6		

FIGURE 9.4-53 MEASUREMENTS OF CURRENT VOLTAGE GAIN AND DARK CURRENT

	11644				11762			
Gain	V_A (volt)	I_A (amps)	I_{13} (amps)	I_{14} (amps)	V_A (volt)	I_A (amps)	I_{13} (amps)	I_{14}(amps)
10^4	1480	2×10^{-8}	4.5×10^{-9}	1.2×10^{-8}	1420	2×10^{-8}	4.8×10^{-9}	1.1×10^{-8}
10^5	2080	2×10^{-7}	4.1×10^{-8}	1.3×10^{-7}	1960	2×10^{-7}	4.6×10^{-8}	1.2×10^{-7}
10^6	3020	2×10^{-6}	3.9×10^{-7}	1.4×10^{-6}	2750	2×10^{-6}	4.2×10^{-7}	1.4×10^{-6}
I_D	3000	4.4×10^{-11} Amp @ G = 10^6			2700	9×10^{-11} Amp @ G = 10^6		

	11647				11664			
Gain	V_A (volt)	I_A (amps)	I_{13} (amps)	I_{14} (amps)	V_A (volt)	I_A (amps)	I_{13} (amps)	I_{14} (amps)
10^4	1610	2×10^{-8}	4.4×10^{-9}	1.1×10^{-8}	1600	2×10^{-8}	4×10^{-9}	1.1×10^{-8}
10^5	2300	2×10^{-7}	4.3×10^{-8}	1.3×10^{-7}	2210	2×10^{-7}	3.7×10^{-8}	1.9×10^{-7}
10^6	3500	2×10^{-6}	4.1×10^{-7}	1.4×10^{-6}	3150	2×10^{-6}	3.5×10^{-7}	1.2×10^{-6}
I_D	3600	7×10^{-11} Amp @ G = 10^6			3300	5.5×10^{-11} Amp @ G = 10^6		

FIGURE 9.4-54 MEASUREMENTS OF CURRENT VOLTAGE GAIN AND DARK CURRENT

	11644				11762			
Gain	V_A (volt)	I_A (amps)	I_{13} (amps)	I_{14} (amps)	V_A (volt)	I_A (amps)	I_{13} (amps)	I_{14}(amps)
10^4	1480	2×10^{-8}	4.1×10^{-9}	1.1×10^{-8}	1420	2×10^{-8}	4.8×10^{-9}	1.1×10^{-8}
10^5	2080	2×10^{-7}	3.8×10^{-8}	1.3×10^{-7}	1950	2×10^{-7}	4.4×10^{-8}	1.3×10^{-7}
10^6	3020	2×10^{-6}	3.7×10^{-7}	1.4×10^{-6}	2730	2×10^{-6}	4.2×10^{-7}	1.4×10^{-6}
I_D	3000	4.6×10^{-11} Amp @ G = 10^6			2700	9.0×10^{-11} Amp @ G = 10^6		

	11647				11664			
Gain	V_A (volt)	I_A (amps)	I_{13} (amps)	I_{14} (amps)	V_A (volt)	I_A (amps)	I_{13} (amps)	I_{14} (amps)
10^4	1610	2×10^{-8}	4.3×10^{-9}	1.1×10^{-8}	1600	2×10^{-8}	4.1×10^{-9}	1.1×10^{-8}
10^5	2290	2×10^{-7}	4.1×10^{-8}	1.3×10^{-7}	2210	2×10^{-7}	3.9×10^{-8}	1.2×10^{-7}
10^6	3470	2×10^{-6}	3.9×10^{-7}	1.4×10^{-6}	3150	2×10^{-6}	3.7×10^{-7}	1.4×10^{-6}
I_D	3500	7.1×10^{-11} Amp @ G = 10^6			3300	5.5×10^{-11} Amp @ G = 10^6		

FIGURE 9.4-55 MEASUREMENTS OF CURRENT VOLTAGE GAIN AND DARK CURRENT

ORBIT 2800

	11644				11762			
Gain	V_A (volt)	I_A (amps)	I_{13} (amps)	I_{14} (amps)	V_A (volt)	I_A (amps)	I_{13} (amps)	I_{14} (amps)
10^4	1590	2×10^{-8}	4.3×10^{-9}	1.25×10^{-8}	1500	2×10^{-8}	4.9×10^{-9}	1.2×10^{-8}
10^5	2260	2×10^{-7}	4.1×10^{-8}	1.25×10^{-7}	2070	2×10^{-7}	4.6×10^{-8}	1.25×10^{-7}
10^6	3360	2×10^{-6}	3.7×10^{-7}	1.4×10^{-6}	2840	2×10^{-6}	4.1×10^{-7}	1.35×10^{-6}
I_D	3360	7.5×10^{-11} Amp @ G = 10^6			2840	8.7×10^{-11} Amp @ G = 10^6		

	11647				11664			
Gain	V_A (volt)	I_A (amps)	I_{13} (amps)	I_{14} (amps)	V_A (volt)	I_A (amps)	I_{13} (amps)	I_{14} (amps)
10^4	1720	2×10^{-8}	5.1×10^{-9}	1.1×10^{-8}	1640	2×10^{-8}	5.3×10^{-9}	1.1×10^{-8}
10^5	2470	2×10^{-7}	4.5×10^{-8}	1.2×10^{-7}	2350	2×10^{-7}	4.2×10^{-8}	1.2×10^{-7}
10^6	3700	2×10^{-6}	3.5×10^{-7}	1.3×10^{-6}	3380	2×10^{-6}	3.8×10^{-7}	1.3×10^{-6}
I_D	3700	8.6×10^{-11} Amp @ G = 10^6			3380	8.9×10^{-11} Amp @ G = 10^6		

FIGURE 9.4-58 MEASUREMENTS OF CURRENT VOLTAGE GAIN AND DARK CURRENT

	11644				11762			
Gain	V_A (volt)	I_A (amps)	I_{13} (amps)	I_{14} (amps)	V_A (volt)	I_A (amps)	I_{13} (amps)	I_{14}(amps)
10^4	1580	2×10^{-8}	4.3×10^{-9}	1.2×10^{-8}	1500	2×10^{-8}	4.9×10^{-9}	1.2×10^{-8}
10^5	2250	2×10^{-7}	4.1×10^{-8}	1.3×10^{-7}	2080	2×10^{-7}	4.6×10^{-8}	1.2×10^{-7}
10^6	3250	2×10^{-6}	3.7×10^{-7}	1.4×10^{-6}	2850	2×10^{-6}	4.1×10^{-7}	1.3×10^{-6}
I_D	3250	7.1×10^{-11} Amp @ G = 10^6			2850	1.2×10^{-10} Amp @ G = 10^6		

	11647				11664			
Gain	V_A (volt)	I_A (amps)	I_{13} (amps)	I_{14} (amps)	V_A (volt)	I_A (amps)	I_{13} (amps)	I_{14} (amps)
10^4	1720	2×10^{-8}	5.3×10^{-9}	1.1×10^{-8}	1680	2×10^{-8}	5.1×10^{-9}	1.1×10^{-8}
10^5	2470	2×10^{-7}	4.2×10^{-8}	1.2×10^{-7}	2360	2×10^{-7}	4.5×10^{-8}	1.2×10^{-7}
10^6	3700	2×10^{-6}	3.8×10^{-7}	1.35×10^{-6}	3400	2×10^{-6}	3.5×10^{-7}	1.3×10^{-6}
I_D	3660	9.1×10^{-11} Amp @ G = 10^6			3400	9.5×10^{-11} Amp @ G = 10^6		

FIGURE 9.4-59 MEASUREMENTS OF CURRENT VOLTAGE GAIN AND DARK CURRENT

ORBIT 2910

11644					11762			
Gain	V_A (volt)	I_A (amps)	I_{13} (amps)	I_{14} (amps)	V_A (volt)	I_A (amps)	I_{13} (amps)	I_{14}(amps)
10^4	1620	2×10^{-8}	4.3×10^{-9}	1.2×10^{-8}	1510	2×10^{-8}	4.8×10^{-9}	1.1×10^{-8}
10^5	2260	2×10^{-7}	4.1×10^{-8}	1.3×10^{-7}	2090	2×10^{-7}	4.4×10^{-8}	1.2×10^{-7}
10^6	3300	2×10^{-6}	3.8×10^{-7}	1.4×10^{-6}	2870	2×10^{-6}	4.1×10^{-7}	1.3×10^{-6}
I_D	3300	8.1×10^{-11} Amp @ G = 10^6			2870	1.2×10^{-10} Amp @ G = 10^6		

11647					11664			
Gain	V_A (volt)	I_A (amps)	I_{13} (amps)	I_{14} (amps)	V_A (volt)	I_A (amps)	I_{13} (amps)	I_{14} (amps)
10^4	1710	2×10^{-8}	4.3×10^{-9}	1.1×10^{-8}	1680	2×10^{-8}	4.1×10^{-9}	1.1×10^{-8}
10^5	2470	2×10^{-7}	4.0×10^{-8}	1.2×10^{-7}	2350	2×10^{-7}	3.9×10^{-8}	1.2×10^{-7}
10^6	3690	2×10^{-6}	4.0×10^{-7}	1.3×10^{-6}	3370	2×10^{-6}	3.6×10^{-7}	1.4×10^{-6}
I_D	3690	9.5×10^{-11} Amp @ G = 10^6			3370	8.5×10^{-11} Amp @ G = 10^6		

FIGURE 9.4-60 MEASUREMENTS OF CURRENT VOLTAGE GAIN AND DARK CURRENT

	11644				11762			
Gain	V_A (volt)	I_A (amps)	I_{13} (amps)	I_{14} (amps)	V_A (volt)	I_A (amps)	I_{13} (amps)	I_{14}(amps)
10^4	1540	2×10^{-8}	4.3×10^{-9}	1.2×10^{-8}	1470	2×10^{-8}	4.7×10^{-9}	1.1×10^{-8}
10^5	2170	2×10^{-7}	4.1×10^{-8}	1.3×10^{-7}	2020	2×10^{-7}	4.3×10^{-8}	1.2×10^{-7}
10^6	3220	2×10^{-6}	3.8×10^{-7}	1.4×10^{-6}	2860	2×10^{-6}	4.0×10^{-7}	1.3×10^{-6}
I_D	3220	9.2×10^{-11} Amp @ G = 10^6			2860	1.3×10^{-10} Amp @ G = 10^6		

	11647				11664			
Gain	V_A (volt)	I_A (amps)	I_{13} (amps)	I_{14} (amps)	V_A (volt)	I_A (amps)	I_{13} (amps)	I_{14} (amps)
10^4	1750	2×10^{-8}	4.3×10^{-9}	1.1×10^{-8}	1660	2×10^{-8}	4.0×10^{-9}	1.1×10^{-8}
10^5	2530	2×10^{-7}	4.0×10^{-8}	1.2×10^{-7}	2330	2×10^{-7}	3.9×10^{-8}	1.2×10^{-7}
10^6	3700	2×10^{-6}	3.9×10^{-7}	1.3×10^{-6}	3320	2×10^{-6}	3.7×10^{-7}	1.4×10^{-6}
I_D	3700	1×10^{-11} Amp @ G = 10^6			3320	7.4×10^{-11} Amp @ G = 10^6		

FIGURE 9.4-61 MEASUREMENTS OF CURRENT VOLTAGE GAIN AND DARK CURRENT

ORBIT 2960

	11644				11762			
Gain	V_A (volt)	I_A (amps)	I_{13} (amps)	I_{14} (amps)	V_A (volt)	I_A (amps)	I_{13} (amps)	I_{14} (amps)
10^4	1620	2×10^{-8}	4.3×10^{-9}	1.2×10^{-8}	1520	2×10^{-8}	4.8×10^{-9}	1.1×10^{-8}
10^5	2270	2×10^{-7}	4×10^{-8}	1.3×10^{-7}	2100	2×10^{-7}	4.4×10^{-8}	1.2×10^{-7}
10^6	3300	2×10^{-6}	3.8×10^{-7}	1.4×10^{-6}	2880	2×10^{-6}	4.1×10^{-7}	1.3×10^{-6}
I_D	3300	8.7×10^{-11} Amp @ G = 10^6			2880	9.5×10^{-11} Amp @ G = 10^6		

	11647				11664			
Gain	V_A (volt)	I_A (amps)	I_{13} (amps)	I_{14} (amps)	V_A (volt)	I_A (amps)	I_{13} (amps)	I_{14} (amps)
10^4	1700	2×10^{-8}	4.3×10^{-9}	1.1×10^{-8}	1630	2×10^{-8}	4.1×10^{-9}	1.1×10^{-8}
10^5	2540	2×10^{-7}	4×10^{-8}	1.2×10^{-7}	2350	2×10^{-7}	4.0×10^{-8}	1.2×10^{-7}
10^6	3700	2×10^{-6}	3.9×10^{-7}	1.3×10^{-6}	3380	2×10^{-6}	3.7×10^{-7}	1.4×10^{-6}
I_D	3700	1×10^{-10} Amp @ G = 10^6			3380	7.8×10^{-11} Amp @ G = 10^6		

FIGURE 9.4-62 MEASUREMENTS OF CURRENT VOLTAGE GAIN AND DARK CURRENT

	11644				11762			
Gain	V_A (volt)	I_A (amps)	I_{13} (amps)	I_{14} (amps)	V_A (volt)	I_A (amps)	I_{13} (amps)	I_{14}(amps)
10^4	1600	2×10^{-8}	4.3×10^{-9}	1.2×10^{-8}	1510	2×10^{-8}	4.8×10^{-9}	1.1×10^{-8}
10^5	2260	2×10^{-7}	4×10^{-8}	1.3×10^{-7}	2100	2×10^{-7}	4.4×10^{-8}	1.2×10^{-7}
10^6	3340	2×10^{-6}	3.8×10^{-7}	1.4×10^{-6}	2890	2×10^{-6}	4.0×10^{-7}	1.3×10^{-6}
I_D	3340	9×10^{-11} Amp @ G = 10^6			2890	8.5×10^{-11} Amp @ G = 10^6		

	11647				11664			
Gain	V_A (volt)	I_A (amps)	I_{13} (amps)	I_{14} (amps)	V_A (volt)	I_A (amps)	I_{13} (amps)	I_{14} (amps)
10^4	1700	2×10^{-8}	4.3×10^{-9}	1.1×10^{-8}	1630	2×10^{-8}	4.1×10^{-9}	1.1×10^{-8}
10^5	2540	2×10^{-7}	4.1×10^{-8}	1.2×10^{-7}	2360	2×10^{-7}	4.0×10^{-8}	1.2×10^{-7}
10^6	3700	2×10^{-6}	4.0×10^{-7}	1.3×10^{-6}	3380	2×10^{-6}	3.9×10^{-7}	1.4×10^{-6}
I_D	3700	8.5×10^{-11} Amp @ G = 10^6			3380	7.6×10^{-11} Amp @ G = 10^6		

FIGURE 9.4-63 MEASUREMENTS OF CURRENT VOLTAGE GAIN AND DARK CURRENT

	11644				11762			
Gain	V_A (volt)	I_A (amps)	I_{13} (amps)	I_{14} (amps)	V_A (volt)	I_A (amps)	I_{13} (amps)	I_{14} (amps)
10^4	1600	2×10^{-8}	4.3×10^{-9}	1.2×10^{-8}	1500	2×10^{-8}	4.6×10^{-9}	1.1×10^{-8}
10^5	2270	2×10^{-7}	4×10^{-8}	1.3×10^{-7}	2070	2×10^{-7}	4.3×10^{-8}	1.2×10^{-7}
10^6	3370	2×10^{-8}	3.8×10^{-7}	1.4×10^{-6}	2900	2×10^{-8}	4.1×10^{-7}	1.3×10^{-6}
I_D	3370	9×10^{-11} Amp @ G = 10^6			2900	8.1×10^{-11} Amp @ G = 10^6		

	11647				11664			
Gain	V_A (volt)	I_A (amps)	I_{13} (amps)	I_{14} (amps)	V_A (volt)	I_A (amps)	I_{13} (amps)	I_{14} (amps)
10^4	1720	2×10^{-8}	4.3×10^{-9}	1.1×10^{-8}	1630	2×10^{-8}	4.1×10^{-9}	1.1×10^{-8}
10^5	2500	2×10^{-7}	4.1×10^{-8}	1.2×10^{-7}	2360	2×10^{-7}	4.0×10^{-8}	1.2×10^{-7}
10^6	3670	2×10^{-6}	3.9×10^{-7}	1.3×10^{-6}	3400	2×10^{-6}	3.7×10^{-7}	1.4×10^{-6}
I_D	3670	9.5×10^{-11} Amp @ G = 10^6			3400	8.1×10^{-11} Amp @ G = 10^6		

FIGURE 9.4-64 MEASUREMENTS OF CURRENT VOLTAGE GAIN AND DARK CURRENT

SECTION 10.0
REFERENCES

1. G. W. Meisenholter, "Planet Illumination", JPL Technical Report 32-361, November, 1962.

2. F. W. Sears, "Optics", page 331, Addison-Wesley Publishing Co., 1958.

3. G. Shortley and D. Williams, "Elements of Physics", page 381, Prentice Hall 1953.

4. V. G. Fessenkov, "Physics and Astronomy of the Moon", Chapter 4, Edited by Zdenek Kopal, Academic Press, 1962.

5. "Handbook of Geophysics and Space Environments", Air Force Cambridge Research Laboratory, McGraw-Hill, 1965.